Design and synthesis of the novel orexin receptor ligands with 1,3,5-trioxazatriquinane skeleton

Mao Amezawa

February 2023

Design and synthesis of the novel orexin receptor ligands with 1,3,5-trioxazatriquinane skeleton

Mao Amezawa
Doctoral Program in Chemistry

Submitted to the
Degree Programs in Pure and Applied Sciences of the
Graduate School of Science and Technology
in Partial Fulfillment of the Requirements
for the Degree of Doctor of Philosophy in
Science

at the University of Tsukuba

Table of contents

List of abbreviation

ABC	ATP Binding Cassette
Ac	acetyl
Alloc	allyloxycarbonyl
ANOVA	analysis of variance
aq.	aqueous solution
ATP	adenosine triphosphate
BBB	blood-brain barrier
BCRP	breast cancer resistance protein
Bn	benzyl
Boc	*tert*-butoxy carbonyl
Bu	butyl
Bz	benzoyl
BSA	bovine serum albumin
Cbz	benzyloxy carbonyl
CD	circular dichroism
CHO	chinese hamster ovary
CHP	cumene hydroperoxide
CL_{int}	intrinsic clearance
CNS	central nervous system
CSA	camphorsulfonic acid
Cy	cyclohexyl
DAMGO	[D-Ala^2, *N*-Me-Phe^4, Gly^5-ol]-enkephalin
DCM	dichloromethane
DDQ	2,3-dichloro-5,6-dicyano-*p*-benzoquinone
DET	diethyl tartrate
DIPEA	diisopropylethylamine
DIPT	di-isopropyl tartrate

DMEM	Dulbecco's modified Eagle medium
DMF	*N*, *N*-dimethylformamide
DMPK	drug metabolism and pharmacokinetics
DMSO	dimethyl sulfoxide
DOR	δ opioid receptor
DORA	dual orexin receptor antagonist
DOS	diversity oriented synthesis
DPDPE	[D-Phe^{2,5}]-enkephalin
EC_{50}	median effective concentration
ECL	extracellular loop
ED_{50}	median effective dose
Ee	enantiomeric excess
EEG	electroencephalogram
E_{max}	maximum effect
EMG	electromyography
eq.	equivalent
ESI	electrospray ionization
Et	ethyl
FBS	fetal bovine serum
FDA	food and drug administration
GDP	guanosine diphosphate
GPC	gel permeation chromatography
GPCR	G-protein-coupled receptor
GTP	guanosine triphosphate
HLM	human liver microsome
HBSS	Hank’s balanced salt solution
HEK	human embryonic kidney
HPLC	high-performance liquid chromatography
HTS	high-throughput screening

IC_{50}	half maximal inhibitory concentration
i.c.v.	intracerebroventricular
i.p.	intraperitoneal
IR	infrared
i.v.	intracerebroventricular
K_i	inhibition constant
KO	knockout
KOR	κ opioid receptor
*m*CPBA	*m*-chloroperoxybenzoic acid
Me	methyl
MeO	methoxy
Moc	methoxycarbonyl
MOR	μ opioid receptor
MS	molecular sieve
Ms	mesyl
MTPA	α-methoxy-α-(trifluoromethyl)phenylacetyl chloride
NMO	*N*-methylmorpholine *N*-oxide
NMR	nuclear magnetic resonance
NOE	nuclear overhauser effect
NREM	nonrapid eye movement
Oct	octyl
OX_1R	orexin 1 receptor
OX_2R	orexin 2 receptor
OXA	orexin A
OXB	orexin B
OXR	orexin receptor
P_{app}	apparent permeability coefficient
P-gp	P-glycoprotein
PDA	photodiode array

PDB	protein data bank
Ph	phenyl
Piv	pivaloyl
PMB	*p*-methoxybenzyl
PMI	principal moment of inertia
PMP	*p*-methoxy phenyl
PNB	*p*-nitrobenzyl
ppm	parts per million
PPTS	pyridinium *p*-toluenesulfonate
Pr	propyl
r.t.	room temperature
REM	rapid eye movement
s.c.	subcutaneous
SEM	standard error of the mean
1-SORA	selective orexin 1 receptor antagonist
2-SORA	selective orexin 2 receptor antagonist
TBAF	tetrabutylammonium fluoride
TBHP	*tert*-butyl hydroperoxide
TBS	*tert*-butyldimethylsilyl
TFA	trifluoroacetic acid
THF	tetrahydrofuran
TPAP	tetrapropylammonium perruthenate
TLC	thin-layer chromatography
TosMIC	tosylmethyl isocyanide
TriMER	1,3,5-trioxazatriquinane bearing multiple effective residue
Troc	2,2,2-trichlotoethoxycarbonyl
UPLC	ultra-performance liquid chromatography
UV	ultraviolet
VEH	vehicle

Chapter 1 General introduction

1.1 Screening for drug discovery and chemical library

Hit identification is the first crucial step for successful drug development, which can generally take more than 10 years from target validation to its approval (Figure 1).[1] This process identifies the right small molecules, also called hits or hit compounds that bind to the target and induce the desired activity. High-quality starting hits can be expected to increase the efficiency of the hit identification process consequently the entire drug discovery project.

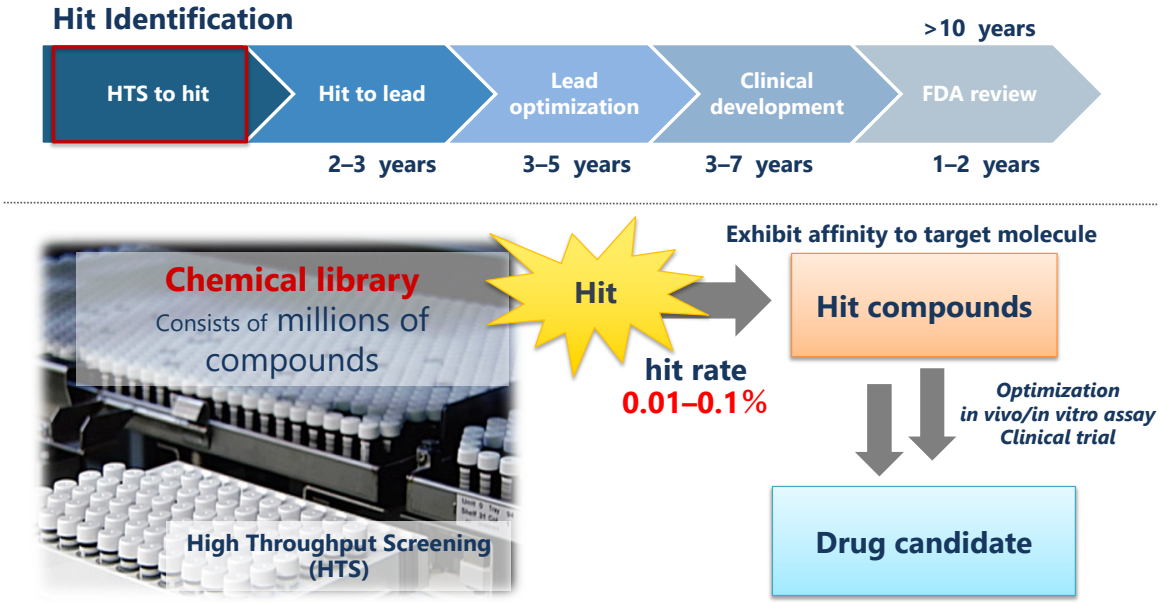

Figure 1. The timeline of drug discovery and probable success rate in each phase

In order to find hit compounds leading drug candidate, high-throughput screening (HTS) that enables rapid evaluation of a huge number of compounds, termed chemical library, using pharmacological assays has been used. However, hit identification process with HTS generally has a very low hit rate (0.01–0.1%)[2] as the method finds few active compounds from a large group of compounds. In addition, such large chemical libraries are expensive and difficult to obtain; thus, an inexpensive and efficient screening library is in demand.

Two factors are essential for hit compounds: 1) pharmacophores that enable interactions with target biomolecules (e.g., hydrogen bond, ionic bond, and hydrophobic interaction), and 2) core scaffold for three-dimensional placement of pharmacophores (Figure 2).[3] In other words, the hit identification process explores the combination of these factors and the chemical library is required to include a large number of each factors

as possible. Therefore, various synthetic chemical approaches have been developed to prepare more compounds.

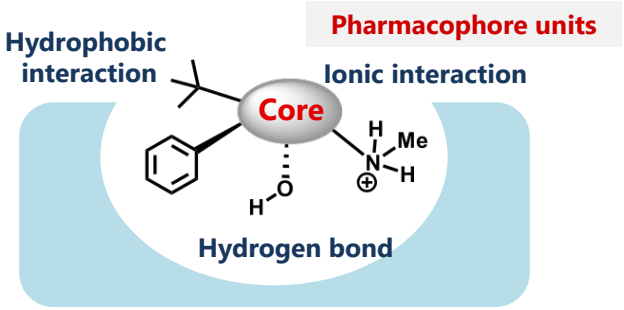

Figure 2. Two factors that are essential for a hit compound

In 1963, Merrifield *et al.* proposed chemical libraries using combinatorial chemistry[4] based on solid-phase peptide synthesis (Figure 3a).[5] In this method, starting materials are supported on the solid phase with covalent bonds, excess reactants are easily removed by washing, and many compounds are synthesized rapidly at once. However, the reactions that can be used for this method are limited to conjugation reactions such as condensation and coupling reactions that connect each component linearly, consequently, the synthesized compounds have poor three-dimensionality. In contrast, chemical libraries based on diversity-oriented synthesis (DOS) put forward by Schriber[6] *et al.* in 2000 have enabled a highly three-dimensionally diverse core skeleton from common starting materials, which offers diverse reactivity as an intermediate via rearrangement reactions and so on (Figure 3b).[7,8] Although complex and highly three-dimensional skeletons can be efficiently synthesized using DOS approach, the molecular design and synthetic strategy tend to be complicated, and achieving the high stereoselectivity is challenging. In addition, the number of compounds to be evaluated tends to increase exponentially as more substituents are introduced from randomly along with the core skeletons. Both chemical libraries are complementary and offer excellent methods that have been used for the synthesis of many valuable compounds. However, the number of compounds in the chemical library determined by the multiplication of these two factors increases exponentially depending on the number of each factor. Consequently, hit rates of HTS using such a library necessarily decrease.

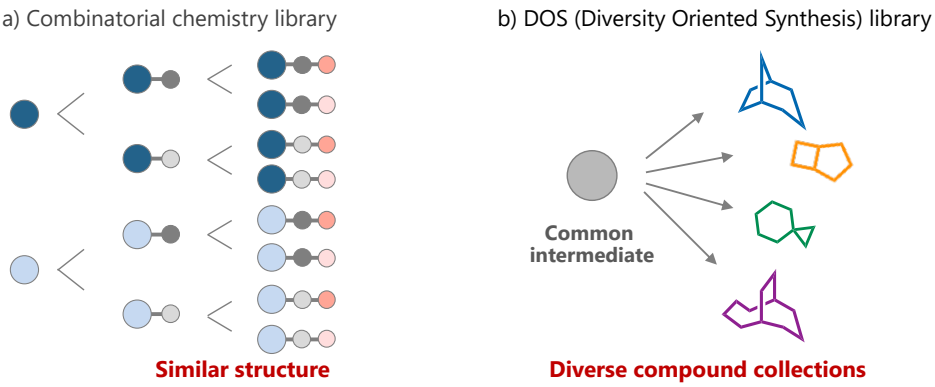

Figure 3. Chemical libraries with (a) combinatorial synthesis and (b) diversity-oriented synthesis (DOS)

The three-dimensionality of the molecule can be visualized using the normalized ratios of principal moments of inertia (PMI)[9] graphical representation. PMI can be determined with several software packages such as MOE and Cerius2. The lowest energy conformer of compounds is calculated and the three principal moments of inertia I_1, I_2, and I_3 ($I_1 < I_2 < I_3$) are determined. The normalization is performed by dividing the two lower PMI values (I_1 and I_2) by the highest value (I_3) to obtain two values for each compound (I_1/I_3 and I_2/I_3). Finally, they are plotted on an isosceles triangle and assessed the three-dimensionality as shown in Figure 4.

The PMI analysis of the existing drug or drug candidate compounds in ChemBL (open database of bioactive compounds), which was obtained from existing chemical libraries via combinatorial chemistry or DOS, suggested that 75% of the compound structures were planar and linear, not a spherical (Figure 4).[10] The same tendency was also observed in the library analysis of the pharmaceutical company, AstraZeneca.[11]

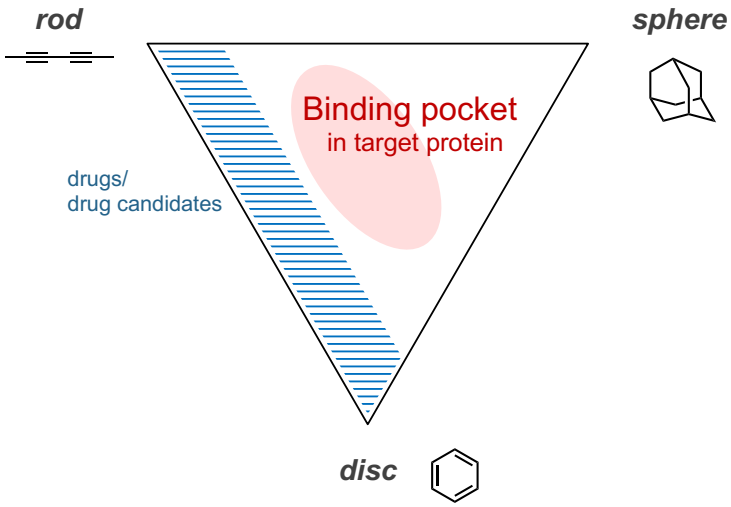

Figure 4. Schematic illustration of the PMI analysis of the existing drug or drug candidate compounds and the structure of the binding pocket in the target proteins[10]

In contrast, focusing on the structure of the binding pocket in the target proteins, the PMI ratio of binding pocket tend to distribute in rather a sphere-like region with few linear and planar ones, especially in G-protein-coupled receptors (GPCRs).[12] These results suggest that there are few existing ligands that can effectively utilize the three-dimensional binding pocket and these planar and linear molecules changes their conformation to fit the binding site. Recently, several libraries focusing on the three-dimensionality of the molecule have been reported.[13] For example, Fujii *et al.* reported an azanorbornane library possessing triazole based on the click reaction.[14] Though azanorbornane is the sp^3-rich sphere-like core structure, the orientation of two substituents on the scaffold is limited in two directions (*endo*- and *exo*-), which causes poor three-dimensional chemical space. Similarly, chemical libraries based on the saturated heterocyclic core structures such as piperidine and pyrrolidine has a limit of arrangement of the sidechains.[15] A chemical library with cyclopentanes can be arranged with six sidechains at most,[16] but applicable reactions and substituents are limiting, which causes a small chemical space. In addition, the core structures of these libraries are relatively small to fix the conformation of sidechains. As the three-dimensionality of the compounds depends on the orientation of sidechains, the hit discovery using above mentioned libraries tends to inefficient.

Thus, to obtain hit compounds efficiently from a small number of library compounds, i.e., to increase the hit rate, the reduction of the absolute number of combinations of the two factors, pharmacophores and scaffolds, while maintaining their quality that complements the actual binding pocket in the proteins would be important. In other words, if the core skeleton has enough three-dimensionality and properties can distribute several pharmacophores in appropriate manner, the number of scaffolds would be limited, leading to a high hit rate from a small group of library compounds.

1.2 1,3,5-Trioxazatriquinane skeleton in medicinal chemistry research

The 1,3,5-trioxazatriquinane skeleton (**1**) is a bowl-like heterocyclic skeleton that was serendipitously discovered by Nagase *et al.* as a byproduct during the synthesis of morphinan derivatives (Scheme 1).[17–19] In the early period since the discovery, this skeleton was utilized to develop the twin drug KNT-123 (**4**) and the triplet drug KNT-93 (**5**), which have two or three morphinan moieties derived from naltrexone (Figure 5).[20–24] Each compound exhibited different opioid receptor type selectivity and activity, especially, **5** showed μ opioid receptor agonist activity 11-fold more potent than morphine in mice in the acetic acid-induced writhing test.[20]

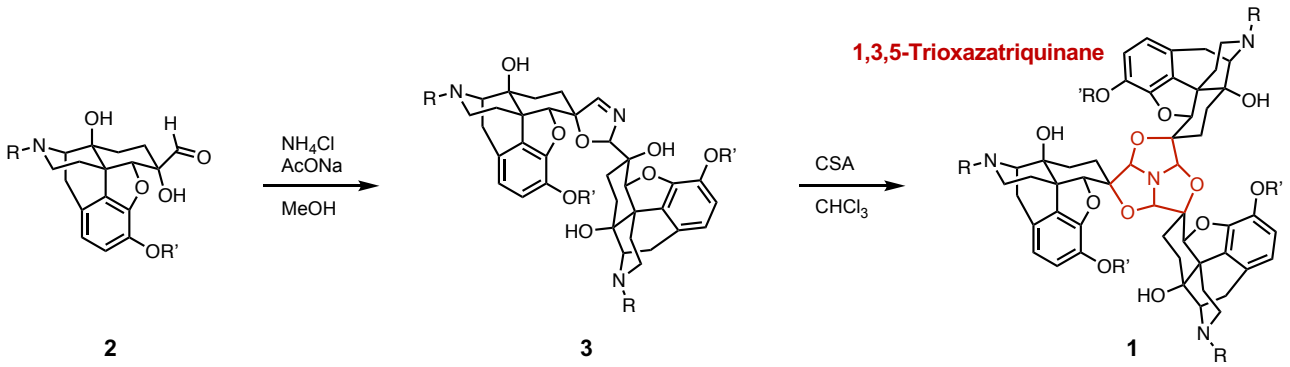

Scheme 1. Discovery of the 1,3,5-trioxazatriquinane skeleton and its features

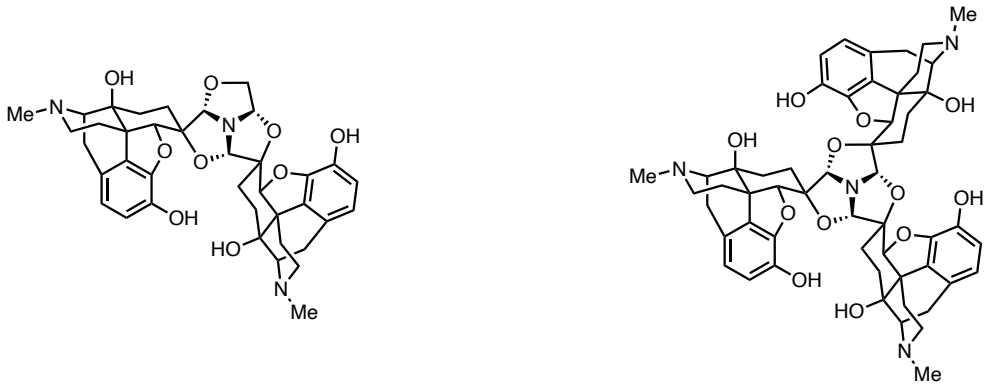

Figure 5. Twin drug and triplet drugs with the 1,3,5-trioxazatriquinane skeleton

In the course of the research, 1,3,5-trioxazatriquinane skeleton has been considered to possess the potential to offer a novel inventive chemical library owing to its attractive properties as follows (Figure 6): 1) it can be synthesized in only four steps *via* a trimerization of α-hydroxyaldehydes derived from the corresponding ketones (Scheme 2), 2) six side chains can be arranged three-dimensionally on the rigid bowl-like core scaffold,

3) a maximum of 16 isomers (8 regioisomers with each enantiomer) can be synthesized at once based on the three quaternary chiral carbon centers and the orientation of the central nitrogen atom (convex or concave).

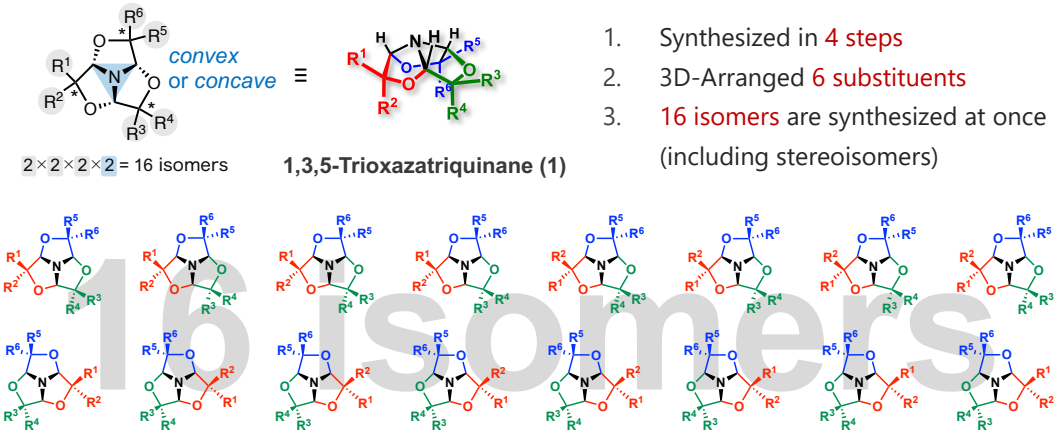

Figure 6. 1,3,5-Trioxazatriquinane skeleton and its unique features

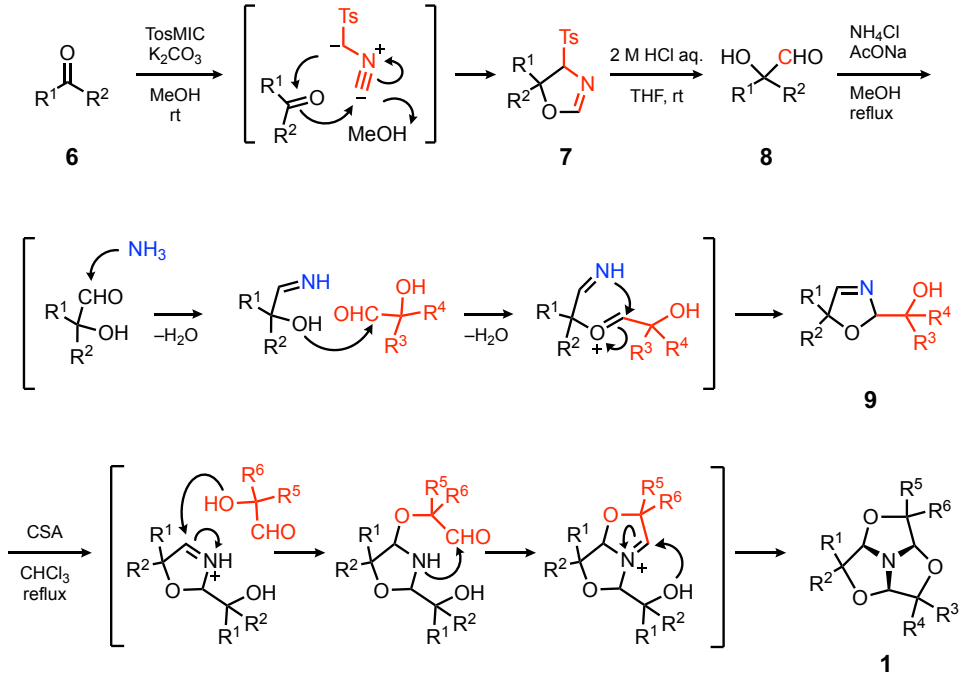

Scheme 2. Synthesis of the 1,3,5-trioxazatriquinane skeleton and its proposed mechanism

Focusing on the above-mentioned attractive characters of the skeleton, Nagase *et al.* synthesized 46 derivatives with 1,3,5-trioxazatriquinane skeleton for the screening of opioid receptor ligands and identified 6 hit compounds in a high hit rate (13%, Figure 7). Especially, SYK-146 showed potent and selective κ opioid receptor (KOR) agonist activity[24,25] (EC_{50} = 6.09 nM for KOR) similar to nalfurafine (**21**), one of the well-known KOR agonists. Despite the simple structure, SYK-146 reproduced multiple pharmacophores of existing

potent KOR agonists U-69,593 and U-50,488H. Intriguingly, all hit compounds in the screening possessed two phenethyl amine units on each side chain, which is one of the common structures in neurotransmitters and central nervous system (CNS) drugs, such as dopamine (**10**) and morphine (**11**). Accordingly, 1,3,5-trioxazatriquinanes has been assumed to be potentially a template scaffold for exploring hit compounds or drugs with the orientations of pharmacophore units on their sidechains. And the authors conceived that 1,3,5-trioxazatriquinanes bearing multiple effective residues (TriMERs) could be an effective conformational restricting scaffold for exploring the shape of a drug, including the orientation of pharmacophore units and applied for ligand screening against GPCRs.[26]

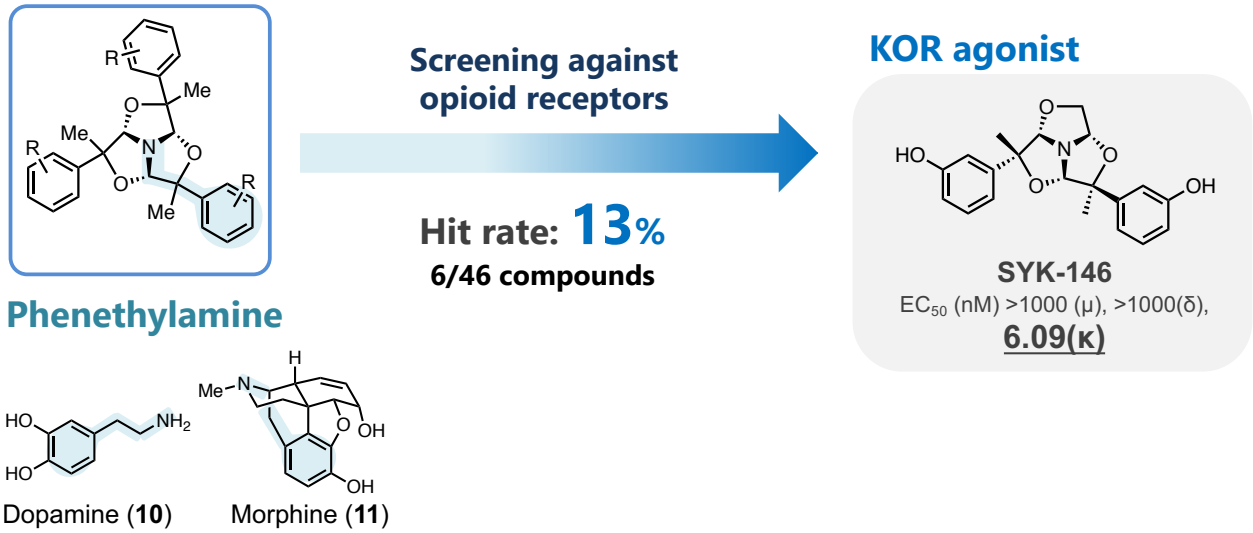

Figure 7. Screening of TriMER library against opioid receptors

1.3 Orexin and orexin receptors

Orexin (orexin-A (OXA) and orexin-B (OXB))[27] is an endogenous neuropeptide mainly localized in neurons within and around the lateral hypothalamus discovered by Yanagisawa, Sakurai *et al*. in 1998. It involves fundamental physiological effects such as feeding behavior,[28,29] sleep-wake cycle,[28,29] reward/addiction,[30,31] and stress responses.[32–34] Orexins were initially considered as neuropeptides that control feeding behavior because orexin-producing neurons are particularly localized in the lateral hypothalamic area, which is deeply involved in feeding, and the intracerebroventricular (i.c.v.) administration of orexins increases the amount of food intake. Afterward, the lack of orexin-producing cells was found to induce an unstable sleep-wake cycle; thus, the role of orexins in the control of the sleep–wake cycle has received immense inerest.[35]

OXA and OXB are derived from a common precursor prepro-orexin and bind to orexin receptors. OXA involves of 33 amino acids with two intramolecular disulfide bonds, while OXB is a linear peptide comprising 28 amino acids. Orexin receptors, consisting of the orexin 1 receptor (OX_1R) and orexin 2 receptor (OX_2R), are G protein-coupled receptors that mainly conjugate with excitatory Gq protein.[36] OX_1R has a high affinity for OXA than OXB, while OX_2R is known to have equal affinity for both receptors.

As mentioned above, orexin-producing neurons are localized in the lateral hypothalamus, but their axonal projections are widely distributed throughout the CNS.[37,38] Electrophysiological experiments revealed that noradrenergic, histaminergic, dopaminergic and serotonergic nerves are activated by orexin.[39–41] Accordingly, orexins are involved in physiological events, such as energy metabolism,[42] autonomic functions,[43,44] emotional memory,[33] reward seeking[30] and stress responses,[32] in addition to controlling feeding behavior and sleep–wake cycles. In this context, OXR ligands are expected to be innovative novel drug candidates in the treatment of sleep disorders, obesity and addiction.[45]

In particular, the activation of orexin receptors has a crucial role in the regulation of wakefulness, making them a key target for the treatment of sleep disorders such as insomnia and hypersomnia and the drug discovery research targeting these receptors has been vigorously investigated.[46–49] Primally, the development of these antagonists as a treatment for insomnia[49] with new mechanisms has preceded, and various OX_1R-selective antagonists (1-SORAs), OX_2R-selective antagonists (2-SORAs) and OX_1R/OX_2R dual antagonists (DORAs) have been developed (Figure 8). More recently, as DORAs, suvorexant (**14**, Belsomra®)[50] was approved in 2014, followed by lemborexant (**15**, Dayvigo®)[51] in 2019, and daridorexant (**16**, Quviviq®)[52] in 2022. Additionally, 1-SORA has been attracted interest for the treatment of drug addiction or anxiety.

Pharmacological studies involving a series of OXR antagonists that showed that OX_1R is involved in emotion, reward systems and autonomic regulation.[37,53]

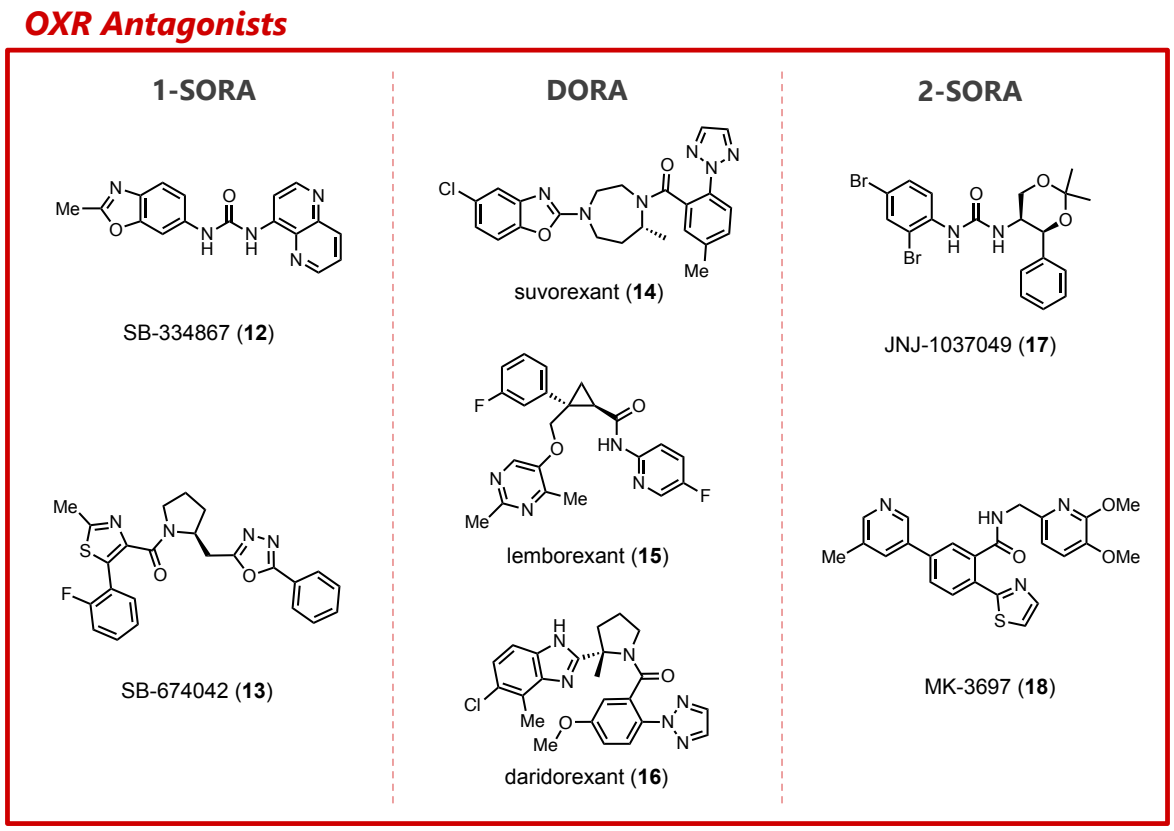

Figure 8. The example of OXR antagonists

By contrast, OXR agonists have been expected as a potential treatment of hypersomnia, especially narcolepsy, a chronic sleep disorder characterized by excessive daytime sleepiness and disruptions in the normal sleep-wake cycle.[54,55] The most common symptoms of narcolepsy is excessive daytime sleepiness, sleep attacks, cataplexy, hypnagogic hallucinations, and sleep paralysis. The prevalence of narcolepsy is estimated to be around 1 in 2,000 people in the US and 1 in 600 people in Japan. Narcolepsy is a lifelong condition, and although there is no fundamental therapeutic yet, its symptoms are currently managed through a combination of lifestyle modifications and drug treatment using CNS stimulants such as modafinil and methylphenidate, tricyclic antidepressants, and sodium oxybate, although they often have severe effects. Therefore, novel chemotherapeutic agents based on new mechanisms are desired against narcolepsy.

Previous genetic studies have revealed that narcolepsy-like sleep abnormalities such as cataplexy and sleep fragmentation were caused by a deficient of prepro-orexin and OXR in rodents[35,56] and canines.[57] Moreover, 90% of human narcolepsy type I (narcolepsy with cataplexy) patients had reduced levels of orexin in the

brain.[58–61] Importantly, OX_2R-knockout mice showed a typical narcoleptic phenotype, while OX_1R-knockout mice exhibited no apparent sleep/wakefulness-related phenotype. Therefore, the OX_2R agonist has been expected as a potential chemotherapeutic agent for narcolepsy.[56] Although orexin administration in the brain effectively ameliorates the symptoms of narcolepsy, orexin is a peptide, which is easily hydrolyzed by oral administration and does not easily penetrate the BBB, making its direct clinical use difficult. Accordingly, OX_2R agonists with small molecules have been required for a long time.

In 2015, the first nonpeptidic OX_2R agonist YNT-185 (**19**, EC_{50} = 2,750 nM for OX_1R, EC_{50} = 28 nM for OX_2R)[62] was discovered by Nagase *et al.* (Figure 9). It was also effective *in vivo* and ameliorated narcoleptic symptoms in prepro-orexin-knockout mice.[63] Since this report, several small-molecule OX_2R agonists with various scaffolds have been reported.[64–69] In particular, TAK-925 (**20**, EC_{50} = 5.5 nM for OX_2R, OX_1R/OX_2R > 5,000),[70] has recently entered phase I clinical trials for the treatment of narcolepsy and hypersomnia. Recently, approximately ten ligands have been reported that possessed the scaffold such as diarylsulfonamides,[62,64–67,71,72] piperidines,[70] pyrrolidines,[73] azulenes,[74,75] and trialkylureas[69]. However, no ligand was approved for clinical use, and further investigation based on the novel scaffolds remains important. Therefore, both OXR antagonists and agonists have been fascinated as a target of drug discovery and the novel ligands have been desired.[76]

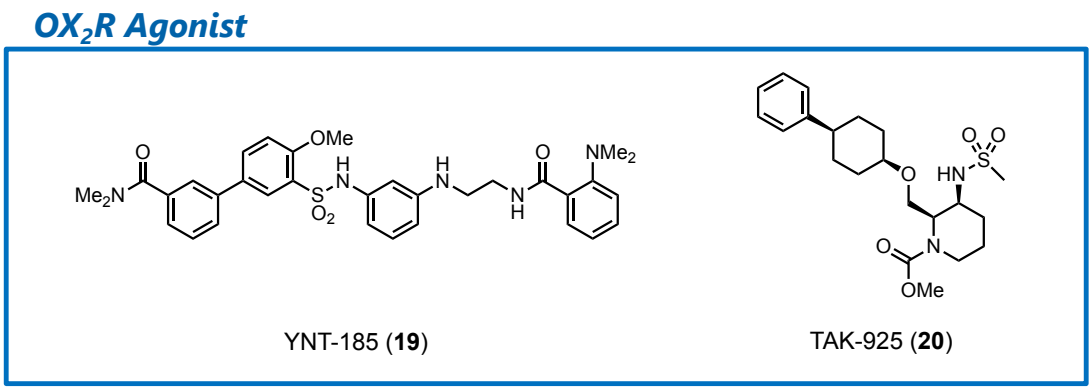

Figure 9. The example of OXR agonists

In 2017, Nagase *et al.* conducted the screening of morphinan chemical library against orexin receptors inspired by the report that the coexistence of dynorphin, an endogenous KOR agonist, and orexin in the same vesicle in the orexin neuron[77] was revealed and discovered that KOR agonist nalfurafine (**21**) shows moderate antagonistic effects on orexin 1 receptors (K_i = 250 nM for OX_1R, Figure 10).[78] After the optimization of the side chain on nalfurafine, the potent selective OX_1R antagonist YNT-1310 (**22**, K_i = 1.36 nM for OX_1R), which had no affinity against KOR. Focusing on the fact that opioid receptors and orexin receptors share ligand scaffolds such as morphinan skeleton, the author conceived that the 1,3,5-trioxazatriquinane skeleton that showed affinity against opioid receptors can be expected to show affinity against orexin receptors.

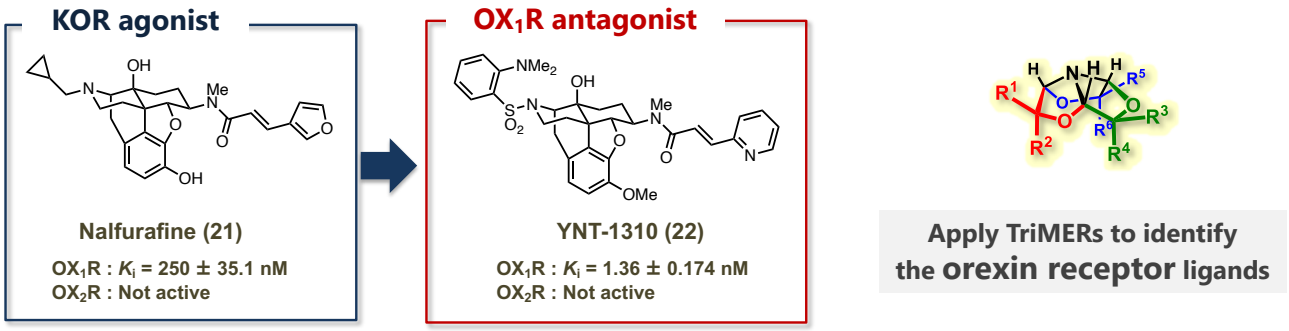

Figure 10. Transformation of the KOR agonist into the OXR antagonist

In this dissertation, in order to discover novel ligands for orexin receptors, which have attracted attention as drug targets for sleep disorders, the author conducted medicinal chemistry research based on the screening approach using 1,3,5-trioxazatriquinanes bearing multiple effective residues (TriMERs).

In Chapter 2, the author conducted the design, synthesis, and evaluation of a novel TriMER library and successfully identified novel TriMER-type OXR antagonists in a high hit rate. Subsequently, the structural optimization of hit compounds led to obtain potent 1-SORA and DORA with a 1,3,5-trioxazatriquinane skeleton, which shows in vivo activity in mice. After the determination of their eutomers, the docking simulations with the model of orexin receptors suggested that these antagonists take a similar U-shape structure and the 1,3,5-trioxazatriquinane core structure interacts with the hydrophobic subpocket in orexin receptors.

In Chapter 3, since none of TriMER derivatives showed agonist activity against orexin receptors in the screening in Chapter 2, the conversion of TriMER-type OXR antagonists into agonists was investigated based on their structure. Incorporating the accessory site theory into the molecular design, a new slim TriMER template by removing sites that interfere with the agonistic activity from TriMER-type antagonists were designed, and a series of derivatives with various substituents were synthesized and evaluated the activity

against orexin receptors. As a result of assay, TriMER derivatives with Boc and octane sulfonamide groups showed full agonist activity against OX_2R. To determine the absolute stereochemistry of these hit compounds, the first asymmetric synthesis of a 1,3,5-trioxazatriquinane skeleton using a Katsuki–Sharpless asymmetric epoxidation as the key reaction was conducted and successfully obtained a set of the individual stereoisomers. After evaluating their activity, derivatives with an (*R*)-1,3,5-trioxazatriquinane core were determined as eutomers for OX_2R agonist activity.

These results indicate that the library approach utilizing the TriMERs might be useful for the hit discovery process targeting not only opioid and orexin receptors, but other G-protein coupled receptors.

Chapter 2 Discovery of orexin receptor antagonists with 1,3,5-trioxazatriquinane skeleton

2.1 Design of TriMER library toward identification of novel OXR ligands

As mentioned in Chapter 1, since opioid receptors and orexin receptors share ligand scaffolds such as morphinan skeleton, the author conceived that the 1,3,5-trioxazatriquinane skeleton, which bound to opioid receptors, also show the affinity against other drug targets such as orexin receptors. Therefore, to evaluate the diversity level of TriMER skeleton as a library template, a computational analysis based on the normalized principal moment-of-inertia (PMI) ratios (described in Section **1.1**)[9] of the simple TriMERs with two aromatic rings and one methylene-oxy bridge, which showed good results in the previous reports targeting opioid receptors, were conducted. The PMI analysis of such TriMERs illustrated that the molecular shapes of each isomer are distributed within a three-dimensionality area corresponding to the binding pocket of the protein[12] (Figure 11). In other words, 1,3,5-trioxazatriquinane can be used to introduce various of pharmacophores to expand the diversity of the aromatic rings on their rigid scaffold which can superimpose with the protein pocket shape. To validate the utility of TriMER in the hit discovery research, the author designed and synthesized a novel-focused library and screened them against orexin receptors.

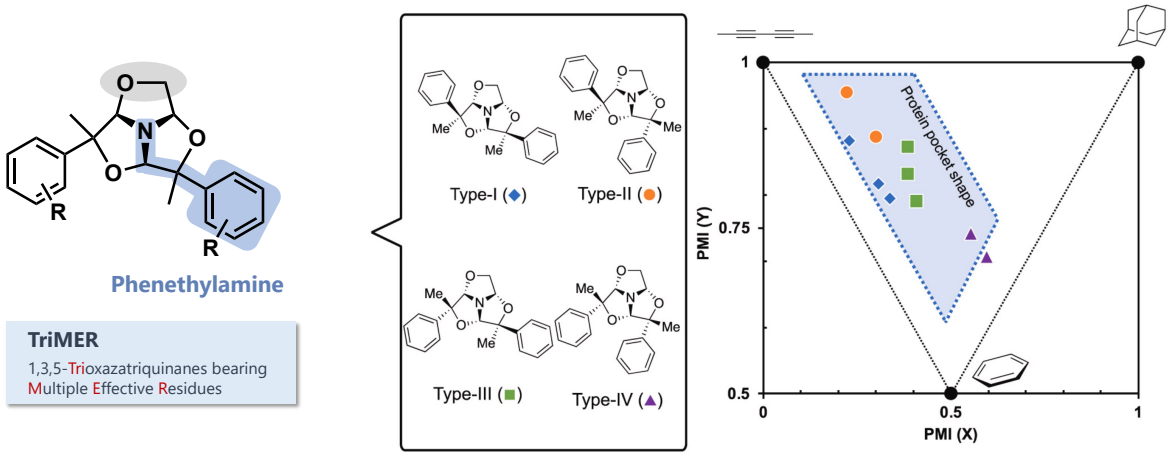

Figure 11. Geometrical diversity of TriMERs with two phenyl residues: Population analysis of TriMER derivative illustrating the geometrical diversity of Type-I (blue), Type-II (orange), Type-III (green), and Type-IV (purple) compounds bearing two phenyl residues. The populations are superimposed over the diversity area of the protein pocket shape reported by Wirth et al.[12] highlighted in light blue. The stable structures for each molecule within 7 kcal/mol were calculated using the Conformational Search function in MOE software package ver. 2019.0102 (Chemical Computing Group, Inc., Montreal, Canada) with LowModeMD method, MMFF94x force field, dielectric constant of 80, and no non-bonded interaction cutoff, and the principal moment of inertia (PMI) was calculated.

First, 72 novel TriMERs with two phenethylamines were designed with a combination of three components according to our previous report[26] (Figure 12): three regioisomers on the aromatic rings (*o*-, *m*-, and *p*-), four stereoisomers derived from the TriMER scaffold (type I–IV), and six substituents on phenyl rings (NO_2, NH_2, NMe_2, NHBoc, NHBz, and $NHSO_2Ph$).

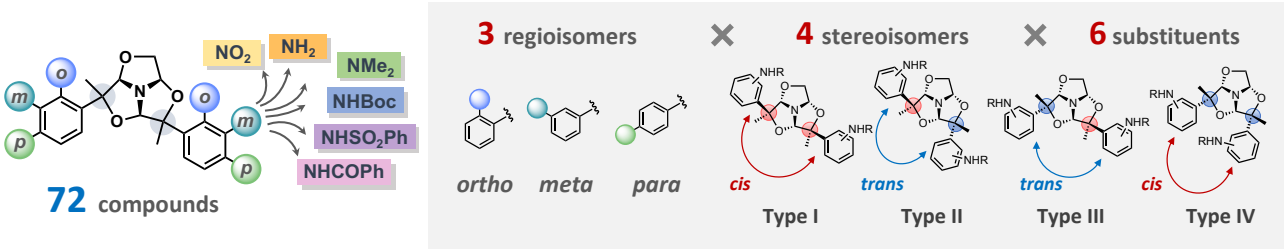

Figure 12. Design of the novel TriMER library

2.2 Synthesis of the novel OXR antagonist with 1,3,5-trioxazatriquinane skeleton

Each TriMER was synthesized from the corresponding nitroacetophenones **23–25** (Scheme 3). *m*- or *p*-Nitroacetophenone was converted to α-hydroxyaldehyde by hydrolysis with HCl aq. following the introduction of carbon using TosMIC (tosylmethyl isocyanide). Similarly, this synthetic method was attempted with *o*-nitroacetophenone, but the starting material **25** was recovered on the ortho position because of steric hindrance on the ortho position. Notably, constructing α-hydroxyaldehyde with TosMIC was difficult using bulky ketones possessing phthalimide, dibenzyl amino group, and other *o*-substitute acetophenones (OMe, Cl, and F). Thus, α-hydroxyaldehyde was obtained from α-hydroxyaldehyde from *o*-nitroacetophenone using different methods; Wittig reaction utilizing (methoxymethyl) triphenylphosphonium chloride to introduce the methylene group, epoxidation with *m*CPBA, and the cleavage of the epoxide with HCl aq. Next, each α-hydroxyaldehyde was reacted with ammonium chloride and sodium acetate, and the corresponding oxazoline dimers **29–31** were obtained. Then, the glycolaldehyde dimer was added in the presence of camphorsulfonic acid in order to construct the 1,3,5-trioxazatriquinane core, which provided four regioisomers; two *cis*-TriMER (type-I and IV) and two *trans*-TriMER (type-II and III). These regioisomers were separated by crystallization, silica gel chromatography and recycling GPC (gel permeation chromatography).

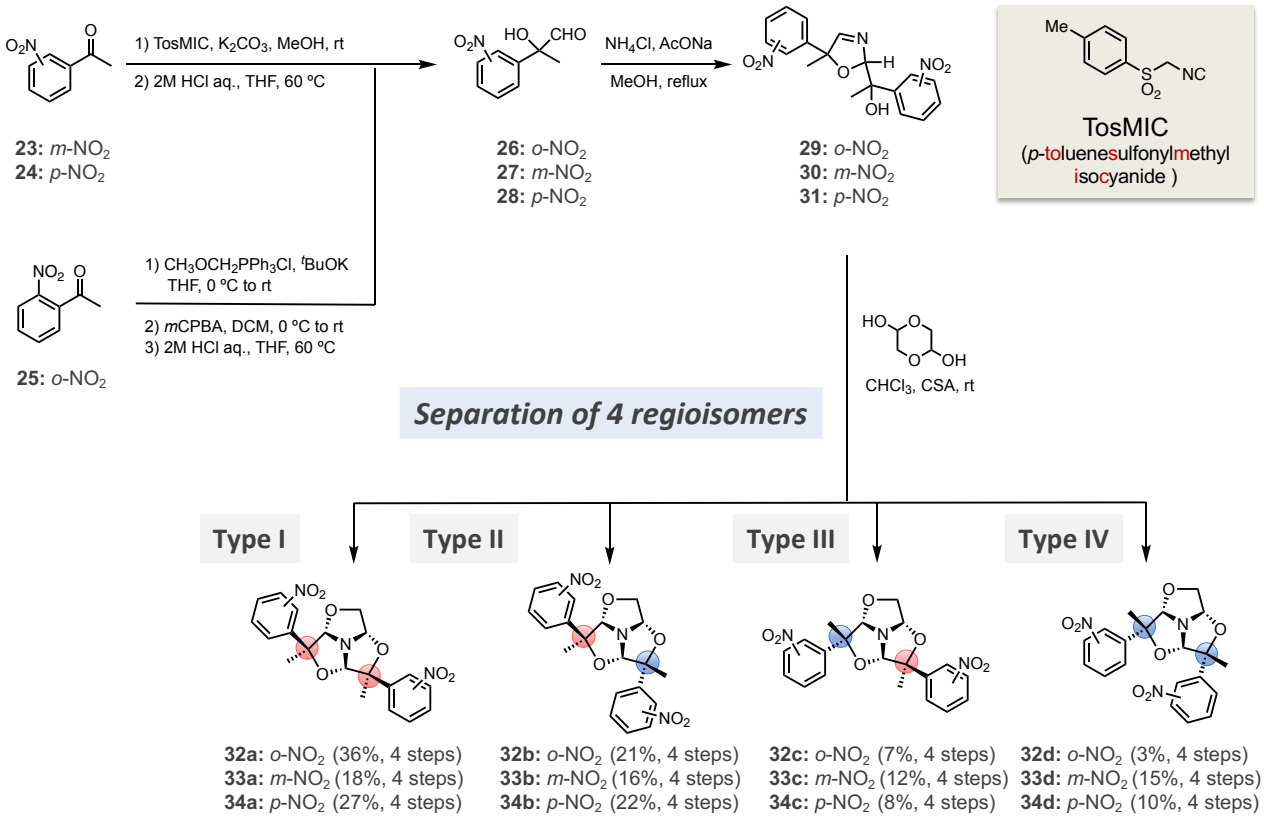

Scheme 3. Synthesis of the novel TriMER library with nitro groups

The configurations of the core and side chains of the four stereoisomers were determined using 2D-NMR experiments. Stereochemistry was determined by the observed NOE relationships correlating the proton of the aromatic ring and the methyl group with the methine proton, which showed a characteristic at 5 ppm with two singlets and one doublet (Figure 13, details of the NOESY spectrum are provided in ethe experimental section).

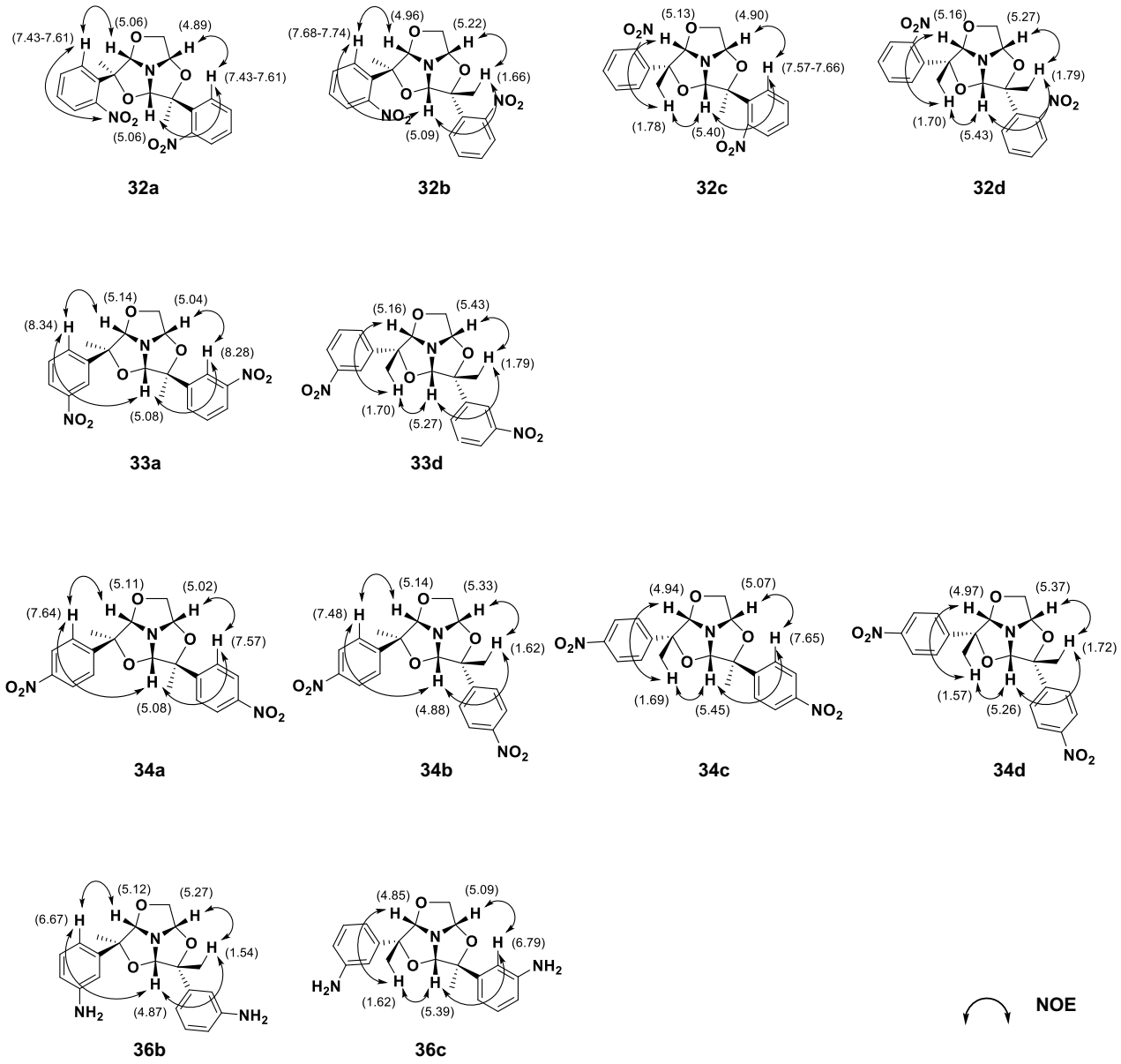

Figure 13. Determination of the stereochemical configurations of TriMERs by NOE-correlation

The nitro groups on phenyl groups were reduced by hydrogenation to corresponding anilines **35a**–**37d** (Scheme 4), and they were derivatized by demethylation and condensation to construct library compounds with NHBoc (**38a**–**40d**), NMe_2 (**41a**–**43d**), $NHSO_2Ph$ (**44a**–**46d**), and NHBz (**47a**–**49d**).

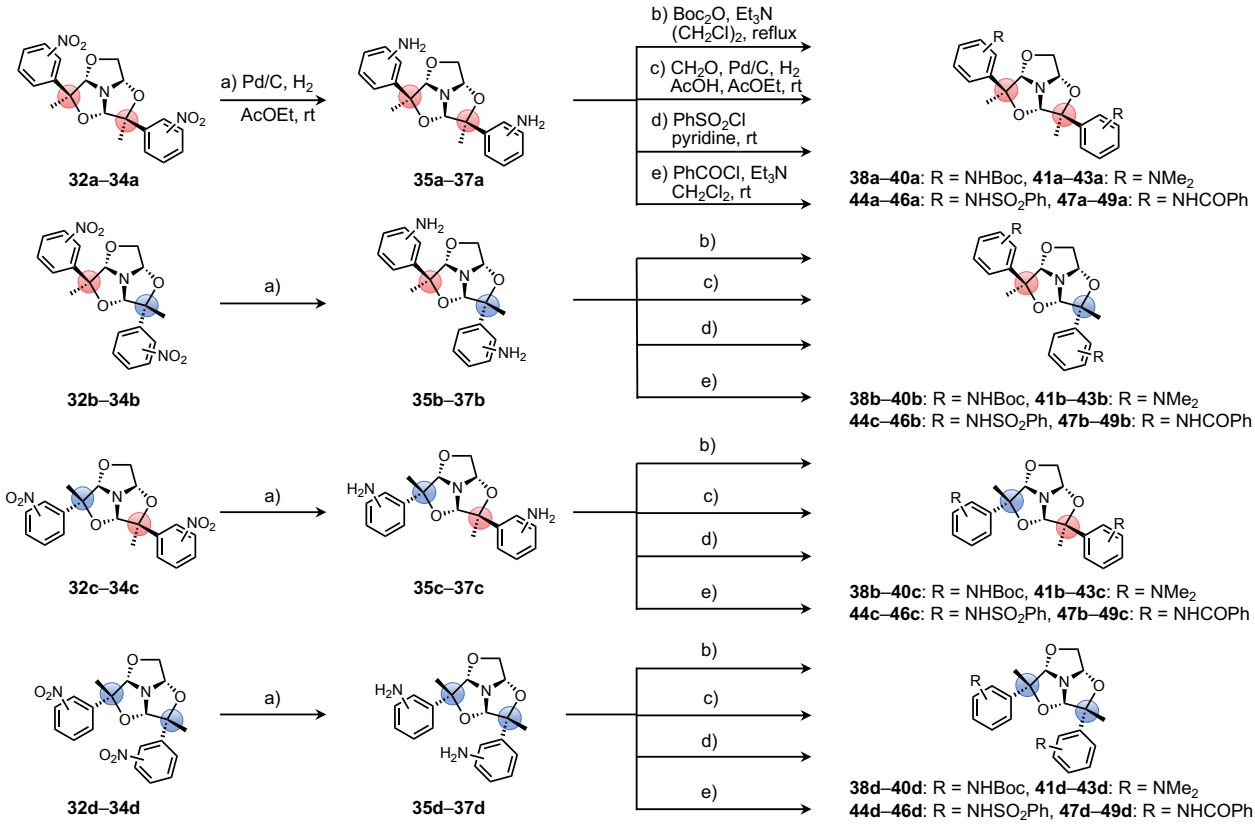

Scheme 4. Synthesis of the novel TriMER derivatives

2.3 Biological evaluation of synthetic TriMER derivatives and optimization of substituents

Using a focused library with 72 TriMERs, cell-based calcium assays were conducted to evaluate the OXR agonist/antagonistic activities in a Chinese hamster ovary (CHO) cell line stably expressing human OX_1R ($CHOOX_1R$) or OX_2R ($CHOOX_2R$). The agonistic activity was measured based on the increase in intracellular Ca^{2+} concentration after the application of test compounds or endogenous OXR ligand OXA as a control and evaluated the activation rate was evaluated using the test compounds (Figure 14). The antagonistic activity was also measured based on the increase in the intracellular Ca^{2+} concentration, and the inhibition rate was evaluated by the test compounds.

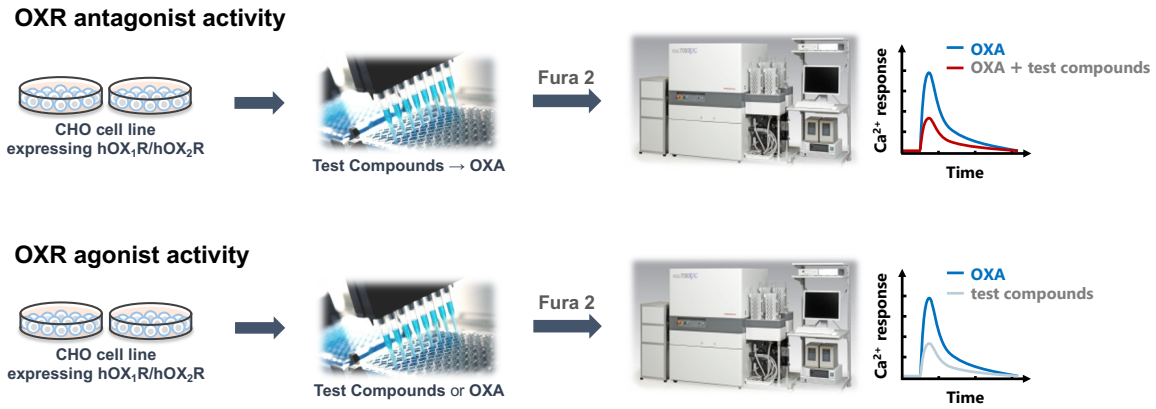

Figure 14. The method of *in vitro* assay to evaluate the OXR agonist/antagonist activities

As a result of screening of 72 compounds, five hit compounds were obtained which showed < 50% inhibitory activity against orexin A-induced OXR activation in the 1.0 μM hit range, although none of the tested TriMERs exhibited significant agonistic activity, even at 10 μM (Figure 15).

In the heat map shown in Figure 15, the compounds with higher activities are shown in darker blue. The results showed that hit compounds were biased toward *m*-derivatives, compared to different substitution positions on the aromatic ring (*o*- and *p*-). Furthermore, focused on the stereochemistry of the core skeleton, type-I and type-IV derivatives with *cis*-configuration have more potent affinities to both OX_1R and OX_2R. Specifically, potent OXR antagonist activity was observed for the four compounds denoted by the red frame.

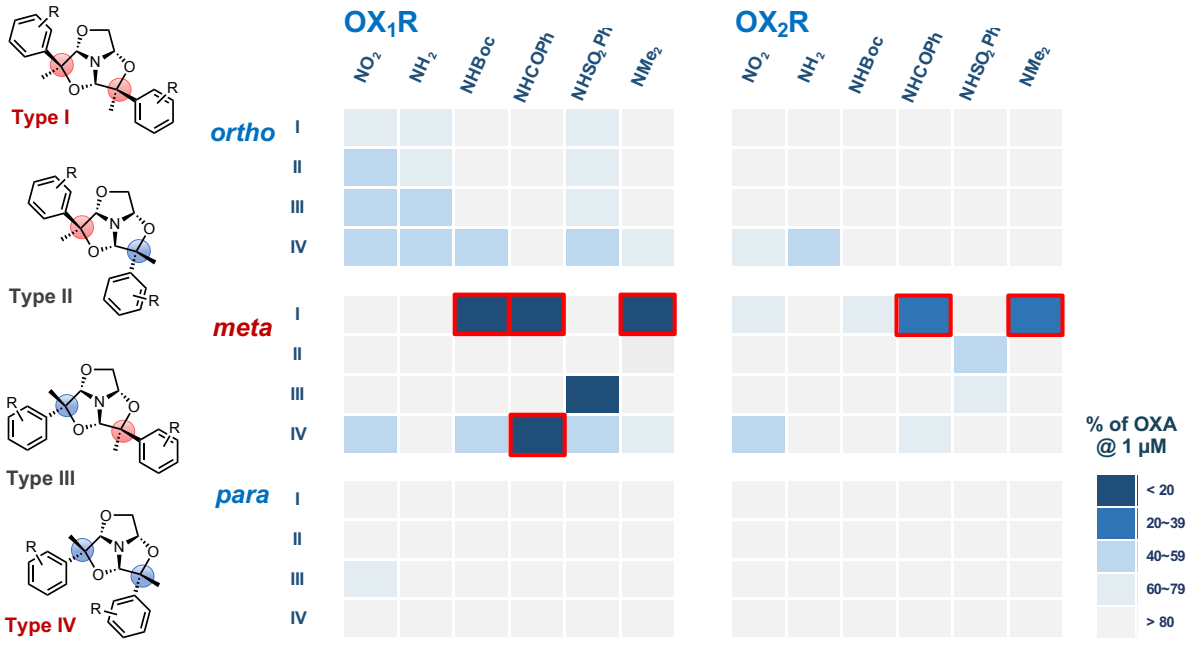

Figure 15. Heat map of the 72 tested compounds against OX_1R/OX_2R

Five hit compounds are summarized in Table 1 with K_i. They had in common a type-I or IV (*cis*-oriented side chain), a *m*-configuration with the anilines and a bulky substituent at the terminal of the side chains, except for **45c** (*m*-*N*-SO_2Ph; K_i = 222 nM for OX_2R) with a type-III core. Type-I derivatives exhibited the highest hit-rate and potent dual $OX_{1/2}R$ antagonistic activity, especially with *m*-*N*-Boc (**39a**; K_i = 34.2 nM for OX_1R, K_i = 180 nM for OX_2R) and *m*-*N*-Bz (**48a**; K_i = 23.4 nM for OX_1R, K_i = 15.1 nM for OX_2R). Type-IV derivatives, with *m*-*N*-Bz exhibited potent selective OX_1R antagonistic activity (**48d**; K_i = 25.4 nM for OX_1R). Notably, YNT-2206 (**48a**) and YNT-2209 (**48d**), which possess the same *m*-*N*-Bz substituents and core unit with *cis* configuration, exhibited a different receptor selectivity with only a difference in core stereochemistry. They had a similar OX_1R antagonist activity but different OX_2R antagonist activity. This structure-activity relationship information suggested that the *cis* configuration of side residues on the bowl-like skeleton plays an important role in the suitable orientation of the terminal lipophilic substituent upon receptor binding.

To further improve the antagonistic activity of dual $OX_{1/2}R$ antagonist (DORA) YNT-2206 (**48a**) and selective OX_1R antagonist (1-SORA) YNT-2209 (**48d**), the structure optimization of the aromatic rings was conducted. Derivatives with several arylamides (**50a**–**58d**) were synthesized by the condensation reaction with the corresponding carboxylic acid against aniline intermediates **36a** and **36d**. As a result, the introduction of MeO group at the terminal of aromatic rings increased the affinity, and 4-MeO derivatives YNT-2293 (**52a**: K_i = 3.99 nM for OX_1R, K_i = 6.01 nM for OX_2R) and YNT-2294 (**52d**: K_i = 1.87 nM for OX_1R) were the most

effective (Table 2). The receptor selectivity of DORA YNT-2206 (**48a**) and 1-SORA YNT-2209 (**48d**) were maintained in 4-MeO derivative DORA YNT-2293 (**52a**) and 1-SORA YNT-2294 (**52d**). These substituent effects were also observed in NMe_2 derivatives with type-IV skeleton, and **55d** carrying 4-NMe_2 groups revealed 1-SORA (K_i = 3.88 nM). The 2-pyridine carboxamide derivatives **56a** (K_i = 14.9 nM for OX_1R, K_i = 69.6 nM for OX_2R) and **56d** (K_i = 18.3 nM for OX_1R) showed higher affinity for the corresponding receptors than the 3- and 4-pyridine carboxamide derivatives (**57a**, **58a**, **57d**, and **58d**).

Table 1. Assay results of the TriMER derivatives for OXR antagonism

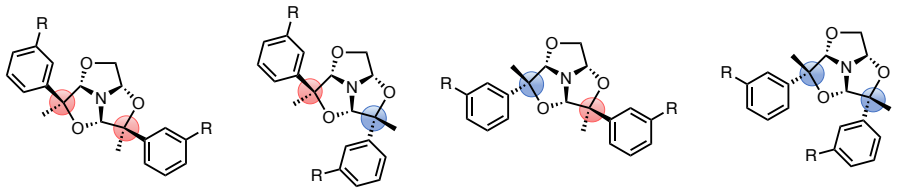

Compounds	Core type	R	K_i (nM) [a]	
			OX_1R	OX_2R
39a	I	NHBoc	34.2 ± 8.93	180 ± 43.1
42a	I	NMe_2	– [b]	655 ± 184
45c	III	$NHSO_2Ph$	– [b]	222 ± 70.2
YNT-2206 (**48a**)	I	NHBz	23.4 ± 0.95	15.1 ± 2.19
YNT-2209 (**48d**)	IV	NHBz	25.4 ± 3.70	– [b]

[a] K_i values represent the mean ± SEM. These values were calculated using IC_{50} values of TriMER derivatives and at least three independent calcium assays performed in triplicate (Cheng–Prusoff equation). [b] K_i value was not calculated. IC_{50} value was over 10 μM (cutoff value) or was not obtain from concentration–response curve.

Table 2. Assay results of the TriMER derivatives for OXR antagonism

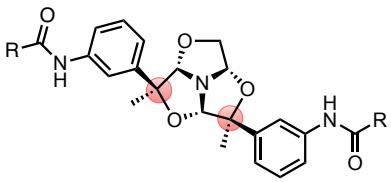

Type-I

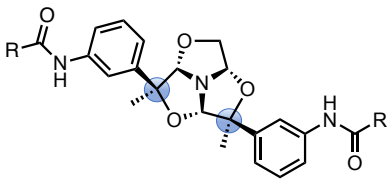

Type-IV

Compounds	Core type	R	K_i (nM) [a]	
			OX_1R	OX_2R
YNT-2206 (**48a**)	I	Ph	23.4 ± 0.95	15.1 ± 2.19
YNT-2209 (**48d**)	IV	Ph	25.4 ± 3.70	– [b]
50a	I	2-MeO-C_6H_4	18.0 ± 3.45	56.0 ± 17.5
51a	I	3-MeO-C_6H_4	7.66 ± 1.50	5.38 ± 0.83
YNT-2293 (**52a**)	I	4-MeO-C_6H_4	3.99 ± 0.47	6.01 ± 1.52
50d	IV	2-MeO-C_6H_4	32.8 ± 1.43	722 ± 40.3
51d	IV	3-MeO-C_6H_4	2.86 ± 0.27	– [b]
YNT-2294 (**52d**)	IV	4-MeO-C_6H_4	1.87 ± 0.30	– [b]
53a	I	2-Me_2N-C_6H_4	– [b]	– [b]
54a	I	3-Me_2N-C_6H_4	– [b]	– [b]
55a	I	4-Me_2N-C_6H_4	– [b]	– [b]
53d	IV	2-Me_2N-C_6H_4	634 ± 158	– [b]
54d	IV	3-Me_2N-C_6H_4	7.85 ± 1.89	– [b]
55d	IV	4-Me_2N-C_6H_4	3.88 ± 0.98	– [b]
56a	I	2-pyridine	14.9 ± 3.97	69.6 ± 15.2
57a	I	3-pyridine	691 ± 179	261 ± 58.0
58a	I	4-pyridine	– [b]	179 ± 35.7
56d	IV	2-pyridine	18.3 ± 2.71	– [b]
57d	IV	3-pyridine	52.0 ± 17.2	– [b]
58d	IV	4-pyridine	104 ± 39.2	– [b]

[a] K_i values represent the mean ± SEM. These values were calculated using IC_{50} values of benzamide derivatives and at least three independent calcium assays performed in triplicate (Cheng–Prusoff equation). [b] K_i value was not calculated. IC_{50} value was over 10 μM (cutoff value) or was not obtain from concentration–response curve.

Besides, in order to evaluate the receptor selectivity against opioid receptors (μ, δ, and κ) with DORA YNT-2293 (**52a**) and 1-SORA YNT-2294 (**52d**), the opioid receptor binding assay was conducted (Figure 16). It was found that neither ligand bound to opioid receptors because the IC_{50} values were over 10 μM, or no concentration response curve was obtained, suggesting that 1,3,5-trioxazatriquinane in this screening is a selective scaffold for orexin receptors.

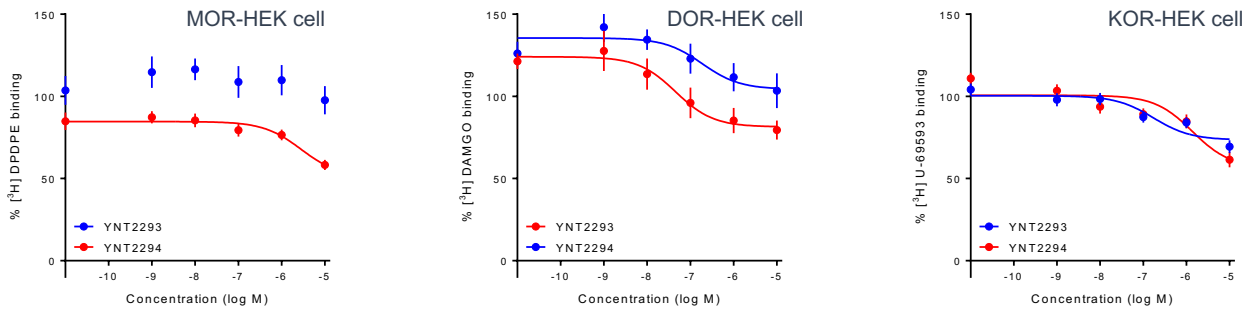

Figure 16. Binding assay against opioid receptors (μ (MOR), δ (DOR), and κ (KOR)): Binding affinity for μ, δ, or κ opioid receptors in test compounds was measured by displacement of [^{3}H]-DAMGO, [^{3}H]-DPDPE, or [^{3}H]-U69,593, respectively. Radioactivity in the test samples was determined by a MicroBeta scintillation counter. Sigmoidal concentration–response curve and K_i value were calculated by Prism software (version 6.05).

2.4 Pharmacokinetics and *in vivo* assay of YNT-2293 and YNT-2294

As for ligands with good properties YNT-2293 (**52a**) and YNT-2294 (**52d**), additional assays on metabolic stability and pharmacokinetics (DMPK) were evaluated. First, Caco-2 permeability[79] of each compound was evaluated in both directions (apical to basolateral (A-B) and basolateral to apical (B-A)) at plasma pH (pH 7.4). YNT-2294 (**52d**) exhibited moderate permeability (P_{app} = 11.9 × 10^{-6} cm/s (A-B) and efflux ratio 1.8) (Table 3). To investigate the involvement of the P-glycoprotein (P-gp) transporter involved in pharmaceutical efflux, which is expressed on apical cell surfaces, those inhibitors were added, such as verapamil, a P-gp/ABC family B1 (ABCB1) inhibitor, and breast cancer resistance protein (BCRP) were added. Pg-p substrate identification is an important factor in assessing brain transit because Pg-p is known to be expressed in the blood-brain barrier (BBB) and to interferes with the brain transit of drugs. As a result, the permeability of YNT-2294 (**52d**) was slightly increased when the inhibitors of these transporters were added, although the efflux ratio (B-A/A-B) was lower than that without these inhibitors. Interestingly, YNT-2293 (**52a**) could not measure the permeability due to the low recovery, although it possessed a similar structure to YNT-2294 (**52d**). In the presence of 1% bovine cerium albumin (BSA), the system significantly improved the recovery of YNT-2294 (**52d**), suggesting that YNT-2294 (**52d**) was not recovered because of specific adsorption on the trans-well plate. After that, YNT-2294 (**52d**) showed moderate permeability (P_{app} = 1.4 × 10^{-6} cm/s (A-B) and efflux ratio 0.2). Next, the metabolic stability of YNT-2293 (**52a**) and YNT-2294 (**52d**) was evaluated *in vitro* with human liver microsomes (HLMs).[80] Both compounds exhibited similar clearance in HLMs; CL_{int} was approximately 183 μL/min/mg, and the estimated half-life was approximately 40 min. These results suggested that these derivatives had moderate permeability with no significant efflux activity and fast clearance. The permeability of YNT-2294 (**52d**) was reasonable as a CNS drug lead compound (P_{app} > 10, Pg-p efflux < 2.5),[81] but further development would be worthful, (e.g., improvement of clearance).

Table 3. Results of membrane permeability and metabolic stability of YNT-2293 (**52a**) and YNT-2294 (**52d**)

compd	Membrane permeability[a] $P_{app, A-B}$, $\times 10^{-6}$ cm s^{-1} [B-A/A-B]				Metabolic stability (HLM)[e] CL_{int} (μL min^{-1} mg^{-1}) [Half life]
	Caco-2	+ BSA[b]	+ verapamil[c]	+ KO143[d]	
52a	–[e]	1.4 [0.2]	–[e]	–[e]	183.5 [38 min]
52d	11.9 [1.8]	N.T.	19.4 [1.1]	16.6 [1.6]	182.7 [39 min]

[a]Bidirectional Caco-2 permeability with pH 7.4/7.4 for donor/receiver chambers, respectively. A = apical, l basolateral. P_{app} is the apparent permeability coefficient (10^{-6} cm/s). For ABC transporter substrate assessm the assays are run with [b]1% BSA or [c]100 μM verapamil or [d]10 μM KO143 on both the A and B sides. [e]Detect was lower than the limit of quantitation in receiver sample due to low recovery. [e]Compounds were treated in mg/mL human liver microsomes (HLMs) at 37 °C. N.T., not tested.

Next, the brain permeability of YNT-2293 (**52a**) and YNT-2294 (**52d**) in mice was evaluated based on the results of *in vitro* permeability and stability (Figure 17). The concentrations of the test compounds in the brain were quantified using LC-MS/MS system at 0.5, 1, and 3 h, after 3 or 10 mg/kg intraperitoneal administration. Both compounds exhibited a good concentration in the brain with the administration of 10 mg/kg compounds and the high brain concentration was maintained for more than 1 h. After 0.5 h injecting them, the value of concentration was 54.7 and 33.9 pmol/g brain, respectively, with over those K_i values. In the case of 3 mg/kg injection, the highest concentrations of them in the brain were a little higher than their K_i values. Considering the above facts, YNT-2293 (**52a**) and YNT-2294 (**52d**) were able to penetrate the BBB and have suitable properties to further conduct *in vivo* evaluation.

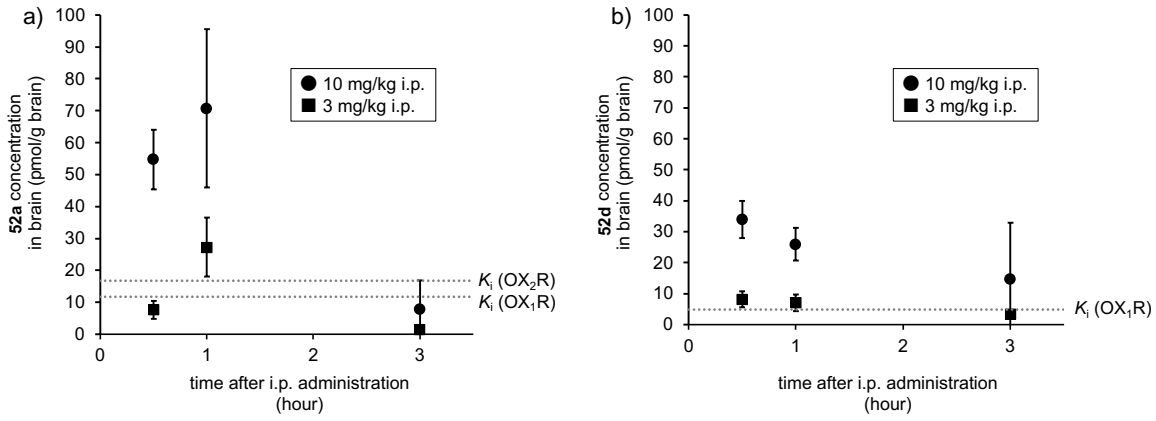

Figure 17. Binding assay against opioid receptors (μ (MOR), δ (DOR), or κ (KOR)): The concentrations of **52a** (a) and **52d** (b) in brain at 0.5, 1 and 3 hours after 10 mg/kg and 3 mg/kg i.p. administration in C57BL/6J mice. Each value represents the mean ± S.D. (four or three mice for each point). Closed circle, 10 mg/kg; Closed square, 3 mg/kg. The data of **52d** at 3 hours were obtained from two mice and the brain concentrations of other mice were under the limit of quantification.

Finally, as YNT-2293 (**52a**) and YNT-2294 (**52d**) showed a reasonable brain permeability and metabolic stability, the *in vivo* effects of these antagonists were evaluated. Since $OX_{1/2}R$ dual antagonism induces an increase in the sleep state, electroencephalogram (EEG)/electromyography (EMG) in wild-type mice was utilized to measure the effect on the sleep–wake state with DORA YNT-2293 (**52a**) (Figure 18). In this experiment 10 mg/kg of YNT-2293 (**52a**) or the vehicle was injected into wild-type mice intraperitoneally. Compared to the vehicle administration, YNT-2293 (**52a**) significantly decreased the total time of wakefulness and increased the total time of NREM sleep during zeitgeber time (ZT) 12–18.

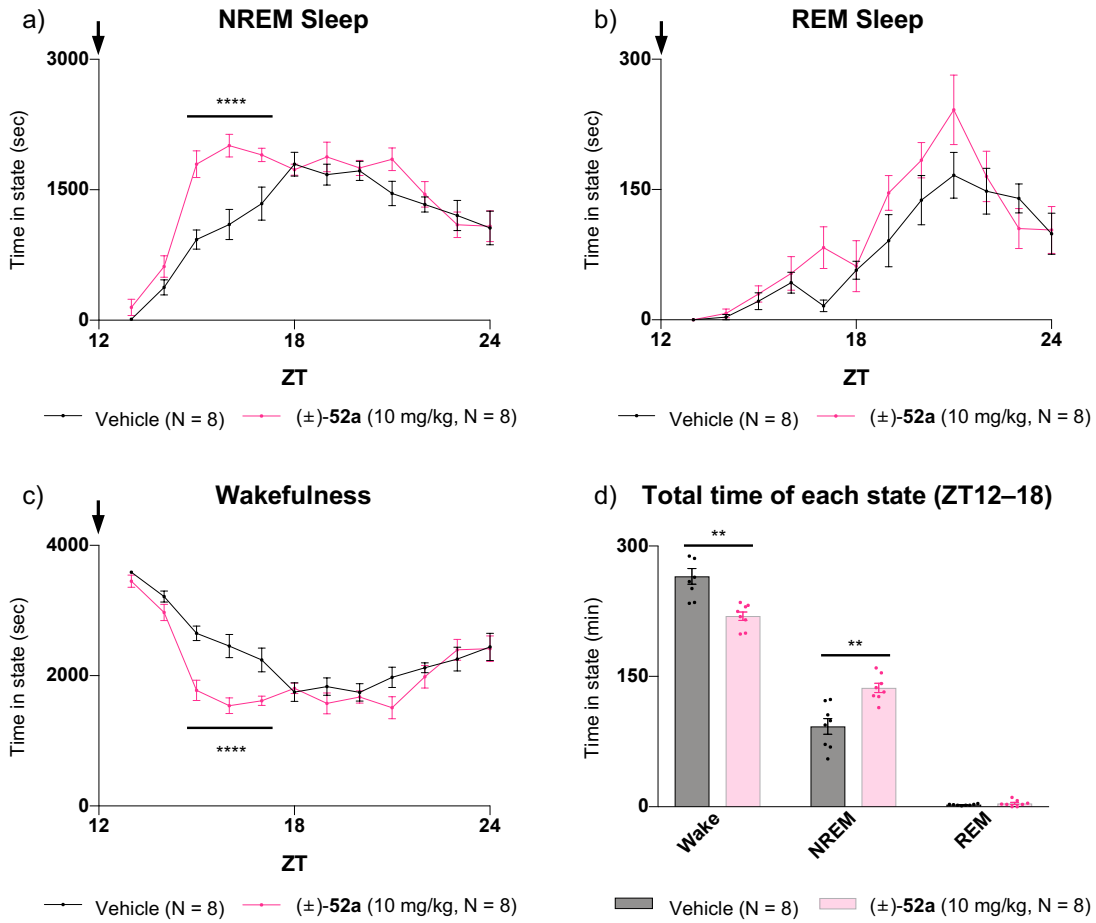

Figure 18. Effect of DORA YNT-2293 (**52a**) on sleep/wake state in mice. (a) Hourly plots of total time in NREM sleep, (b) REM sleep, and (c) wakefulness. Data are presented as the mean ± SEM of 8 mice. ****P < 0.0001 for vehicle vs. **52a** by two-way ANOVA. Each arrow indicates an injection. (d) Time spent in NREM sleep, REM sleep, and wakefulness during ZT12–18 after vehicle or **52a** administration. Data are presented as the mean ± SEM of 8 mice. **P < 0.01 for vehicle vs. **52a** by two-tailed Student's *t*-test.

Further, it is well-known the selective inhibition of OX_1R suppresses motivated behaviors,[82] and intracerebroventricular (i.c.v.) administration of orexin A causes an OX_1R activation following a substantial increase of locomotor activity in wild-type mice. Accordingly, 1-SORA YNT-2294 (**52d**) was evaluated for the suppression of locomotor activity in mice which is caused by the activation of OX_1R with OXA (Figure 19). When the locomotor activity of mice not treated with the compound was set at 100%, the values for the case with only OXA treatment increased approximately threefold, whereas intraperitoneal treatment with the YNT-2294 (**52d**) suppressed this effect in a dose-dependent manner.

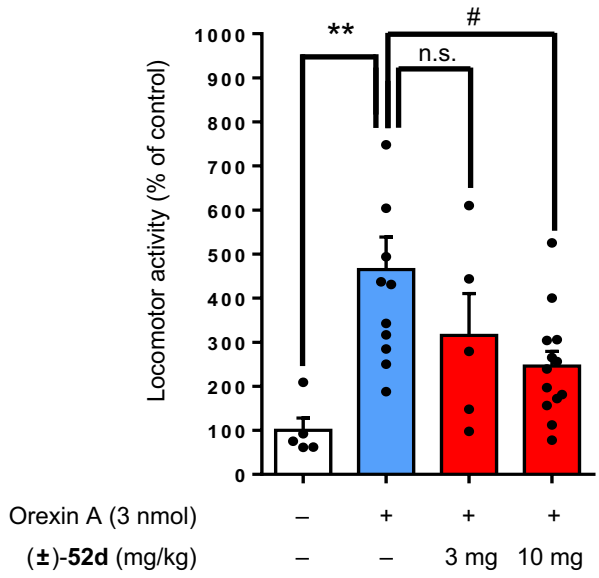

Figure 19. Effect of 1-SORA YNT-2294 (**52d**) on motivated behavior in mice. Orexin A-induced locomotor activity was suppressed by intraperitoneal pretreatment with **52d** (10 mg/kg) 30 min before intracerebroventricular injection of orexin A. Data are presented as the mean ± SEM of 5–13 mice. **P< 0.01, #P< 0.05, one-way ANOVA followed by Bonferroni test; n.s., not significant.

2.5 Optical resolution of YNT-2293 and YNT-2294 and determination of their eutomers

Finally, to consider the structural differences and intriguing receptor selectivity between YNT-2293 (**52a**) and YNT-2294 (**52d**). Their stereochemistry was determined by optical resolution and circular dichroism (CD) spectrum to identify the eutomers, the enantiomers which have more potent affinity to the target. At first, optical resolution was conducted for both compounds by chiral HPLC with a ChiralPak AD-H column, and the (+)- and (–)-isomers were determined by measuring the optical rotation (Figure 20).

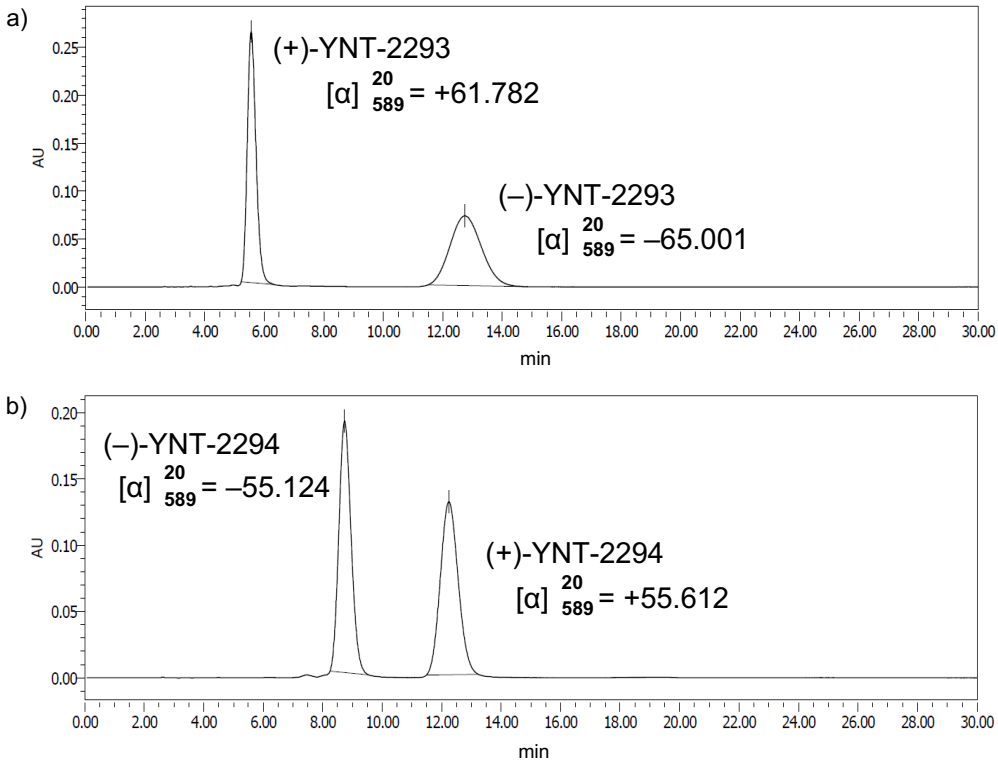

Figure 20. Chiral HPLC analysis of (a) YNT-2293 (**52a**) and (b) YNT-2294 (**52d**). Chiral HPLC chromatogram of isolated YNT-2293 (**52a**) with Chiralpak AD-H (Eluent: hexane/2-propanol = 1/1, Flow rate: 1 mL/min) and YNT-2294 (**52d**) with Chiralpak AD-H (Eluent: hexane/2-propanol = 3/2, Flow rate: 1 mL/min).

Then, the stereochemistry of each enantiomer was determined by CD. The CD spectrum is conventionally used to determine the absolute conformation of complex molecule, such as natural products, macromolecules, and metal complexes, and it is known that the Cotton effect, which is the opposite absorption between the (+) and (–)-isomers can be observed. This method can determine the absolute conformation by comparing the experimentally measured spectrum with the calculated results with the stable conformation. In the case of YNT-2293 (Figure 21a), (2a*S*,4*S*,4a*S*,6*S*,6a*S*)-YNT-2293 showed a negative Cotton effect curve is defined at 270 nm in the simulated spectrum. Referring to the experiential data, (–)-YNT-2293 (red line) corresponds to

the (*S*)-core isomer. In contrast, (2a*S*,4*R*,4a*S*,6*R*,6a*S*)-YNT-2294 have a positive Cotton effect curve is defined at 280 nm in the simulated spectrum (Figure 21b). Referring to the experiential data, (+)-YNT-2294 (red line) corresponds to the (*S*)-core isomer.

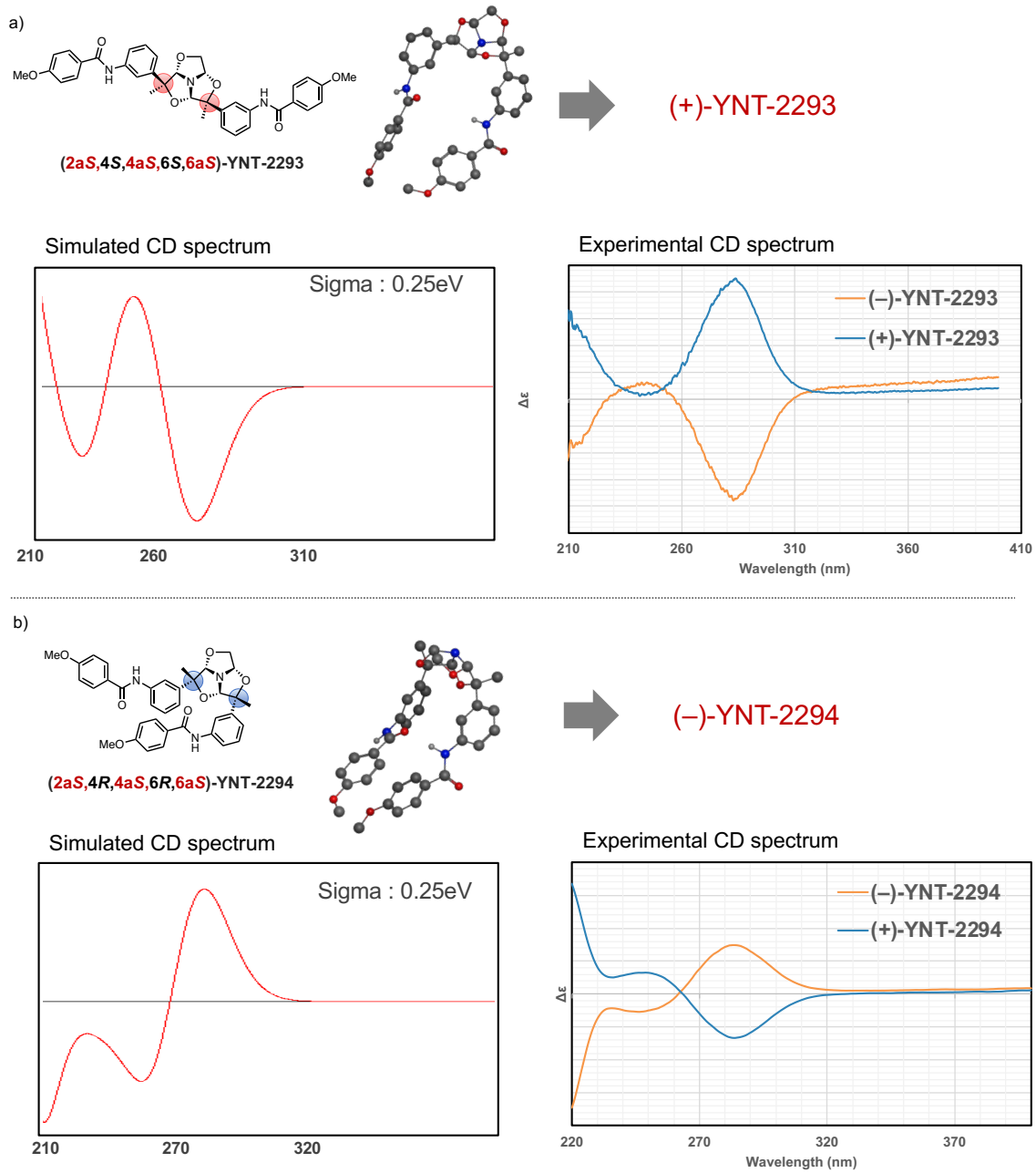

Figure 21. CD spectrum of (a) YNT-2293 (**52a**) and (b) YNT-2294 (**52d**): CD spectra measurements were carried out with acetonitrile at 20 °C. The instrument settings were bandwidth, 1.0 nm; data pitch, 0.2 nm; speed, 100 nm/min; accumulation, 16; and wavelengths, 400–220 nm. Theoretical calculations of the CD spectra started with a preliminary MMFF conformational search using Molecular Operating Environment® (MOE).

As the absolute configuration of each derivative was obtained above, their affinities with OXRs were evaluated to determine the eutomers (Table 4). As a result, (–)-YNT-2293 (**52a**) and (+)-YNT-2294 (**52d**) were revealed to be eutomer, respectively. (–)-**52a** had a 20-times more potent OXR antagonistic activity for OX_1R (K_i = 5.23 nM) than its (+)-isomer (K_i = 110 nM) and twice the affinity of racemic **52a** (K_i = 11.7 nM). In contrast, both isomers had similar affinity for OX_2R (K_i = 26.6 nM and 34.8 nM, respectively). On the other hand, (+)-YNT-2294 (**52d**) had an 80-times more potent OXR antagonistic activity for OX_1R (K_i = 2.17 nM) than its (–)-enantiomer (K_i = 161 nM), although it showed no affinity for OX_2R. These results revealed that two *cis*-side chains in (–)-**52a** and (+)-**52d** had well overlapped each other, and the core skeletons were flipped for arrangement of the heteroatoms' similar positions.

Table 4. Assay results of OXR antagonistic activity with racemic/enantiopure YNT-2293 and YNT-2294

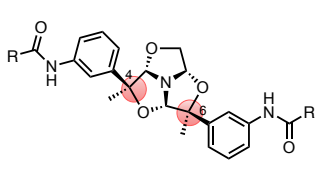

(–)-(2a*S*,4*S*,4a*S*,6*S*,6a*S*)-**52a**

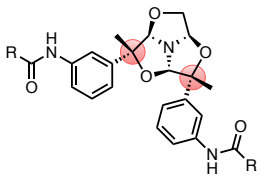

(+)-(2a*R*,4*R*,4a*R*,6*R*,6a*R*)-**52a**

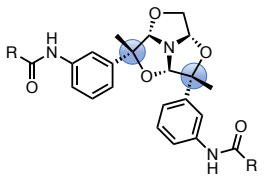

(–)-(2a*S*,4*R*,4a*S*,6*R*,6a*S*)-**52d**

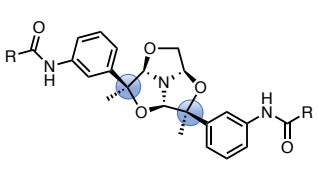

(+)-(2a*R*,4*S*,4a*R*,6*S*,6a*R*)-**52d**

R = 4-MeO-C_6H_4

Compounds	K_i (nM) [a]	
	OX_1R	OX_2R
(±)-**52a**	11.7 ± 2.13	16.7 ± 9.37
(+)-**52a**	110 ± 28.1	26.6 ± 6.70
(–)-**52a**	5.23 ± 1.02	34.8 ± 9.47
(±)-**52d**	4.93 ± 1.00	– [b]
(+)-**52d**	2.17 ± 0.69	– [b]
(–)-**52d**	161 ± 39.2	– [b]

[a] K_i values represent the mean ± SEM. These values were calculated using IC_{50} values of each isomer and at least three independent calcium assays performed in triplicate (Cheng–Prusoff equation). [b] K_i value was not detected. IC_{50} value was over 10 μM (cutoff value) or was not obtain from concentration–response curve.

2.6 Docking simulation of (–)-YNT-2293 and (+)-YNT-2294 with OXRs

After the determination of the eutomers, a docking simulation was conducted for (–)-YNT-2293 and (+)-YNT-2294 by utilizing the crystal structures of human OX_1R with SB-334867[83,84] (PDB ID: 6TQ7, Figure 22).[85] Although SB-334867 is 1-SORA, the binding pocket of OX_2R was technically constructed from the SB-334867/OX_1R crystal structure by threonine substitutions $S103^{2.61}$ and $A127^{3.33}$ to reproduce the corresponding $T111^{2.61}$ and $T135^{3.33}$, respectively. SB-334867 interacted as a pair of two molecules with OX_1R by hydrogen bonding with $E^{45.52}$ of ECL2-stabilizing salt bridge ($E204^{45.52}$–$H216^{5.39}$)-mediated water molecule and π-stacking with $H^{7.39}$ indicated by dashed lines.

In the case of TriMERs, (–)-YNT-2293 (**52a**) and (+)-YNT-2294 (**52d**) have similar binding forms owing to the flipping the 1,3,5-trioxazatriquinane core structure, which covers the pharmacophore those of SB-334867. TriMER occupied a hydrophobic subpocket comprising $A^{2.60}$, $S^{2.61}$ ($T^{2.61}$ in OX_2R), $V^{2.64}$, $I^{3.28}$ $P^{3.29}$, $Q^{3.32}$, and $Y^{2.64}$ covered by the ECL2 which is occupied by common OXR antagonists in each known crystal structure.[85–88]

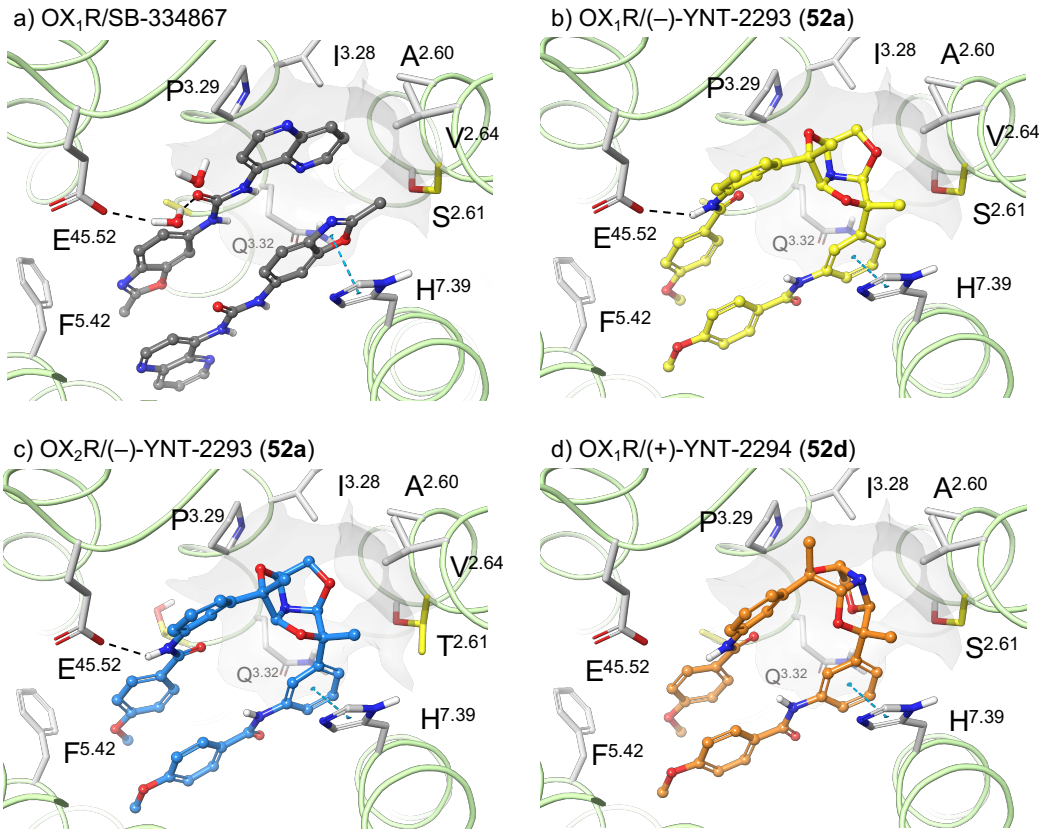

Figure 22. Results of docking simulation with OX_1R and OX_2R: Binding modes of (a) SB-334867 in complex with OX_1R (PDB ID: 6TQ7)[85], (b) (–)-**52a** with OX_1R, (c) (–)-**52a** with OX_2R, and (d) (+)-**52d** with OX_1R determined by our docking procedure. Hydrogen-bonding interactions and π-stacking are indicated by dashed lines.

Additionally, the ether oxygens of 1,3,5-trioxazatriquinane core possibly interact with the hydroxyl moiety of $S^{2.61}$ (in OX_1R) or $T^{2.61}$ (in OX_2R) with direct hydrogen or indirect water-mediated bonding. The left benzamide moiety of the 1,3,5-trioxazatriquinane core and $E^{45.52}$ interact with direct hydrogen bonds without the water molecule. Notably, the *cis*-configuration of the sidechain enables fitting the binding pocket similar to a pair of SB-334867 with van der Waals contacts and π-stacking between the right aryl residue and $H^{7.39}$.

The orthosteric sites of OX_1R and OX_2R have high homology (82%) with differences in only two residues: $S103^{2.61}$/$T111^{2.61}$ and $A127^{3.33}$/$T135^{3.33}$ (Figure 23). This slight difference in the shape of the hydrophobic cavity and the 1,3,5-trioxazatriquinane scaffold plays an important role in the receptor selectivity of (–)-**52a** and (+)-**52d**. When (–)-**52a** (blue one) binds to OX_2R, it slightly shifts to the left side to avoid the steric crash with the γ-methyl group of $T111^{2.61}$, avoiding the collision between the terminal benzamide unit on the left part and the γ-methyl group of $T135^{3.33}$.

On the other hand, if (+)-**52d** (orange one) binds to OX_1R similarly to that of (–)-**52a** in OX_2R, the left terminal aromatic ring of (+)-**52d** has a steric repulsion with $T135^{3.33}$ in OX_2R. Thus, the 1,3,5-trioxazatriquinane core rotates to avoid steric hindrance. Nevertheless, the methyl group on the 1,3,5-trioxazatriquinane core of (+)-**52d** (indicated as orange mesh) causes of the steric crash between the ECL2, limiting the rotation of the core unit. Receptor selectivity depends on the binding modes of (–)-**52a** and (+)-**52d** upon the interaction with ECL2.

The involvement of ECL2 in the reported OXR antagonists was demonstrated by mutagenesis experiments,[87,89] and that the hydrogen-bonding network of the salt bridge enable the stabilization of the binding complex. The result show that the receptor selectivity of these two compounds is controlled by the stereochemistry of the scaffold, even though they have the same side chains.

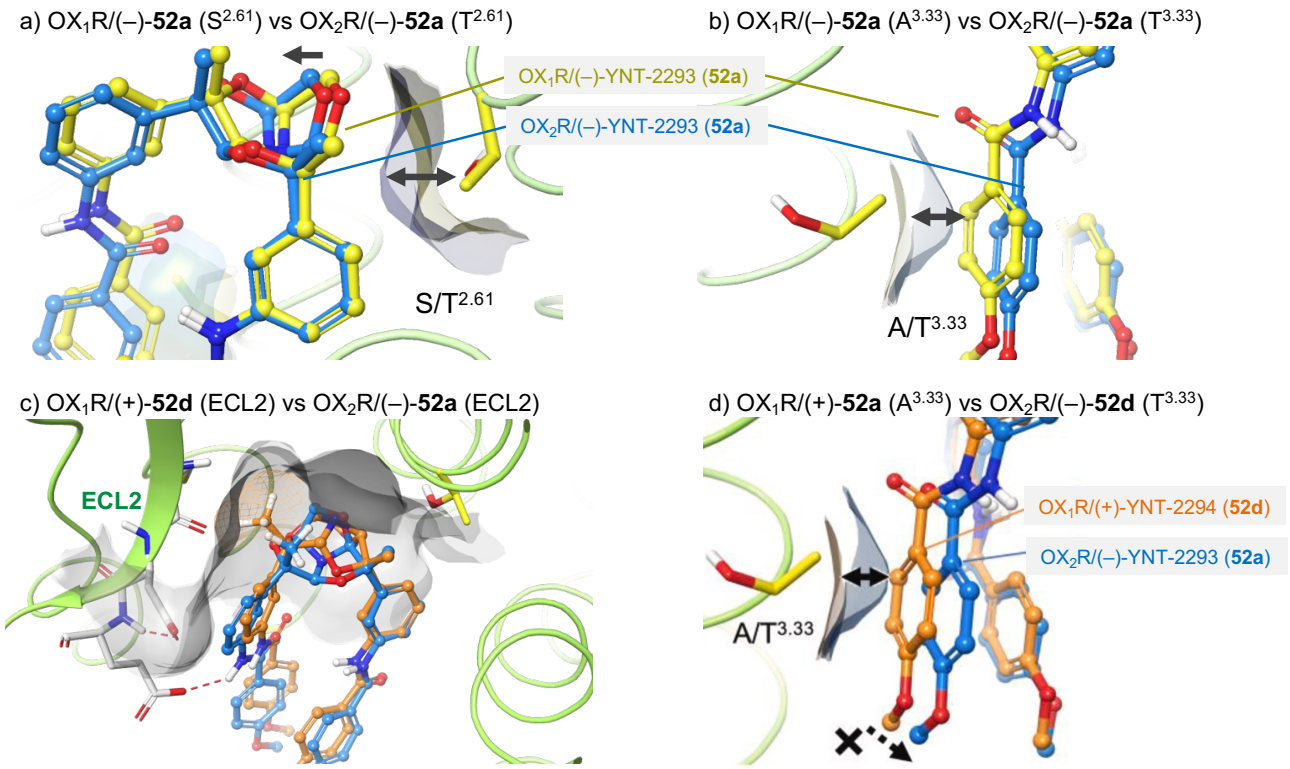

Figure 23. Discussion on receptor selectivity based on the results of docking simulation: Expanded views around the (a) S/T$^{2.61}$ residues and (b) A/T$^{3.33}$ residues in the superimposition of (−)-**52a** with OX$_1$R (yellow) and (−)-**52a** with OX$_2$R (blue), (c) ECL2 and hydrophobic pocket and (d) A/T$^{3.33}$ residues in the superimposition of (+)-**52d** with OX$_1$R (orange) and (−)-**52a** with OX$_2$R (blue). The orange mesh indicates the surface of convex methyl group of (+)-**52d**.

2.7 Conclusion

In this chapter, upon the discovery of the novel orexin receptor ligands, the author utilized the unique bowl-type heterocyclic compound 1,3,5-trioxazatriquinane as a scaffold for screening and found the novel OXR antagonists with different receptor selectivity. The author designed and synthesized a novel TriMER-focused library consisting of 72 compounds which had two phenethylamine moieties and evaluated it using with cell-based assays. As a result, the screening hit rate was high (7%), and 5 hit compounds were obtained. According to the structure–activity relationship, the hit compounds took the *cis*-configuration bearing a pair of *m*-aniline residues, and they had bulky substituents at the terminals of the side chains in common. Especially in stereoisomers YNT-2206 (**48a**, DORA, K_i = 23.4 nM for OX_1R, K_i = 15.1 nM for OX_2R) and YNT-2209 (**48d**, 1-SORA, K_i = 25.4 nM for OX_1R) with *m*-*N*-Bz had potent OXR antagonistic activity with different receptor selectivity on OX_1R. The optimization of the benzamide moiety provided more potent OXR antagonists while maintaining the receptor selectivity; YNT-2293 (**52a**, K_i = 3.99 nM for OX_1R, K_i = 6.01 nM for OX_2R) as DORA and YNT-2294 (**52d**, K_i = 1.87 nM for OX_1R) as 1-SORA, which possessed 4-MeO benzamide groups in common. Both ligands exhibited significant receptor selectivity against opioid receptors, reasonable brain permeability and metabolic stability. Moreover, **52a** and **52d** were effective *in vivo*: DORA **52a** showed a significant sleep-inducing effect with EEG/EMG, whereas 1-SORA **52d** suppressed the locomotor activity induced by OXA, respectively. Finally, the author discussed the pharmacophores of both ligands and receptor selectivity. After the absolute configuration was determined, the eutomers (–)-(2a*S*,4*S*,4a*S*,6*S*,6a*S*)-**52a** and (+)-(2a*R*,4*R*,4a*R*,6*R*,6a*R*)-**52d** were obtained. The docking simulation results suggested that both ligands bound to OXRs quite similarly by flipping the 1,3,5-trioxatriquinane core structure. In addition, the interaction with ECL2 and (–)-**52a** and (+)-**52d** would be crucial for a different receptor selectivity for OX_1R.

In summary, the discovery of the efficient DORA and 1-SORA was achieved from TriMERs, although, none of the library compounds in this screening exhibited the OXR agonistic activity. Therefore, further investigation is required to attain the OXR agonist.

Chapter 3 Design and synthesis of orexin receptor agonists with 1,3,5-trioxazatriquinane skeleton

3.1 Design of the novel OXR agonist based on TriMER-type OXR antagonists

In the screening described in Chapter 2 using TriMER derivatives with aromatic rings, no compounds exhibited OXR agonist activity. To develop OXR agonists utilizing the 1,3,5-trioxazatriquinane skeleton common with TriMER-type antagonists, the structural transformation of these antagonists to have OXRs agonist activity was conducted.

It is generally accepted that antagonists are larger and bulkier than the corresponding agonists to inhibit the movement of the receptor necessary for the agonistic activity, and they have hydrophobic extra motifs called accessory sites[90]. For example, acetylcholine receptor ligands indicated that those antagonists have extra phenyl rings in that structure (Figure 24). Inspired by this concept, the author hypothesized that the TriMER-type OXR agonists could be obtained by removing the accessory sites from the antagonists and maintaining the pharmacophore units on TriMER. From the docking study of TriMER-type OXR antagonists YNT-2293 (**52a**) and YNT-2294 (**52d**), the side chain aromatic rings act as accessory sites to prevent the inward conformational changes of the receptors which are important for the agonistic activity (Figure 25).[91] In addition, the 1,3,5-trioxazatriquinnane core interacts with a hydrophobic cavity that is important for both the agonist[65,92] and the antagonist.[85] Thus, the design and synthesis of the novel OX_2R agonists based on TriMER-type OXR antagonists were conducted by removal of aromatic rings.

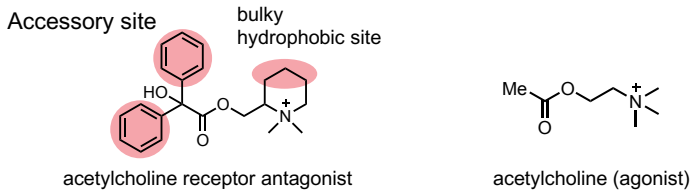

Figure 24. Concepts of accessory sites and the example of acetylcholine receptor ligands

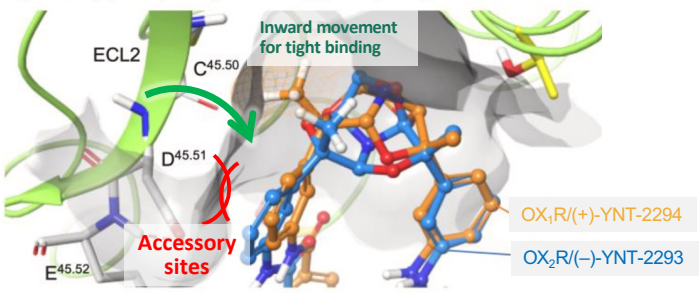

Figure 25. Proposed accessory sites of TriMER-type OXR antagonists based on the docking study

First, the derivatives lacking one or two aromatic rings at the terminal of the TriMER-type OXR antagonists were evaluated the antagonist activity (Table 5). However, the hetero-TriMER derivatives removing the one aromatic ring (e.g., mono-Boc, mono-Ms, and mono-Ac derivatives) showed weak OXR antagonistic activity, and the aniline derivatives obtained by removing the two aromatic rings showed neither agonist nor antagonist activity, even though they were enantiopure. In other words, the scaffolds directly attached to the aromatic rings with TriMER make it difficult to obtain agonists, requiring substantial modification.

Table 5. Assay results of TriMER derivatives removing the one or two aromatic rings

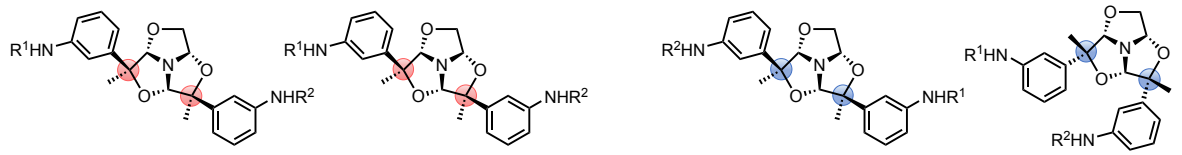

Type-I Type-IV

Compounds	Core type	R^1	R^2	IC_{50} (nM)	
				OX_1R	OX_2R
YNT-2293 (**52a**)	I	4-MeO-Bz	4-MeO-Bz	3.99 ± 0.47	6.01 ± 1.52
YNT-2294 (**52d**)	IV	4-MeO-Bz	4-MeO-Bz	1.87 ± 0.30	– [b]
59a	I	4-MeO-Bz	H	1560 ± 147	402 ± 7.75
60a	I	4-MeO-Bz	SO_2Me	504 ± 2.20	129 ± 17.5
61d	IV	4-MeO-Bz	Boc	68.5 ± 4.20	– [b]

[a] IC_{50} values represent the mean ± SEM. [b] IC_{50} value was over 10 μM (cutoff value) or was not obtain from concentration–response curve.

Thus, a novel slim *cis*-type TriMER scaffold was designed by removing both aromatic rings directly attaching the 1,3,5-trioxazatriquinane skeleton thought to be accessory sites and alternatively introducing amino-methylene groups (Figure 26). Since only Type-I and Type-IV TriMER derivatives with a *cis* side-chain configuration previously showed affinity against OXRs, novel TriMER derivatives were designed based on templates TriMER-type antagonists with *cis* configuration (Type-I and IV). In this design, TriMERs with amino groups can be carried out synthesized from protected diols **64,** and these diols can be sequentially converted to amines after the construction of the 1,3,5-trioxazatriquiuane skeleton following the introduction of several alkyl and aryl substituents via amide, carbamate, and sulfonamide conjugates by the condensation reaction. As the starting material, ketone with protected alcohol was synthesized from benzyloxyacetone. This synthetic route has mainly two advantages that are useful as a library: 1) the intermediate causes less steric

hindrance and is stable to enable the modification, and 2) the precursors of amino-methylene TriMERs can be transformed into various TriMERs, such as the oxidation of alcohol and Huisgen cycloaddition with azide.

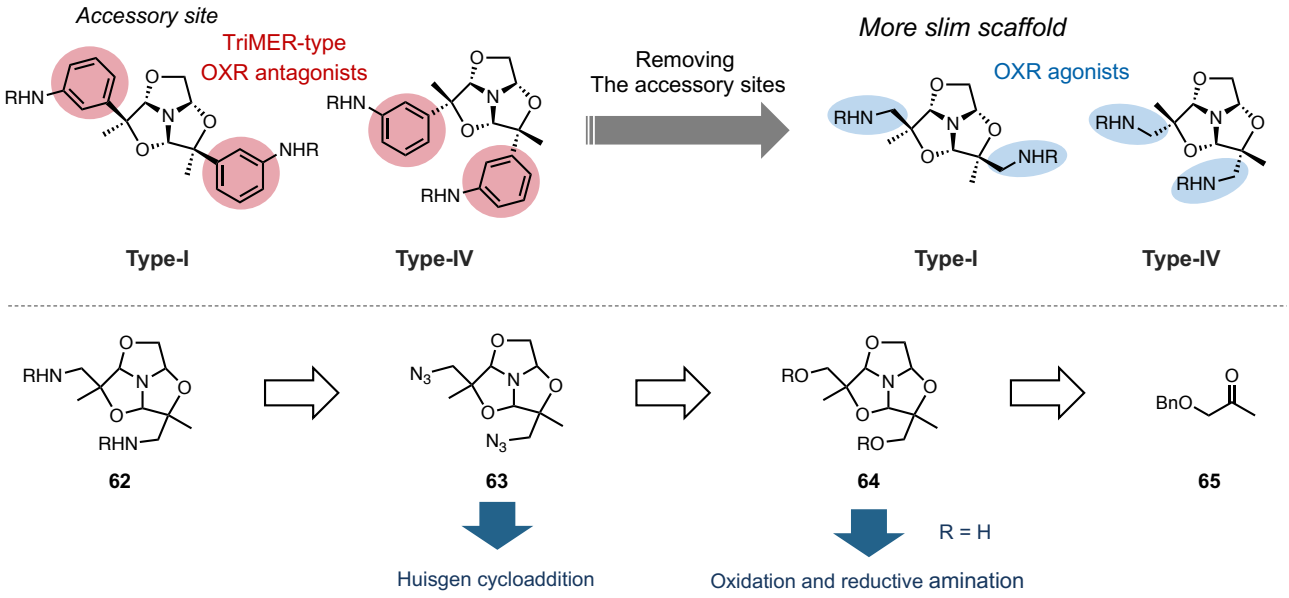

Figure 26. Design of slim TriMER derivatives from TriMER-type OXR antagonists and its synthesis plan

In addition, intermediate **62** was synthesized directly from ketones using protected amines. The ketone **67** with dibenzyl-protected amine was synthesized from 1-chloroacetone (**66**) and derivatized up to oxazoline dimer **68** (Scheme 5), although the trimerization with the glycolaldehyde dimer did not proceed even under high-temperature conditions, likely due to steric hindrance caused by the bulky nitrogen atoms' protecting groups. On the other hand, TriMER was obtained from ketones **70** with phthalimide groups in low yield. Even the first step of reaction with the TosMIC reaction was not proceeded as with the *o*-NO_2 derivative described in Chapter 2, which must be due to the steric hindrance around the nitrogen atom. Based on these results, TriMER synthesis was conducted from benzyloxyacetone.

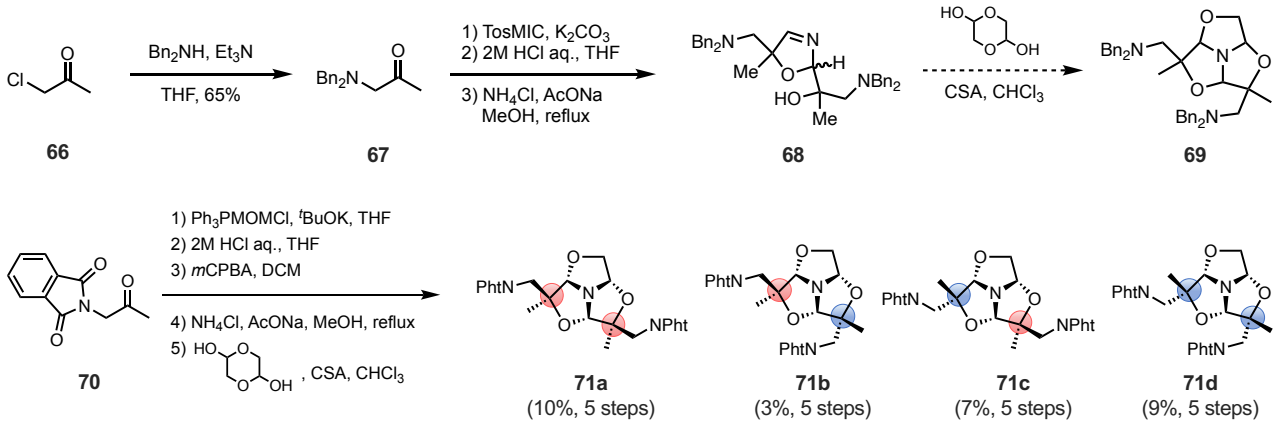

Scheme 5. Investigation of protecting group on starting material

3.2 Synthesis of TriMERs with aminomethylene side chains

TriMER intermediates **75a**–**75d** were synthesized from benzyloxyacetone (**65**) according to our previous report[91] (Scheme 6). First, α-hydroxyaldehyde **72** was synthesized by the reaction with TosMIC following hydrolysis. In this process, previously suspending K_2CO_3 solution was used as the base but replaced by ^{t}BuOK, which significantly reduced the reaction time (12 h → 2 h). This process was applied for flow synthesis using a microreactor (see the experimental procedure).

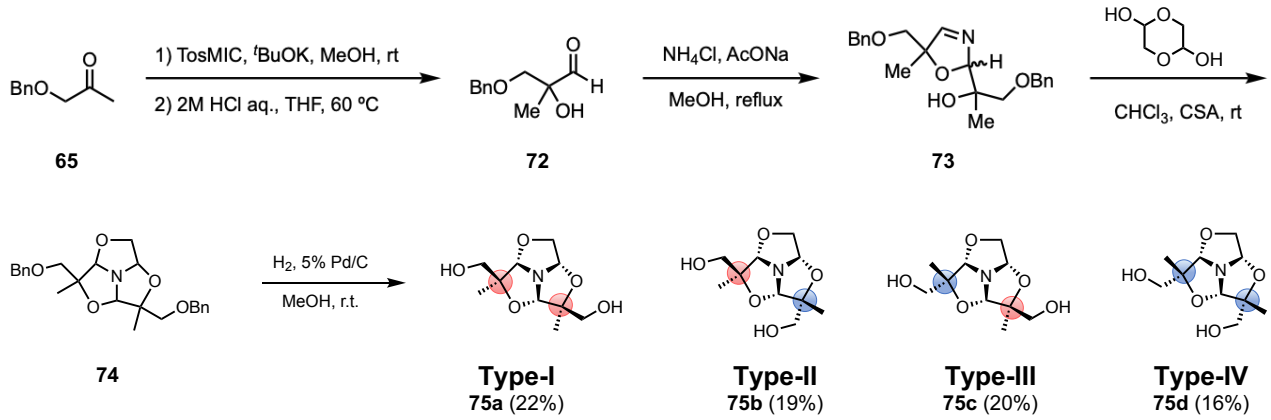

Scheme 6. Synthesis of TriMER intermediate **75a**–**75d**

TriMERs **74** with the benzyloxy group were subsequently synthesized by oxazoline dimer formation and trimerization with the glycolaldehyde dimer. Because the separation of the four isomers, especially in *trans*-isomers (Type II and III), was not successful by column chromatography, four isomers were separated after benzyl deprotection and conversed to diols **75a**–**d**. In the preparation of **75a**–**d**, a minimum of two purification operations are required with a 500-fold silica gel for crude in the $CHCl_3$/EtOH/MeOH system followed by the recrystallization. Due to the different morphology of compounds, i.e. TriMERs **32a**–**34d** with nitrophenyl groups in Chapter 2 were solid and **75a**–**d** with diol group were syrup, the recrystallization approach can't be utilized and other approaches such as reverse phase and gel permeation chromatography that were effective for the separation of other TriMER derivatives also couldn't work well. In addition, despite the further investigations to separate the four isomers after the derivatization of **75a**–**d** using condensation reaction, the most efficient way to separate the four isomers was the utilization of normal phase silica-gel chromatography after the synthesis of diols **75a**–**d** using 15 μm spherical silica gel on the medium-pressure liquid chromatography (MPLC) system, Reveleris®, which can detect the compounds by not only UV absorbance but also evaporative light scattering detection (ELSD) (Figure 27). By using this method, gram-scale separation

in one step was achieved. The stereochemistry of **75a–d** was determined from NOE correlations using 2D NMR as in Chapter 2.

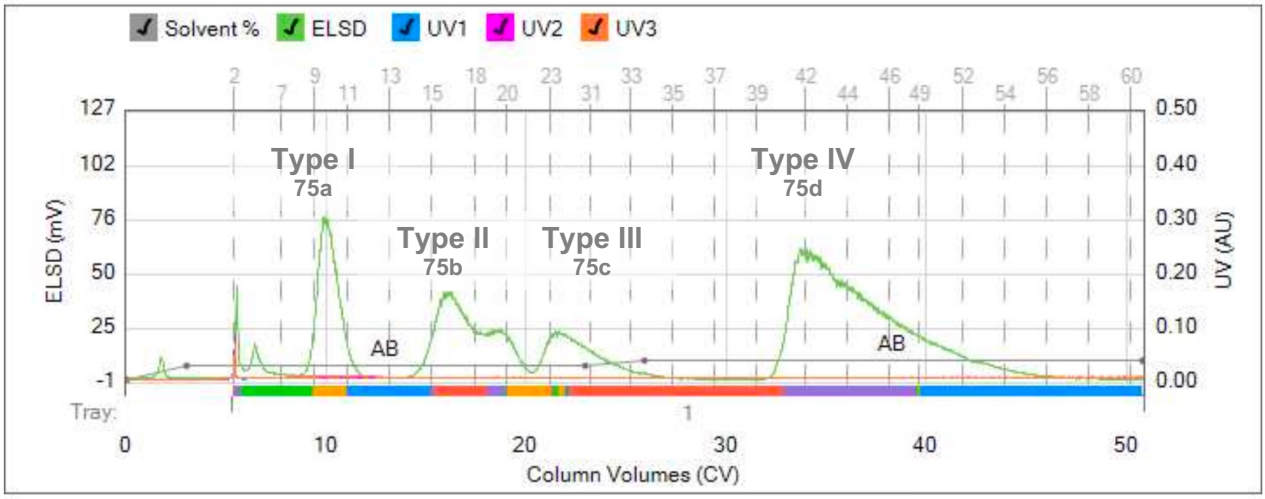

Figure 27. Separation of four isomers (**75a**–**d**) by Reveleris®: MPLC chromatogram of **75a**–**d** with FlashPure Select (Share 15 µm silica gel, 12 g; Eluent: $CHCl_3$/MeOH/EtOH = 99/0.5/0.5, Flow rate: 20 mL/min).

Next, each alcohol **75a–d** was converted to mesylate **76a–d**, which had a good leaving group, followed by the introduction of azide groups, and hydrogenation to give diamines **78a–d**, respectively (Scheme 7). For the reduction of the azide, Staudinger reaction using phosphines was not compatible because of decomposition of the core skeleton. Finally, each amine **78a–d** was derivatized to obtain the TriMERs with amide, carbamate, and sulfonamide derivatives by a condensation reaction. From the intermediates **75** and **77**, several other reactions as well as condensation were applied. Alcohols **75a** could be converted to aldehyde **98a** by Parikh-Doering oxidation, following reductive amination obtaining benzyl amine derivative **99a**. On the other hand, azide **77d** introduced phenyl triazole with Huisgen cycloaddition (Scheme 8).

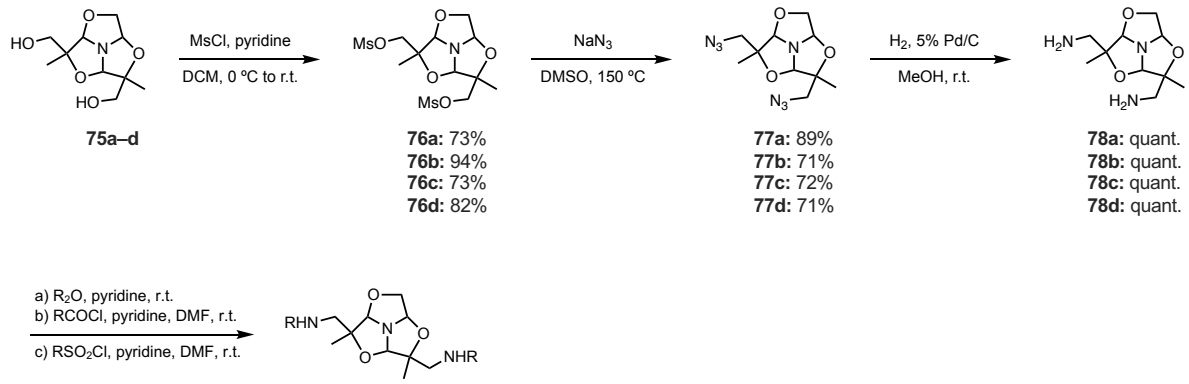

75a–d

76a: 73%
76b: 94%
76c: 73%
76d: 82%

77a: 89%
77b: 71%
77c: 72%
77d: 71%

78a: quant.
78b: quant.
78c: quant.
78d: quant.

List of synthetic TriMER derivatives

Core type	Amide derivatives (R)								
	Ac	Piv	Bz	2-MeOBz	3-MeOBz	4-MeOBz		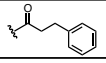	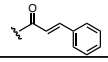
Type-I	**79a** (82%)	**80a** (61%)	**81a** (70%)	**82a** (95%)	**83a** (98%)	**84a** (96%)	**85a** (30%)	**86a** (98%)	**87a** (77%)
Type-IV	**79d** (96%)	**80d** (66%)	**81d** (64%)	**82d** (90%)	**83d** (88%)	**84d** (97%)	**85d** (89%)	**86d** (62%)	**87d** (52%)

Core type	Carbamate derivatives (R)					Sulfonamide derivatives (R)				
	Boc	Moc	Alloc	Troc	Cbz	SO_2Me	$SO_2{}^nPr$	$SO_2{}^nBu$	$SO_2C_8H_{17}$	SO_2Ph
Type-I	**88a** (96%)	**89a** (96%)	**90a** (53%)	**91a** (85%)	**92a** (99%)	**93a** (28%)	**94a** (44%)	**95a** (56%)	**96a** (24%)	**97a** (15%)
Type-IV	**88d** (97%)	**89d** (75%)	**90d** (58%)	**91d** (63%)	**92d** (88%)	**93d** (33%)	**94d** (32%)	**95d** (41%)	**96d** (21%)	**97d** (28%)

Scheme 7. Synthesis of TriMERs with diamine and derivatization

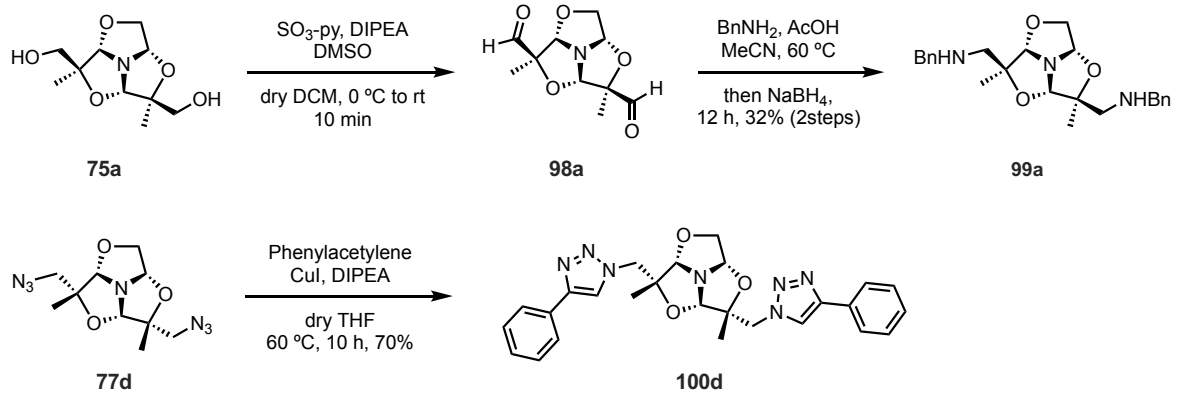

75a

98a

99a

77d

100d

Scheme 8. Synthesis of other TriMER derivatives

3.3 Biological evaluation of synthetic TriMER derivatives

The OX_1R and OX_2R agonist and antagonistic activities of the TriMERs were evaluated with the same assay system used in Chapter 2; cell-based calcium assays with a Chinese hamster ovary (CHO) cell line stably expressing hOX_1R and hOX_2R at a 10 μM substrate concentration. Hit compounds were defined as the compounds that showed >60% activation against OX_2R compared to OXA, and in the heat map, the more active compounds are shown in darker blue (Figure 28). As a result, six compounds (**94d**, **99d**–**102d**, and **102a**) were obtained without antagonistic activity against OXRs.

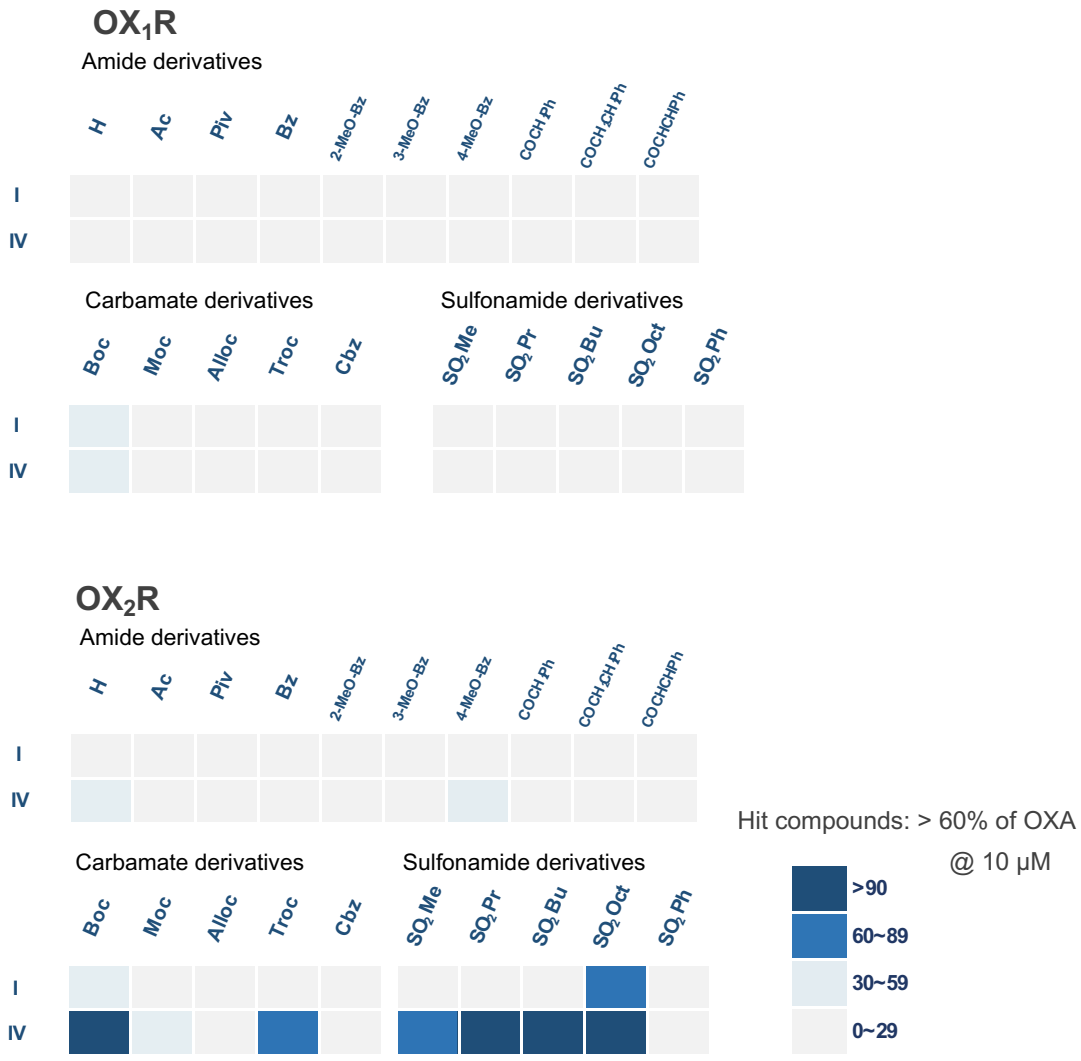

Figure 28. Heat map visualization of the screening results using synthetic TriMERs in the orexin receptor agonist activity

All hit compounds showed OX_2R selectivity, and particularly potent activity was detected in Type IV with those having *cis* side chains orientated downward (Table 6). **78d** had weak OXR agonistic activity despite possessing only amino groups at the side chains, suggesting that the Type IV skeleton would be the active skeleton for OX_2R. Paying attention to the substituents, the derivatives with carbamate and sulfonamide tend to exhibit a potent OXR agonist activity, especially TriMERs with Boc groups and octane sulfonamides showed higher affinity to them.

Table 6. Assay results of hit compounds

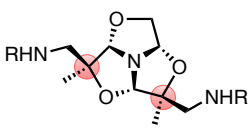

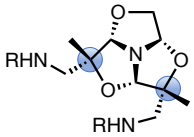

Compounds	Core type	R	% of OXA [a]	
			OX_1R	OX_2R
88d	**IV**	Boc	54.0	171.9
93d	**IV**	SO_2Me	5.66	61.4
94d	**IV**	$SO_2{}^nPr$	14.2	92.3
95d	**IV**	$SO_2{}^nBu$	11.1	91.4
96d	**IV**	$SO_2C_8H_{17}$	23.6	101.2
96a	**I**	$SO_2C_8H_{17}$	11.8	61.2

[a] The value obtained for 10 μM of each compound was used, whereby the agonist activity of endogenous OXR ligand orexin A (OXA) was set to 100%.

On the other hand, none of the amide derivatives including Ac (**79a**, **79d**), Piv (**80a**, **80d**), and aromatic rings such as benzamide (**81a**–**84a**, **81d**–**84d**), phenylacetamide (**85a**, **85d**), phenylpropionamide (**86a**, **86d**), and cinnamamide (**87a**, **87d**), with either skeleton type, showed OX_2R agonist activity (Table 7). Intriguingly, only diol (**75d**) and cinnamamide (**87a**) showed slightly weak antagonist activity. These results suggested that this slim scaffold was appropriate for OXR agonist investigation.

Table 7. All assay results of synthetic TriMER derivatives

OXR agonistic activity

Comp.	Core type	R^1	R^2	% of OXA [a]	
				OX_1R	OX_2R
79a	I	Ac	H	5.73	6.14
79d	IV	Ac	H	6.30	6.31
80a	I	Piv	H	3.30	19.4
80d	IV	Piv	H	1.12	0.39
81a	I	Bz	H	4.49	2.41
81d	IV	Bz	H	4.98	2.39
82a	I	2-MeO-Bz	H	1.61	1.14
82d	IV	2-MeO-Bz	H	1.77	0.96
83a	I	3-MeO-Bz	H	1.47	1.11
83d	IV	3-MeO-Bz	H	2.68	1.34
84a	I	4-MeO-Bz	H	5.01	5.16
84d	IV	4-MeO-Bz	H	6.34	45.3
85a	I	$COCH_2Ph$	H	2.27	2.28
85d	IV	$COCH_2Ph$	H	6.92	29.6
86a	I	$COCH_2CH_2Ph$	H	4.64	2.94
86d	IV	$COCH_2CH_2Ph$	H	5.96	4.19
87a	I	COCHCHPh	H	6.48	3.09
87d	IV	COCHCHPh	H	8.24	4.79
88a	I	Boc	H	30.1	40.2
88b	II	Boc	H	2.21	2.72
88c	III	Boc	H	4.94	2.99
88d	IV	Boc	H	54.0	171.9
89a	I	Moc	H	2.79	4.41
89d	IV	Moc	H	2.89	46.92
90a	I	Alloc	H	2.79	1.41
90d	IV	Alloc	H	3.26	1.64
91a	I	Troc	H	3.59	1.77
91d	IV	Troc	H	4.65	58.62
92a	I	Cbz	H	2.61	1.01
92d	IV	Cbz	H	4.01	1.56
93a	I	SO_2Me	H	6.27	4.42
93d	IV	SO_2Me	H	5.66	61.4
94a	I	$SO_2{}^nPr$	H	7.54	3.58
94d	IV	$SO_2{}^nPr$	H	14.2	92.3
95a	I	$SO_2{}^nBu$	H	7.54	3.58
95d	IV	$SO_2{}^nBu$	H	11.1	91.4
96a	I	$SO_2C_8H_{17}$	H	11.8	61.2
96b	II	$SO_2C_8H_{17}$	H	3.86	3.17
96c	III	$SO_2C_8H_{17}$	H	3.71	3.15
96d	IV	$SO_2C_8H_{17}$	H	23.6	101.2
97a	I	SO_2Ph	H	4.38	3.59
97d	IV	SO_2Ph	H	4.38	2.87
98d	IV	Boc	Me	4.47	2.89
99d	IV	$SO_2C_8H_{17}$	Me	2.65	2.08
101d	IV	$CONH^tBu$	H	2.81	2.02
100d	IV	Ph triazole	H	13.7	19.2
102d	IV	COOEt	H	4.58	2.78
103d	IV	COO^nPr	H	0.36	0.49
104d	IV	COO^nBu	H	0.95	0.3
105d	IV	COO^iPr	H	0.89	0.3
106d	IV	COO^iBu	H	1.29	1.98
107d	IV	$COOCH_2C(CH_3)_3$	H	1.68	2.44
108d	IV	COOPh	H	2.31	2.06
109d	IV	COEt	H	2.37	1.56
110d	IV	COBu	H	2.21	1.37
111d	IV	COC_8H_{17}	H	2.5	0.93

OXR antagonistic activity

Comp.	Core type	R^1	R^2	% of OXA [a]	
				OX_1R	OX_2R
79a	I	Ac	H	105.1	125.9
79d	IV	Ac	H	118.5	118.5
80a	I	Piv	H	108.7	98.3
80d	IV	Piv	H	84.1	122.9
81a	I	Bz	H	110.9	97.3
81d	IV	Bz	H	120.4	124.9
82a	I	2-MeO-Bz	H	147.7	107.9
82d	IV	2-MeO-Bz	H	138.8	112.9
83a	I	3-MeO-Bz	H	136.6	124.9
83d	IV	3-MeO-Bz	H	110.8	113.2
84a	I	4-MeO-Bz	H	103.9	92.9
84d	IV	4-MeO-Bz	H	169.6	176.2
85a	I	$COCH_2Ph$	H	109.6	104.5
85d	IV	$COCH_2Ph$	H	104.5	100.5
86a	I	$COCH_2CH_2Ph$	H	121.9	122.8
86d	IV	$COCH_2CH_2Ph$	H	131.8	124.6
87a	I	COCHCHPh	H	31.4	79.1
87d	IV	COCHCHPh	H	115.8	126
88a	I	Boc	H	109.6	94.8
88b	II	Boc	H	117.2	95.7
88c	III	Boc	H	118.1	126
88d	IV	Boc	H	192.2	151.6
89a	I	Moc	H	105.7	106.5
89d	IV	Moc	H	94.6	67.6
90a	I	Alloc	H	117.9	128.9
90d	IV	Alloc	H	103.3	93.7
91a	I	Troc	H	83.5	95.4
91d	IV	Troc	H	75.9	85.5
92a	I	Cbz	H	103.4	98.4
92d	IV	Cbz	H	73	94.2
93a	I	SO_2Me	H	85.9	76.3
93d	IV	SO_2Me	H	94.9	82.3
94a	I	$SO_2{}^nPr$	H	94.6	77.8
94d	IV	$SO_2{}^nPr$	H	106.3	94.1
95a	I	$SO_2{}^nBu$	H	119.9	139.7
95d	IV	$SO_2{}^nBu$	H	105.6	99.2
96a	I	$SO_2C_8H_{17}$	H	112.1	91
96b	II	$SO_2C_8H_{17}$	H	115.3	126.1
96c	III	$SO_2C_8H_{17}$	H	130.3	126.6
96d	IV	$SO_2C_8H_{17}$	H	220.3	198.5
97a	I	SO_2Ph	H	136	136
97d	IV	SO_2Ph	H	121.3	122.5
98d	IV	Boc	Me	84.7	107.2
99d	IV	$SO_2C_8H_{17}$	Me	94.8	95.1
101d	IV	$CONH^tBu$	H	104.8	99
100d	IV	Ph triazole	H	62.7	97.9
102d	IV	COOEt	H	105.2	139.17
103d	IV	COO^nPr	H	98.3	99.2
104d	IV	COO^nBu	H	123.5	111.1
105d	IV	COO^iPr	H	115.3	96.2
106d	IV	COO^iBu	H	108.2	106.9
107d	IV	$COOCH_2C(CH_3)_3$	H	92.3	99.5
108d	IV	COOPh	H	100.1	93.2
109d	IV	COEt	H	111.6	115.3
110d	IV	COBu	H	112.9	96.4
111d	IV	COC_8H_{17}	H	99.3	84.6

[a] The value obtained at 10 μM was used. The agonist activity of endogenous OXR ligand orexin A (OXA) was set as 100%. Darker blue compounds have more potent OXR agonistic activity. [b] The value obtained at 10 μM was used. The endogenous OXR ligand orexin A (OXA) is set at 100% and evaluated how much inhibiting that with synthetic compounds. Darker red compounds have more potent OXR antagonistic activity.

Next, the structure–activity relationships of the surrounding compounds were investigated. Among the carbamate derivatives (Table 8), Boc derivative **88d** with a Type-IV skeleton exhibited the most potent OX_2R agonist activity against OX_2R, whereas the other carbamate derivatives with methyl (Moc; **89a**, **89d**), allyl (Alloc; **90a**, **90d**), 2,2,2-trichloroethoxycarbonyl (Troc; **91a**, **91d**), or benzyl (Cbz; **92a**, **92d**) groups showed no or weak agonistic activity. The length and bulkiness of the alkyl chain on carbamate oxygen were investigated (**102d**–**108d**) and these results suggested that the bulky *tert*-butoxy group is crucial for the OX_2R agonist activity.

Table 8. Assay results of all TriMER derivatives surrounding Boc derivatives (Excerpt from Table 5)

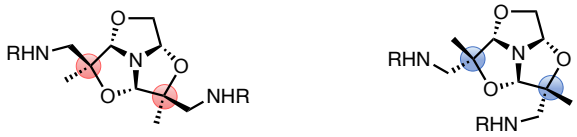

Compounds	Core type	R	% of OXA [a]	
			OX_1R	OX_2R
88d	**IV**	Boc	54.0	171.9
88a	**I**	Boc	30.1	40.2
89d	**IV**	Moc	3.26	1.64
90d	**IV**	Alloc	2.89	46.92
91d	**IV**	Troc	4.65	58.62
92d	**IV**	Cbz	4.01	1.56
102d	**IV**	COOEt	4.58	2.78
103d	**IV**	$COO^{n}Pr$	0.36	0.49
104d	**IV**	$COO^{n}Bu$	0.95	0.30
105d	**IV**	$COO^{i}Pr$	0.89	0.30
106d	**IV**	$COOCH_2{}^{i}Pr$	1.29	1.98
107d	**IV**	$COOCH_2{}^{t}Bu$	1.68	2.44
108d	**IV**	COOPh	2.31	2.06

[a] The value obtained for 10 μM of each compound was used, whereby the agonist activity of endogenous OXR ligand orexin A (OXA) was set to 100%.

Among the sulfonamide derivatives, octane sulfonamide derivative **96d** with a Type-IV skeleton exhibited the most potent OX_2R agonist activity against OX_2R (Table 9). Alkyl sulfonamide derivatives **93d**–**96d** showed more potent agonist activity with increasing alkyl chain length. On the other hand, alkyl amide derivatives showed no agonist activity against OX_2R (**109d**–**111d**). In addition, **96a** only exhibited moderate agonist activity in the Type-I derivatives. Besides, benzene sulfonamide **97d** did not show any agonist activity against OXRs. The results suggest that the removal of the aromatic rings on the side chains, which were directly attached to the 1,3,5-trioxazatriquinane skeleton core, and the installation of bulkier/longer alkyl groups were effective for the transformation of TriMER-type OXR antagonists to OX_2R agonists.

Table 9. Assay results of all TriMERs surrounding octane sulfonamide derivatives (from Table 5)

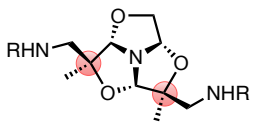

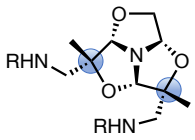

Compounds	Core type	R	% of OXA [a]	
			OX_1R	OX_2R
93d	**IV**	SO_2Me	5.66	61.4
94d	**IV**	$SO_2{}^nPr$	14.2	91.4
95d	**IV**	$SO_2{}^nBu$	11.1	92.3
96d	**IV**	$SO_2C_8H_{17}$	23.6	101.2
96a	**I**	$SO_2C_8H_{17}$	11.8	61.2
97d	**IV**	SO_2Ph	4.38	2.87
109d	**IV**	COEt	2.37	1.56
110d	**IV**	$CO{}^nBu$	2.21	1.37
111d	**IV**	COC_8H_{17}	2.50	0.93

[a] The value obtained for 10 μM of each compound was used, whereby the agonist activity of endogenous OXR ligand orexin A (OXA) was set to 100%.

Finally, the effects of the core scaffold and amide protons were investigated (Table 10). As for the Boc derivative and octane sulfonamide derivatives, Type-II and Type-III derivatives with a *trans* configuration (**88b**, **88c**, **96b**, and **96c**) were also synthesized and evaluated. As expected, these compounds exhibited no OXR agonistic activity. Additionally, to investigate pharmacophores further, *N*-Me carbamate (**98d**), *N*-Me sulfonamide (**99d**), and *N*-*tert*-butyl urea (**101d**) were prepared (Scheme 9), neither of which exhibited no agonistic activity against OXR. These results suggest that the protons of the carbamate/sulfonamide, rather than urea groups, are involved in the OX_2R agonist activity.

Table 10. Investigation of the effects of core scaffold and protons

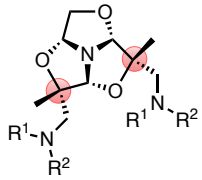

Type-I

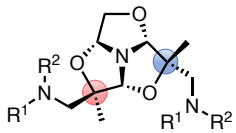

Type-II

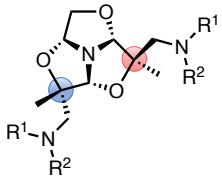

Type-III

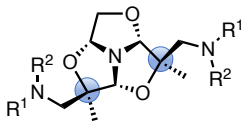

Type-IV

Compounds	Core type	R^1	R^2	% of OXA [a]	
				OX_1R	OX_2R
88a	**I**	Boc	H	30.1	40.2
88b	**II**	Boc	H	2.21	2.72
88c	**III**	Boc	H	4.94	2.99
88d	**IV**	Boc	H	54.0	171.9
98d	**IV**	Boc	Me	4.47	2.89
101d	**IV**	$CONH^tBu$	H	2.81	2.02
96a	**I**	$SO_2C_8H_{17}$	H	11.8	61.2
96b	**II**	$SO_2C_8H_{17}$	H	3.86	3.17
96c	**III**	$SO_2C_8H_{17}$	H	3.71	3.15
96d	**IV**	$SO_2C_8H_{17}$	H	23.6	101.2
99d	**IV**	$SO_2C_8H_{17}$	Me	2.65	2.08

[a] The value obtained for 10 μM of each compound was used, whereby the agonist activity of endogenous OXR ligand orexin A (OXA) was set to 100%.

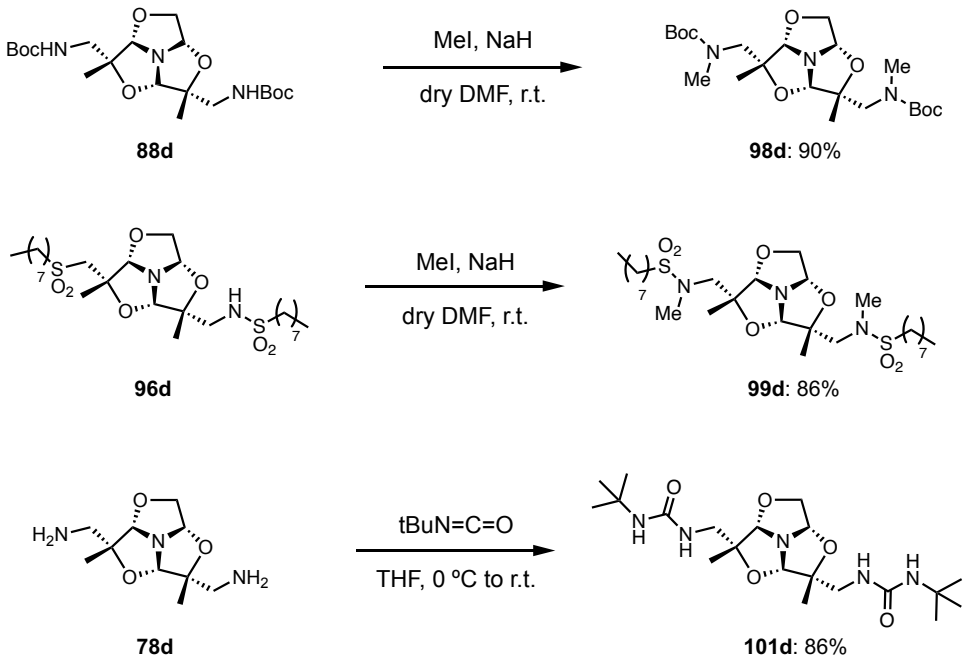

Scheme 9. Derivatization of TriMERs with methylation and urea synthesis

3.4 Stereoselective synthesis of TriMERs

As described above, screening results revealed that novel TriMER derivatives with slim scaffolds successfully exhibited OXR agonist activity, but **88d** and **96d** were not considered significantly potent, enough to determine their EC_{50} values. Thus, it was necessary to obtain optical isomers and optimize them after revealing the active stereo configuration for further pharmacological evaluation and derivatization.

Conventionally, TriMER synthesis yields four regioisomers of Type I–IV in a single synthetic operation along with their enantiomers, yielding a total of eight isomers (Figure 29). This property is useful for early-stage screening of compound libraries, as compounds with various stereochemistry and side chains can be obtained at once.[91] However, it is difficult to obtain the TriMER with the desired stereochemistry separately because TriMER with undesired stereochemistry is also obtained, and multiple and longtime purifications are required for purification, which is inefficient for a hit compound optimization stage. Moreover, due to the lack of the UV absorption of these compounds, optical resolution using chiral columns was not applicable. Hence, the author decided to attempt the first asymmetric synthesis of diols **75a** and **75d**, specifically the stereoselective synthesis of OXR-active *cis*-TriMERs was conducted.

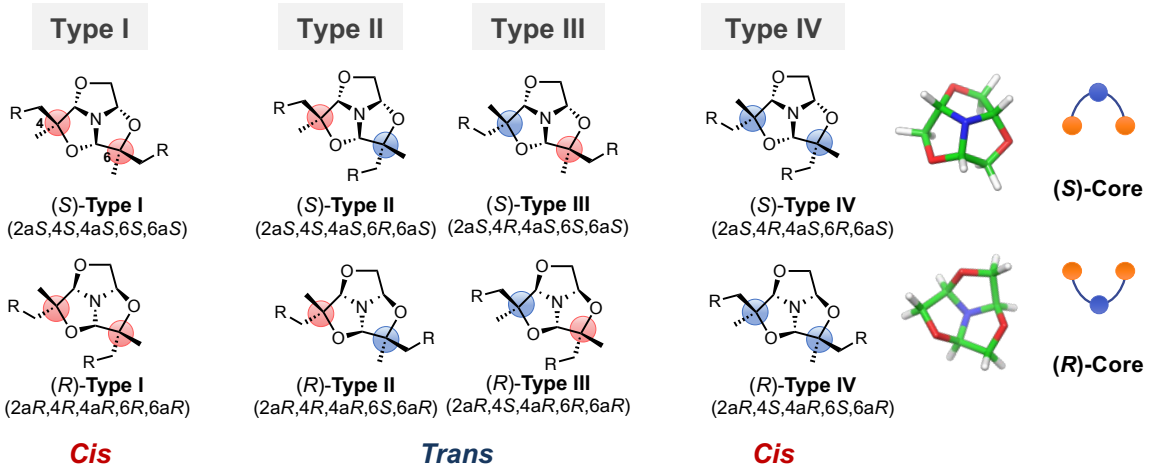

Figure 29. Each enantiomer of TriMER carrying two substituents

For the asymmetric synthesis of TriMERs, the origin of stereochemistry on the skeleton was reconsidered (Figure 30). Coloring the stereochemistry in each part of the eight isomers suggested that those stereocenters are originated from the corresponding α-hydroxyaldehydes and that the stereochemistry of the 1,3,5-trioxazatriquinane skeleton was derived from those of the quaternary carbon of those oxazolinedimers. Consequently, the *cis*-type TriMERs (Type-I and -IV) were produced selectively from the reaction with two

optically pure α-hydroxyaldehydes possessing the same stereochemistry. Hence, in this chapter, the stereoselective synthesis of α-hydroxyaldehydes is presented first. The advantage of this method is not only the yield improvement but also the simplification of the purification as the predicted isomers obtained in this procedure are only Type-I and -IV, which can be easily separated by silica gel column chromatography (Figure 31).

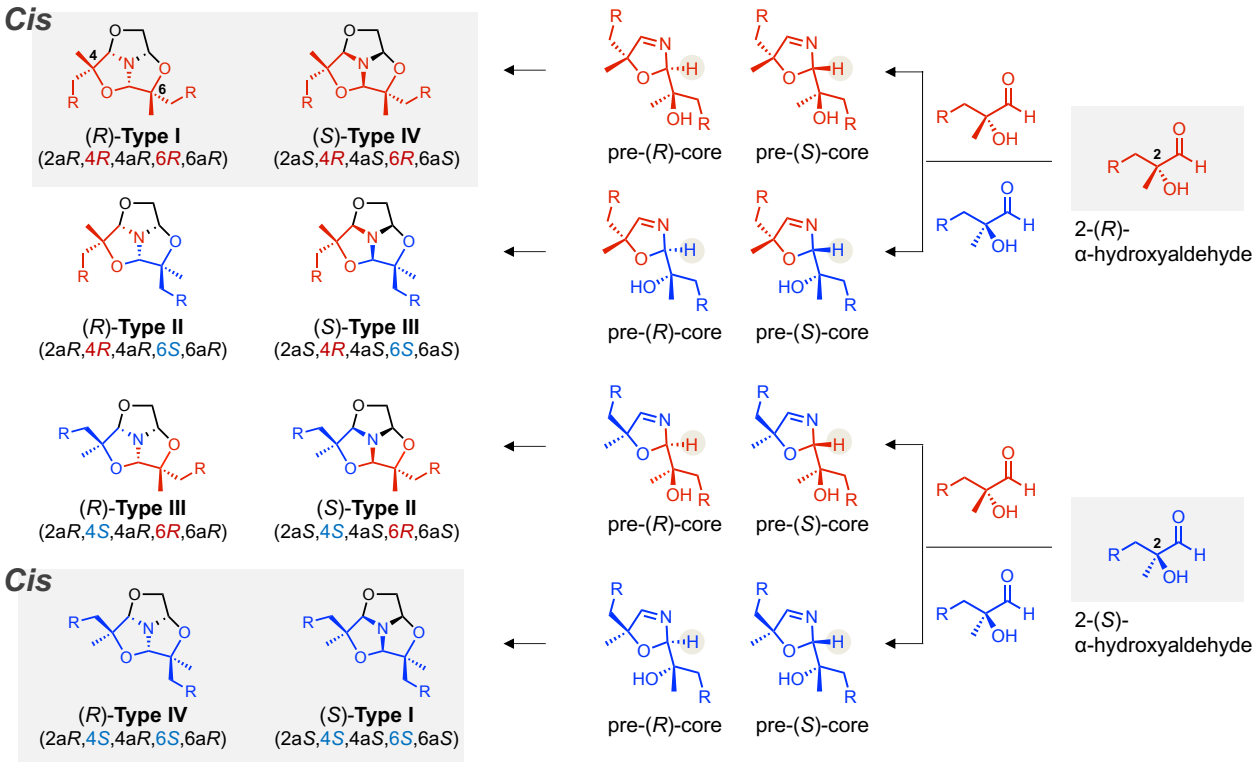

Figure 30. Stereochemistry of TriMERs and those origin

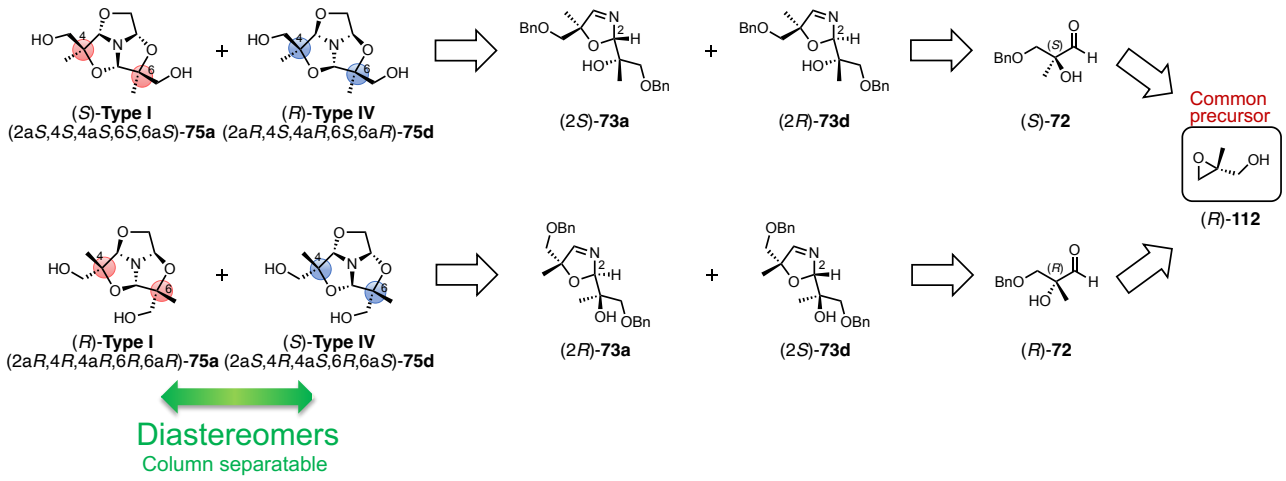

Figure 31. Retrosynthesis of chiral *cis*-TriMERs

The asymmetric synthesis of TriMERs was mainly conducted by following the route of racemic synthesis. The respective chiral α-hydroxyaldehydes **72a** and **72d** were assumed to be obtained from chiral epoxy alcohols (*R*)-**112** as common intermediates, which was prepared by Katsuki–Sharpless asymmetric epoxidation.[93] The advantage of this method is that both enantiomers can be derivatized from the common intermediate more effectively.

The reason for utilizing the Katsuki–Sharpless asymmetric epoxidation is utilized to introduce the chiral center with high enantioselectivity. Although diols can be obtained using Sharpless dihydroxylation, it was not employed as it leads to significantly low enantioselectivity (ca. 45% ee.).[94]

3.5 First asymmetric synthesis of TriMERs

The asymmetric synthesis of the 1,3,5-trioxazatriquinane skeleton was begun with the synthesis of the common intermediate (*R*)-**112**, which was synthesized by Katsuki–Sharpless asymmetric epoxidation[95] with β-methallyl alcohol (**113**)[93] (Table 11). In this reaction, improving the yield was challenging because the low reactivity of the starting material led to long reaction times and the product was unstable. Under general Sharpless epoxidation conditions (Entry 1),[95] few amounts of product was obtained despite taking long reaction times. Considering the decomposition of TBHP, to accelerate reaction times and improve the yields, the reagent equivalents were significantly increased to obtain only the target product with low enantioselectivity.

During this process, the losses in the extraction and purification stages were also improved. Initially, NaOH aq. was used to quench, but the degradation of the product was observed. Thus, the use of milder conditions with Rochelle salt (sodium potassium tartrate) and potassium persulfate was utilized, which reduced the degradation of the target product, and 12% of the target product was isolated. In the purification, a two-step purification step with $P(OMe)_3$ was also conducted (Scheme 10).[96] This method involves the quenching by $P(OMe)_3$ and *in situ* esterification, followed by recrystallization to improve ee. after the hydrolysis to obtain enantiopure epoxy alcohol. However, using this substrate, the by-product obtained from phosphorus was difficult to separate. Although enantioselectivity was 99% ee. after recrystallization (determined by chiral UPLC), the low yield of the subsequent hydrolysis made it challenging to apply. The peroxide was changed to cumene hydroperoxide (CHP), which is more stable for degradation, and the tartaric acid ester was changed from D-DET to D-DIPT, which forms more stable complexes with titanium (Entry 4 and 5). As a result, the reaction times were shortened, the yield was improved (45%), and enantioselectivity was increased (99% ee.). Finally, it was decided to use the purification method with single-column chromatography and distillation purification after epoxidation.

Table 11. Investigation of the Sharpless asymmetric epoxidation

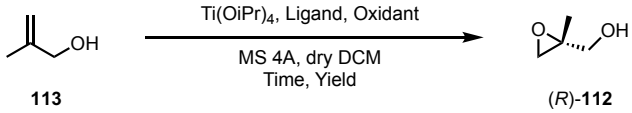

Ent	Ti(O^{i}Pr)	Ligand	Oxidant	**113** : (*R*)-**112**	Time	Yield	*ee.*
1	0.05 eq.	D-DET (0.06 eq.)	TBHP (2.1 eq.)	5:1	48h	–	–
2	0.10 eq.	D-DET (0.15 eq.)	TBHP (2.1 eq.)	2:1	72h	–	–
3	1.00 eq.	D-DET (1.20 eq.)	TBHP (2.1 eq.)	0:100	36h	12%	92%
4	1.00 eq.	D-DET (1.20 eq.)	CHP (2.1 eq.)	0:100	36h	36%	93%
5	0.10 eq.	D-DIPT (1.20 eq.)	CHP (1.5 eq.)	0:100	27h	45%	99%

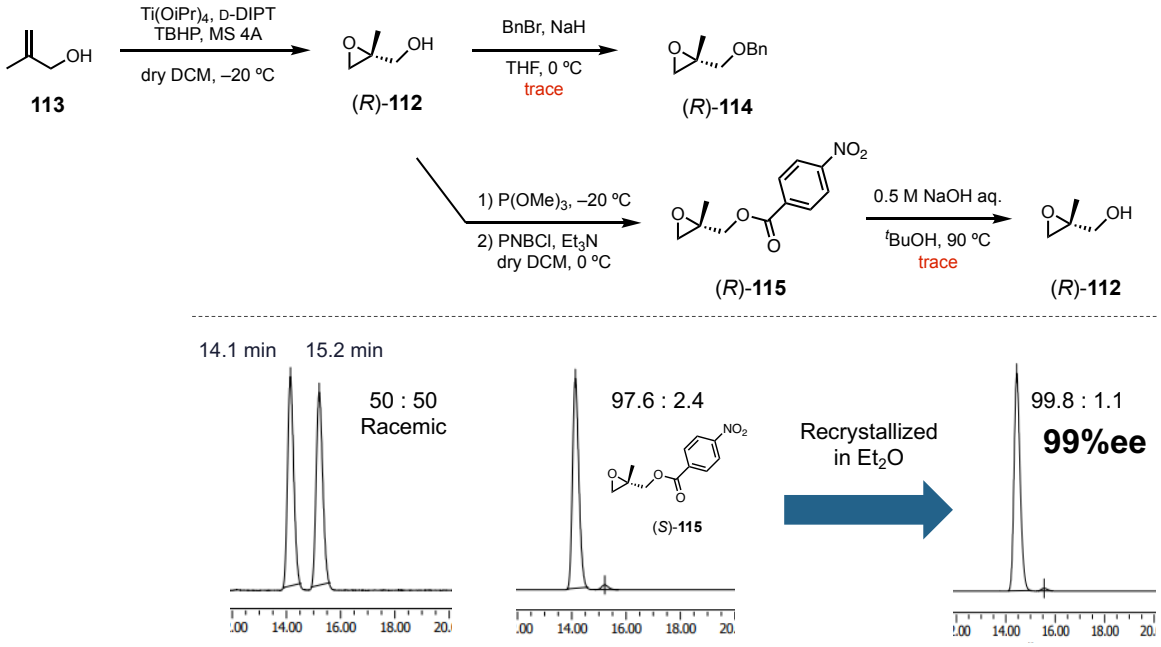

Chiralpak AD-H (Eluent: hexane/2-propanol = 95/5, Flow rate: 1 mL/min, 254 nm)

Scheme 10. Investigation of the purification method

The absolute stereochemistry of (*R*)-**112** (99% ee.) was determined by the Mosher's method,[97] and crude (*R*)-**112** was converted to (*S*)-**116** by condensation with (*S*)-MTPACl (α-methoxy-α-(trifluoromethyl)phenylacetyl chloride) (Scheme 11). For racemic **116**, the epoxide was prepared after epoxidation with β-methallylalcohol with *m*CPBA, and condensation with (*S*)-MTPACl was conducted in the same way. The optical purity of each was confirmed by chiral UPLC, and ee. was determined from the integral ratio of the ^{1}H NMR spectrum of the racemic derivative with reference to that reported previously (Figure 32)[98].

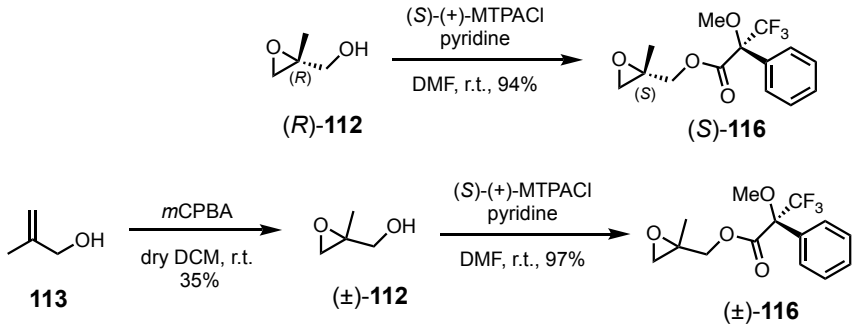

Scheme 11. Synthesis of Mosher's ester

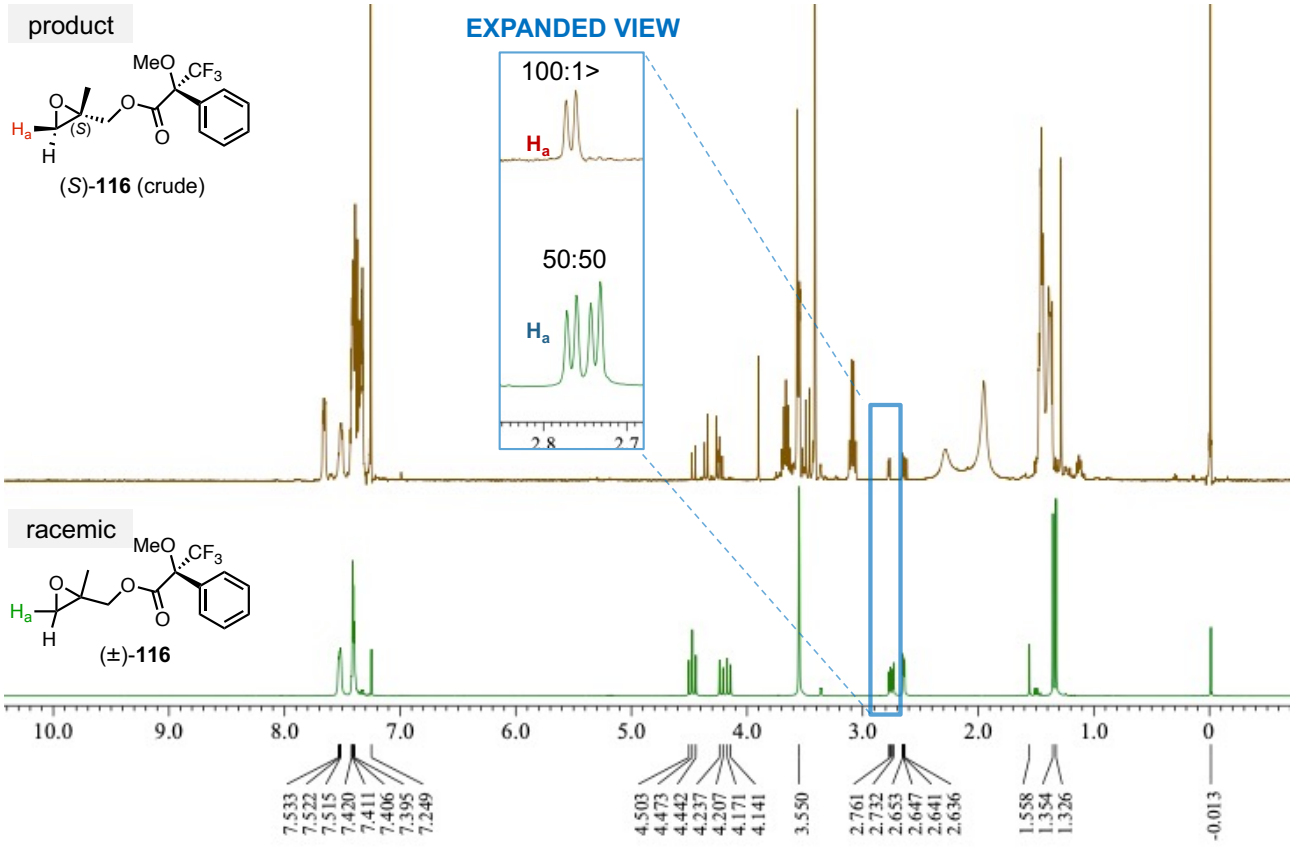

Figure 32. Determination of ee. with Mosher's method

This epoxidation reaction and the following reactions were achieved with 20 g scale. Firstly, diols (–)**75a** and (+)-**75d** were synthesized (Scheme 12a). After the cleavage of the epoxide with BnOH to form a diol (*R*)-**117**, α-hydroxy aldehyde (*S*)-**72** was synthesized by the oxidation of the primary alcohol. As the Swern and Parick-Doering oxidations resulted in complex mixtures, TPAP oxidation was utilized instead, which needed only filtration after the reaction. Optically pure α-hydroxyaldehydes (*S*)-**72** in hand, chiral diols (–)-(2a*S*,4*S*,4a*S*,6*S*,6a*S*)-**75a** and (+)-(2a*R*,4*S*,4a*R*,6*S*,6a*R*)-**75d**, were successfully and stereoselectively obtained using the same three steps as those in the racemic synthesis and after removing the benzyl groups, diols were separated using silica gel chromatography easily. Besides, (2*R*)-**73d** and (2*S*)-**73a** were separated and utilized by the trimerization with the glycolaldehyde dimer (Table 12), but the ratios of the products did not change. Thus, this reaction was conducted with a mixture of diastereomers.

On the other hand, optical pure α-hydroxy aldehyde (*R*)-**72** was synthesized by the benzyl protection of the epoxy alcohol of (*R*)-**113**, followed by hydrolysis and oxidation (Scheme 12b). In this process, the amount of BnBr was important to obtain good yield since excess BnBr can accelerate the reaction but induce the decomposition of the product (Table 13). Subsequently, diols (–)-**75a** and (+)-**75d** were synthesized in the same manner.

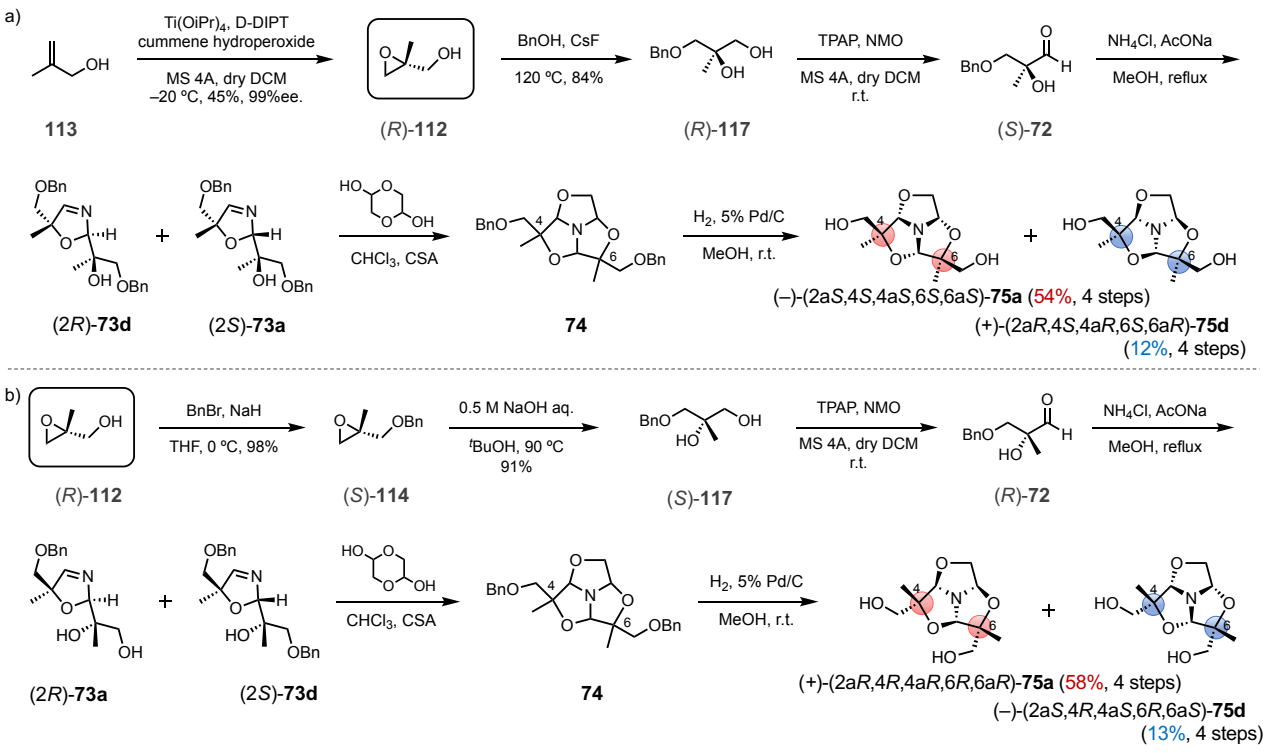

Scheme 12. Asymmetric synthesis of Asymmetric synthesis of (a) (–)-**75a** and (+)-(2aR,4S,4aR,6S,6aR)-**75d**, and (b) (–)-(2aR,4R,4aR,6R,6aR)-**75a** and (+)-(2aS,4R,4aS,6R,6aS)-**75d**

Table 12. Investigation of trimerization with enantiopure oxazolinedimer (2*R*)-**73d** and (2*S*)-**73a**

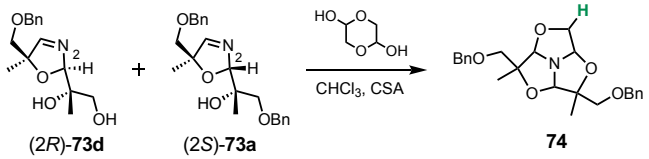

(2*R*)-**73d** (2*S*)-**73a** **74**

SM	Yield	**80a**	**80d**
			^{1}H-NMR ratio
(2*R*)-**73d**	90%	84	16
(2*S*)-**73a**	91%	82	18
73	89%	84	16

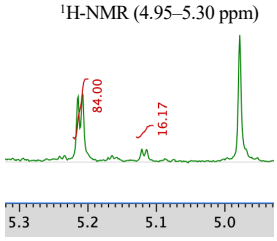

Table 13. Investigation of the benzylation reaction of epoxyalcohol

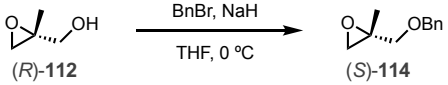

(*R*)-**112** (*S*)-**114**

Entry	NaH (eq.)	BnBr (eq.)	Time	Yield
1	3.0	84	14 h	47%
2	3.0	82	42 h	98%

Finally, the synthesis of optically pure *N*-Boc derivatives (+)-**88a**, (+)-**88d**, (–)-**88a**, and (–)-**88d** along with octane sulfonamide derivatives (+)-**96a**, (+)-**96d**, (–)-**96a**, and (–)-**96d** were accomplished with the same procedure used for the racemic compounds (Scheme 13).

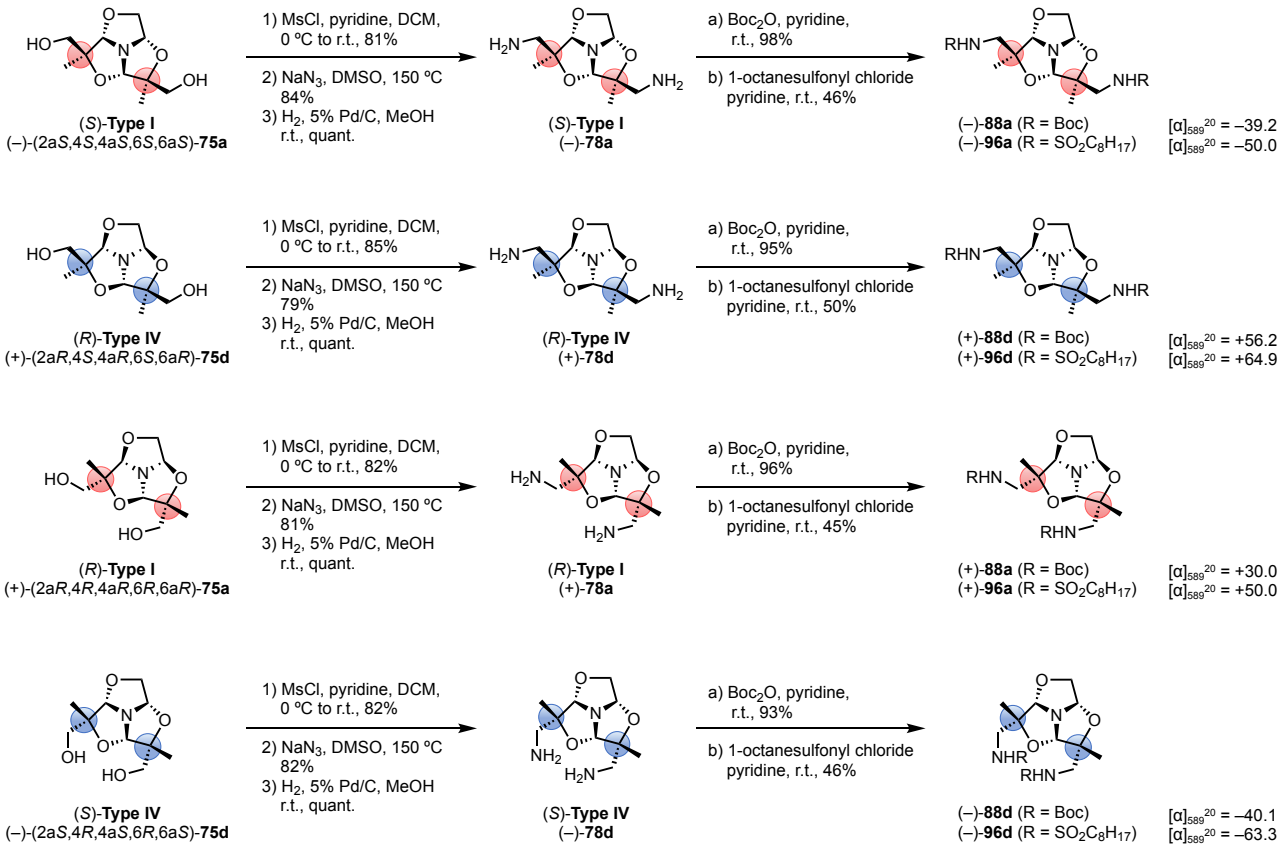

Scheme 13. Synthesis of chiral *cis*-TriMERs carrying Boc and octane sulfonamide groups

3.6 Evaluation of derivatives

The chiral Type-I and Type-IV isomers were evaluated for the OXR agonistic activity *in vitro* (Table 14).

Table 14. Assay results of chiral *cis*-TriMER derivatives for OXR agonist activity

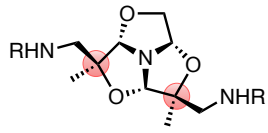

(*S*)-**Type I**
(–)-(2a*S*,4*S*,4a*S*,6*S*,6a*S*)

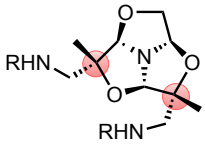

(*R*)-**Type I**
(+)-(2a*R*,4*R*,4a*R*,6*R*,6a*R*)

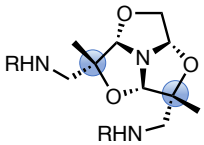

(*S*)-**Type IV**
(–)-(2a*S*,4*R*,4a*S*,6*R*,6a*S*)

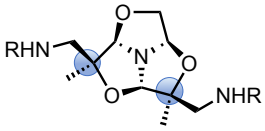

(*R*)-**Type IV**
(+)-(2a*R*,4*S*,4a*R*,6*S*,6a*R*)

Compounds	Core type	**R**	EC_{50} (μM) [E_{max} (%)[a]]	
			OX_1R	OX_2R
(±)-**88a**	(*rac*)-**I**	Boc	_[b] [30.1][c]	_[b] [40.2][c]
(–)-**88a**	(*S*)-**I**	Boc	_[b] [4.97][c]	_[b] [69.4][c]
(+)-**88a**	(*R*)-**I**	Boc	_[b] [3.91]	_[b] [2.71]
(±)-**96a**	(*rac*)-**I**	$SO_2C_8H_{17}$	_[b] [11.8][c]	_[b] [61.2][c]
(–)-**96a**	(*S*)-**I**	$SO_2C_8H_{17}$	_[b] [1.92][c]	_[b] [6.23]
(+)-**96a**	(*R*)-**I**	$SO_2C_8H_{17}$	_[b] [4.86][c]	_[b] [3.95]
(±)-**88d**	(*rac*)-**IV**	Boc	_[b] [54.0][c]	_[b] [171.9][c]
(–)-**88d**	(*S*)-**IV**	Boc	_[b] [4.31][c]	_[b] [2.59][c]
(+)-**88d**	(*R*)-**IV**	Boc	_[b] [5.07]	3.87 ± 0.1760 [105]
(±)-**96d**	(*rac*)-**IV**	$SO_2C_8H_{17}$	_[b] [23.6][c]	_[b] [101.2][c]
(–)-**96d**	(*S*)-**IV**	$SO_2C_8H_{17}$	_[b] [5.29][c]	2.42 ± 0.1730 [97.3]
(+)-**96d**	(*R*)-**IV**	$SO_2C_8H_{17}$	_[b] [5.66][c]	1.62 ± 0.969 [91.4]

[a] E_{max} is expressed as a percentage of the OXA maximum. [b] Not tested due to the low potency. [c] The value obtained 10 μM of each compound was used when the agonist activity of endogenous OXR ligand orexin A (OXA) is s 100%.

As a result, the OX_2R agonists were found in (*R*)-Type-IV core structures, while none of Type-I derivatives showed any OXR agonist activity. In each case, the (+)-isomers ((+)-**88d** (EC_{50} = 3.87 μM) and (+)-**96d** (EC_{50} = 1.62 μM)) with an (*R*)-Type-IV configuration exhibited more potent OX_2R-selective agonist activity than the (–)-isomers which suggested (*R*)-Type-IV was a eutomer. These results suggest that not only the structure of the side chains, but also the stereochemistry of the core structure is important for the expression of OX_2R agonist activity. Intriguingly, octane sulfonamide derivative (–)-**96d** (EC_{50} = 2.42 μM) with an (*S*)-Type-IV configuration (EC_{50} = 2.42 μM for OX_2R) showed higher potency than the eutomer of the Boc derivative (+)-**88d**. The same phenomenon, that the distomer also interacts with the receptor was also observed in the TriMER-type OXR antagonists; DORA (–)-YNT-2293 (**57a**) and 1-SORA (+)-YNT-2294 (**57d**) possess (*S*)-Type-I and (*R*)-Type-IV core structures, respectively, while those enantiomers also show weak but detectable affinity against the receptors. The binding pockets of OX_1R and OX_2R differ in only two residues ($S103^{2.61}$/$T111^{2.61}$ and $A127^{3.33}$/$T135^{3.33}$), which give rise to a larger volume in the OX_1R-binding pocket than that of OX_2R.[65] In our previous docking study, the methyl group on the (*R*)-Type-IV core of TriMER-type antagonist **2** faced $S103^{2.61}$ (OX_1R) consisting of the hydrophobic pocket, which would cause the receptor selectivity over OX_2R due to the steric interactions with spatially more demanding $T111^{2.61}$ residue.[41] In contrast, the agonists found in the present study possess (*S*)- and (*R*)-Type-IV core structures and show OX_2R selectivity. These observations imply that the (*S*)- and (*R*)-Type-IV cores would also occupy a similar binding pocket as (+)-**57d**, albeit that the steric interaction with $T111^{2.61}$ (OX_2R) can be expected to be alleviated through the induced fitting to express the agonist activity due to slim and flexible side-chain residues and octan sulfonamide groups, while the bulky Boc residues on (–)-**88d** with an (*S*)-Type-IV core would prohibit its structural changes. On the other hand, these interactions can be expected to be attenuated due to a larger volume of the binding pocket for OX_1R than for OX_2R, which ultimately does not cause the induced fitting by the OX_1R. Although the docking simulation of these OX_2R agonists has failed due to its flexibility and weak activity, a more detailed discussion will most likely be possible in the near future using more potent derivatives.

3.7 Conclusion

In this chapter, in order to discover the OXR agonists with novel scaffold, the design and synthesis of novel TriMER-type OX_2R agonists based on the TriMER-type OXR antagonists were achieved. The results of docking calculations for TriMER-type OXR antagonists and OXRs suggested that phenyl rings on TriMER inhibited the movement of the receptor, which is required for agonistic activity, because of steric hindrance. Applying the "accessory sites" concept, OXR antagonists were transformed into OX_2R agonists by removing the bulky side chain aromatic rings and adding the amino-methylene units. Therefore, the author designed the novel TriMER bearing the protected diol as an intermediate that is stable enough to modify and can be transformed into various TriMERs, such as aldehyde and triazole.

TriMERs bearing diol group were synthesized in 5 steps according to the authors' previous report.[91] The purification of diols **75a**–**d** was successfully conducted with MPLC, and diols were converted to diamines in 3 steps; mesylation of diol, following substitution with azides and hydrogenation. Subsequently, the condensation reaction afforded to obtain amide, carbamate, and sulfonamide derivatives. *In vitro* assays identified six TriMER derivatives **88d**, **93d**–**96d** and **96a** with a *cis*-side-chain orientation as OX_2R agonists, and, among them, the derivatives with a Type-IV core and Boc (**88d**) and octane sulfonamide (**96d**) groups on the side chains showed full agonist activity against OX_2R at a concentration of 10 μM.

Then, to determine the absolute stereochemistry of eutomers of these OX_2R agonists, the first asymmetric synthesis of the *cis*-TriMERs was performed. After retrosynthetic analysis of each TriMER, it was revealed that the stereochemistry of TriMERs is derived from that of corresponding α-hydroxyaldehydes and *cis*-TriMERs can be synthesized from the corresponding single isomers of α-hydroxyaldehydes, respectively. Therefore, the author devised a new synthetic route using the Katsuki–Sharpless asymmetric epoxidation of β-methallylalcohol because the optically pure (*R*)- and (*S*)-α-hydroxyaldehydes would be obtained from the common epoxy alcohol intermediate, respectively. After obtaining each α-hydroxyaldehydes ((*R*)- and (*S*)-**72**) from a chiral epoxy alcohol (*R*)-**112**, (*S*)-**72** and (*R*)-**72** were converted to chiral TriMERs bearing diol group (–)-**75a** and (+)-**75d**, and (+)-**75a** and (–)-**75d**, which successfully led to each isomer of **88d** and **96d**. As a result of the pharmacological evaluation of each isomer, (+)-**88d** (EC_{50} = 3.87 μM for OX_2R) and (+)-**96d** (EC_{50} = 1.62 μM for OX_2R) were determined as eutomers for OX_2R agonist activity. These results provide a new class of skeleton consisting of an (*R*)-Type IV core with slim methylene linkers and larger hydrophobic substituents at the terminals of the side chains via carbamates/sulfonamides as OX_2R agonists.

Chapter 4 Conclusion

In this dissertation, a novel unique library of 1,3,5-trioxazatriquiunane skeletons called TriMER was designed and synthesized to develop both OXR antagonists and agonists from a single skeleton and achieved the first asymmetric synthesis of TriMERs from chiral α-hydroxy aldehydes. This approach can obtain the hit compound within a high hit-rate and modify the receptor selectivity or affinity utilizing a single skeleton.

In drug discovery research, hit identification is a crucial process to obtain the small molecule bound to the target proteins, which is usually conducted by a high-throughput screening using a large number of compounds (chemical library). However, a HTS utilizing conventional libraries used to have a low hit rate (0.01–0.1%) and thus, a more efficient screening approach is desired. Here, the author focused on "the feature of hit compound" consisting of two factors; 1) pharmacophores that enable interactions with target biomolecules (e.g., hydrogen bond, ionic bond, and hydrophobic interaction), and 2) core scaffold for three-dimensional placement of pharmacophores and designed a novel chemical library that can procreate the hit identification process. To archive such a chemical library, the author particularly aimed the 1,3,5-trioxazatirquinane skeleton that possesses attractive character in medicinal chemistry research, such as 1) it can be synthesized in only four steps *via* a trimerization of α-hydroxyaldehydes derived from the corresponding ketones, 2) six side chains can be arranged three-dimensionally on the rigid bowl-like core scaffold, and 3) a maximum of 16 isomers (8 regioisomers with each enantiomer) can be synthesized at once based on the three quaternary chiral carbon centers and the orientation of the central nitrogen atom (convex or concave) and applied it to discover novel ligands for orexin receptors, which have attracted attention as drug targets for sleep disorders.

In Chapter 2, based on the results that opioid receptors and orexin receptors share ligand scaffolds, the author conceived that the TriMERs bound to opioid receptors also show an affinity against orexin receptors and conducted the design, synthesis, and evaluation of a novel TriMER library. Based on the computational analysis using the PMI ratios of the simple TriMER derivatives, the author focused on a TriMER template with two aromatic rings and one methylene-oxy bridge and designed a novel TriMER library consisting of 72 TriMER derivatives. Then the TriMER library was synthesized from the corresponding nitroacetophenones according to the previous report and evaluated their OXR agonist/antagonistic activities in a CHO cell line stably expressing human OX_1R or OX_2R. As a result of the screening, five hit compounds were identified with a high hit-rate (7%), although none of the tested TriMERs exhibited significant agonistic activity. Most hit compounds commonly had the *cis*-configuration of the side chains and bulky substituents such as benzamide groups at the terminals of the side chains. The optimization of the substituents on the benzamide moiety led to

obtaining potent DORA **52a** and 1-SORA **52d**. The most interesting point is that both antagonists have the same planner structure and the only difference in the stereochemistry on the scaffold (Type-I and Type-IV). As **52a** and **52d** showed reasonable brain permeability and metabolic stability, their *in vivo* effects were evaluated: DORA **52a** showed a significant sleep-inducing effect with EEG/EMG, whereas 1-SORA **52d** suppressed the locomotor activity induced by OXA. Finally, to gain structural insights into the differences between **52a** and **52d** in receptor selectivity, a docking simulation was conducted after the determination of those eutomers. The binding forms of the eutomers (−)-**52a** and (+)-**52d** take a similar U-shape structure in the receptor pockets by flipping the 1,3,5-trioxatriquinane core structure, and the differences between the binding structures of (−)-**52a** and (+)-**52d** suggested that the interaction with ECL2 would be important for the receptor selectivity. The fact that the 1,3,5-trioxatriquinane showed high affinity not only for opioid receptors but orexin receptors suggests that the 1,3,5-trioxatriquinane could be an effective scaffold to explore a novel ligand for GPCRs and the TriMER library approach might be useful for the hit discovery process targeting other GPCRs.

In Chapter 3, the author investigated the conversion study of TriMER-type antagonists into agonists by removing the structural motifs involved in the antagonistic activity as none of the TriMER derivatives in Chapter 2 exhibited OXR agonist activity. Based on the results of the docking simulation of TriMER-type antagonists, the author focused on the phenyl rings directly attached to the 1,3,5-trioxatriquinane core structure as the accessory sites and designed a series of derivatives with a new slim TriMER skeleton. The derivative synthesis was commenced with obtaining TriMERs with a diol group from benzyloxyacetone (**65**) according to the conventional TriMER synthesis followed by conversion of diol to diamine and condensation reactions to obtain amide, carbamate, and sulfonamide derivatives. *In vitro* assays of synthetic TriMER derivatives identified six hit compounds showing the OX_2R agonist activity, especially the derivatives with Boc (**88d**) and octane sulfonamide (**96d**) groups on the side chains showed full agonist activity against OX_2R. Then, to determine the absolute stereochemistry of eutomers of **88d** and **96d**, the first asymmetric synthesis of the 1,3,5-trioxazatriquinane skeleton was conducted using the Katsuki–Sharpless asymmetric epoxidation of β-methallylalcohol as a key step. After obtaining chiral α-hydroxyaldehydes (*S*)-**72** and (*R*)-**72** from a chiral epoxyalcohol (*R*)-**112**, (*S*)-**72** and (*R*)-**72** were then converted to chiral TriMERs bearing diol group (–)-**75a** and (+)-**75d**, and (+)-**75a** and (–)-**75d**, respectively, which successfully led to each isomer of **88d** and **96d**. As a result of the pharmacological evaluation of each isomer, (+)-**88d** (EC_{50} = 3.87 μM for OX_2R) and (+)-**96d** (EC_{50} = 1.62 μM for OX_2R) were determined as eutomers for OX_2R agonist activity. These results provide a new class of skeleton consisting of an (*R*)-Type IV core with slim methylene linkers and larger hydrophobic substituents at the terminals of the side chains via carbamates/sulfonamides as OX_2R agonists.

Conventional libraries used in drug discovery research are huge, expensive, and ordinally suffer from low hit rates. Though especially in the GPCR family accepts ligands of diverse shapes and sizes, the ligand-binding pockets show similarity despite the diversity in the ligands.[99] The achievement of this study shows that TriMERs have a high affinity not only for opioid receptors but orexin receptors and play an important role as a "template compound" that satisfies the two factors required for a hit compound: 1) a pharmacophore which can interact with the target molecule (e.g., hydrophobic interactions or hydrogen bonds), and 2) a core scaffold that allows the pharmacophore to be arranged three-dimensionally. This study offers a novel library template with a high hit rate and rich in three-dimensionality though it is small, as opposed to the conventional "low hit rate libraries" that have required screening of large numbers of compounds. To the best of our knowledge, the chemical library template with a single skeleton adjusting the three-dimensionality has not been discovered previously, therefore this is an innovative method which can efficiently obtain the hit compound with high hit-rate and SAR comparing directly. This research is expected to accelerate drug discovery research as it can streamline the ligand search process, which is a real bottleneck in drug discovery research and enable to be utilized as a screening tool compound that can be applied to other drug targets.

Experimental section

Chemistry

General

All reagents and solvents were purchased from the following commercial suppliers: Tokyo Chemical Industry., Sigma-Aldrich, Inc., Kanto Chemical Co., Inc., Wako Pure Chemical Ind., Ltd., and Nacalai Tesuque. All commercially available chemicals and solvents were used without further purification. In general, reaction mixtures were magnetically stirred at the respective temperature under an argon atmosphere. All synthetic compounds were checked with analytical thin-layer chromatography (TLC, Merck Co., Ltd., Kieselgel 60 F_{254}, 0.25 mm), visualized under UV light at 254 nm and phosphomolybdic acid in a sulfuric acid aqueous solution, Hanessian stain, dinitrophenylhydrazine, potassium permanganate, ninhydrin or *p*-anisaldehyde followed by heating. Column chromatography was carried out on silica gel (a: spherical, neutral, 40–50 μm, Kanto Chemical Co., Japan; b: spherical, neutral, CHROMATOREX PSQ60B, 60 μm, Fuji Silysia Chemical Ltd.). Preparative TLC was performed on Kieselgel 60 F_{254} (0.50 mm) plates (Merck Co., Ltd.). Infrared (IR) spectra were recorded on a JASCO FT/IR-4100Plus. Nuclear magnetic resonance (NMR) spectra were obtained on a JEOL JNM-ECS 400 at 400 MHz for ^{1}H NMR and 100 MHz for ^{13}C NMR. NMR chemical shifts are quoted in ppm using tetramethylsilane (TMS, δ 0 ppm) as the reference for ^{1}H NMR spectroscopy and $CDCl_3$ (δ 77.16 ppm) for ^{13}C NMR spectroscopy. Some compounds were observed as a mixture of rotamers. Gel permeation chromatography (GPC) was performed on SSC-8200-25 recycle HPLC system (Senshu Scientific Co., Ltd) equipped with YMC-GPC T4000 column (10 μm, 600 mm × 20 mm), with UV detection at 254 nm, and RI detection. Mass spectra (MS) were obtained on a JEOL JMS-T100LP spectrometer. The purity (≥95%) of the assayed compounds was determined by analytical HPLC. Analytical HPLC was performed on ACQUITY UPLC system (Waters Co., Ltd) equipped with ACQUITY UPLC BEH C18 column (1.7 μm, 50 mm × 2.1 mm), with PDA detection at 254 nm, at column temperature of 40 ºC. The chiral resolution was performed using SSC-8200-25 recycling preparative HPLC system (Senshu Scientific Co., Ltd.) with a DAICEL CHIRALPAK AD-H (5 μm, 20 mm I.D.×250 mmL), with PDA detection at 254 nm at 25 °C. The optical purity was analyzed using ACQUITY UPLC system (Waters Co., Ltd) with a DAICEL CHIRALPAK AD-H (5 μm, 4.6 mm I.D. × 250 mmL), with PDA detection at 254 nm at 25 °C. Optical rotations were measured with Anton Paar MCP 100 Polarimeter. Circular dichroism (CD) spectra were recorded on J-820 circular dichroism spectropolarimeter (JASCO Co., Ltd.). Measurements were carried out at 20 °C using a 10 mm

quartz cell in a volume of 3.5 mL. Compounds (1.0 mg) were dissolved in MeOH (5.0 mL). The instrument settings were bandwidth, 1.0 nm; data pitch, 0.2 nm; speed, 100 nm/min; accumulation, 16; and wavelengths, 400–220 nm. Chemical names were generated using ChemDraw Professional 15.0 (Perkin-Elmer Informatics).

4,6-Dimethyl-4,6-bis(2-nitrophenyl)hexahydro-1,3,5-trioxa-2a^1-azacyclopenta[*cd*]pentalene (32a–d)

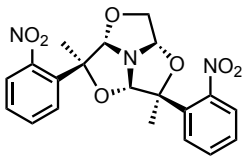

32a

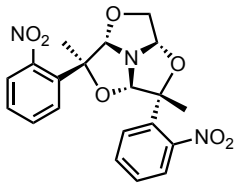

32b

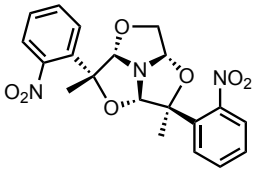

32c

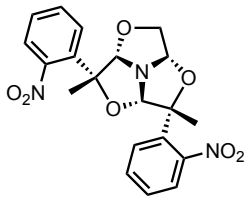

32d

To a solution of potassium *tert*-butoxide (1.56 g, 13.93 mmol) in anhydrous THF (20 mL) were added (methoxymethyl)triphenylphosphonium chloride (5.20 g, 15.14 mmol) at 0 °C under nitrogen flow. After stirring for 1 h, the mixture was added a solution of 2'-nitroacetophenone (**23**) (1.00 g, 6.06 mmol) in 5 mL of anhydrous THF and stirred at room temperature for 8 h. The reaction mixture was poured into water (15 mL) and extracted with $CHCl_3$ (30 mL, 25 mL, 20 mL). The combined organic extracts were dried over anhydrous Na_2SO_4 and concentrated *in vacuo.* The crude product was recrystallized twice from hexane/Et_2O, filtrated, and the filtrate was concentrated. The residue was purified by silica gel chromatography (hexane/ethyl acetate = 20/1) to give the *E*/*Z* mixture of methyl enol ether (976.6 mg, 5.05 mmol) as a yellow oil.

To a solution of the *E*/*Z* mixture of methyl enol ether in 1,2-dichloromethane (25 mL) was added *m*CPBA (1.31 g, 7.58 mmol) at 0 °C and stirred for 1 h and then at room temperature for 9.5 h. The reaction mixture was poured into sat. $Na_2S_2O_3$ aq. solution (30 mL) and extracted with $CHCl_3$ (5 mL, 25 mL, 20 mL). The combined organic layers were washed with brine (5 mL), dried over anhydrous Na_2SO_4, and concentrated *in vacuo.* The residue was purified by silica gel chromatography (hexane/ethyl acetate = 5/1) to give the mixture of epoxide (1.68 g) as a colorless solid.

To a solution of the epoxide mixture in THF (5 mL) was added 2 M HCl aqueous solution (8 mL) at room temperature and the mixture was stirred at 60 °C for 8 h under Ar atmosphere. After cooling to room temperature, the mixture was neutralized with saturated $NaHCO_3$ aqueous solution (12 mL) and extracted with $CHCl_3$ (25 mL, 25 mL, 20 mL). The combined organic layers were dried over anhydrous Na_2SO_4 and concentrated *in vacuo* to obtain the crude mixture of α-hydroxyaldehyde **26** (1.15 g), which was used in the next reaction without further purification.

To a solution of the crude mixture of α-hydroxyaldehyde **26** (986.6 mg) in MeOH (20 mL) were added NH_4Cl (1.25 g, 15.17 mmol) and NaOAc (406.5 mg, 7.58 mmol) at room temperature and the mixture was refluxed for 4 h under Ar atmosphere. After cooling to room temperature, MeOH was removed under reduced pressure. The residue was poured into sat. $NaHCO_3$ aq. solution (10 mL) and extracted with $CHCl_3$ (30 mL, 25 mL, 20 mL). The combined organic layers were dried over anhydrous Na_2SO_4 and concentrated *in vacuo.* The residue was purified by silica gel

chromatography (hexane/ethyl acetate = 2/1) to give the isomeric mixture of **29** (840.3 mg, 2.26 mmol, 37% in 4 steps) as a brown amorphous.

To a solution of the isomeric mixture of **29** (840.3 mg, 2.26 mmol) in $CHCl_3$ (10 ml) were added glycolaldehyde dimer (273.8 mg, 2.26 mmol) and 10-camphorsulfonic acid (1.05 g, 4.53 mmol) at room temperature and the mixture was stirred at the same temperature for 14 h under Ar atmosphere. The reaction mixture was poured into sat. $NaHCO_3$ aq. solution (15 mL) and extracted with $CHCl_3$ (10 mL, 25 mL, 20 mL). The combined organic layers were washed with brine (15 mL), dried over anhydrous Na_2SO_4 and concentrated *in vacuo*. The residue was purified by silica gel column chromatography (hexane/ethyl acetate = 5/1) and recycle GPC ($CHCl_3$) to obtain compounds **32a** (371.9 mg, 36%), **32b** (222.1 mg, 21%), **32c** (75.7 mg, 7%) and **32d** (35.7 mg, 3%) as a colorless solid, respectively.

32a

IR (KBr, cm^{-1}) 2952, 1531, 1375, 1106.

^1H NMR (400 MHz, $CDCl_3$) δ 1.79 (s, 3H), 1.87 (s, 3H), 3.75 (dd, *J* = 3.2, 10.1 Hz, 1H), 4.21 (d, *J* = 10.1 Hz, 1H), 4.89 (d, *J* = 3.2 Hz, 1H), 5.06 (s, 2H), 7.37–7.40 (m, 1H), 7.43–7.61 (m, 7H).

^{13}C NMR (100 MHz, $CDCl_3$) δ 23.4, 23.6, 71.4, 86.9, 87.5, 96.3, 99.6, 100.8, 124.3, 124.6, 127.7, 127.9, 128.9, 129.2, 131.7, 132.0, 134.7, 135.0, 149.3, 149.4.

HR-MS (ESI): Calcd for $C_{20}H_{19}N_3NaO_7$ $[M+Na]^+$, 436.1121. Found, 436.1121.

32b

IR (KBr, cm^{-1}) 2939, 1529, 1360, 1111.

^1H NMR (400 MHz, $CDCl_3$) δ 1.60 (s, 3H), 1.66 (s, 3H), 3.85 (dd, *J* = 2.8, 10.1 Hz, 1H), 4.26 (d, *J* = 10.1 Hz, 1H), 4.96 (s, 1H), 5.09 (s, 1H), 5.22 (d, *J* = 2.8 Hz, 1H), 7.42–7.48 (m, 2H), 7.61–7.64 (m, 1H), 7.68–7.74 (m, 2H), 7.78–7.83 (m, 2H), 7.88–7.90 (m, 1H).

^{13}C NMR (100 MHz, $CDCl_3$) δ 23.16, 23.20, 71.5, 88.1, 88.2, 94.6, 98.7, 100.1, 124.3, 125.7, 128.1, 128.2, 129.0, 129.6, 132.7, 133.6, 136.2, 136.3, 148.0, 148.6.

HR-MS (ESI): Calcd for $C_{20}H_{19}N_3NaO_7$ $[M+Na]^+$, 436.1121. Found, 436.1120.

32c

IR (KBr, cm^{-1}) 2943, 1528, 1364, 1108.

^{1}H NMR (400 MHz, $CDCl_3$) δ 1.78 (s, 3H), 1.83 (s, 3H), 3.67 (dd, *J* = 2.8, 10.4 Hz, 1H), 3.99 (d, *J* = 10.4 Hz, 1H), 4.90 (d, *J* = 2.8 Hz, 1H), 5.13 (s, 1H), 5.40 (s, 1H), 7.41–7.48 (m, 2H), 7.57–7.66 (m, 4H), 7.76–7.78 (m, 1H), 7.94–7.96 (m, 1H).

^{13}C NMR (100 MHz, $CDCl_3$) δ 23.4, 23.8, 71.7, 87.7, 87.9, 95.7, 98.1, 100.8, 124.5, 124.9, 127.8, 128.4, 129.1, 129.5, 132.1, 132.9, 135.4, 136.4, 147.9, 149.3.

HR-MS (ESI): Calcd for $C_{20}H_{19}N_3NaO_7$ $[M+Na]^+$, 436.1121. Found, 436.1136.

32d

IR (KBr, cm^{-1}) 2945, 1525, 1358, 1106.

^{1}H NMR (400 MHz, $CDCl_3$) δ 1.70 (s, 3H), 1.79 (s, 3H), 3.75 (dd, *J* = 2.8, 10.1 Hz, 1H), 4.02 (d, *J* = 10.1 Hz, 1H), 5.16 (s, 1H), 5.27 (d, *J* = 2.8 Hz, 1H), 5.43 (s, 1H), 7.21–7.32 (m, 3H), 7.40–7.44 (m, 1H), 7.52–7.56 (m, 1H), 7.65–7.67 (m, 1H), 7.79–7.83 (m, 1H).

^{13}C NMR (100 MHz, $CDCl_3$) δ 23.2, 23.4, 71.8, 88.1, 88.3, 94.4, 97.7, 100.5, 124.2, 124.3, 128.1, 128.2, 129.4, 129.8, 132.9, 136.3, 136.8, 147.5, 148.1.

HR-MS (ESI): Calcd for $C_{20}H_{19}N_3NaO_7$ $[M+Na]^+$, 436.1121. Found, 436.1105.

4,6-Dimethyl-4,6-bis(3-nitrophenyl)hexahydro-1,3,5-trioxa-2a^1-azacyclopenta[*cd*]pentalene (33a–d)

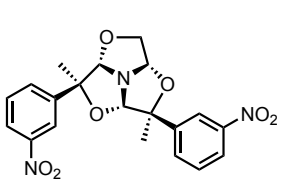

33a

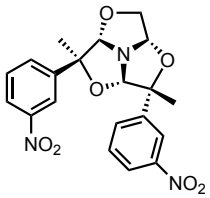

33b

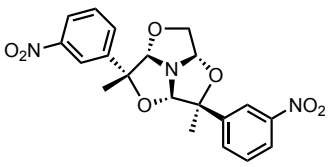

33c

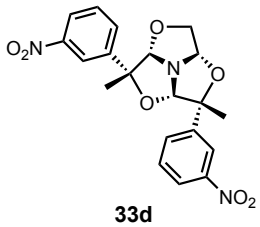

33d

To a solution of 3'-nitroacetophenone (**24**) (3.05 g, 18.5 mmol) in MeOH (90 mL) were added *p*-toluene sulfonylmethyl isocyanide (TosMIC, 7.21 g, 36.9 mmol) and K_2CO_3 (5.10 g, 36.9 mmol) at room temperature and the mixture was stirred for 18 h at the same temperature under Ar atmosphere. After removal of MeOH under reduced pressure, the residue was poured into brine (40 mL) and extracted with $CHCl_3$ (80 mL, 60 mL, 40 mL). The combined organic extracts were dried over anhydrous Na_2SO_4 and concentrated *in vacuo* to obtain the crude mixture of oxazoline (5.61 g), which was used in the next reaction without further purification.

To a solution of the crude mixture of oxazoline (5.61 g) in THF (15 mL) was added 2 M HCl (24 mL) at room temperature and the mixture was stirred at 60 °C for 5.5 h under Ar atmosphere. After cooling to room temperature, the mixture was neutralized with saturated $NaHCO_3$ aqueous solution (30 mL) and extracted with $CHCl_3$ (85 mL, 80 mL, 60 mL). The combined organic layers were dried over anhydrous Na_2SO_4 and concentrated *in vacuo* to obtain the crude mixture of α-hydroxyaldehyde **27** (4.37 g), which was used in the next reaction without further purification.

To a solution of the crude mixture of α-hydroxyaldehyde **27** (4.37 g) in MeOH (30 mL) were added NH_4Cl (1.99 g, 37.3 mmol) and NaOAc (6.12 g, 74.6 mmol) at room temperature and the mixture was refluxed for 4 h under Ar atmosphere. After cooling to room temperature, MeOH was removed under reduced pressure. The residue was poured into saturated $NaHCO_3$ aqueous solution (30 mL) and extracted with $CHCl_3$ (80 mL, 60 mL, 40 mL). The combined organic layers were washed with brine (10 mL), dried over anhydrous Na_2SO_4, and concentrated *in vacuo.* The residue was purified by silica gel chromatography (hexane/ethyl acetate = 2/1) to give the isomeric mixture of **30** (2.98g, 8.03 mmol, 87% in 3 steps) as a brown amorphous.

To a solution of isomeric mixture of **30** (2.48 g, 6.67 mmol) in $CHCl_3$ (10 ml) were added glycolaldehyde dimer (273.8 mg, 2.26 mmol) and 10-camphorsulfonic acid (1.05 g, 4.53 mmol) at room temperature and the mixture was stirred at the same temperature for 14 h under Ar atmosphere. The reaction mixture was poured into sat. $NaHCO_3$ aq. solution (15 mL) and extracted with $CHCl_3$ (10 mL, 25 mL, 20 mL). The combined organic layers were washed with brine (15 mL), dried over anhydrous Na_2SO_4, and concentrated *in vacuo*. The residue was purified by silica

gel column chromatography (hexane/ethyl acetate = 5/1) and recycle GPC ($CHCl_3$) to obtain compounds **33a** (0.57g, 18%), **33b** (0.50 g, 16%), **33c** (0.38 g, 12%) and **33d** (0.48 g, 15%) as colorless solid, respectively.

33a

IR (KBr, cm^{-1}) 2929, 1526, 1450, 1350, 1102.

^1H NMR (400 MHz, $CDCl_3$) δ 1.72 (s, 6H), 3.85 (dd, *J* = 2.8, 10.0 Hz, 1H), 4.35 (d, *J* = 10.0 Hz, 1H), 5.04 (d, *J* = 2.8 Hz, 1H), 5.08 (s, 1H), 5.14 (s, 1H), 7.56 (dd, *J* = 8.0, 16.0 Hz, 1H), 7.62 (dd, *J* = 8.0, 16.0 Hz, 1H), 7.69–7.72 (m, 1H), 7.80–7.83 (m, 1H), 8.13–8.16 (m, 1H), 8.19–8.21 (m, 1H), 8.28–8.29 (m, 1H), 8.34–8.35 (m, 1H).

^{13}C NMR (100 MHz, $CDCl_3$) δ 24.21, 24.22, 71.5, 86.8, 87.2, 95.6, 99.8, 101.2, 120.2 (×2), 122.9, 123.0, 129.9, 130.1, 131.2, 131.4, 144.7, 144.8, 148.7, 148.8.

HR-MS (ESI): Calcd for $C_{20}H_{19}N_3NaO_7$ $[M+Na]^+$, 436.1121. Found, 436.1111.

33b

IR (KBr, cm^{-1}) 2901, 1526, 1352, 1116.

^1H NMR (400 MHz, $CDCl_3$) δ 1.47 (s, 3H), 1.65 (s, 3H), 3.94 (dd, *J* = 2.8, 10.0 Hz, 1H), 4.42 (d, *J* = 10.0 Hz, 1H), 4.86 (s, 1H), 5.16 (s, 1H), 5.33 (d, *J* = 2.8 Hz, 1H), 7.54–7.60 (m, 2H), 7.64–7.66 (m, 1H), 8.14–8.17 (m, 2H) 8.19–8.22 (m, 1H), 8.40 (m, 1H).

^{13}C NMR (100 MHz, $CDCl_3$) δ 22.6, 23.9, 71.5, 86.7, 87.1, 95.3, 100.1, 101.3, 120.1, 121.6, 122.7, 122.9, 128.9, 129.9, 131.1, 132.5, 142.7, 144.6, 148.2, 148.6.

HR-MS (ESI): Calcd for $C_{20}H_{19}N_3NaO_7$ $[M+Na]^+$, 436.1121. Found, 436.1119.

33c

IR (KBr, cm^{-1}) 2903, 1529, 1351, 1106.

^1H NMR (400 MHz, $CDCl_3$) δ 1.72 (s, 3H), 1.77 (s, 3H), 3.70 (dd, *J* = 2.8, 10.1 Hz, 1H), 4.13 (d, *J* = 10.5 Hz, 1H), 4.93 (s, 1H), 5.08 (d, *J* = 2.8 Hz, 1H), 5.46 (s, 1H), 7.56–7.64 (m, 2H), 7.81–7.83 (m, 2H), 8.18–8.22 (m, 2H), 8.35–8.37 (m, 2H).

^{13}C NMR (100 MHz, $CDCl_3$) δ 23.3, 24.6, 71.7, 86.8, 87.3, 95.3, 99.8, 101.7, 120.4, 121.0, 122.7, 122.9, 129.2, 130.0, 131.4, 132.0, 143.2, 144.9, 148.3, 148.8.

HR-MS (ESI): Calcd for $C_{20}H_{19}N_3NaO_7$ $[M+Na]^+$, 436.1121. Found, 436.1115.

33d

IR (KBr, cm^{-1}) 2914, 1524, 1353, 1110.

^{1}H NMR (400 MHz, $CDCl_3$) δ 1.59 (s, 3H), 1.77 (s, 3H), 3.78 (dd, *J* = 2.8, 10.5 Hz, 1H), 4.20 (d, *J* = 10.7 Hz, 1H), 4.94 (s, 1H), 5.21 (s, 1H), 5.38 (d, *J* = 2.8 Hz, 1H), 7.37–7.44 (m, 2H), 7.66 (dd, *J* = 8.2, 16.0 Hz, 1H), 7.88 (m, 1H), 7.93–7.96 (m, 1H), 8.06–8.09 (m, 1H), 8.24–8.27 (m, 1H), 8.35 (m, 1H).

^{13}C NMR (100 MHz, $CDCl_3$) δ 22.4, 22.9, 71.7, 86.8, 86.9, 95.1, 100.2, 101.7, 121.05, 121.04, 122.5, 122.8, 129.0, 129.2, 131.6, 132.5, 142.9, 148.0, 148.2.

HR-MS (ESI): Calcd for $C_{20}H_{19}N_3NaO_7$ $[M+Na]^+$, 436.1121. Found, 436.1129.

4,6-Dimethyl-4,6-bis(4-nitrophenyl)hexahydro-1,3,5-trioxa-2a[1]-azacyclopenta[*cd*]pentalene (34a–d)

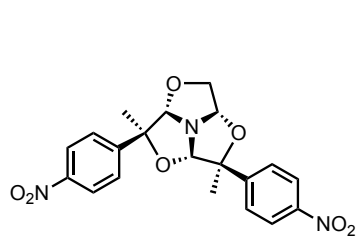

34a

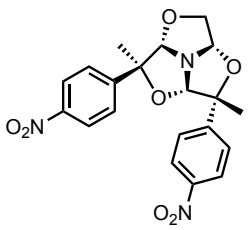

34b

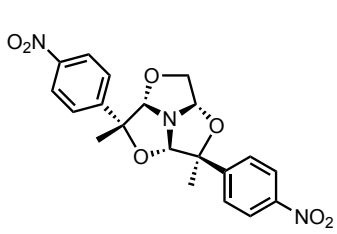

34c

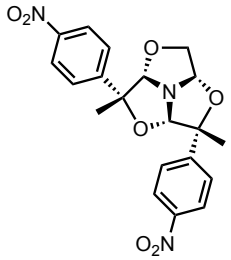

34d

According to the synthetic protocol of **33a**–**d**, 4'-nitroacetophenone (**24**, 1.00 g, 6.06 mmol) was converted to compound **34a** (0.34 g, 27%), **34b** (0.28 g, 22%), **34c** (0.10 g, 12%) and **34d** (0.13 g, 18%) as colorless solid, respectively.

34a

IR (KBr, cm^{-1}) 2917, 1517, 1348, 1116.

^{1}H NMR (400 MHz, $CDCl_3$) δ 1.699 (s, 3H), 1.704 (s, 3H), 3.84 (dd, *J* = 2.8, 10.1 Hz, 1H), 4.33 (d, *J* = 10.1 Hz, 1H), 5.02 (d, *J* = 2.8 Hz, 1H), 5.08 (s, 1H), 5.11 (s, 1H), 7.56–7.58 (m, 2H), 7.63–7.65 (m, 2H), 8.20–8.23 (m, 2H), 8.26–8.28 (m, 2H).

^{13}C NMR (100 MHz, $CDCl_3$) δ 24.11, 24.14, 71.4, 87.1, 87.5, 95.5, 99.6, 101.2, 124.0, 124.2, 126.1, 126.2, 147.5, 147.6, 149.6, 149.7.

HR-MS (ESI): Calcd for $C_{20}H_{19}N_3NaO_7$ $[M+Na]^+$, 436.1121. Found, 436.1111.

34b

IR (KBr, cm^{-1}) 2926, 1519, 1116.

^{1}H NMR (400 MHz, $CDCl_3$) δ 1.43 (s, 3H), 1.62 (s, 3H), 3.93 (dd, *J* = 2.8, 10.1 Hz, 1H), 4.39 (d, *J* = 10.1 Hz, 1H), 4.88 (s, 1H), 5.14 (s, 1H), 5.33 (d, *J* = 2.8 Hz, 1H), 7.47–7.49 (m, 2H), 7.66–7.69 (m, 2H), 8.22–8.27 (m, 4H).

^{13}C NMR (100 MHz, $CDCl_3$) δ 22.9, 23.8, 71.4, 87.1, 87.3, 95.4, 100.2, 101.1, 123.3, 124.0, 126.0, 127.0, 147.4, 147.6, 148.0, 149.5.

HR-MS (ESI): Calcd for $C_{20}H_{19}N_3NaO_7$ $[M+Na]^+$, 436.1121. Found, 436.1127.

34c

IR (KBr, cm^{-1}) 2925, 1520, 1349, 1122.

^{1}H NMR (400 MHz, $CDCl_3$) δ 1.69 (s, 3H), 1.74 (s, 3H), 3.70 (dd, *J* = 2.8, 10.1 Hz, 1H), 4.11 (d, *J* = 10.1 Hz, 1H), 4.94 (s, 1H), 5.07 (d, *J* = 2.8 Hz, 1H), 5.45 (s, 1H), 7.65 (d, *J* = 8.2 Hz, 4H), 8.26 (d, *J* = 9.2 Hz, 2H), 8.28 (d, *J* = 9.2 Hz, 2H).

^{13}C NMR (100 MHz, $CDCl_3$) δ 23.3, 24.4, 71.7, 87.1, 87.6, 95.3, 99.7, 101.8, 123.5, 124.1, 126.2, 126.7, 147.3, 147.6, 148.3, 149.8.

HR-MS (ESI): Calcd for $C_{20}H_{19}N_3NaO_7$ $[M+Na]^+$, 436.1121. Found, 436.1117.

34d

IR (KBr, cm^{-1}) 2930, 1520, 1350, 1118.

^{1}H NMR (400 MHz, $CDCl_3$) δ 1.57 (s, 3H), 1.72 (s, 3H), 3.79 (dd, *J* = 2.8, 10.1 Hz, 1H), 4.17 (d, *J* = 10.1 Hz, 1H), 4.97 (s, 1H), 5.26 (s, 1H), 5.37 (d, *J* = 2.8 Hz, 1H), 7.15–7.17 (m, 2H), 7.66–7.68 (m, 2H), 8.09–8.11 (m, 2H), 8.26–8.28 (m, 2H).

^{13}C NMR (100 MHz, $CDCl_3$) δ 23.0, 23.2, 71.7, 87.21, 87.24, 95.2, 100.3, 101.7, 123.3, 123.4, 126.4, 126.9, 147.2, 147.4, 148.0, 148.3.

HR-MS (ESI): Calcd for $C_{20}H_{19}N_3NaO_7$ $[M+Na]^+$, 436.1121. Found, 436.1099.

2,2'-((2*aS/R*,4*S/R*,4*aS/R*,6*S/R*,6*aS/R*)-4,6-Dimethylhexahydro-1,3,5-trioxa-2a^1-azacyclopenta[*cd*] pentalene-4,6-diyl)dianiline (35a)

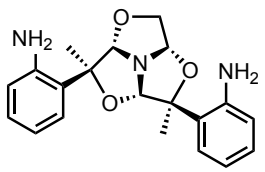

To a solution of **32a** (107 mg, 0.258 mmol) in ethyl acetate (20 mL) was added 5% Pd/C (Degussa type, 109.1 mg, 19.9 mol%) at room temperature. The mixture was stirred for 17 h at the same temperature under hydrogen atmosphere (balloon pressure). The reaction mixture was filtrated with Celite and the filtrate was concentrated *in vacuo*. The residue was purified by silica gel column chromatography (chloroform/methanol = 40/1) to give **35a** (91.1 mg, 100%) as a colorless amorphous.

IR (KBr, cm^{-1}) 3477, 3375, 2933, 1127.

^{1}H NMR (400 MHz, $CDCl_3$) δ 1.73 (s, 3H), 1.75 (s, 3H), 3.79 (dd, *J* = 2.8, 10.1 Hz, 1H), 4.23 (d, *J* = 10.1 Hz, 1H), 4.58 (brs, 4H), 4.92 (d, *J* = 2.8 Hz, 1H), 5.26 (s, 1H), 5.41 (s, 1H), 6.59–6.64 (m, 2H), 6.67–6.74 (m, *2*H), 6.98–7.05 (m, 2H), 7.08–7.13 (m, 2H).

^{13}C NMR (100 MHz, $CDCl_3$) δ 20.2, 20.9, 70.6, 87.3, 87.7, 95.1, 97.0, 99.6, 117.6, 117.7, 117.9, 118.0, 123.7, 123.8, 126.2, 126.4, 128.8, 145.1, 145.2.

HR-MS (ESI): Calcd for $C_{20}H_{23}N_3NaO_3$ $[M+Na]^+$, 376.1637. Found, 376.1651.

2,2'-((2*aS/R*,4*R/S*,4*aS/R*,6*S/R*,6*aS/R*)-4,6-Dimethylhexahydro-1,3,5-trioxa-2a^1-azacyclopenta[*cd*] pentalene-4,6-diyl)dianiline (35b)

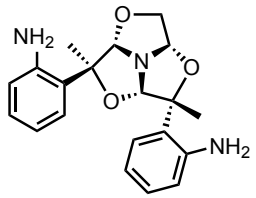

According to the synthetic protocol of **35a**, **32b** (172 mg, 0.417 mmol) was converted to **35b** (138 mg, 94%) as a pale-brown amorphous.

IR (KBr, cm^{-1}) 3469, 3378, 2931, 1114.

^{1}H NMR (400 MHz, $CDCl_3$) δ 1.56 (s, 3H), 1.61 (s, 3H), 3.90 (dd, *J* = 2.8, 10.1 Hz, 1H), 4.29 (d, *J* = 10.1 Hz, 1H), 4.44 (brs, 2H), 4.52 (brs, 2H), 4.88 (s, 1H), 5.35 (d, *J* = 2.8 Hz, 1H), 5.45 (s, 1H), 6.64–6.73 (m, 4H), 7.04–7.14 (m, 4H).

^{13}C NMR (100 MHz, $CDCl_3$) δ 20.4, 22.2, 70.8, 87.4, 89.1, 95.1, 99.0, 99.7, 117.5, 117.6, 117.85, 117.89, 123.5, 124.7, 126.0, 127.4, 128.2, 128.9, 145.2, 145.3.

HR-MS (ESI): Calcd for $C_{20}H_{23}N_3NaO_3$ $[M+Na]^+$, 376.1637. Found, 376.1651.

2,2'-((2*aS/R*,4*S/R*,4*aS/R*,6*R/S*,6*aS/R*)-4,6-Dimethylhexahydro-1,3,5-trioxa-2a^1-azacyclopenta[*cd*] pentalene-4,6-diyl)dianiline (35c)

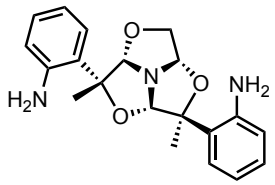

According to the synthetic protocol of **35a**, **32c** (136 mg, 0.329 mmol) was converted to **35c** (112 mg, 96%) as a pale-brown amorphous.

IR (KBr, cm^{-1}) 3467, 3378, 2929, 1118.

^{1}H NMR (400 MHz, $CDCl_3$) δ 1.69 (s, 3H), 1.75 (s, 3H), 3.75 (dd, *J* = 2.8, 10.1 Hz, 1H), 4.17 (d, *J* = 10.1Hz, 1H), 4.52 (brs, 4H), 4.95 (d, *J* = 2.8 Hz, 1H), 5.11 (s, 1H), 5.69 (s, 1H), 6.64–6.69 (m, 2H), 6.72–6.78 (m, 2H), 7.05–7.12 (m, 2H), 7.19–7.21 (m, 2H).

^{13}C NMR (100 MHz, $CDCl_3$) δ 20.9, 22.1, 71.2, 88.0, 88.8, 94.8, 97.2, 102.1, 117.7, 118.0, 123.8, 126.3, 127.7, 128.4, 128.9, 145.2.

HR-MS (ESI): Calcd for $C_{20}H_{23}N_3NaO_3$ $[M+Na]^+$, 376.1637. Found, 376.1637.

2,2'-((2*aS/R*,4*R/S*,4*aS/R*,6*R/S*,6*aS/R*)-4,6-Dimethylhexahydro-1,3,5-trioxa-2a^1-azacyclopenta[*cd*] pentalene-4,6-diyl)dianiline (35d)

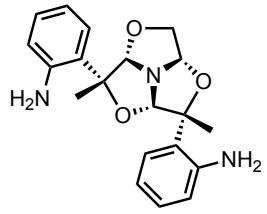

According to the synthetic protocol of **35a**, **32d** (28.0 mg, 0.0677 mmol) was converted to **35d** (22.1 mg, 92%) as a colorless amorphous.

IR (KBr, cm^{-1}) 3460, 3374, 2927, 1118.

^{1}H NMR (400 MHz, $CDCl_3$) δ 1.63 (s, 3H), 1.69 (s, 3H), 3.83 (dd, *J* = 2.8, 10.4 Hz, 1H), 4.18 (brs, 4H), 4.23 (d, *J* = 10.4 Hz, 1H), 5.12 (s, 1H), 5.33 (s, 1H), 5.35 (d, *J* = 2.8 Hz, 1H), 6.49–6.51 (m, 1H), 6.61–6.71 (m, 3H), 6.94–6.99 (m, 2H), 7.04 (ddd, *J* = 1.2, 7.6, 7.6 Hz, 1H), 7.17–7.24 (m, 1H).

^{13}C NMR (100 MHz, $CDCl_3$) δ 22.0, 22.7, 71.3, 89.3, 89.6, 94.8, 100.3, 102.4, 117.3, 117.5, 117.77, 117.82, 117.96, 117.99, 127.6, 127.7, 128.2, 128.4, 145.3, 145.4.

HR-MS (ESI): Calcd for $C_{20}H_{23}N_3NaO_3$ $[M+Na]^+$, 376.1637. Found, 376.1632.

3,3'-((2*aS/R*,4*S/R*,4*aS/R*,6*S/R*,6*aS/R*)-4,6-Dimethylhexahydro-1,3,5-trioxa-2a^1-azacyclopenta[*cd*] pentalene-4,6-diyl)dianiline (36a)

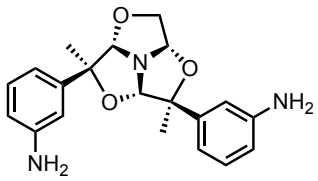

According to the synthetic protocol of **35a**, **33a** (106.7 mg, 0.258 mmol) was converted to **36a** (91.1 mg, 100%) as a colorless amorphous.

IR (KBr, cm^{-1}) 3444, 3365, 2932, 1110.

^{1}H NMR (400 MHz, $CDCl_3$) δ 1.641 (s, 3H), 1.644 (s, 3H), 3.66 (brs, 2H), 3.71 (brs, 2H), 3.77 (dd, *J* = 2.8, 10.1 Hz, 1H), 4.25 (d, *J* = 10.1 Hz, 1H), 5.03 (d, *J* = 2.8 Hz, 1H), 5.09 (s, 1H), 5.11 (s, 1H), 6.54–6.57 (m, 1H), 6.59–6.62 (m, 1H), 6.70–6.71 (m, 1H), 6.73–6.75 (m, 1H), 6.78–6.82 (m, 2H), 7.10 (dd, *J* = 8.0, 8.0 Hz, 1H), 7.16 (dd, *J* = 8.0, 8.0 Hz, 1H).

^{13}C NMR (100 MHz, $CDCl_3$) δ 24.2, 24.3, 71.2, 86.7, 87.3, 95.1, 99.4, 101.4, 111.7, 111.8, 114.3, 114.4, 115.4, 115.5, 129.6, 129.7, 143.8, 146.6, 146.7.

HR-MS (ESI): Calcd for $C_{20}H_{23}N_3NaO_3$ $[M+Na]^+$, 376.1637. Found, 376.1646.

3,3'-((2*aS/R*,4*R/S*,4*aS/R*,6*S/R*,6*aS/R*)-4,6-Dimethylhexahydro-1,3,5-trioxa-2a^1-azacyclopenta[*cd*] pentalene-4,6-diyl)dianiline (36b)

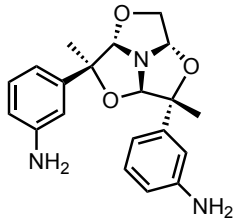

According to the synthetic protocol of **35a**, **33b** (172 mg, 0.417 mmol) was converted to **36b** (138 mg, 94%) as a colorless amorphous.

IR (KBr, cm^{-1}) 3438, 3361, 2929, 1112.

^{1}H NMR (400 MHz, $CDCl_3$) δ 1.44 (s, 3H), 1.53 (s, 3H), 3.66 (brs, 4H), 3.87 (dd, *J* = 2.8, 10.1 Hz, 1H), 4.31 (d, *J* = 10.1 Hz, 1H), 4.87 (s, 1H), 5.12 (s, 1H), 5.27 (d, *J* = 2.8 Hz, 1H), 6.56–6.59 (m, 1H), 6.60–6.63 (m, 1H), 6.70–6.71 (m, 1H), 6.83–6.86 (m, 1H), 6.88–6.89 (m, 1H), 7.12 (dd, *J* = 7.8, 7.8 Hz, 1H), 7.16 (dd, *J* = 7.8, 7.8 Hz, 1H).

^{13}C NMR (100 MHz, $CDCl_3$) δ 23.5, 24.1, 71.3, 87.0, 87.1, 94.8, 99.7, 101.2, 111.7, 113.2, 114.1, 114.3, 115.3, 116.4, 128.8, 129.6, 142.3, 143.7, 146.0, 146.7.

HR-MS (ESI): Calcd for $C_{20}H_{23}N_3NaO_3$ $[M+Na]^+$, 376.1637. Found, 376.1633.

3,3'-((2*aS/R*,4*S/R*,4*aS/R*,6*R/S*,6*aS/R*)-4,6-Dimethylhexahydro-1,3,5-trioxa-2a^1-azacyclopenta[*cd*] pentalene-4,6-diyl)dianiline (36c)

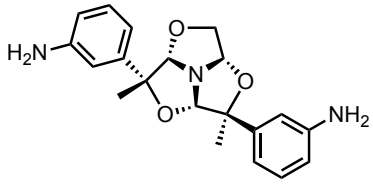

According to the synthetic protocol of **35a**, **33c** (136 mg, 0.329 mmol) was converted to **36c** (112 mg, 96%) as a colorless amorphous.

IR (KBr, cm^{-1}) 3437, 3361, 2931, 1115.

^{1}H NMR (400 MHz, $CDCl_3$) δ 1.62 (s, 3H), 1.70 (s, 3H), 3.65 (dd, *J* = 2.8, 10.1 Hz, 1H), 3.70 (brs, 4H), 4.12 (d, *J* = 10.1 Hz, 1H), 4.85 (s, 1H), 5.09 (d, *J* = 2.8 Hz, 1H), 5.39 (s, 1H), 6.60–6.63 (m, 2H), 6.79–6.88 (m, 4H), 7.168 (dd, *J* = 8.0, 8.0 Hz, 1H), 7.173 (dd, *J* = 8.0, 8.0 Hz, 1H).

^{13}C NMR (100 MHz, $CDCl_3$) δ 23.5, 24.5, 71.6, 86.9, 87.4, 94.9, 99.5, 102.0, 111.8, 112.6, 114.3, 115.3, 115.8, 129.1, 129.7, 142.5, 144.0, 146.2, 146.7.

HR-MS (ESI): Calcd for $C_{20}H_{23}N_3NaO_3$ $[M+Na]^+$, 376.1637. Found, 376.1644.

3,3'-((2*aS/R*,4*R/S*,4*aS/R*,6*R/S*,6*aS/R*)-4,6-Dimethylhexahydro-1,3,5-trioxa-2a^1-azacyclopenta[*cd*] pentalene-4,6-diyl)dianiline (36d)

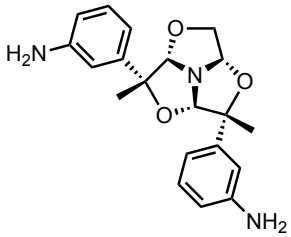

According to the synthetic protocol of **35a**, **33d** (636 mg, 0.154 mmol) was converted to **36d** (153 mg, 99%) as a colorless amorphous.

IR (KBr, cm^{-1}) 3387, 3336, 2933, 1115.

^{1}H NMR (400 MHz, $CDCl_3$) δ 1.51 (s, 3H), 1.68 (s, 3H), 3.74 (dd, *J* = 2.8, 10.1 Hz, 1H), 3.75 (brs, 4H), 4.20 (d, *J* = 10.1 Hz, 1H), 4.87 (s, 1H), 5.05 (s, 1H), 5.30 (d, *J* = 2.8 Hz, 1H), 6.50–6.53 (m, 2H), 6.61–6.62 (m, 1H), 6.68 (ddd, *J* = 0.9, 2.3, 7.8 Hz, 1H), 6.82–6.85 (m, 1H), 7.06 (dd, *J* = 8.0, 8.0 Hz, 1H), 7.08–7.10 (m, 1H), 7.18 (dd, *J* = 8.0, 8.0 Hz, 1H).

^{13}C NMR (100 MHz, $CDCl_3$) δ 21.9, 23.3, 71.8, 87.0, 94.6, 100.3, 102.2, 113.3, 113.7, 114.7, 115.1, 116.2, 128.75, 128.80, 141.8, 142.3, 145.6, 146.3.

HR-MS (ESI): Calcd for $C_{20}H_{23}N_3NaO_3$ $[M+Na]^+$, 376.1637. Found, 376.1636.

4,4'-((2*aS/R*,4*S/R*,4*aS/R*,6*S/R*,6*aS/R*)-4,6-Dimethylhexahydro-1,3,5-trioxa-2a^1-azacyclopenta[*cd*] pentalene-4,6-diyl)dianiline (37a)

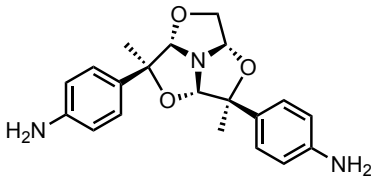

According to the synthetic protocol of **35a**, **34a** (102 mg, 0.246 mmol) was converted to **37a** (86.6 mg, 100%) as a colorless amorphous.

IR (KBr, cm^{-1}) 3425, 3369, 2931, 1115.

^{1}H NMR (400 MHz, $CDCl_3$) δ 1.62 (s, 3H), 1.63 (s, 3H), 3.67 (brs, 4H), 3.76 (dd, *J* = 2.8, 10.1 Hz, 1H), 4.24 (d, *J* = 10.1 Hz, 1H), 4.97 (d, *J* = 2.8 Hz, 1H), 5.04 (s, 1H), 5.06 (s, 1H), 6.61–6.63 (m, 2H), 6.67–6.69 (m, 2H), 7.13–7.16 (m, 2H), 7.21–7.24 (m, 2H).

^{13}C NMR (100 MHz, $CDCl_3$) δ 24.2, 24.3, 71.2, 86.5, 87.0, 94.9, 99.3, 101.4, 115.1, 115.2, 126.1, 126.2, 132.2, 132.4, 145.7, 145.8.

HR-MS (ESI): Calcd for $C_{20}H_{23}N_3NaO_3$ $[M+Na]^+$, 376.1637. Found, 376.1639.

4,4'-((2*aS/R*,4*R/S*,4*aS/R*,6*S/R*,6*aS/R*)-4,6-Dimethylhexahydro-1,3,5-trioxa-2a^1-azacyclopenta[*cd*] pentalene-4,6-diyl)dianiline (37b)

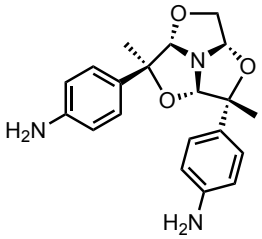

According to the synthetic protocol of **35a**, **34b** (50.3 mg, 0.122 mmol) was converted to **37b** (23.7 mg, 55%) as a colorless amorphous.

IR (KBr, cm^{-1}) 3455, 3364, 1118.

^{1}H NMR (400 MHz, $CDCl_3$) δ 1.45 (s, 3H), 1.54 (s, 3H), 3.65 (brs, 4H), 3.86 (dd, *J* = 2.8, 10.1 Hz, 1H), 4.30 (d, *J* = 10.1 Hz, 1H), 4.75 (s, 1H), 5.09 (s, 1H), 5.25 (d, *J* = 2.8 Hz, 1H), 6.63–6.65 (m, 2H), 6.67–6.70 (m, 2H), 7.09–7.11 (m, 2H), 7.30–7.32 (m, 2H).

^{13}C NMR (100 MHz, $CDCl_3$) δ 22.8, 24.1, 71.4, 86.7, 94.6, 99.8, 101.4, 114.6, 115.2, 126.1, 127.4, 130.8, 132.2, 145.6, 145.7.

HR-MS (ESI): Calcd for $C_{20}H_{23}N_3NaO_3$ $[M+Na]^+$, 376.1637. Found, 376.1635.

4,4'-((2*aS/R*,4*S/R*,4*aS/R*,6*R/S*,6*aS/R*)-4,6-Dimethylhexahydro-1,3,5-trioxa-2a^1-azacyclopenta[*cd*] pentalene-4,6-diyl)dianiline (37c)

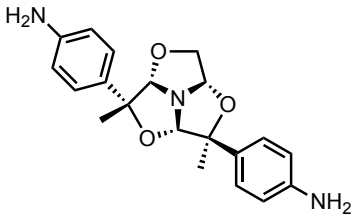

According to the synthetic protocol of **35a**, **34c** (25.4 mg, 0.0612 mmol) was converted to **37c** (20.2 mg, 93%) as a colorless amorphous.

IR (KBr, cm^{-1}) 3466, 3373, 2903, 1111.

^{1}H NMR (400 MHz, $CDCl_3$) δ 1.62 (s, 3H), 1.68 (s, 3H), 3.64 (dd, *J* = 2.8, 10.1 Hz, 1H), 3.67 (brs, 4H), 4.11 (d, *J* = 10.1 Hz, 1H), 4.76 (s, 1H), 5.04 (d, *J* = 2.8 Hz, 1H), 5.35 (s, 1H), 6.69 (d, *J* = 8.8 Hz, 2H), 6.70 (d, *J* = 8.8 Hz, 2H), 7.24 (d, *J* = 8.8 Hz, 2H), 7.30 (d, *J* = 8.8 Hz, 2H).

^{13}C NMR (100 MHz, $CDCl_3$) δ 22.9, 24.5, 71.5, 86.5, 87.2, 94.8, 99.3, 102.0, 114.9, 115.2, 126.2, 126.8, 131.0, 132.5, 145.7, 145.8.

HR-MS (ESI): Calcd for $C_{20}H_{23}N_3NaO_3$ $[M+Na]^+$, 376.1637. Found, 376.1648.

4,4'-((2*aS/R*,4*R/S*,4*aS/R*,6*R/S*,6*aS/R*)-4,6-Dimethylhexahydro-1,3,5-trioxa-2a^1-azacyclopenta [*cd*]pentalene-4,6-diyl)dianiline (37d)

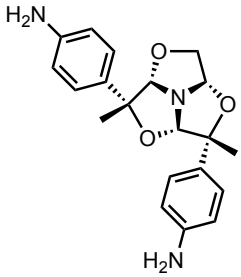

According to the synthetic protocol of **35a**, **34d** (60.7 mg, 0.147 mmol) was converted to **37d** (51.6 mg, 99%) as a colorless amorphous.

IR (KBr, cm^{-1}) 3431, 3357, 2926, 1119.

^{1}H NMR (400 MHz, $CDCl_3$) δ 1.51 (s, 3H), 1.66 (s, 3H), 3.62 (brs, 4H), 3.73 (dd, *J* = 2.0 10.1 Hz, 1H), 4.18 (d, *J* = 10.1 Hz, 1H), 4.83 (s, 1H), 5.02 (s, 1H), 5.29 (d, *J* = 2.0 Hz, 1H), 6.59 (d, *J* = 8.0 Hz, 2H), 6.70 (d, *J* = 8.0 Hz, 2H), 7.01 (d, *J* = 8.0 Hz, 2H), 7.35 (d, *J* = 8.0 Hz, 2H).

^{13}C NMR (100 MHz, $CDCl_3$) δ 22.3, 23.1, 71.7, 86.78, 86.83, 94.4, 99.8, 102.0, 114.6, 114.8, 126.6, 127.4, 130.6, 131.3, 145.4, 145.7.

HR-MS (ESI): Calcd for $C_{20}H_{23}N_3NaO_3$ $[M+Na]^+$, 376.1637. Found, 376.1652.

Determination of the relative configurations of the synthesized compounds.

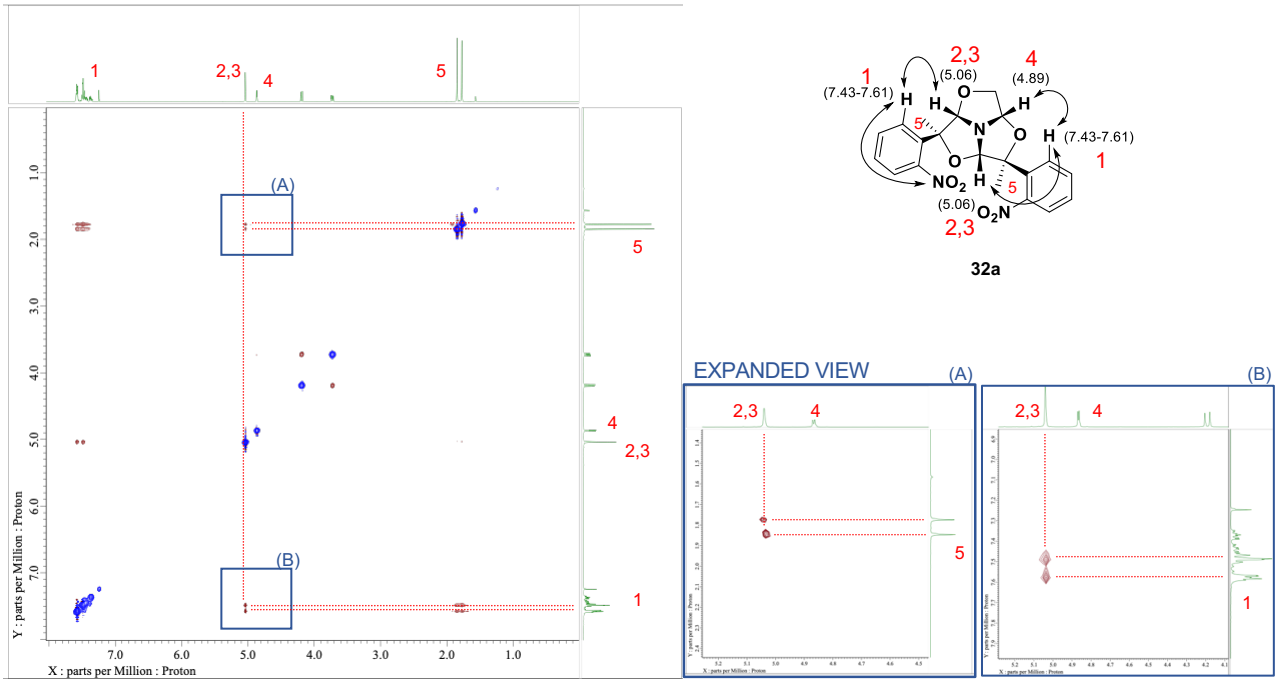

Figure S1. NOESY spectrum of **32a**

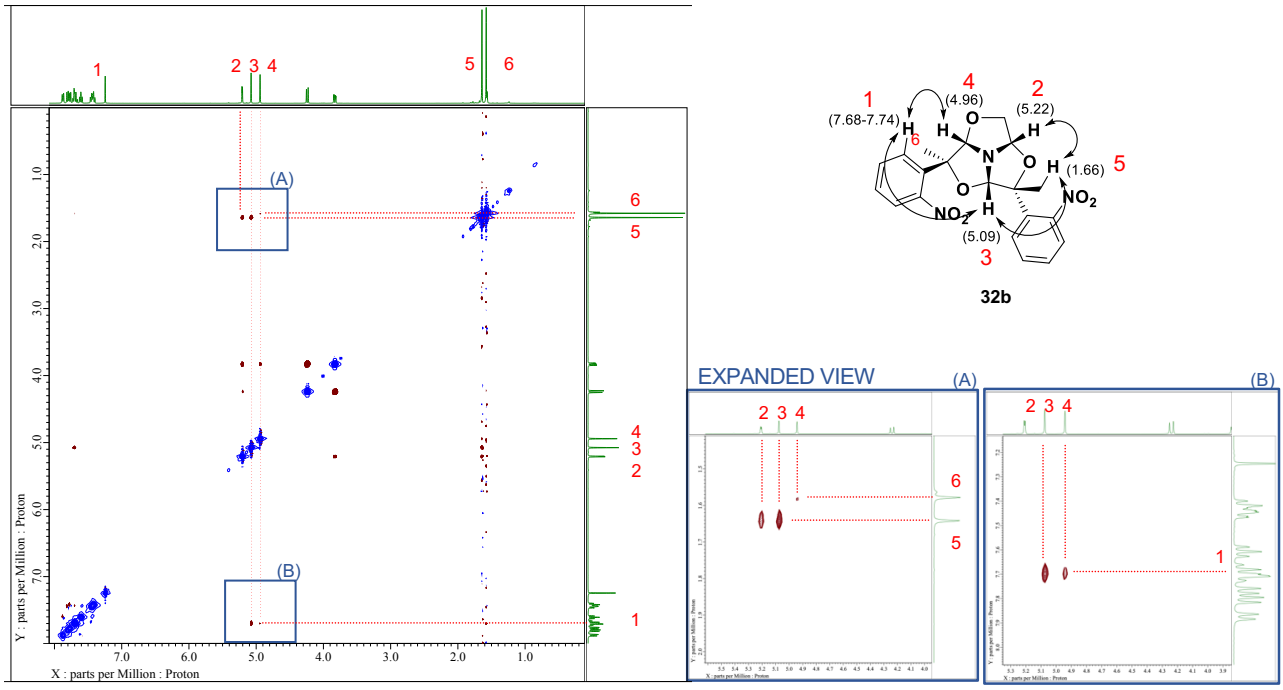

Figure S2. NOESY spectrum of **32b**

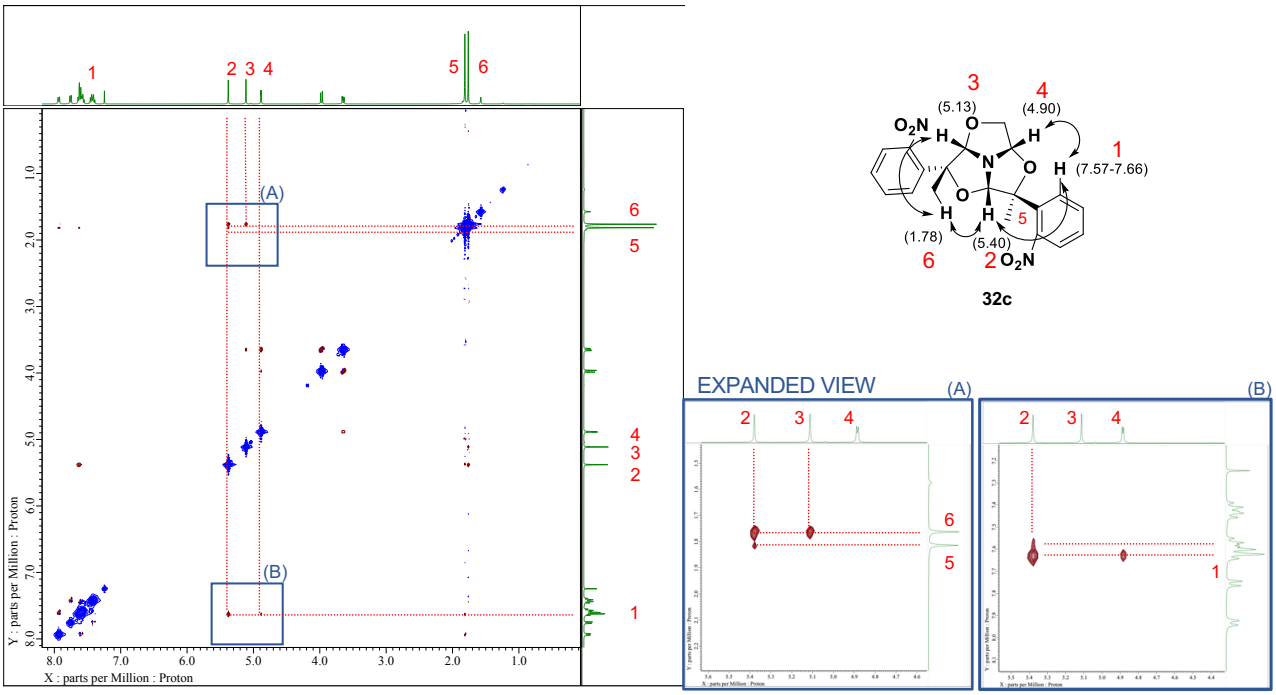

Figure S3. NOESY spectrum of **32c**

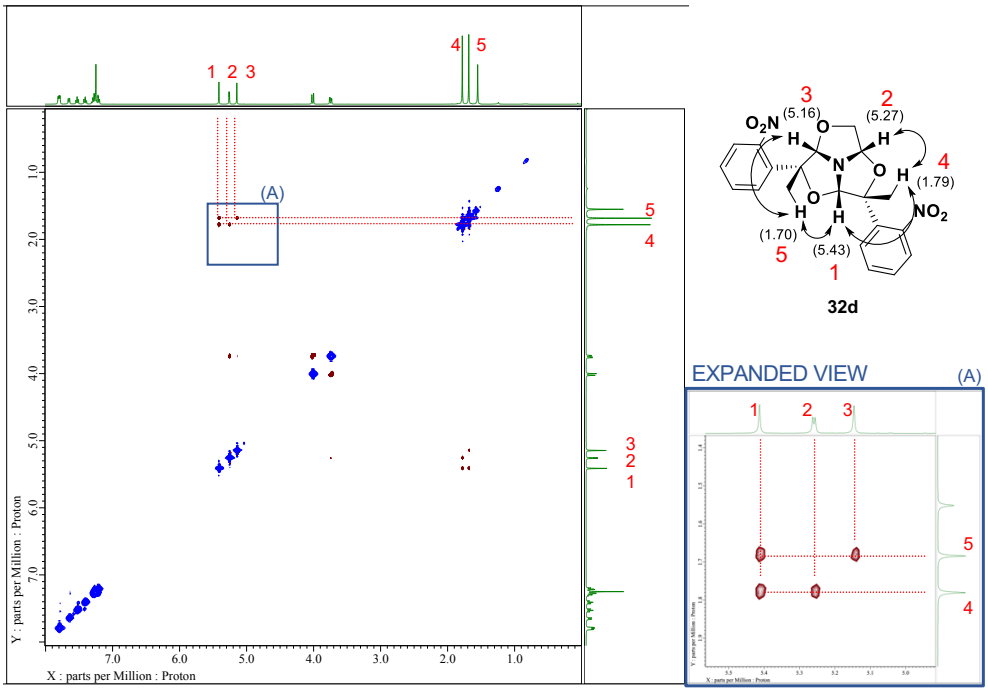

Figure S4. NOESY spectrum of **32d**

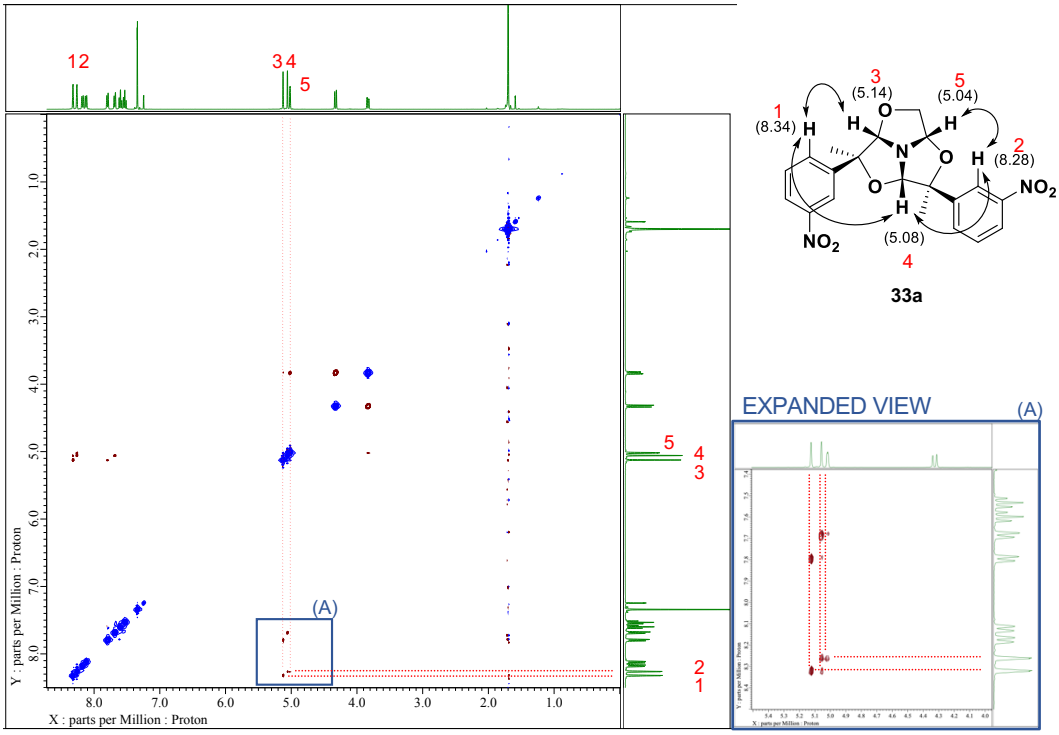

Figure S5. NOESY spectrum of **33a**

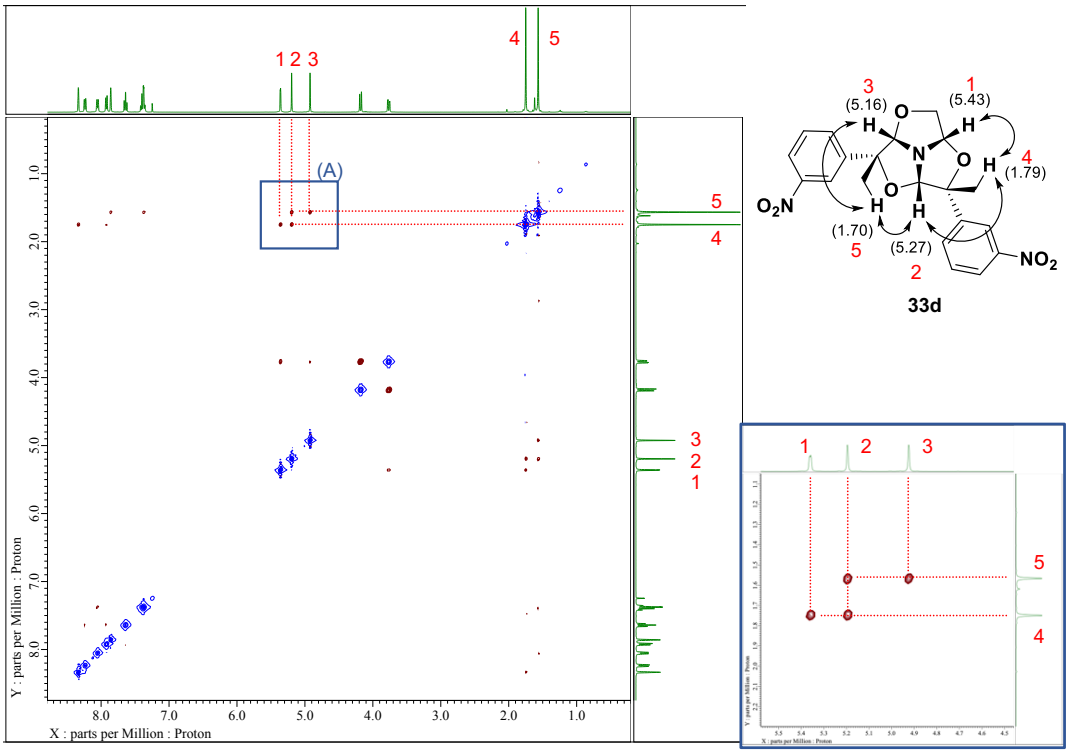

Figure S6. NOESY spectrum of **33d**

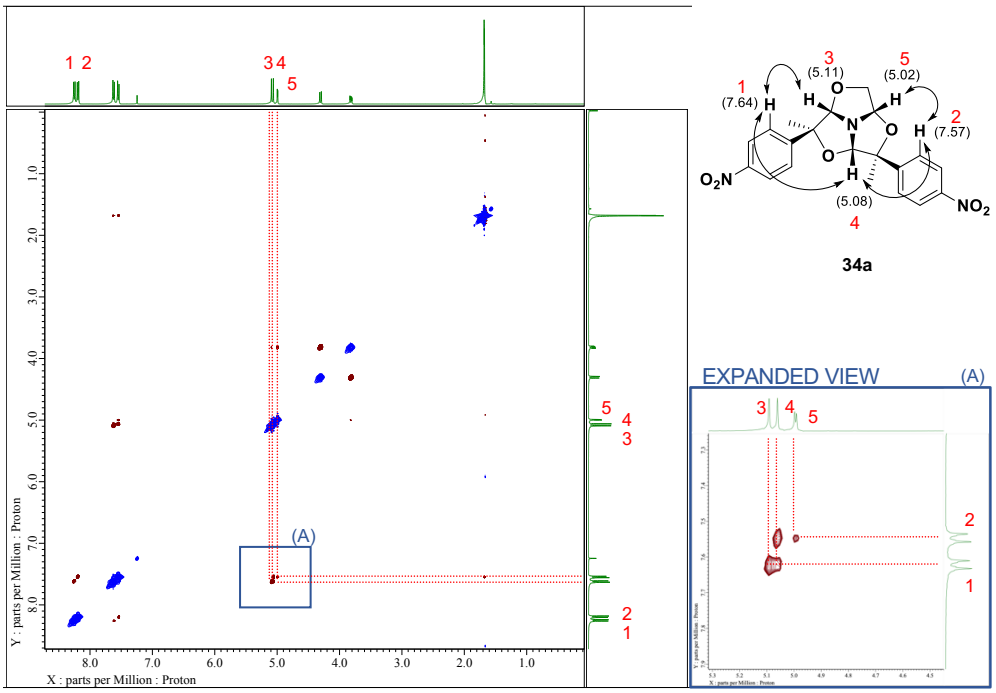

Figure S7. NOESY spectrum of **34a**

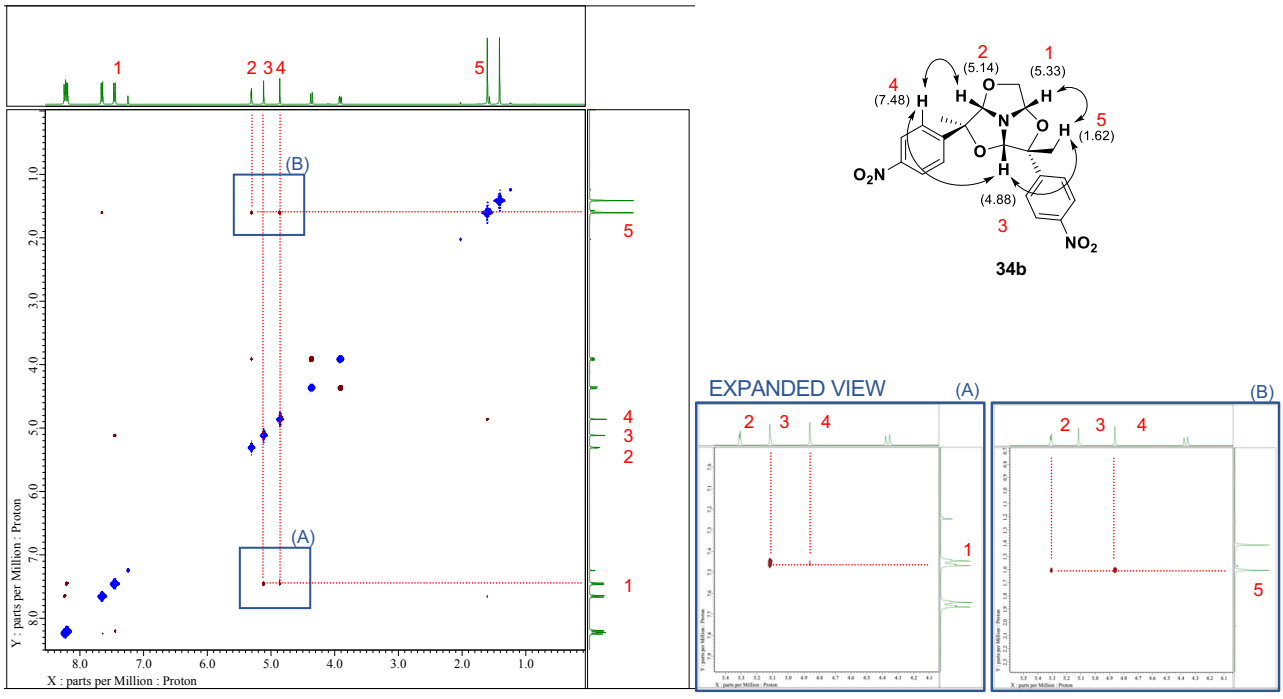

Figure S8. NOESY spectrum of **34b**

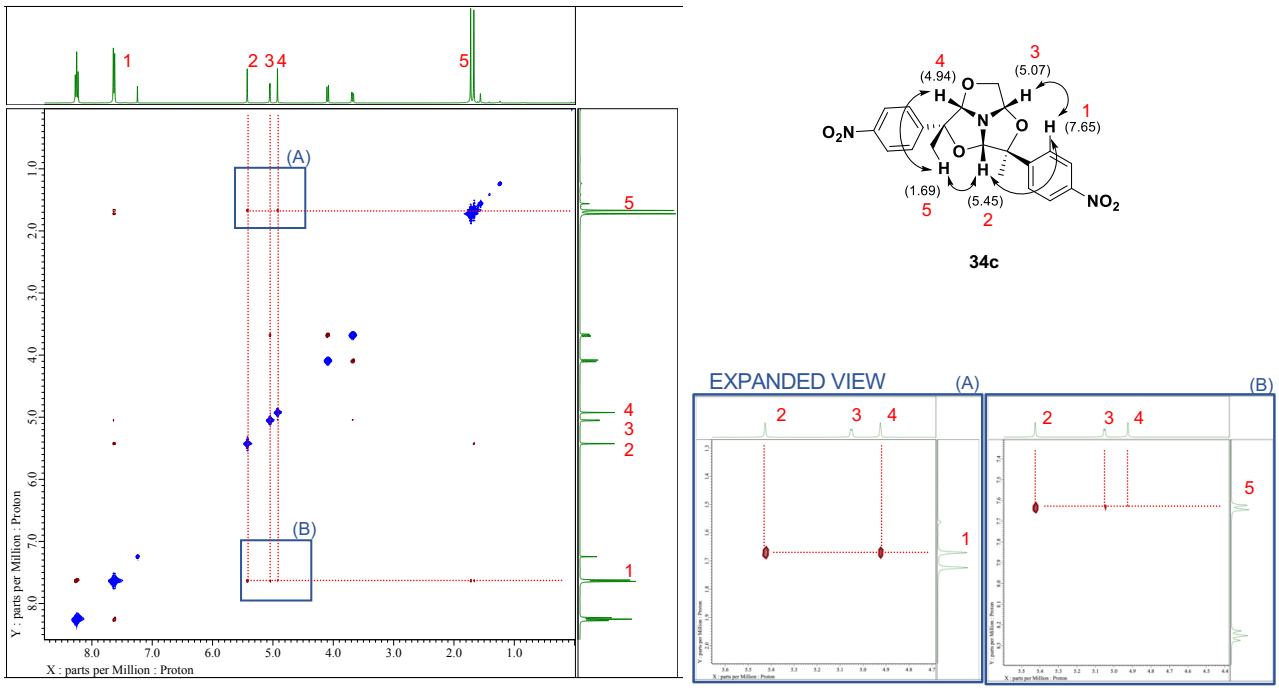

Figure S9. NOESY spectrum of **34c**

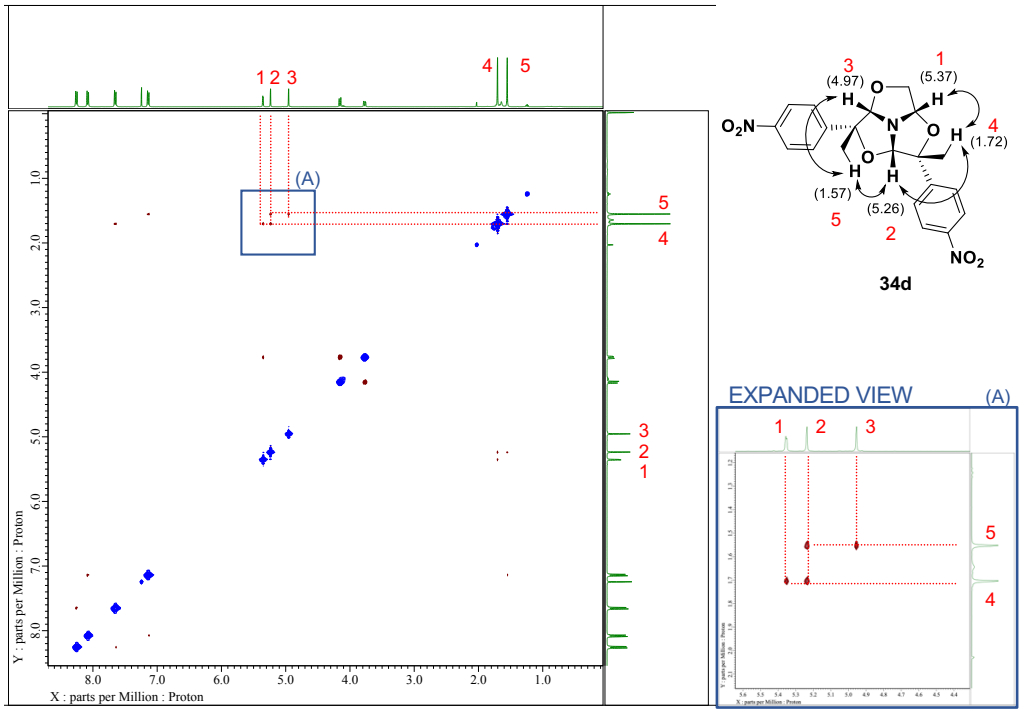

Figure S10. NOESY spectrum of **34d**

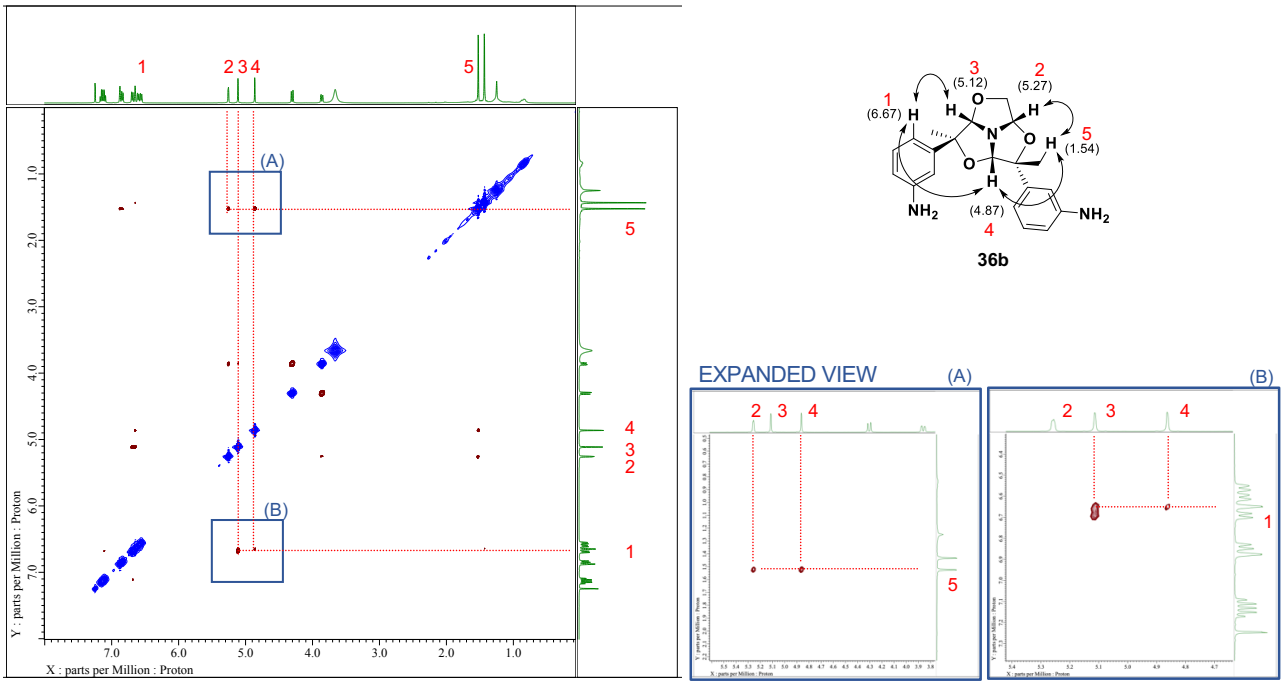

Figure S11. NOESY spectrum of **36b**

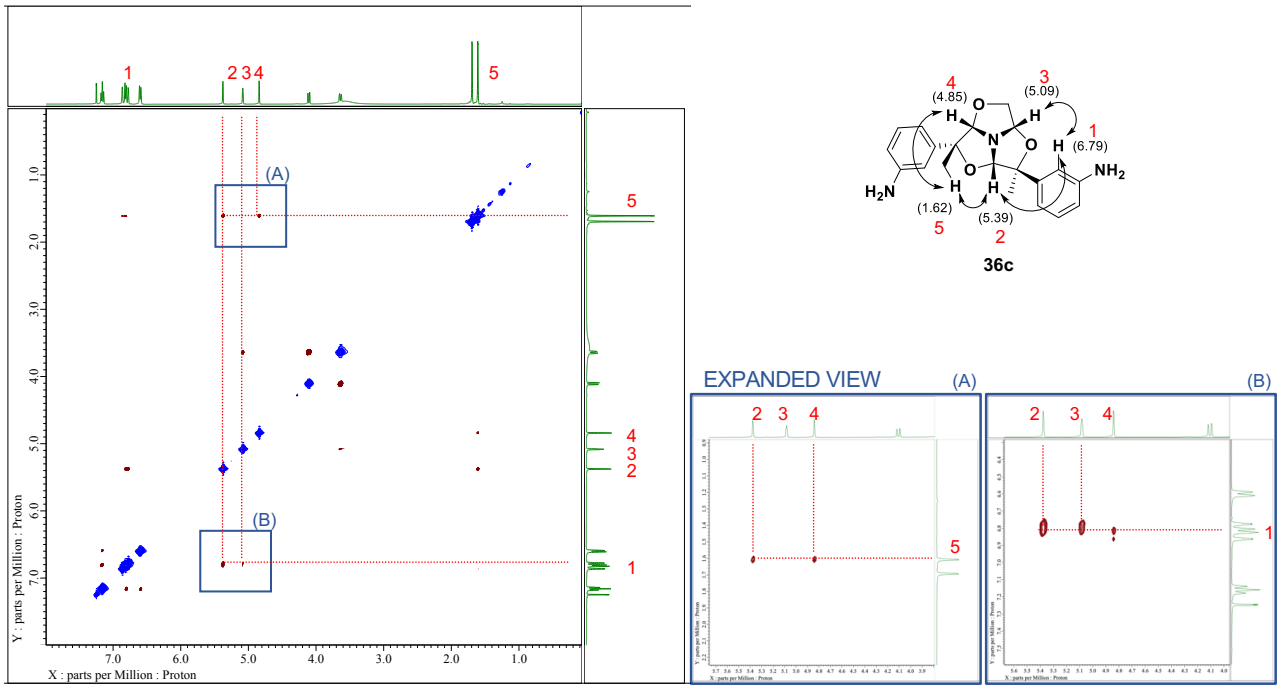

Figure S12. NOESY spectrum of **36c**

Di-*tert*-butyl(((2*aS/R*,4*S/R*,4*aS/R*,6*S/R*,6*aS/R*)-4,6-dimethylhexahydro-1,3,5-trioxa-2a^1-azacyclopenta [*cd*]pentalene-4,6-diyl)bis(2,1-phenylene))dicarbamate (38a)

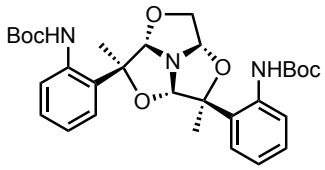

To a solution of **35a** (4.9 mg, 0.0139 mmol) in 1,2-dichlorimethane (1 mL) were added Boc_2O (20 μL, 0.0871 mmol) and triethylamine (20 μL, 0.144 mmol) at room temperature and the mixture was refluxed for 17 h under Ar atmosphere. After cooling to room temperature, the reaction mixture was poured into saturated $NaHCO_3$ aqueous solution (2 mL) and extracted with $CHCl_3$ (6 mL, 5 mL, 4 mL). The combined organic layers were dried over anhydrous Na_2SO_4 and concentrated *in vacuo.* The residue was purified by preparative TLC (chloroform/methanol = 40/1) to give **38a** (4.9 mg, 64%) as a colorless solid.

IR (KBr, cm^{-1}) 3373, 2978, 2929, 1728, 1162, 1119.

^{1}H NMR (400 MHz, $CDCl_3$) δ 1.42 (s, 9H), 1.53 (s, 9H), 1.60 (s, 3H), 1.63 (s, 3H), 3.94 (dd, *J* = 2.8, 10.1 Hz, 1H), 4.38 (d, *J* = 10.1 Hz, 1H), 4.68 (s, 1H), 5.40 (d, *J* = 2.8 Hz, 1H), 5.47 (s, 1H), 6.98–7.04 (m, 2H), 7.14–7.16 (m, 1H), 7.18–7.20 (m, 1H), 7.23–7.32 (m, 2H), 8.11–8.18 (m, 2H), 8.24 (brs, 1H), 8.69 (brs, 1H).

^{13}C NMR (100 MHz, $CDCl_3$) δ 21.3, 22.8, 28.4, 28.5, 70.7, 79.6, 80.2, 87.7, 95.7, 98.9, 100.4, 121.6, 122.5, 122.7, 125.2, 126.9, 127.1, 128.5, 129.0, 137.5, 137.6, 153.1, 153.3.

HR-MS (ESI): Calcd for $C_{30}H_{39}N_3NaO_7$ $[M+Na]^+$, 576.2686. Found, 576.2663.

Di-*tert*-butyl(((2*aS/R*,4*S/R*,4*aS/R*,6*S/R*,6*aS/R*)-4,6-dimethylhexahydro-1,3,5-trioxa-2a^1-azacyclopenta [*cd*]pentalene-4,6-diyl) bis(3,1-phenylene))dicarbamate (38b)

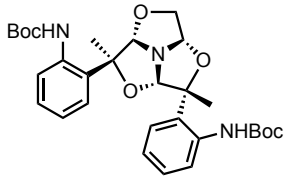

According to the synthetic protocol of **38a**, **35b** (10.0 mg, 0.0283 mmol) was converted to **38b** (7.5 mg, 48%) as a colorless solid.

IR (KBr, cm^{-1}) 3330, 2978, 2933, 1705, 1159, 1111. ^{1}H NMR (400 MHz, $CDCl_3$) δ 1.50 (s, 9H), 1.53 (s, 9H), 1.66 (s, 6H), 3.78 (dd, *J* = 2.8, 10.0 Hz, 1H), 4.27 (d, *J* = 10.0 Hz, 1H), 5.03 (d, *J* = 2.8 Hz, 1H), 5.12 (s, 1H), 5.15 (s, 1H), 6.49 (brs, 1H), 6.57 (brs, 1H), 7.03–7.05 (m, 1H), 7.09–7.11 (m, 1H), 7.22–7.35 (m, 6H), 7.46–7.48 (m, 1H). ^{13}C NMR (100 MHz, $CDCl_3$) δ 24.20, 24.24, 28.5, 71.3, 80.7, 86.8, 87.3, 95.2, 99.5, 101.5, 115.4, 117.8, 119.7, 119.9, 129.3, 129.4, 138.7, 138.8, 143.4, 143.6, 152.77, 152.82.

HR-MS (ESI): Calcd for $C_{30}H_{39}N_3NaO_7$ $[M+Na]^+$, 576.2686. Found, 576.2709.

Di-*tert*-butyl(((2*aS/R*,4*S/R*,4*aS/R*,6*S/R*,6*aS/R*)-4,6-dimethylhexahydro-1,3,5-trioxa-2a^1-azacyclopenta [*cd*]pentalene-4,6-diyl)bis(4,1-phenylene))dicarbamate (38c)

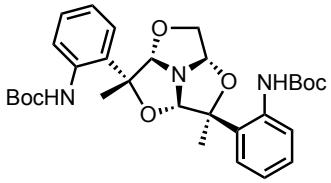

According to the synthetic protocol of **38a**, **35c** (5.00 mg, 0.0141 mmol) was converted to **38c** (7.7 mg, 99%) as a colorless solid.

IR (KBr, cm^{-1}) 3339, 2978, 2929, 1729, 1160, 1102.

^{1}H NMR (400 MHz, $CDCl_3$) δ 1.50 (s, 9H), 1.52 (s, 9H), 1.63 (s, 3H), 1.64 (s, 3H), 3.78 (dd, *J* = 2.8, 10.1 Hz, 1H), 4.26 (d, *J* = 10.1 Hz, 1H), 4.98 (d, *J* = 2.8 Hz, 1H), 5.05 (s, 1H), 5.08 (s, 1H), 6.45 (brs, 1H), 6.49 (brs, 1H), 7.27–7.36 (m, 8H).

^{13}C NMR (100 MHz, $CDCl_3$) δ 24.3 (×2), 28.5, 71.3, 80.8, 86.6, 87.0, 93.0, 95.1, 99.4, 101.4, 118.7, 118.8, 125.76, 125.82, 137.0, 137.1, 137.7, 137.8, 152.8, 152.9.

HR-MS (ESI): Calcd for $C_{30}H_{39}N_3NaO_7$ $[M+Na]^+$, 576.2686. Found, 576.2679.

Di-*tert*-butyl(((2*aS/R*,4*R/S*,4*aS/R*,6*S/R*,6*aS/R*)-4,6-dimethylhexahydro-1,3,5-trioxa-2a^1-azacyclopenta [*cd*]pentalene-4,6-diyl)bis(2,1-phenylene))dicarbamate (38d)

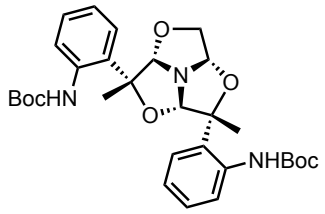

According to the synthetic protocol of **38a**, **35d** (4.9 mg, 0.0139 mmol) was converted to **38d** (7.7 mg, 100%) as a colorless solid.

IR (KBr, cm^{-1}) 3372, 2979, 1731, 1161, 1120.

^{1}H NMR (400 MHz, $CDCl_3$) δ 1.48 (s, 9H), 1.52 (s, 9H), 1.74 (s, 3H), 1.78 (s, 3H), 3.82 (dd, *J* = 2.8, 10.1 Hz, 1H), 4.31 (d, *J* = 10.1 Hz, 1H), 4.82 (d, *J* = 2.8 Hz, 1H), 5.28 (s, 1H), 5.40 (s, 1H), 6.90–6.94 (m, 1H), 7.01–7.05 (m, 2H), 7.18 (dd, *J* = 1.2, 8.0 Hz, 1H), 7.24–7.28 (m, 1H), 7.32 (ddd, *J* = 1.2, 8.0, 8.0 Hz, 1H), 8.04–8.08 (m, 1H), 8.23–8.25 (m, 1H), 8.55 (brs, 1H), 8.99 (brs, 1H).

^{13}C NMR (100 MHz, $CDCl_3$) δ 21.1, 23.0, 28.49 (×3), 28.54 (×3), 70.4, 80.4 (×2), 87.8, 88.0, 95.3, 96.8, 100.4, 121.2, 122.2, 122.8, 122.9, 125.5, 126.4, 126.9, 127.5, 128.9, 129.1, 137.46, 137.50, 153.2, 153.3.

HR-MS (ESI): Calcd for $C_{30}H_{39}N_3NaO_7$ $[M+Na]^+$, 576.2686. Found, 576.2711.

Di-*tert*-butyl(((2*aS/R*,4*R/S*,4*aS/R*,6*S/R*,6*aS/R*)-4,6-dimethylhexahydro-1,3,5-trioxa-2a^1-azacyclopenta [*cd*]pentalene-4,6-diyl) bis(3,1-phenylene))dicarbamate (39a)

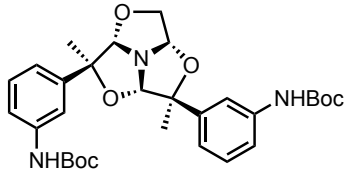

According to the synthetic protocol of **38a**, **36a** (10.0 mg, 0.0283 mmol) was converted to **39a** (11.6 mg, 74%) as a colorless solid.

IR (KBr, cm^{-1}) 3340, 2977, 2931, 1710, 1160, 1115.

^{1}H NMR (400 MHz, $CDCl_3$) δ 1.43 (s, 3H), 1.52 (s, 9H), 1.53 (s, 9H), 1.55 (s, 3H), 3.88 (dd, *J* = 2.8, 10.1 Hz, 1H), 4.31 (d, *J* = 10.1 Hz, 1H), 4.89 (s, 1H), 5.15 (s, 1H), 5.27 (d, *J* = 2.8 Hz, 1H), 6.56 (brs, 2H), 6.96–7.00 (m, 1H), 7.16–7.19 (m, 1H), 7.24–7.44 (m, 6H).

^{13}C NMR (100 MHz, $CDCl_3$) δ 24.20, 24.20, 28.5, 71.3, 80.7, 86.8, 87.3, 95.2, 99.5, 101.5, 115.4, 117.8, 119.7, 119.9, 129.3, 129.4, 138.7, 138.8, 143.4, 143.6, 152.77, 152.82.

HR-MS (ESI): Calcd for $C_{30}H_{39}N_3NaO_7$ $[M+Na]^+$, 576.2686. Found, 576.2673.

Di-*tert*-butyl(((2*aS/R*,4*R/S*,4*aS/R*,6*S/R*,6*aS/R*)-4,6-dimethylhexahydro-1,3,5-trioxa-2a^1-azacyclopenta [*cd*]pentalene-4,6-diyl)bis(4,1-phenylene))dicarbamate (39b)

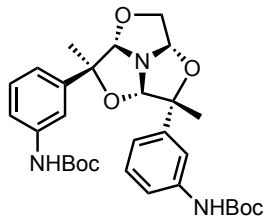

According to the synthetic protocol of **38a**, **36b** (5.0 mg, 0.0141 mmol) was converted to **39b** (8.2 mg, 100%) as a colorless solid.

IR (KBr, cm^{-1}) 3342, 2977, 2929, 1728, 1161, 1119.

^{1}H NMR (400 MHz, $CDCl_3$) δ 1.43 (s, 3H), 1.51 (s, 9H), 1.52 (s, 9H), 1.55 (s, 3H), 3.88 (dd, *J* = 2.8, 10.1 Hz, 1H), 4.32 (d, *J* = 10.1 Hz, 1H), 4.77 (s, 1H), 5.11 (s, 1H), 5.26 (d, *J* = 2.8 Hz, 1H), 6.47 (brs, 1H), 6.50 (brs, 1H), 7.21–7.23 (m, 2H), 7.31–7.70 (m, 4H), 7.41–7.43 (m, 2H).

^{13}C NMR (100 MHz, $CDCl_3$) δ 22.9, 24.1, 28.5, 71.4, 86.8, 94.8, 99.8, 101.3, 118.0, 118.8, 125.7, 126.9, 137.0, 137.5, 137.7, 152.9.

HR-MS (ESI): Calcd for $C_{30}H_{39}N_3NaO_7$ $[M+Na]^+$, 576.2686. Found, 576.2693.

Di-*tert*-butyl(((2*aS/R*,4*S/R*,4*aS/R*,6*R/S*,6*aS/R*)-4,6-dimethylhexahydro-1,3,5-trioxa-2a^1-azacyclopenta [*cd*]pentalene-4,6-diyl)bis(2,1-phenylene))dicarbamate (39c)

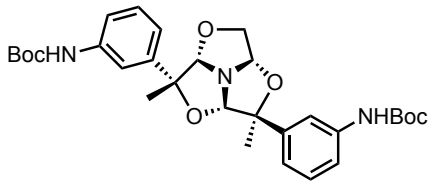

According to the synthetic protocol of **38a**, **36c** (5.3 mg, 0.0150 mmol) was converted to **39c** (4.3 mg, 52%) as a colorless solid.

IR (KBr, cm^{-1}) 3371, 2927, 1728, 1161, 1111.

^{1}H NMR (400 MHz, $CDCl_3$) δ 1.490 (s, 9H), 1.494 (s, 9H), 1.69 (brs, 3H), 1.80 (s, 3H), 3.77 (dd, *J* = 2.8, 10.1 Hz, 1H), 4.19 (d, *J* = 10.1 Hz, 1H), 4.86 (d, *J* = 2.8 Hz, 1H), 5.14 (brs, 1H), 5.78 (s, 1H), 7.06 (ddd, *J* = 1.2, 7.6, 7.6 Hz, 1H), 7.25–7.34 (m, 5H), 8.11–8.13 (m, 2H), 8.58 (brs, 1H).

^{13}C NMR (100 MHz, $CDCl_3$) δ 21.9, 23.7, 28.5, 28.6, 70.9, 80.4, 87.8, 95.0, 97.4, 99.2, 122.3, 122.9, 125.5, 127.4, 127.8, 128.4, 129.1, 137.6, 153.3.

HR-MS (ESI): Calcd for $C_{30}H_{39}N_3NaO_7$ $[M+Na]^+$, 576.2686. Found, 576.2697.

Di-*tert*-butyl(((2*aS/R*,4*S/R*,4*aS/R*,6*R/S*,6*aS/R*)-4,6-dimethylhexahydro-1,3,5-trioxa-2a^1-azacyclopenta [*cd*]pentalene-4,6-diyl)bis(3,1-phenylene))dicarbamate (39d)

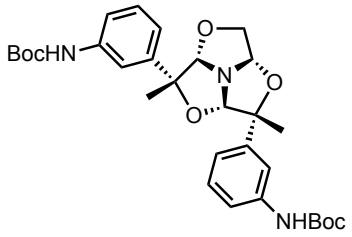

According to the synthetic protocol of **38a**, **36d** (5.0 mg, 0.0141 mmol) was converted to **39d** (5.6 mg, 72%) as a colorless solid.

IR (KBr, cm^{-1}) 3351, 2932, 1708, 1160, 1119.

^{1}H NMR (400 MHz, $CDCl_3$) δ 1.515 (s, 9H), 1.522 (s, 9H), 1.64 (s, 3H), 1.71 (s, 3H), 3.65 (dd, *J* = 2.8, 10.1 Hz, 1H), 4.10 (d, *J* = 10.1 Hz, 1H), 4.87 (s, 1H), 5.09 (d, *J* = 2.8 Hz, 1H), 5.40 (s, 1H), 6.52–6.53 (m, 2H), 7.10–7.16 (m, 2H), 7.28–7.33 (m, 3H), 7.35–7.46 (m, 3H).

^{13}C NMR (100 MHz, $CDCl_3$) δ 23.5, 24.6, 28.5, 71.6, 80.6, 80.7, 86.9, 87.5, 95.0, 99.6, 101.9, 115.3, 115.7, 117.6, 117.8, 119.8, 120.2, 128.9, 129.4, 138.2, 138.8, 142.3, 143.8, 152.8.

HR-MS (ESI): Calcd for $C_{30}H_{39}N_3NaO_7$ $[M+Na]^+$, 576.2686. Found, 576.2680.

Di-*tert*-butyl(((2*aS/R*,4*S/R*,4*aS/R*,6*R/S*,6*aS/R*)-4,6-dimethylhexahydro-1,3,5-trioxa-2a^1-azacyclopenta [*cd*]pentalene-4,6-diyl)bis(4,1-phenylene))dicarbamate (40a)

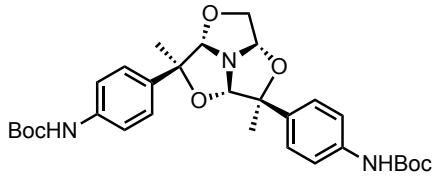

According to the synthetic protocol of **38a**, **37a** (5.0 mg, 0.0141 mmol) was converted to **40a** (5.8 mg, 74%) as a colorless solid.

IR (KBr, cm^{-1}) 3340, 2978, 2930, 1729, 1161, 1119.

^{1}H NMR (400 MHz, $CDCl_3$) δ 1.51 (s, 9H), 1.52 (s, 9H), 1.63 (s, 3H), 1.68 (s, 3H), 3.65 (dd, *J* = 2.8, 10.1 Hz, 1H), 4.10 (d, *J* = 10.1 Hz, 1H), 4.81 (s, 1H), 5.04 (d, *J* = 2.8 Hz, 1H), 5.38 (s, 1H), 6.48 (brs, 1H), 6.50 (brs, 1H), 7.34–7.43 (m, 8H).

^{13}C NMR (100 MHz, $CDCl_3$) δ 23.2, 24.6, 28.5, 71.6, 86.7, 87.3, 94.9, 99.5, 101.9, 118.3, 118.8, 125.8, 126.4, 135.8, 137.3, 137.6, 137.7, 152.9.

HR-MS (ESI): Calcd for $C_{30}H_{40}N_3O_7$ $[M+H]^+$, 554.2866. Found, 554.2894.

Di-*tert*-butyl(((2*aS/R*,4*R/S*,4*aS/R*,6*R/S*,6*aS/R*)-4,6-dimethylhexahydro-1,3,5-trioxa-2a^1-azacyclopenta [*cd*]pentalene-4,6-diyl)bis(2,1-phenylene))dicarbamate (40b)

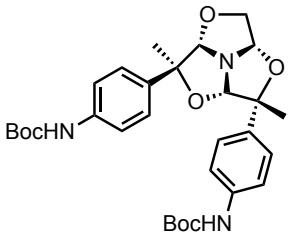

According to the synthetic protocol of **38a**, **37b** (5.0 mg, 0.0142 mmol) was converted to **40b** (5.6 mg, 71%) as a colorless solid.

IR (KBr, cm^{-1}) 3385, 2978, 2928, 1726, 1165, 1116.

^{1}H NMR (400 MHz, $CDCl_3$) δ 1.32 (brs, 9H), 1.48 (s, 9H), 1.54 (brs, 3H), 1.70 (s, 3H), 3.92 (dd, *J* = 2.8, 10.1 Hz, 1H), 4.26 (d, *J* = 10.1 Hz, 1H), 5.21 (s, 1H), 5.30 (brs, 1H), 5.04 (d, *J* = 2.8 Hz, 1H), 6.99–7.07 (m, 2H), 7.14–7.20 (m, 2H), 7.25–7.29 (m, 3H), 7.41–8.59 (m, 3H).

^{13}C NMR (100 MHz, $CDCl_3$) δ 23.0, 23.2, 28.3, 28.6, 71.3, 79.4, 80.1, 89.5, 100.7, 113.6, 123.0, 123.2, 126.0, 126.1, 127.2, 128.1, 128.6, 138.0, 138.2, 151.0, 151.3.

HR-MS (ESI): Calcd for $C_{30}H_{39}N_3NaO_7$ $[M+Na]^+$, 576.2686. Found, 576.2670.

Di-*tert*-butyl(((2*aS/R*,4*R/S*,4*aS/R*,6*R/S*,6*aS/R*)-4,6-dimethylhexahydro-1,3,5-trioxa-2a^1-azacyclopenta [*cd*]pentalene-4,6-diyl)bis(3,1-phenylene))dicarbamate (40c)

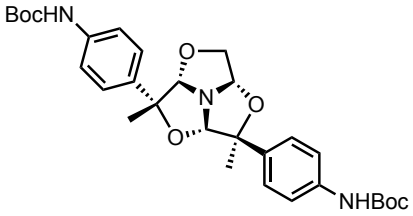

According to the synthetic protocol of **38a**, **37c** (10.0 mg, 0.0283 mmol) was converted to **40c** (12.7 mg, 81%) as a colorless solid.

IR (KBr, cm^{-1}) 3336, 2977, 1728, 1161, 1121.

^{1}H NMR (400 MHz, $CDCl_3$) δ 1.50 (s, 9H), 1.518 (s, 9H), 1.524 (s, 3H), 1.68 (s, 3H), 3.75 (dd, *J* = 2.8, 10.1 Hz, 1H), 4.18 (d, *J* = 10.1 Hz, 1H), 4.92 (s, 1H), 5.13 (s, 1H), 5.31 (d, *J* = 2.8 Hz, 1H), 6.37 (brs, 1H), 6.55 (brs, 1H), 6.77–6.80 (m, 1H), 6.99 (brs, 1H), 7.16 (dd, *J* = 8.0, 8.0 Hz, 1H), 7.19–7.21 (m, 1H), 7.26–7.30 (m, 1H), 7.33 (dd, *J* = 8.0, 8.0 Hz, 1H), 7.40–7.41 (m, 1H), 7.45–7.48 (m, 1H).

^{13}C NMR (100 MHz, $CDCl_3$) δ 22.8, 23.6, 28.50, 28.52, 71.8, 80.4, 80.5, 87.1, 87.2, 94.7, 100.2, 101.9, 115.8, 116.8, 117.5, 117.9, 120.2, 121.0, 128.5, 128.7, 138.0, 141.9, 142.1, 152.8, 153.0.

HR-MS (ESI): Calcd for $C_{30}H_{39}N_3NaO_7$ $[M+Na]^+$, 576.2686. Found, 576.2664.

Di-*tert*-butyl(((2*aS/R*,4*R/S*,4*aS/R*,6*R/S*,6*aS/R*)-4,6-dimethylhexahydro-1,3,5-trioxa-2a^1-azacyclopenta [*cd*]pentalene-4,6-diyl)bis(4,1-phenylene))dicarbamate (40d)

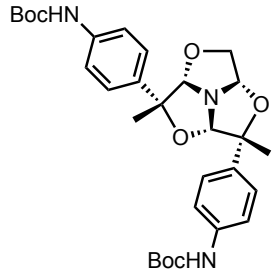

According to the synthetic protocol of **38a**, **37c** (5.0 mg, 0.0141 mmol) was converted to **40d** (6.1 mg, 78%) as a colorless solid.

IR (KBr, cm^{-1}) 3339, 2977, 2930, 1728, 1161, 1120.

^{1}H NMR (400 MHz, $CDCl_3$) δ 1.50 (s, 9H), 1.51 (s, 3H), 1.54 (s, 9H), 1.67 (s, 3H), 3.74 (dd, *J* = 2.8, 10.1 Hz, 1H), 4.17 (d, *J* = 10.1 Hz, 1H), 4.86 (s, 1H), 5.07 (s, 1H), 5.31 (d, *J* = 2.8 Hz, 1H), 6.41 (brs, 1H), 6.52 (brs, 1H), 7.06–7.08 (m, 2H), 7.22–7.27 (m, 2H), 7.35–7.38 (m, 2H), 7.43–7.46 (m, 2H).

^{13}C NMR (100 MHz, $CDCl_3$) δ 22.5, 23.1, 28.4, 28.5, 71.7, 86.86, 86.92, 94.6, 100.0, 102.0, 117.8, 118.0, 126.2, 126.9, 135.2, 135.8, 137.3, 137.7, 152.8.

HR-MS (ESI): Calcd for $C_{30}H_{39}N_3NaO_7$ $[M+Na]^+$, 576.2686. Found, 576.2671.

2,2'-((2*aS/R*,4*S/R*,4*aS/R*,6*S/R*,6*aS/R*)-4,6-Dimethylhexahydro-1,3,5-trioxa-2a^1-azacyclopenta[*cd*] pentalene-4,6-diyl)bis(*N,N*-dimethylaniline) (41a)

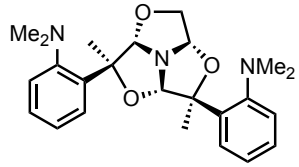

To a solution of **35a** (10.0 mg, 0.0283 mmol) in ethyl acetate (0.5 mL) were added formaldehyde (37% Solution, 104.4 μL, 1.415 mmol) and acetic acid (50 μL) at room temperature. After stirring for 10 min, the mixture was added 5% Pd/C (Degussa type, 10.0 mg, 17.7 mol%) and continued to stir for 2h under hydrogen atmosphere (balloon pressure). The reaction mixture was filtrated with Celite and the filtrate was washed with $CHCl_3$ (5 mL, 4 mL, 3 mL) and $CHCl_3$/MeOH mixtures (3/1, 5 mL × 3). After removal of organic solvent under reduced pressure, the residue was extracted with $CHCl_3$ (8 mL, 5 mL, 3 mL). The combined organic layers were dried over anhydrous Na_2SO_4 and concentrated *in vacuo.* The residue was purified by preparative TLC (hexane/ethyl acetate = 3/1) to give the mixture of **41a** (10.1 mg, 87%) as a colorless solid.

IR (KBr, cm^{-1}) 2935, 1483, 1140.

^{1}H NMR (400 MHz, $CDCl_3$) δ 1.82 (s, 3H), 1.85 (s, 3H), 2.60 (s, 6H), 2.65 (s, 6H), 3.78 (dd, *J* = 2.8, 10.1 Hz, 1H), 4.28 (d, *J* = 10.1 Hz, 1H), 5.11 (d, *J* = 2.8 Hz, 1H), 5.39 (s, 1H), 5.47 (s, 1H), 7.16 (ddd, *J* = 1.2, 8.0, 8.0 Hz, 1H), 7.18 (ddd, *J* = 1.2, 8.0, 8.0 Hz, 1H), 7.26 (ddd, *J* = 1.2, 8.0, 8.0 Hz, 1H), 7.27 (ddd, *J* = 1.2, 8.0, 8.0 Hz, 1H), 7.37 (dd, *J* = 1.2, 8.0 Hz, 1H), 7.38 (dd, *J* = 1.2, 8.0 Hz, 1H), 7.56 (dd, *J* = 1.2, 8.0 Hz, 1H), 7.73 (dd, *J* = 1.2, 8.0 Hz, 1H).

^{13}C NMR (100 MHz, $CDCl_3$) δ 23.0, 23.3, 47.3, 47.5, 71.4, 87.2, 88.2, 95.1, 99.2, 101.5, 125.0, 125.1, 126.06, 126.14, 126.6, 128.86, 128.90, 138.8, 139.5, 152.9, 153.1.

HR-MS (ESI): Calcd for $C_{24}H_{32}N_3O_3$ $[M+H]^+$, 410.2444. Found, 410.2431.

3,3'-((2*aS/R*,4*S/R*,4*aS/R*,6*S/R*,6*aS/R*)-4,6-Dimethylhexahydro-1,3,5-trioxa-2a^1-azacyclopenta[*cd*] pentalene-4,6-diyl)bis(*N*,*N*-dimethylaniline) (41b)

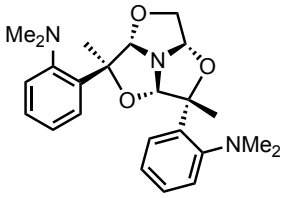

According to the synthetic protocol of **41a**, **35b** (10.0 mg, 0.0283 mmol) was converted to **41b** (7.9 mg, 68%) as a colorless solid.

IR (KBr, cm^{-1}) 2923, 1496, 1112.

^{1}H NMR (400 MHz, $CDCl_3$) δ 1.69 (s, 6H), 2.93 (s, 6H), 2.97 (s, 6H), 3.79 (dd, *J* = 2.8, 10.1 Hz, 1H), 4.28 (d, *J* = 10.1 Hz, 1H), 5.08 (d, *J* = 2.8 Hz, 1H), 5.12 (s, 1H), 5.23 (s, 1H), 6.59–6.63 (m, 1H), 6.64–6.67 (m, 2H), 6.76–6.83 (m, 3H), 7.18 (dd, *J* = 8.0, 8.0 Hz, 1H), 7.23 (dd, *J* = 8.0, 8.0 Hz, 1H).

^{13}C NMR (100 MHz, $CDCl_3$) δ 24.38, 24.44, 40.9, 71.4, 87.1, 87.6, 95.2, 99.8, 101.9, 109.1, 109.2, 111.75, 111.84, 113.4, 113.6, 129.2, 129.4, 143.3, 143.5, 150.9.

HR-MS (ESI): Calcd for $C_{24}H_{31}N_3NaO_3$ $[M+Na]^+$, 432.2263. Found, 432.2248.

4,4'-((2*aS/R*,4*S/R*,4*aS/R*,6*S/R*,6*aS/R*)-4,6-Dimethylhexahydro-1,3,5-trioxa-2a^1-azacyclopenta[*cd*] pentalene-4,6-diyl)bis(*N*,*N*-dimethylaniline) (41c)

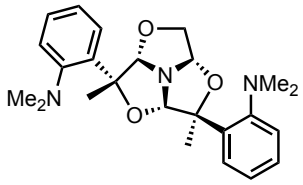

According to the synthetic protocol of **41a**, **35c** (10.1 mg, 0.0286 mmol) was converted to **41c** (9.3 mg, 80%) as a colorless solid.

IR (KBr, cm^{-1}) 2932, 1523, 1124.

^{1}H NMR (400 MHz, $CDCl_3$) δ 1.647 (s, 3H), 1.652 (s, 3H), 2.90 (s, 6H), 2.94 (s, 6H), 3.77 (dd, *J* = 2.8, 10.1 Hz, 1H), 4.24 (d, *J* = 10.1 Hz, 1H), 4.99 (d, *J* = 2.8 Hz, 1H), 5.08 (s, 1H), 5.09 (s, 1H), 6.66–6.67 (m, 2H), 6.72–6.75 (m, 2H), 7.22–7.24 (m, 2H), 7.30–7.33 (m, 2H).

^{13}C NMR (100 MHz, $CDCl_3$) δ 24.10, 24.14, 40.7, 71.2, 86.4, 86.9, 95.0, 99.3, 101.4, 112.57, 112.65, 125.9, 126.0, 130.0, 130.2, 150.0, 150.02.

HR-MS (ESI): Calcd for $C_{24}H_{32}N_3O_3$ $[M+H]^+$, 410.2444. Found, 410.2459.

2,2'-((2*aS/R*,4*R/S*,4*aS/R*,6*S/R*,6*aS/R*)-4,6-Dimethylhexahydro-1,3,5-trioxa-2a^{1}-azacyclopenta[*cd*] pentalene-4,6-diyl)bis(*N,N*-dimethylaniline) (41d)

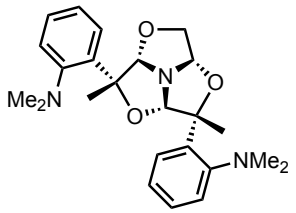

According to the synthetic protocol of **41a**, **35d** (10.0 mg, 0.0283 mmol) was converted to **41d** (7.9 mg, 68%) as a colorless solid.

IR (KBr, cm^{-1}) 2936, 1490, 1101.

^{1}H NMR (400 MHz, $CDCl_3$) δ 1.50 (s, 3H), 1.63 (s, 3H), 2.59 (s, 6H), 2.79 (brs, 6H), 3.88 (dd, *J* = 2.8, 10.1 Hz, 1H), 4.33 (d, *J* = 10.1 Hz, 1H), 5.23 (d, *J* = 2.8 Hz, 1H), 5.33 (s, 1H), 5.43 (s, 1H), 7.15–7.24 (m, *2*H), 7.27–7.34 (m, 2H), 7.39 (dd, *J* = 1.2, 7.6 Hz, 1H), 7.42 (dd, *J* = 1.2, 7.6 Hz, 1H), 7.67 (dd, *J* = 1.2, 7.6 Hz, 1H), 7.77 (dd, *J* = 1.2, 7.6 Hz, 1H).

^{13}C NMR (100 MHz, $CDCl_3$) δ 23.2, 47.3, 47.8, 71.3, 87.9, 88.2, 93.6, 99.7, 101.6, 123.5, 125.1, 125.79, 125.84, 126.5, 127.4, 128.2, 128.8, 139.7, 139.9, 151.6, 152.9.

HR-MS (ESI): Calcd for $C_{24}H_{32}N_3O_3$ $[M+H]^+$, 410.2444. Found, 410.2428.

3,3'-((2*aS/R*,4*R/S*,4*aS/R*,6*S/R*,6*aS/R*)-4,6-Dimethylhexahydro-1,3,5-trioxa-2a^1-azacyclopenta[*cd*] pentalene-4,6-diyl)bis(*N*,*N*-dimethylaniline) (42a)

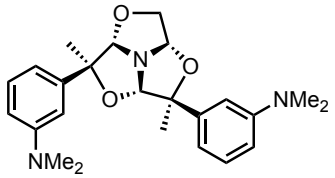

According to the synthetic protocol of **41a**, **36b** (10.0 mg, 0.0283 mmol) was converted to **42a** (6.9 mg, 60%) as a colorless solid.

IR (KBr, cm^{-1}) 2925, 1498, 1119.

^{1}H NMR (400 MHz, $CDCl_3$) δ 1.48 (s, 3H), 1.56 (s, 3H), 2.94 (s, 6H), 2.99 (s, 6H), 3.89 (dd, *J* = 2.8, 10.1 Hz, 1H), 4.33 (d, *J* = 10.1 Hz, 1H), 4.94 (s, 1H), 5.19 (s, 1H), 5.28 (d, *J* = 2.8 Hz, 1H), 6.63–6.66 (m, 1H), 6.68–6.73 (m, 3H), 6.81–6.83 (m, 1H), 6.94 (dd, *J* = 1.2, 2.4 Hz, 1H), 7.21 (dd, *J* = 8.0, 8.0 Hz, 1H), 7.25 (dd, *J* = 8.0, 8.0 Hz, 1H).

^{13}C NMR (100 MHz, $CDCl_3$) δ 23.9, 24.3, 40.8, 40.9, 71.4, 87.3, 87.5, 94.9, 99.7, 101.5, 109.2, 110.9, 111.7, 111.8, 113.4, 114.5, 128.5, 129.3, 142.0, 143.3, 150.3, 150.9.

HR-MS (ESI): Calcd for $C_{24}H_{32}N_3O_3$ $[M+H]^+$, 410.2444. Found, 410.2430.

4,4'-((2*aS/R*,4*R/S*,4*aS/R*,6*S/R*,6*aS/R*)-4,6-Dimethylhexahydro-1,3,5-trioxa-2a^1-azacyclopenta[*cd*] pentalene-4,6-diyl)bis(*N,N*-dimethylaniline) (42b)

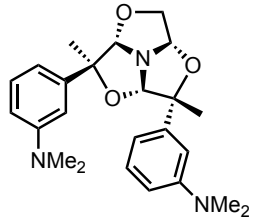

According to the synthetic protocol of **41a**, **36b** (7.6 mg, 0.0215 mmol) was converted to **42b** (9.4 mg, 81%) as a colorless solid.

IR (KBr, cm^{-1}) 2925, 1523, 1110.

^{1}H NMR (400 MHz, $CDCl_3$) δ 1.49 (s, 3H), 1.55 (s, 3H), 2.92 (s, 6H), 2.96 (s, 6H), 3.87 (dd, *J* = 2.8, 10.1 Hz, 1H), 4.31 (d, *J* = 10.1 Hz, 1H), 4.77 (s, 1H), 5.12 (s, 1H), 5.25 (d, *J* = 2.8 Hz, 1H), 6.69–6.75 (m, 4H), 7.19–7.21 (m, 2H), 7.39–7.41 (m, 2H).

^{13}C NMR (100 MHz, $CDCl_3$) δ 22.9, 24.1, 40.71, 40.74, 71.4, 86.66, 94.6, 99.8, 101.4, 111.8, 112.6, 125.9, 127.2, 128.6, 130.0, 149.8, 150.0.

HR-MS (ESI): Calcd for $C_{24}H_{32}N_3O_3$ $[M+H]^+$, 410.2444. Found, 410.2447.

2,2'-((2*aS/R*,4*S/R*,4*aS/R*,6*R/S*,6*aS/R*)-4,6-Dimethylhexahydro-1,3,5-trioxa-2a^1-azacyclopenta[*cd*] pentalene-4,6-diyl)bis(*N,N*-dimethylaniline) (42c)

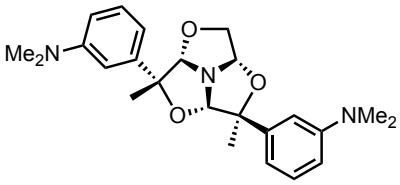

According to the synthetic protocol of **41a**, **36c** (10.0 mg, 0.0283 mmol) was converted to **42c** (7.3 mg, 63%) as a colorless solid.

IR (KBr, cm^{-1}) 2935, 1486, 1135.

^{1}H NMR (400 MHz, $CDCl_3$) δ 1.66 (s, 3H), 1.84 (s, 3H), 2.64 (s, 6H), 2.68 (s, 6H), 3.62 (dd, *J* = 2.8, 10.1 Hz, 1H), 4.08 (d, *J* = 10.1 Hz, 1H), 5.12 (d, *J* = 2.8 Hz, 1H), 5.21 (s, 1H), 5.65 (s, 1H), 7.19–7.25 (m, 2H), 7.29–7.34 (m, 2H), 7.38 (dd, *J* = 1.2, 7.6 Hz, 1H), 7.44 (dd, *J* = 1.2, 7.6 Hz, 1H), 7.59 (dd, *J* = 1.2, 7.6 Hz, 1H), 7.83 (dd, *J* = 1.2, 7.6 Hz, 1H).

^{13}C NMR (100 MHz, $CDCl_3$) δ 22.2, 23.3, 46.8, 47.3, 71.5, 86.7, 88.2, 94.8, 98.1, 101.7, 123.8, 125.2, 126.1, 126.2, 126.5, 127.1, 128.4, 128.9, 139.7, 140.5, 151.2, 153.2.

HR-MS (ESI): Calcd for $C_{24}H_{32}N_3O_3$ $[M+H]^+$, 410.2444. Found, 410.2427.

3,3'-((2*aS/R*,4*S/R*,4*aS/R*,6*R/S*,6*aS/R*)-4,6-Dimethylhexahydro-1,3,5-trioxa-2a^1-azacyclopenta[*cd*] pentalene-4,6-diyl)bis(*N,N*-dimethylaniline) (42d)

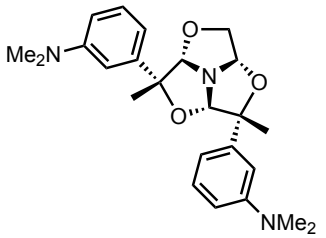

According to the synthetic protocol of **41a**, **36b** (10.0 mg, 0.0283 mmol) was converted to **42b** (7.3 mg, 63%) as a colorless solid.

IR (KBr, cm^{-1}) 2906, 1496, 1119.

^{1}H NMR (400 MHz, $CDCl_3$) δ 1.65 (s, 3H), 1.74 (s, 3H), 2.97 (s, 6H), 2.98 (s, 6H), 3.66 (dd, *J* = 2.8, 10.1 Hz, 1H), 4.13 (d, *J* = 10.1 Hz, 1H), 4.88 (s, 1H), 5.15 (d, *J* = 2.8 Hz, 1H), 5.44 (s, 1H), 6.66–6.68 (m, 2H), 6.75–6.79 (m, 2H), 6.83–6.84 (m, 1H), 6.98–6.99 (m, 1H), 7.25 (dd, *J* = 8.0, 8.0 Hz, 1H), 7.23–7.28 (m, 1H).

^{13}C NMR (100 MHz, $CDCl_3$) δ 23.8, 24.7, 40.7, 40.9, 71.8, 87.2, 87.9, 95.0, 99.9, 102.1, 109.2, 110.0, 111.6, 111.8, 113.6, 113.7, 128.8, 129.4, 142.2, 143.7, 150.4, 151.0.

HR-MS (ESI): Calcd for $C_{24}H_{31}N_3NaO_3$ $[M+H]^+$, 432.2263. Found, 432.2279.

4,4'-((2*aS/R*,4*S/R*,4*aS/R*,6*R/S*,6*aS/R*)-4,6-Dimethylhexahydro-1,3,5-trioxa-2a^1-azacyclopenta[*cd*] pentalene-4,6-diyl)bis(*N,N*-dimethylaniline) (43a)

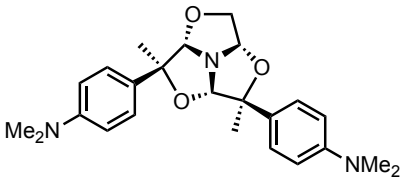

According to the synthetic protocol of **41a**, **37a** (10.0 mg, 0.0283 mmol) was converted to **43a** (7.3 mg, 63%) as a colorless solid.

IR (KBr, cm^{-1}) 2926, 1524, 1117.

^{1}H NMR (400 MHz, $CDCl_3$) δ 1.64 (s, 3H), 1.70 (s, 3H), 2.945 (s, 6H), 2.950 (s, 6H), 3.64 (dd, *J* = 2.8, 10.1 Hz, 1H), 4.12 (d, *J* = 10.1 Hz, 1H), 4.77 (s, 1H), 5.05 (d, *J* = 2.8 Hz, 1H), 5.38 (s, 1H), 6.74–6.76 (m, 4H), 7.31–7.34 (m, 2H), 7.38–7.40 (m, 2H).

^{13}C NMR (100 MHz, $CDCl_3$) δ 22.9, 24.5, 40.7, 40.8, 71.6, 86.5, 87.2, 94.9, 99.3, 102.0, 112.2, 112.7, 126.0, 126.5, 128.9, 130.4, 149.9, 150.1.

HR-MS (ESI): Calcd for $C_{24}H_{32}N_3O_3$ $[M+H]^+$, 410.2444. Found, 410.2439.

2,2'-((2*aS/R*,4*R/S*,4*aS/R*,6*R/S*,6*aS/R*)-4,6-Dimethylhexahydro-1,3,5-trioxa-2a^1-azacyclopenta[*cd*] pentalene-4,6-diyl)bis(*N,N*-dimethylaniline) (43b)

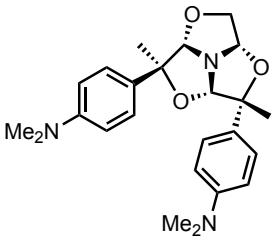

According to the synthetic protocol of **41a**, **37b** (10.0 mg, 0.0283 mmol) was converted to **43b** (5.9 mg, 51%) as a colorless solid.

IR (film, cm^{-1}) 2933, 1490, 1115. ^{1}H NMR (400 MHz, $CDCl_3$) δ 1.59 (s, 3H), 1.72 (s, 3H), 2.59 (brs, 6H), 2.69 (brs, 6H), 3.72 (dd, *J* = 2.8, 10.0 Hz, 1H), 4.15 (d, *J* = 10.0 Hz, 1H), 5.25 (s, 1H), 5.30 (d, *J* = 2.8 Hz, 1H), 5.56 (s, 1H), 6.73 (ddd, *J* = 1.6, 8.0 Hz, 1H), 6.85–6.90 (m, 1H), 7.14–7.19 (m, 2H), 7.24–7.28 (m, 1H), 7.33 (ddd, *J* = 1.6, 8.0, 8.0 Hz, 1H), 7.41 (dd, *J* = 1.6, 8.0 Hz, 1H), 7.63 (dd, *J* = 1.6, 8.0 Hz, 1H). ^{13}C NMR (100 MHz, $CDCl_3$) δ 22.1, 22.6, 46.7 (×2), 46.9 (×2), 71.3, 86.7, 87.7, 93.8, 98.0, 101.7, 123.5, 123.6, 125.8, 126.0, 126.6, 126.8, 128.0, 128.2, 140.2, 140.6, 151.1, 151.4. HR-MS (ESI): Calcd for $C_{24}H_{32}N_3O_3$ $[M+H]^+$, 410.2444. Found, 410.2424.

3,3'-((2*aS/R*,4*R/S*,4*aS/R*,6*R/S*,6*aS/R*)-4,6-Dimethylhexahydro-1,3,5-trioxa-2a^1-azacyclopenta[*cd*] pentalene-4,6-diyl)bis(*N,N*-dimethylaniline) (43c)

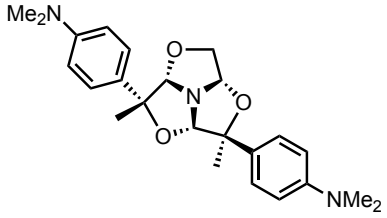

According to the synthetic protocol of **41a**, **37c** (5.1 mg, 0.144 mmol) was converted to **43c** (3.9 mg, 66%) as a colorless solid.

IR (KBr, cm^{-1}) 2916, 1604, 1121.

^{1}H NMR (400 MHz, $CDCl_3$) δ 1.54 (s, 3H), 1.69 (s, 3H), 2.78 (s, 6H), 2.94 (s, 6H), 3.75 (dd, *J* = 2.8, 10.1 Hz, 1H), 4.20 (d, *J* = 10.1 Hz, 1H), 4.91 (s, 1H), 5.17 (s, 1H), 5.32 (d, *J* = 2.8 Hz, 1H), 6.49–6.56 (m, 3H), 6.63–6.66 (m, 1H), 6.85–6.87 (m, 1H), 6.93 (dd, *J* = 2.0, 2.0 Hz, 1H), 7.10–7.14 (m, 1H), 7.23 (dd, *J* = 8.0, 8.0 Hz, 1H).

^{13}C NMR (100 MHz, $CDCl_3$) δ 23.2, 23.4, 40.6, 40.8, 71.8, 87.2, 87.6, 94.6, 100.1, 102.1, 110.2, 110.4, 111.2, 111.3, 113.5, 114.6, 128.4, 128.5, 142.0, 150.19, 150.24.

HR-MS (ESI): Calcd for $C_{24}H_{31}N_3NaO_3$ $[M+Na]^+$, 432.2263. Found, 432.2276.

4,4'-((2*aS/R*,4*R/S*,4*aS/R*,6*R/S*,6*aS/R*)-4,6-Dimethylhexahydro-1,3,5-trioxa-2a^1-azacyclopenta[*cd*]pentalene-4,6-diyl)bis(*N*,*N*-dimethylaniline) (43d)

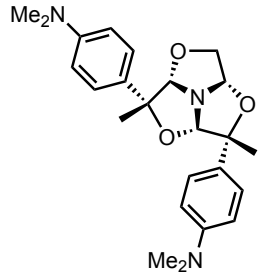

According to the synthetic protocol of **41a**, **37d** (10.0 mg, 0.0283 mmol) was converted to **43d** (7.6 mg, 66%) as a colorless solid.

IR (KBr, cm^{-1}) 2893, 1523, 1119.

^{1}H NMR (400 MHz, $CDCl_3$) δ 1.53 (s, 3H), 1.68 (s, 3H), 2.91 (s, 6H), 2.97 (s, 6H), 3.74 (dd, *J* = 2.8, 10.1 Hz, 1H), 4.20 (d, *J* = 10.1 Hz, 1H), 4.84 (s, 1H), 5.03 (s, 1H), 5.30 (d, *J* = 2.8 Hz, 1H), 6.63–6.66 (m, 2H), 6.76–6.69 (m, 2H), 7.09–7.12 (m, 2H), 7.43–7.45 (m, 2H).

^{13}C NMR (100 MHz, $CDCl_3$) δ 22.3, 23.0, 40.7, 40.9, 71.8, 86.78, 86.82, 94.4, 99.8, 102.0, 112.09, 112.10, 126.3, 127.2, 128.4, 129.1, 149.7, 150.1.

HR-MS (ESI): Calcd for $C_{24}H_{32}N_3O_3$ $[M+H]^+$, 410.2444. Found, 410.2434.

***N,N'*-(((2*aS/R*,4*S/R*,4*aS/R*,6*S/R*,6*aS/R*)-4,6-Dimethylhexahydro-1,3,5-trioxa-2a^1-azacyclopenta[*cd*]pentalene-4,6-diyl)bis(2,1-phenylene))dibenzenesulfonamide (44a)**

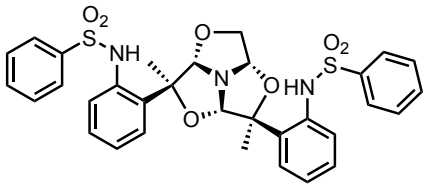

To a solution of **35a** (10.0 mg, 0.0283 mmol) in 1,2-dichlorimethane (1 mL) were added anhydrous pyridine (0.25 mL) and benzenesulfonyl chloride (3.6 μL, 0.0283 mmol) and the mixture was stirred at room temperature for 10 h. After that, the reaction mixture was poured into saturated $NaHCO_3$ aqueous solution (3 mL) and extracted with $CHCl_3$ (9 mL, 5 mL, 3 mL). The combined organic layers were dried over anhydrous Na_2SO_4 and concentrated *in vacuo.* The residue was purified by preparative TLC (hexane/ethyl acetate = 1/1) to give the mixture of **44a** (17.8 mg, 100%) as a colorless solid.

IR (KBr, cm^{-1}) 3247, 1335, 1163, 1092.

^{1}H NMR (400 MHz, $CDCl_3$) δ 1.32 (s, 3H), 1.40 (s, 3H), 3.75 (dd, *J* = 2.8, 10.4 Hz, 1H), 4.28 (d, *J* = 10.4 Hz, 1H), 4.30 (d, *J* = 2.8 Hz, 1H), 5.16 (s, 1H), 5.27 (s, 1H), 6.98–7.10 (m, 4H), 7.23–7.26 (m, 2H), 7.45–7.61 (m, 7H), 7.78–7.83 (m, 3H), 7.88–7.92 (m, 2H), 9.16 (brs, 1H), 9.40 (brs, 1H).

^{13}C NMR (100 MHz, $CDCl_3$) δ 22.4, 23.1, 70.6, 88.2, 88.6, 95.4, 97.5, 100.1, 120.0, 121.1, 124.0, 124.4, 126.6, 126.8, 127.1, 127.2, 127.5, 128.0, 129.2, 129.3, 129.4, 133.3, 136.0, 136.3, 139.9, 140.2.

HR-MS (ESI): Calcd for $C_{32}H_{31}N_3NaO_7S_2$ $[M+Na]^+$, 656.1501. Found, 656.1510.

***N,N'*-(((2*aS/R*,4*S/R*,4*aS/R*,6*S/R*,6*aS/R*)-4,6-Dimethylhexahydro-1,3,5-trioxa-2a^1-azacyclopenta[*cd*]pentalene-4,6-diyl)bis(3,1-phenylene))dibenzenesulfonamide (44b)**

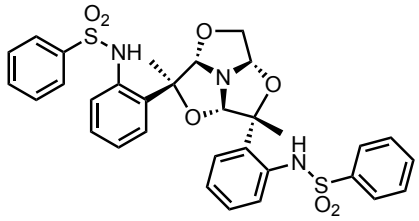

According to the synthetic protocol of **44a**, **35b** (10.0 mg, 0.0283 mmol) was converted to **44b** (6.4 mg, 36%) as a colorless solid.

IR (KBr, cm^{-1}) 3256, 2931, 1327, 1160, 1108, 1092.

^{1}H NMR (400 MHz, $CDCl_3$) δ 1.53 (s, 3H), 1.56 (s, 3H), 3.73 (dd, *J* = 2.8, 10.1 Hz, 1H), 4.22 (d, *J* = 10.1 Hz, 1H), 4.83 (d, *J* = 2.8 Hz, 1H), 4.94 (s, 1H), 4.95 (s, 1H), 6.75 (brs, 1H), 6.85 (brs, 1H), 6.93–6.97 (m, 1H), 7.01–7.04 (m, 1H), 7.11–7.15 (m, 2H), 7.20–7.26 (m, 3H), 7.33–7.46 (m, 5H), 7.49–7.53 (m, 1H), 7.68–7.70 (m, 2H), 7.73–7.75 (m, 2H).

^{13}C NMR (100 MHz, $CDCl_3$) δ 24.0, 24.1, 71.3, 86.7 87.1, 95.2, 99.6, 101.5, 118.9, 119.0, 120.9, 121.2, 122.2, 122.4, 127.3, 127.4, 129.1, 129.3, 129.7, 129.8, 133.1, 133.3, 136.81, 136.84, 138.9, 139.1, 144.0, 144.1.

HR-MS (ESI): Calcd for $C_{32}H_{31}N_3NaO_7S_2$ $[M+Na]^+$, 656.1501. Found, 656.1525.

***N,N'*-(((2*aS/R*,4*S/R*,4*aS/R*,6*S/R*,6*aS/R*)-4,6-Dimethylhexahydro-1,3,5-trioxa-2a^1-azacyclopenta[*cd*]pentalene-4,6-diyl)bis(4,1-phenylene))dibenzenesulfonamide (44c)**

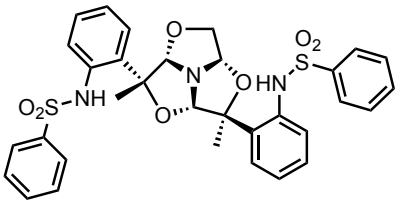

According to the synthetic protocol of **44a**, **35c** (7.0 mg, 0.0198 mmol) was converted to **44c** (12.4 mg, 99%) as a colorless solid.

IR (KBr, cm^{-1}) 3258, 2932, 1331, 1162, 1094.

^{1}H NMR (400 MHz, $CDCl_3$) δ 1.56 (s, 3H), 1.57 (s, 3H), 3.79 (dd, *J* = 2.8, 10.1 Hz, 1H), 4.24 (d, *J* = 10.1 Hz, 1H), 4.94 (s, 1H), 4.96 (d, *J* = 2.8 Hz, 1H), 5.03 (s, 1H), 6.99 (d, *J* = 8.8 Hz, 2H), 7.00 (d, *J* = 8.8 Hz, 2H), 7.16–7.21 (m, 3H), 7.25–7.28 (m, 3H), 7.38–7.42 (m, 4H), 7.49–7.54 (m, 2H), 7.73–7.75 (m, 4H).

^{13}C NMR (100 MHz, $CDCl_3$) δ 24.2, 71.3, 86.7, 87.1, 95.2, 99.4, 101.2, 121.5, 121.7, 126.0, 126.1, 127.2, 129.2, 133.2, 135.8, 135.9, 139.2, 139.3.

HR-MS (ESI): Calcd for $C_{32}H_{31}N_3NaO_7S_2$ $[M+Na]^+$, 656.1501. Found, 656.1492.

***N,N'*-(((2*aS/R*,4*R/S*,4*aS/R*,6*S/R*,6*aS/R*)-4,6-Dimethylhexahydro-1,3,5-trioxa-2a^1-azacyclopenta[*cd*]pentalene-4,6-diyl)bis(2,1-phenylene))dibenzenesulfonamide (44d)**

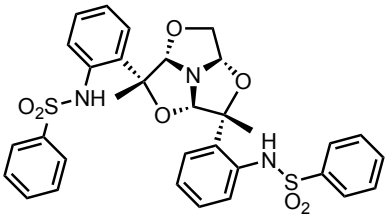

According to the synthetic protocol of **44a**, **35d** (10.2 mg, 0.0289 mmol) was converted to **44d** (17.9 mg, 98%) as a colorless solid.

IR (KBr, cm^{-1}) 3261, 2933, 1335, 1164, 1092.

^{1}H NMR (400 MHz, $CDCl_3$) δ 0.99 (s, 3H), 1.24 (s, 3H), 3.90 (dd, *J* = 2.8, 10.4 Hz, 1H), 4.38 (d, *J* = 10.4 Hz, 1H), 4.80 (s, 1H), 5.28 (d, *J* = 2.8 Hz, 1H), 5.28 (s, 1H), 7.02–7.05 (m, 2H), 7.11–7.17 (m, 1H), 7.23–7.54 (m, 9H), 7.57–7.61 (m, 2H), 7.62–7.70 (m, 1H), 7.75–7.83 (m, 3H), 8.92 (brs, 1H), 9.03 (brs, 1H).

^{13}C NMR (100 MHz, $CDCl_3$) δ 22.8, 23.5, 70.8, 88.4, 90.4, 95.9, 100.1, 100.3, 121.2, 124.2, 126.3, 127.0, 127.5, 127.6, 128.0, 128.6, 129.0, 129.2, 132.9, 133.1, 135.8, 136.0, 139.86, 139.90.

HR-MS (ESI): Calcd for $C_{32}H_{31}N_3NaO_7S_2$ $[M+Na]^+$, 656.1501. Found, 656.1502.

***N,N'*-(((2*aS/R*,4*R/S*,4*aS/R*,6*S/R*,6*aS/R*)-4,6-Dimethylhexahydro-1,3,5-trioxa-2a^1-azacyclopenta[*cd*]pentalene-4,6-diyl)bis(3,1-phenylene))dibenzenesulfonamide (45a)**

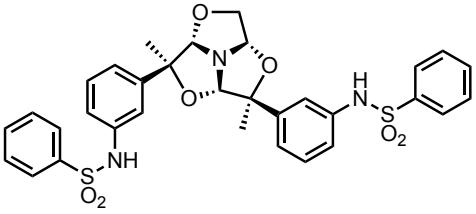

According to the synthetic protocol of **44a**, **36a** (10.0 mg, 0.0283 mmol) was converted to **45a** (5.8 mg, 32%) as a colorless solid.

IR (KBr, cm^{-1}) 3258, 2927, 1327, 1161, 1114, 1092.

^{1}H NMR (400 MHz, $CDCl_3$) δ 1.31 (s, 3H), 1.46 (s, 3H), 3.89 (dd, *J* = 3.2, 10.1 Hz, 1H), 4.25 (d, *J* = 10.0 Hz, 1H), 4.63 (s, 1H), 5.11 (s, 1H), 5.28 (d, *J* = 3.2 Hz, 1H), 6.54 (brs, 1H), 6.63–6.66 (m, 1H), 6.98–7.01 (m, 2H), 7.17 (dd, *J* = 8.0, 8.0 Hz, 1H), 7.20–7.21 (m, 1H), 7.24–7.34 (m, 8H), 7.36–7.40 (m, 1H), 7.44–7.49 (m, 1H), 7.65–7.68 (m, 2H), 7.71–7.74 (m, 2H).

^{13}C NMR (100 MHz, $CDCl_3$) δ 24.3, 24. 4, 71.2, 86.4, 87.4, 95.5, 99.0, 100.7, 118.5, 120.3, 121.06, 121.10, 121.7, 123.0, 127.3, 127.5, 128.9, 129.0, 129.3, 129.9, 132.9, 133.1, 135.8, 137.7, 138.6, 139.0, 143.4, 143.5.

HR-MS (ESI): Calcd for $C_{32}H_{31}N_3NaO_7S_2$ $[M+Na]^+$, 656.1501. Found, 656.1497.

***N,N'*-(((2*aS/R*,4*R/S*,4*aS/R*,6*S/R*,6*aS/R*)-4,6-Dimethylhexahydro-1,3,5-trioxa-2a^1-azacyclopenta[*cd*]pentalene-4,6-diyl)bis(4,1-phenylene))dibenzenesulfonamide (45b)**

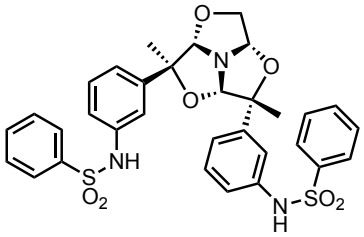

According to the synthetic protocol of **44a**, **36b** (7.0 mg, 0.0198 mmol) was converted to **45b** (11.0 mg, 88%) as a colorless solid.

IR (KBr, cm^{-1}) 3260, 2929, 1330, 1115, 1092.

^{1}H NMR (400 MHz, $CDCl_3$) δ 1.34 (s, 3H), 1.51 (s, 3H), 3.85 (dd, *J* = 2.8, 10.1 Hz, 1H), 4.28 (d, *J* = 10.1 Hz, 1H), 4.71 (s, 1H), 5.03 (s, 1H), 5.23 (d, *J* = 2.8 Hz, 1H), 6.85 (brs, 1H), 7.01–7.06 (m, 5H), 7.13–7.15 (m, 2H), 7.34–7.36 (m, 2H), 7.38–7.47 (m, 4H), 7.50–7.57 (m, 2H), 7.76–7.80 (m, 4H).

^{13}C NMR (100 MHz, $CDCl_3$) δ 22.7, 24.0, 71.4, 86.7, 86.8, 94.9, 99.8, 101.3, 121.2, 121.6, 126.0, 127.3, 127.3, 127.4, 129.1, 129.3, 133.1, 133.2, 135.4, 135.8, 138.0, 139.2, 139.3.

HR-MS (ESI): Calcd for $C_{32}H_{31}N_3NaO_7S_2$ $[M+Na]^+$, 656.1501. Found, 656.1532.

***N,N'*-(((2*aS/R*,4*S/R*,4*aS/R*,6*R/S*,6*aS/R*)-4,6-Dimethylhexahydro-1,3,5-trioxa-2a^1-azacyclopenta[*cd*]pentalene-4,6-diyl)bis(2,1-phenylene))dibenzenesulfonamide (45c)**

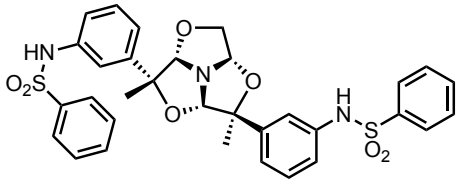

According to the synthetic protocol of **44a**, **36c** (10.0 mg, 0.0283 mmol) was converted to **45c** (9.4 mg, 52%) as a colorless solid.

IR (KBr, cm^{-1}) 3264, 2925, 1333, 1163, 1109, 1092.

^{1}H NMR (400 MHz, $CDCl_3$) δ 1.35 (s, 3H), 1.37 (brs, 3H), 3.68–3.70 (m, 1H), 4.09 (d, *J* = 10.8 Hz, 1H), 4.79 (d, *J* = 2.8 Hz, 1H), 5.03 (brs, 1H), 5.57 (s, 1H), 7.04–7.33 (m, 6H), 7.43–7.59 (m, 7H), 7.78–7.88 (m, 5H), 8.63 (brs, 1H), 9.17 (brs, 1H).

^{13}C NMR (100 MHz, $CDCl_3$) δ 23.1, 23.8, 71.0, 88.5, 95.1, 100.0, 101.7, 102.1, 121.3, 124.3, 126.5, 127.1 (×2), 127.4 (×2), 128.0, 128.3, 128.6, 129.2 (×3), 129.3 (×5), 133.1, 133.4, 135.7, 136.2, 139.1, 139.9.

HR-MS (ESI): Calcd for $C_{32}H_{31}N_3NaO_7S_2$ $[M+Na]^+$, 656.1501. Found, 656.1499.

***N,N'*-(((2*aS/R*,4*S/R*,4*aS/R*,6*R/S*,6*aS/R*)-4,6-Dimethylhexahydro-1,3,5-trioxa-2a^1-azacyclopenta[*cd*]pentalene-4,6-diyl)bis(3,1-phenylene))dibenzenesulfonamide (45d)**

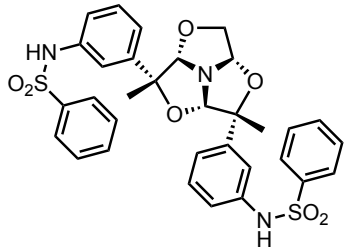

According to the synthetic protocol of **44a**, **36d** (10.0 mg, 0.0283 mmol) was converted to **45d** (6.1 mg, 34%) as a colorless solid.

IR (KBr, cm^{-1}) 3257, 2929, 1328, 1161, 1118, 1092.

^{1}H NMR (400 MHz, $CDCl_3$) δ 1.55 (s, 3H), 1.57 (s, 3H), 3.59 (dd, *J* = 2.8, 10.1 Hz, 1H), 4.00 (d, *J* = 10.1 Hz, 1H), 4.78 (s, 1H), 4.85 (d, *J* = 2.8 Hz, 1H), 5.24 (s, 1H), 6.51 (brs, 1H), 6.52 (brs, 1H), 6.94–6.97 (m, 1H), 7.01–7.03 (m, 1H), 7.09–7.10 (m, 1H), 7.18–7.31 (m, 5H), 7.42–7.47 (m, 4H), 7.52–7.57 (m, 2H), 7.74–7.80 (m, 4H).

^{13}C NMR (100 MHz, $CDCl_3$) δ 23.3, 24.5, 71.5, 86.7, 87.3, 94.9, 99.5, 101.8, 118.9, 119.4, 120.8, 121.4, 122.5, 122.7, 127.5, 129.1, 129.17, 129.22, 129.9, 133.1, 133.2, 136.2, 136.8, 139.0, 139.2, 142.7, 144.3. HR-MS (ESI): Calcd for $C_{32}H_{31}N_3NaO_7S_2$ $[M+Na]^+$, 656.1501. Found, 656.1513.

***N,N'*-(((2*aS/R*,4*S/R*,4*aS/R*,6*R/S*,6*aS/R*)-4,6-Dimethylhexahydro-1,3,5-trioxa-2a^1-azacyclopenta[*cd*]pentalene-4,6-diyl)bis(4,1-phenylene))dibenzenesulfonamide (46a)**

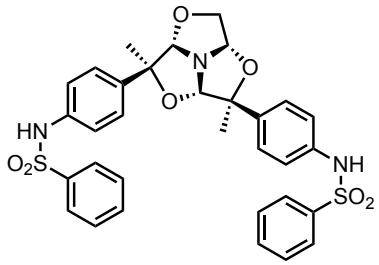

According to the synthetic protocol of **44a**, **37a** (7.0 mg, 0.0198 mmol) was converted to **46a** (12.3 mg, 98%) as a colorless solid.

IR (KBr, cm^{-1}) 3259, 2930, 1330, 1162, 1119, 1092.

^{1}H NMR (400 MHz, $CDCl_3$) δ 1.58 (s, 3H), 1.61 (s, 3H), 3.62 (dd, *J* = 2.8, 10.1 Hz, 1H), 4.04 (d, *J* = 10.1 Hz, 1H), 4.78 (s, 1H), 4.97 (d, *J* = 2.8 Hz, 1H), 5.30 (s, 1H), 6.95 (brs, 1H), 7.03–7.10 (m, 5H), 7.29–7.36 (m, 4H), 7.43–7.49 (m, 4H), 7.52–7.57 (m, 2H), 7.79–7.83 (m, 4H).

^{13}C NMR (100 MHz, $CDCl_3$) δ 23.0, 24.5, 71.5, 86.6, 87.2, 94.9, 99.4, 101.8, 121.1, 121.6, 126.2, 126.8, 127.3, 129.2, 129.3, 133.2, 133.3, 135.6, 135.9, 138.1, 139.3, 139.4, 139.5. HR-MS (ESI): Calcd for $C_{32}H_{31}N_3NaO_7S_2$ $[M+Na]^+$, 656.1501. Found, 656.1526.

***N,N'*-(((2*aS/R*,4*R/S*,4*aS/R*,6*R/S*,6*aS/R*)-4,6-Dimethylhexahydro-1,3,5-trioxa-2a^1-azacyclopenta[*cd*]pentalene-4,6-diyl)bis(2,1-phenylene))dibenzenesulfonamide (46b)**

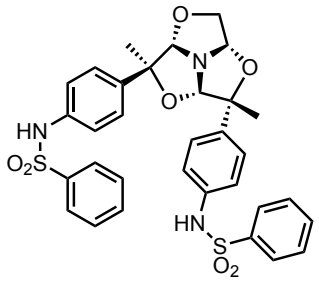

According to the synthetic protocol of **44a**, **37b** (10.0 mg, 0.0283 mmol) was converted to **46b** (12.4 mg, 69%) as a colorless solid.

IR (KBr, cm^{-1}) 3281, 2929, 1339, 1162, 1113, 1092.

^{1}H NMR (400 MHz, $CDCl_3$) δ 1.44 (s, 3H), 1.47 (s, 3H), 3.86–3.92 (m, 1H), 4.30 (d, *J* = 11.2 Hz, 1H), 5.16 (s, 1H), 5.36–5.40 (m, 2H), 6.91–7.36 (m, 14H), 7.39–7.48 (m, 1H), 7.52–7.60 (m, 1H), 7.67–7.73 (m, 2H), 8.18 (brs, 1H), 8.97 (brs, 1H).

^{13}C NMR (100 MHz, $CDCl_3$) δ 23.1, 24.5, 71.2, 89.5, 90.1, 100.5, 101.7, 120.0, 121.1, 125.3, 125.4, 126.9, 127.2, 127.4, 127.9, 128.4, 128.6, 128.9, 129.0, 132.6, 132.7, 135.4, 135.7, 139.7, 140.6.

HR-MS (ESI): Calcd for $C_{32}H_{31}N_3NaO_7S_2$ $[M+Na]^+$, 656.1501. Found, 656.1499.

***N,N'*-(((2*aS/R*,4*R/S*,4*aS/R*,6*R/S*,6*aS/R*)-4,6-Dimethylhexahydro-1,3,5-trioxa-2a^1-azacyclopenta[*cd*]pentalene-4,6-diyl)bis(3,1-phenylene))dibenzenesulfonamide (46c)**

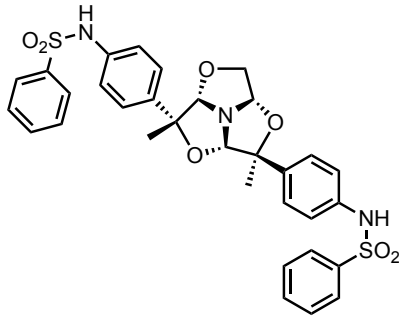

According to the synthetic protocol of **44a**, **37c** (10.0 mg, 0.0283 mmol) was converted to **46c** (8.0 mg, 45%) as a colorless solid.

IR (KBr, cm^{-1}) 3257, 2925, 1328, 1162, 1120, 1091.

^{1}H NMR (400 MHz, $CDCl_3$) δ 1.47 (s, 3H), 1.61 (s, 3H), 3.72 (dd, *J* = 2.8, 10.1 Hz, 1H), 4.07 (d, *J* = 10.1 Hz, 1H), 4.80 (s, 1H), 5.08 (s, 1H), 5.29 (d, *J* = 2.8 Hz, 1H), 6.81–6.85 (m, 2H), 6.94–6.97 (m, 2H), 7.11 (dd, *J* = 8.0, 8.0 Hz, 1H), 7.17–7.20 (m, 1H), 7.23–7.25 (m, 1H), 7.32–7.40 (m, 5H), 7.45–7.49 (m, 2H), 7.73–7.75 (m, 2H), 7.79–7.81 (m, 2H).

^{13}C NMR (100 MHz, $CDCl_3$) δ 22.6, 22.8, 71.5, 86.7, 87.0, 94.8, 99.9, 101.8, 119.7, 120.3, 120.5, 121.2, 122.1, 123.0, 127.38, 127.43, 128.8, 128.86, 128.93, 129.1, 132.8, 133.0, 136.1, 136.2, 139.3, 139.5, 142.2, 142.5.

HR-MS (ESI): Calcd for $C_{32}H_{31}N_3NaO_7S_2$ $[M+Na]^+$, 656.1501. Found, 656.1493.

***N,N'*-(((2*aS/R*,4*R/S*,4*aS/R*,6*R/S*,6*aS/R*)-4,6-Dimethylhexahydro-1,3,5-trioxa-2a^1-azacyclopenta[*cd*]pentalene-4,6-diyl)bis(4,1-phenylene))dibenzenesulfonamide (46d)**

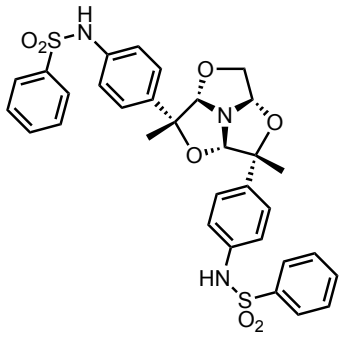

According to the synthetic protocol of **44a**, **37d** (7.0 mg, 0.0198 mmol) was converted to **46d** (11.3 mg, 90%) as a colorless solid.

IR (KBr, cm^{-1}) 3258, 2927, 1331, 1162, 1119, 1092.

^{1}H NMR (400 MHz, $CDCl_3$) δ 1.47 (s, 3H), 1.62 (s, 3H), 3.70 (dd, *J* = 2.8, 10.4 Hz, 1H), 4.10 (d, *J* = 10.4 Hz, 1H), 4.81 (s, 1H), 5.04 (s, 1H), 5.28 (d, *J* = 2.8 Hz, 1H), 6.92–6.96 (m, 6H), 7.07–7.09 (m, 2H), 7.35–7.42 (m, 6H), 7.47–7.52 (m, 2H), 7.75–7.78 (m, 4H).

^{13}C NMR (100 MHz, $CDCl_3$) δ 22.6, 23.0, 71.6, 86.7, 86.8, 94.7, 100.0, 101.8, 121.1, 121.4, 126.5, 127.1, 127.26, 127.30, 129.2, 133.1, 133.3, 135.4, 135.6, 138.1, 139.1, 139.4.

HR-MS (ESI): Calcd for $C_{32}H_{31}N_3NaO_7S_2$ $[M+Na]^+$, 656.1501. Found, 656.1509.

***N,N'*-(((2*aS/R*,4*S/R*,4*aS/R*,6*S/R*,6*aS/R*)-4,6-Dimethylhexahydro-1,3,5-trioxa-2a^1-azacyclopenta[*cd*]pentalene-4,6-diyl)bis(2,1-phenylene))dibenzamide (47a)**

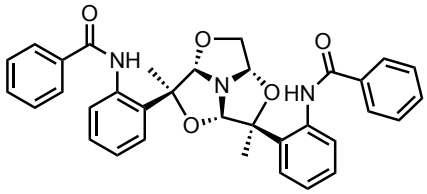

To a solution of **35a** (10.0 mg, 0.0283 mmol) in 1,2-dichlorimethane (1 mL) was added triethylamine (40 μL, 0.287 mmol) and benzoyl chloride (20 μL, 0.0283 mmol) and the mixture was stirred at room temperature for 1 h. After that, the reaction mixture was poured into saturated $NaHCO_3$ aqueous solution (1 mL) and extracted with $CHCl_3$ (7 mL, 5 mL, 5 mL). The combined organic layers were dried over anhydrous Na_2SO_4 and concentrated *in vacuo.* The residue was purified by preparative TLC (ethyl acetate/hexane = 2/1) to give the mixture of **47a** (10.8 mg, 68%) as a colorless solid.

IR (KBr, cm^{-1}) 3357, 2932, 1677, 1534, 1102.

^{1}H NMR (400 MHz, $CDCl_3$) δ 1.71 (s, 3H), 1.87 (s, 3H), 3.86 (dd, *J* = 2.8, 10.8 Hz, 1H), 4.30 (d, *J* = 10.8 Hz, 1H), 4.97 (d, *J* = 2.8 Hz, 1H), 5.33 (s, 1H), 5.56 (s, 1H), 6.98–7.03 (m, 2H), 7.17 (ddd, *J* = 1.2, 8.0, 8.0 Hz, 1H), 7.31–7.35 (m, 2H), 7.42–7.60 (m, 7H), 7.92–7.97 (m, 4H), 8.51–8.53 (m, 1H), 8.66 (dd, *J* = 1.2, 8.0 Hz, 1H), 10.29 (brs, 1H), 10.45 (brs, 1H).

^{13}C NMR (100 MHz, $CDCl_3$) δ 21.9, 22.2, 70.4, 87.9, 88.2, 95.5, 97.1, 99.2, 123.2, 123.3, 124.2, 124.3, 125.7, 125.8, 127.1, 127.7, 128.0, 128.9, 129.0, 129.3, 129.4, 132.07, 132.14, 134.9, 135.0, 137.1, 137.3, 165.0, 165.2.

HR-MS (ESI): Calcd for $C_{34}H_{31}N_3NaO_5$ $[M+Na]^+$, 584.2161. Found, 584.2144.

***N,N'*-(((2*aS/R*,4*S/R*,4*aS/R*,6*S/R*,6*aS/R*)-4,6-Dimethylhexahydro-1,3,5-trioxa-2a^1-azacyclopenta[*cd*]pentalene-4,6-diyl)bis(3,1-phenylene))dibenzamide (47b)**

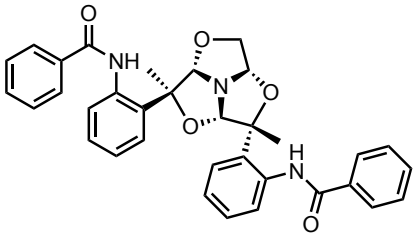

According to the synthetic protocol of **47a, 35b** (10.0 mg, 0.0283 mmol) was converted to **47b** (14.5 mg, 91%) as a colorless solid.

IR (KBr, cm^{-1}) 3301, 2931, 1651, 1543, 1108.

^{1}H NMR (400 MHz, $CDCl_3$) δ 1.696 (s, 3H), 1.701 (s, 3H), 3.76 (dd, *J* = 2.8, 10.1 Hz, 1H), 4.26 (d, *J* = 10.1 Hz, 1H), 5.05 (d, *J* = 2.8 Hz, 1H), 5.10 (s, 1H), 5.28 (s, 1H), 7.19–7.21 (m, 2H), 7.33 (dd, *J* = 8.0, 8.0 Hz, 1H), 7.35–7.43 (m, 5H), 7.47–7.52 (m, 2H), 7.54–7.57 (m, 1H), 7.65–7.67 (m, 2H), 7.79–7.87 (m, 5H), 8.05 (brs, 1H), 8.07 (brs, 1H).

^{13}C NMR (100 MHz, $CDCl_3$) δ 24.0, 24.2, 71.3, 86.8, 87.2, 95.3, 99.6, 101.5, 117.2, 117.6, 119.4, 119.8, 121.2, 121.5, 127.15, 127.18, 128.8, 128.9, 129.4, 129.6, 131.9, 132.0, 134.97, 134.99, 138.2, 138.4, 143.4, 143.7, 166.0, 166.2.

HR-MS (ESI): Calcd for $C_{34}H_{31}N_3NaO_5$ $[M+Na]^+$, 584.2161. Found, 584.2161.

***N,N'*-(((2*aS/R*,4*S/R*,4*aS/R*,6*S/R*,6*aS/R*)-4,6-Dimethylhexahydro-1,3,5-trioxa-2a^1-azacyclopenta[*cd*]pentalene-4,6-diyl)bis(4,1-phenylene))dibenzamide (47c)**

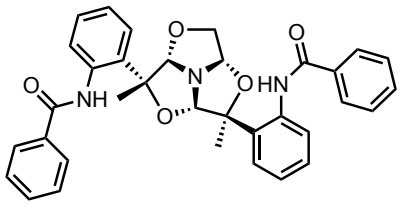

According to the synthetic protocol of **47a**, **35c** (10.0 mg, 0.0283 mmol) was converted to **47c** (12.8 mg, 81%) as a colorless amorphous.

IR (KBr, cm^{-1}) 3423, 2930, 1654, 1524, 1100.

^{1}H NMR (400 MHz, $CDCl_3$) δ 1.67 (s, 6H), 3.80 (dd, *J* = 2.8, 10.1 Hz, 1H), 4.28 (d, *J* = 10.1 Hz, 1H), 5.02 (d, *J* = 2.8 Hz, 1H), 5.12 (s, 1H), 5.13 (s, 1H), 7.37 (d, *J* = 8.8 Hz, 2H), 7.43–7.56 (m, 8H), 7.61 (d, *J* = 8.8 Hz, 2H), 7.67 (d, *J* = 8.8 Hz, 2H), 7.83–7.87 (m, 4H), 7.95 (brs, 1H), 8.00 (brs, 1H).

^{13}C NMR (100 MHz, $CDCl_3$) δ 24.3, 71.3, 86.7, 87.2, 95.2, 99.4, 101.3, 120.4, 120.6, 125.88, 125.95, 127.2, 128.9, 129.0, 132.0, 132.1, 134.9, 137.3, 137.4, 138.60, 138.69, 165.9, 166.0.

HR-MS (ESI): Calcd for $C_{34}H_{31}N_3NaO_5$ $[M+Na]^+$, 584.2161. Found, 584.2190.

***N,N'*-(((2*aS/R*,4*R/S*,4*aS/R*,6*S/R*,6*aS/R*)-4,6-Dimethylhexahydro-1,3,5-trioxa-2a^1-azacyclopenta[*cd*]pentalene-4,6-diyl)bis(2,1-phenylene))dibenzamide (47d)**

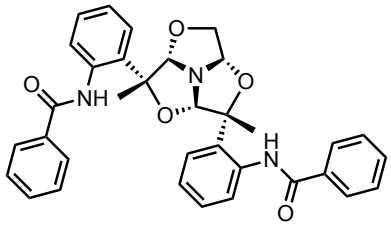

According to the synthetic protocol of **47a**, **35d** (10.0 mg, 0.0283 mmol) was converted to **47d** (15.2 mg, 96%) as a colorless solid.

IR (KBr, cm^{-1}) 3355, 2939, 1673, 1531, 1114.

^{1}H NMR (400 MHz, $CDCl_3$) δ 1.59 (s, 3H), 1.71 (s, 3H), 3.86 (dd, *J* = 2.8, 10.8 Hz, 1H), 4.12 (d, *J* = 10.8 Hz, 1H), 4.76 (s, 1H), 5.41 (d, *J* = 2.8 Hz, 1H), 5.54 (s, 1H), 6.54–6.58 (m, 1H), 6.99–7.00 (m, 1H), 7.13–7.20 (m, 2H), 7.29–7.38 (m, 3H), 7.43 (ddd, *J* = 1.2, 8.0, 8.0 Hz, 1H), 7.47–7.58 (m, 6H), 7.91–7.92 (m, 2H), 8.53 (dd, *J* = 1.2, 8.0 Hz, 2H), 9.68 (brs, 1H), 10.25 (brs, 1H).

^{13}C NMR (100 MHz, $CDCl_3$) δ 20.6, 23.7, 70.2, 87.2, 90.2, 95.8, 98.3, 100.5, 124.3, 124.4, 125.1, 126.7, 127.1, 127.3, 128.6, 128.8, 129.2, 129.3, 131.8, 134.0, 137.2, 165.0, 166.0.

HR-MS (ESI): Calcd for $C_{34}H_{31}N_3NaO_5$ $[M+Na]^+$, 584.2161. Found, 584.2162.

***N,N'*-(((2*aS/R*,4*R/S*,4*aS/R*,6*S/R*,6*aS/R*)-4,6-Dimethylhexahydro-1,3,5-trioxa-2a^1-azacyclopenta[*cd*]pentalene-4,6-diyl)bis(3,1-phenylene))dibenzamide (48a)**

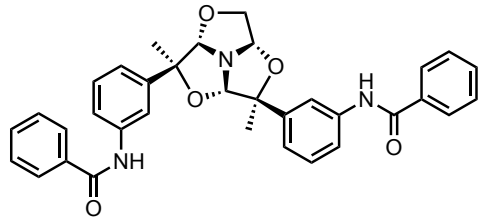

According to the synthetic protocol of **47a**, **36a** (10.0 mg, 0.0283 mmol) was converted to **48a** (11.9 mg, 75%) as a colorless solid.

IR (KBr, cm^{-1}) 3298, 2925, 1652, 1544, 1121.

^{1}H NMR (400 MHz, $CDCl_3$) δ 1.67 (s, 3H), 1.76 (s, 3H), 3.66 (dd, *J* = 2.8, 10.1 Hz, 1H), 4.11 (d, *J* = 10.1 Hz, 1H), 4.90 (s, 1H), 5.13 (d, *J* = 2.8 Hz, 1H), 5.47 (s, 1H), 7.24–7.29 (m, 2H), 7.40 (dd, *J* = 8.0, 8.0 Hz, 1H), 7.41 (dd, *J* = 8.0, 8.0 Hz, 1H), 7.47–7.51 (m, 4H), 7.53–7.59 (m, 2H), 7.60–7.62 (m, 1H), 7.66–7.68 (m, 1H), 7.74–7.90 (m, 4H), 7.90 (brs, 1H), 7.97 (brs, 1H).

^{13}C NMR (100 MHz, $CDCl_3$) δ 23.5, 24.6, 71.7, 86.9, 87.5, 95.0, 99.6, 101.9, 117.0, 117.3, 119.3, 119.4, 121.4, 121.8, 127.2, 128.94, 128.98, 129.04, 129.6, 132.0, 132.1, 135.0, 135.2, 137.8, 138.4, 142.5, 143.9, 165.9.

HR-MS (ESI): Calcd for $C_{34}H_{31}N_3NaO_5$ $[M+Na]^+$, 584.2161. Found, 584.2188.

***N,N'*-(((2*aS/R*,4*R/S*,4*aS/R*,6*S/R*,6*aS/R*)-4,6-Dimethylhexahydro-1,3,5-trioxa-2a^1-azacyclopenta[*cd*]pentalene-4,6-diyl)bis(4,1-phenylene))dibenzamide (48b)**

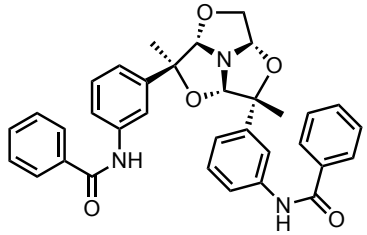

According to the synthetic protocol of **47a**, **36b** (20.0 mg, 0.0566 mmol) was converted to **48b** (26.5 mg, 90%) as a colorless amorphous.

IR (KBr, cm^{-1}) 3423, 2928, 1649, 1528, 1117.

^{1}H NMR (400 MHz, $CDCl_3$) δ 1.47 (s, 3H), 1.60 (s, 3H), 3.91 (dd, *J* = 2.8, 10.1 Hz, 1H), 4.36 (d, *J* = 10.1 Hz, 1H), 4.85 (s, 1H), 5.16 (s, 1H), 5.30 (d, *J* = 2.8 Hz, 1H), 7.33–7.35 (m, 2H), 7.49–7.59 (m, 8H), 7.62–7.64 (m, 2H), 7.67–7.69 (m, 2H), 7.80 (brs, 1H), 7.83 (brs, 1H), 7.86–7.89 (m, 4H).

^{13}C NMR (100 MHz, $CDCl_3$) δ 22.9, 24.1, 71.4, 86.9, 95.0, 99.9, 101.4, 119.6, 120.4, 125.9, 127.0, 127.2, 129.0, 132.0, 132.1, 134.9, 137.1, 137.2, 137.3, 138.6, 165.8, 166.0.

HR-MS (ESI): Calcd for $C_{34}H_{31}N_3NaO_5$ $[M+Na]^+$, 584.2161. Found, 584.2136.

***N,N'*-(((2*aS/R*,4*S/R*,4*aS/R*,6*R/S*,6*aS/R*)-4,6-Dimethylhexahydro-1,3,5-trioxa-2a^1-azacyclopenta[*cd*]pentalene-4,6-diyl)bis(2,1-phenylene))dibenzamide (48c)**

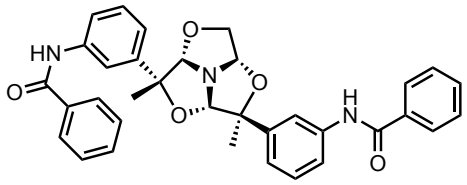

According to the synthetic protocol of **47a**, **36c** (10.0 mg, 0.0283 mmol) was converted to **48c** (16.6 mg, 100%) as a colorless solid.

IR (KBr, cm^{-1}) 3362, 2928, 1672, 1535, 1114.

^{1}H NMR (400 MHz, $CDCl_3$) δ 1.69 (s, 3H), 1.78 (s, 3H), 3.85 (dd, *J* = 2.0, 10.8 Hz, 1H), 4.27 (d, *J* = 10.8 Hz, 1H), 4.97 (d, *J* = 2.0 Hz, 1H), 5.27 (s, 1H), 5.85 (s, 1H), 7.12–7.24 (m, 2H), 7.30–7.62 (m, 11H), 7.87–7.91 (m, 4H), 8.64 (dd, *J* = 1.2, 8.0 Hz, 1H), 10.01 (brs, 1H), 10.37 (brs, 1H).

^{13}C NMR (100 MHz, $CDCl_3$) δ 22.4, 24.0, 71.1, 88.0, 89.5, 94.9, 97.9, 101.9, 123.4, 124.2, 125.6, 127.1, 127.2, 127.6, 128.0, 128.6, 128.7, 128.9, 129.0, 129.4, 130.3, 132.0, 132.1, 133.7, 134.8, 137.4, 164.9, 165.8.

HR-MS (ESI): Calcd for $C_{34}H_{31}N_3NaO_5$ $[M+Na]^+$, 584.2161. Found, 584.2170.

***N,N'*-(((2*aS/R*,4*S/R*,4*aS/R*,6*R/S*,6*aS/R*)-4,6-Dimethylhexahydro-1,3,5-trioxa-2a^1-azacyclopenta[*cd*]pentalene-4,6-diyl)bis(3,1-phenylene))dibenzamide (48d)**

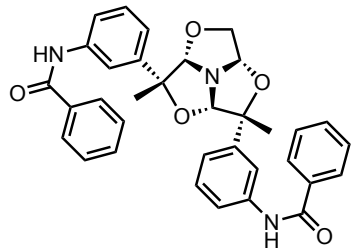

According to the synthetic protocol of **47a**, **36d** (10.0 mg, 0.0283 mmol) was converted to **48d** (15.9 mg, 100%) as a colorless solid.

IR (KBr, cm^{-1}) 3304, 2929, 1652, 1542, 1112.

^{1}H NMR (400 MHz, $CDCl_3$) δ 1.47 (s, 3H), 1.57 (s, 3H), 3.93 (dd, *J* = 3.2, 10.1 Hz, 1H), 4.29 (d, *J* = 10.1 Hz, 1H), 5.05 (s, 1H), 5.24 (s, 1H), 5.35 (d, *J* = 2.8 Hz, 1H), 7.04–7.06 (m, 1H), 7.20–7.28 (m, 4H), 7.32–7.42 (m, 5H), 7.52–7.55 (m, 1H), 7.71–7.73 (m, 2H), 7.80–7.83 (m, 3H), 7.97–7.98 (m, 1H), 8.00–8.01 (m, 1H), 8.18 (brs, 1H), 8.55 (brs, 1H).

^{13}C NMR (100 MHz, $CDCl_3$) δ 24.2, 24.5, 71.2, 86.8, 87.8, 95.6, 98.9, 101.1, 116.6, 117.7, 118.6, 118.8, 120.8, 121.6, 127.1, 127.3, 128.6, 128.7, 128.9, 129.6, 131.7, 131.8, 135.1, 135.4, 137.8, 139.2, 142.9, 143.3, 166.5, 166.7.

HR-MS (ESI): Calcd for $C_{34}H_{31}N_3NaO_5$ $[M+Na]^+$, 584.2161. Found: 584.2180.

***N,N'*-(((2*aS/R*,4*S/R*,4*aS/R*,6*R/S*,6*aS/R*)-4,6-dimethylhexahydro-1,3,5-trioxa-2a^1-azacyclopenta[*cd*] pentalene-4,6-diyl)bis(4,1-phenylene))dibenzamide (49a)**

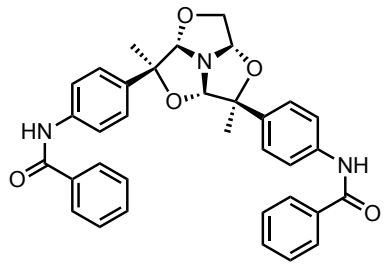

According to the synthetic protocol of **47a**, **37a** (20.0 mg, 0.0566 mmol) was converted to **49a** (1.5 mg, 68%) as a colorless amorphous.

IR (KBr, cm^{-1}) 3306, 2929, 1655, 1518, 1119.

^{1}H NMR (400 MHz, $CDCl_3$) δ 1.68 (s, 3H), 1.74 (s, 3H), 3.68 (dd, *J* = 2.8, 10.1 Hz, 1H), 4.13 (d, *J* = 10.1 Hz, 1H), 4.87 (s, 1H), 5.10 (d, *J* = 2.8 Hz, 1H), 5.44 (s, 1H), 7.46–7.52 (m, 10H), 7.68 (d, *J* = 8.8 Hz, 2H), 7.69 (d, *J* = 8.8 Hz, 2H), 7.85–7.92 (m, 6H).

^{13}C NMR (100 MHz, $CDCl_3$) δ 23.2, 24.6, 71.6, 86.8, 87.4, 95.0, 99.5, 102.0, 119.9, 120.5, 126.0, 126.5, 127.2, 128.95, 128.97, 132.0, 132.1, 134.9, 135.1, 137.2, 137.35, 137.41, 138.8, 165.8, 165.9.

HR-MS (ESI): Calcd for $C_{34}H_{31}N_3NaO_5$ $[M+Na]^+$, 584.2161. Found, 584.2175.

***N,N'*-(((2*aS/R*,4*R/S*,4*aS/R*,6*R/S*,6*aS/R*)-4,6-Dimethylhexahydro-1,3,5-trioxa-2a^1-azacyclopenta[*cd*]pentalene-4,6-diyl)bis(2,1-phenylene))dibenzamide (49b)**

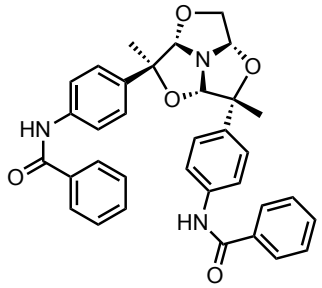

According to the synthetic protocol of **47a**,**37b** (10.0 mg, 0.0283 mmol) was converted to **49b** (16.1 mg, 99%) as a colorless solid.

IR (KBr, cm^{-1}) 3355, 2925, 1665, 1526, 1116.

^{1}H NMR (400 MHz, $CDCl_3$) δ 1.54 (brs, 3H), 1.78 (brs, 3H), 3.47–3.65 (m, 2H), 5.12 (s, 1H), 5.14 (s, 1H), 5.30 (d, *J* = 2.4 Hz, 1H), 7.00–7.53 (m, 16H), 7.96–8.25 (m, 2H), 9.17 (brs, 2H).

^{13}C NMR (100 MHz, $CDCl_3$) δ 21.9, 22.8, 70.4, 88.8, 89.8, 94.9, 101.4, 101.6, 123.9, 124.6, 125.0, 126.4, 127.0, 127.1, 127.6, 127.9, 128.1, 128.6, 128.8, 131.1, 131.4, 134.8, 135.7, 135.9, 136.3, 138.1, 165.4, 167.0.

HR-MS (ESI): Calcd for $C_{34}H_{31}N_3NaO_5$ $[M+Na]^+$, 584.2161. Found, 584.2138.

***N,N'*-(((2*aS/R*,4*R/S*,4*aS/R*,6*R/S*,6*aS/R*)-4,6-Dimethylhexahydro-1,3,5-trioxa-2a^1-azacyclopenta[*cd*]pentalene-4,6-diyl)bis(3,1-phenylene))dibenzamide (49c)**

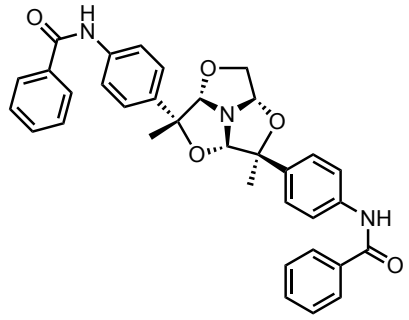

According to the synthetic protocol of **47a**, **37c** (10.0 mg, 0.0283 mmol) was converted to **49c** (15.8 mg, 100%) as a colorless solid.

IR (KBr, cm^{-1}) 3298, 2925, 1652, 1544, 1121.

^{1}H NMR (400 MHz, $CDCl_3$) δ 1.56 (s, 3H), 1.72 (s, 3H), 3.78 (dd, *J* = 2.8, 10.1 Hz, 1H), 4.21 (d, *J* = 10.1 Hz, 1H), 4.96 (s, 1H), 5.18 (s, 1H), 5.35 (d, *J* = 2.8 Hz, 1H), 6.90–6.92 (m, 1H), 7.25 (dd, *J* = 8.0, 8.0 Hz, 1H), 7.29–7.49 (m, 9H), 7.71–7.76 (m, 7H), 8.12 (brs, 1H), 8.15 (brs, 1H).

^{13}C NMR (100 MHz, $CDCl_3$) δ 22.9, 23.6, 71.7, 87.1, 87.2, 94.8, 100.1, 101.9, 117.6, 119.2, 119.8, 120.8, 121.4, 122.7, 127.1, 127.2, 128.67, 128.73, 131.7, 131.8, 134.8, 135.2, 137.5, 137.9, 142.1, 142.2, 166.1, 166.3. HR-MS (ESI): Calcd for $C_{34}H_{31}N_3NaO_5$ $[M+Na]^+$, 584.2161. Found, 584.2162.

***N,N'*-(((2*aS/R*,4*R/S*,4*aS/R*,6*R/S*,6*aS/R*)-4,6-Dimethylhexahydro-1,3,5-trioxa-2a^1-azacyclopenta[*cd*]pentalene-4,6-diyl)bis(4,1-phenylene))dibenzamide (49d)**

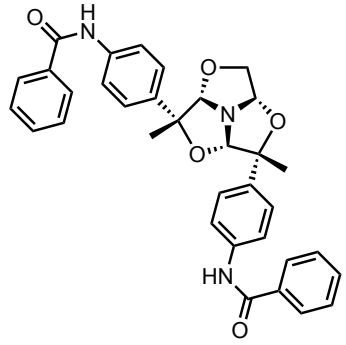

According to the synthetic protocol of **47a**, **37d** (10.0 mg, 0.0283 mmol) was converted to **49d** (14.6 mg, 92%) as a colorless amorphous.

IR (KBr, cm^{-1}) 3423, 2927, 1655, 1522, 1120.

^{1}H NMR (400 MHz, $CDCl_3$) δ 1.53 (s, 3H), 1.70 (s, 3H), 3.75 (dd, *J* = 2.8, 10.1 Hz, 1H), 4.18 (d, *J* = 10.1 Hz, 1H), 4.89 (s, 1H), 5.11 (s, 1H), 5.32 (d, *J* = 2.8 Hz, 1H), 7.12–7.14 (m, 2H), 7.43–7.54 (m, 10H), 7.69 (d, *J* = 8.4 Hz, 2H), 7.82–7.84 (m, 2H), 7.89–7.91 (m, 2H), 7.98 (brs, 1H), 8.18 (brs, 1H).

^{13}C NMR (100 MHz, $CDCl_3$) δ 22.4, 23.2, 71.7, 86.9, 87.0, 94.6, 100.1, 102.0, 119.6 (×4), 126.3 (×2), 127.0 (×2), 127.2 (×2), 127.3 (×2), 128.9 (×4), 131.9 (×2), 135.1 (×2), 136.8, 137.0, 137.3, 137.4, 165.8, 166.0.

HR-MS (ESI): Calcd for $C_{34}H_{31}N_3NaO_5$ $[M+Na]^+$, 584.2161. Found, 584.2156.

***N,N'*-(((2*aS/R*,4*S/R*,4*aS/R*,6*S/R*,6*aS/R*)-4,6-Dimethylhexahydro-1,3,5-trioxa-2a^1-azacyclopenta[*cd*]pentalene-4,6-diyl)bis(3,1-phenylene))bis(2-methoxybenzamide) (50a)**

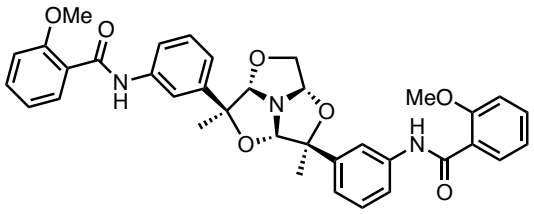

To a solution of **35a** (10.0 mg, 0.0283 mmol) in 1,2-dichlorimethane (1 mL) was added triethylamine (40 μL, 0.287 mmol) and 2-methoxybenzoyl chloride (20 μL, 0.149 mmol) and the mixture was stirred at room temperature for 2 h. After that, the reaction mixture was poured into saturated $NaHCO_3$ aqueous solution (1 mL) and extracted with $CHCl_3$ (5 mL, 4 mL, 3 mL). The combined organic layers were dried over anhydrous Na_2SO_4 and concentrated *in vacuo.* The residue was purified by preparative TLC (hexane/ethyl acetate = 2/1) to give the mixture of **50a** (16.4 mg, 93%) as a colorless solid.

IR (KBr, cm^{-1}) 3357, 2932, 1665, 1546, 1234, 1111, 1022.

^{1}H NMR (400 MHz, $CDCl_3$) δ 1.72 (s, 3H), 1.73 (s, 3H), 3.81 (dd, *J* = 2.8, 10.0 Hz, 1H), 3.99 (s, 3H), 4.07 (s, 3H), 4.30 (d, *J* = 10.0 Hz, 1H), 5.10 (d, *J* = 2.8 Hz, 1H), 5.18 (s, 1H), 5.23 (s, 1H), 6.98–7.05 (m, 2H), 7.09–7.16 (m, 3H), 7.24–7.26 (m, 1H), 7.32 (dd, *J* = 8.0, 8.0 Hz, 1H), 7.39 (dd, *J* = 8.0, 8.0 Hz, 1H), 7.46–7.52 (m, 2H), 7.56–7.61 (m, 2H), 7.69 (dd, *J* = 2.0, 2.0 Hz, 1H), 7.83 (dd, *J* = 2.0, 2.0 Hz, 1H), 8.24 (dd, *J* = 2.0, 8.0 Hz, 1H), 8.27 (dd, *J* = 2.0, 8.0 Hz, 1H), 9.76 (brs, 1H), 9.83 (brs, 1H).

^{13}C NMR (100 MHz, $CDCl_3$) δ 24.27, 24.34, 56.4, 56.5, 71.4, 86.9, 87.4, 95.3, 99.7, 101.5, 111.6, 111.7, 117.3, 117.4, 119.8, 119.9, 120.8, 121.1, 121.77, 121.83 (×2), 121.9, 129.3, 129.4, 132.60, 132.63, 133.39, 133.43, 138.7, 138.8, 143.5, 143.7, 157.3 (×2), 163.4 (×2).

HR-MS (ESI): Calcd for $C_{36}H_{35}N_3NaO_7$ $[M+Na]^+$, 644.2373. Found, 644.2356.

***N,N'*-(((2*aS/R*,4*S/R*,4*aS/R*,6*S/R*,6*aS/R*)-4,6-Dimethylhexahydro-1,3,5-trioxa-2a^1-azacyclopenta[*cd*]pentalene-4,6-diyl)bis(3,1-phenylene))bis(3-methoxybenzamide*)* (51a)**

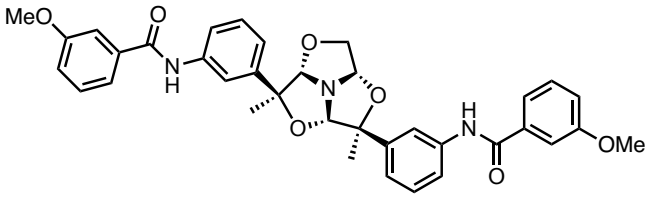

According to the synthetic protocol of **50a**, **36a** (10.0 mg, 0.0283 mmol) was converted to **51a** (15.5 mg, 88%) as a colorless solid.

IR (KBr, cm^{-1}) 3312, 2933, 1654, 1541, 1234, 1108, 1039.

^{1}H NMR (400 MHz, $CDCl_3$) δ 1.69 (s, 3H), 1.70 (s, 3H), 3.76 (dd, *J* = 2.8, 10.1 Hz, 1H), 3.805 (s, 3H), 3.814 (s, 3H), 4.26 (d, *J* = 10.1 Hz, 1H), 5.05 (d, *J* = 2.8 Hz, 1H), 5.11 (s, 1H), 5.25 (s, 1H), 7.01–7.06 (m, 3H), 7.18–7.42 (m, 9H), 7.55 (dd, *J* = 0.8, 8.0 Hz, 1H), 7.64–7.66 (m, 2H), 7.81 (dd, *J* = 2.0, 2.0 Hz, 1H), 8.04 (brs, 1H), 8.06 (brs, 1H).

^{13}C NMR (100 MHz, $CDCl_3$) δ 24.1, 24.2, 55.6, 71.3, 86.8, 87.2, 95.3, 99.6, 101.5, 112.4, 112.6, 117.1, 117.5, 118.22, 118.25, 118.8, 118.9, 119.4, 119.7, 121.2, 121.5, 129.4, 129.6, 129.8, 129.9, 136.4, 138.2, 138.3, 143.4, 143.7, 160.0, 160.1, 165.8, 166.0.

HR-MS (ESI): Calcd for $C_{36}H_{35}N_3NaO_7$ $[M+Na]^+$, 644.2373. Found, 644.2392.

***N,N'*-(((2*aS/R*,4*S/R*,4*aS/R*,6*S/R*,6*aS/R*)-4,6-Dimethylhexahydro-1,3,5-trioxa-2a^1-azacyclopenta[*cd*]pentalene-4,6-diyl)bis(3,1-phenylene))bis(4-methoxybenzamide) (52a)**

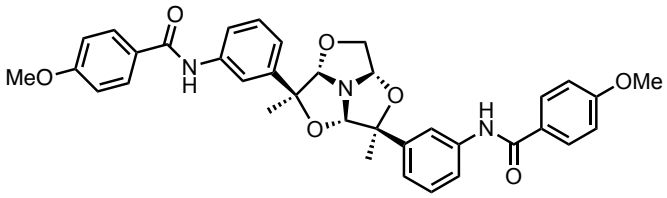

According to the synthetic protocol of **50a**, **37a** (10.0 mg, 0.0283 mmol) was converted to **52a** (15.3 mg, 87%) as a colorless solid.

IR (KBr, cm^{-1}) 3327, 2933, 1649, 1543, 1252, 1107, 1029.

^{1}H NMR (400 MHz, $CDCl_3$) δ 1.687 (s, 3H), 1.692 (s, 3H), 3.73 (dd, *J* = 2.8, 10.1 Hz, 1H), 3.82 (s, 3H), 3.83 (s, 3H), 4.24 (d, *J* = 10.1 Hz, 1H), 5.03 (d, *J* = 2.8 Hz, 1H), 5.08 (s, 1H), 5.29 (s, 1H), 6.81–6.84 (m, 2H), 6.87–6.89 (m, 2H), 7.16–7.19 (m, 2H), 7.30 (dd, *J* = 8.0, 8.0 Hz, 1H), 7.35 (dd, *J* = 8.0, 8.0 Hz, 1H), 7.53 (dd, *J* = 1.6, 8.0 Hz, 1H), 7.64–7.67 (m, 2H), 7.74–7.76 (m, 2H), 7.81–7.83 (m, 3H), 8.06 (brs, 1H), 8.07 (brs, 1H).

^{13}C NMR (100 MHz, $CDCl_3$) δ 24.0, 24.2, 55.5, 55.6, 71.3, 86.8, 87.2, 95.3, 99.7, 101.5, 113.9, 114.0, 117.2, 117.7, 119.4, 119.8, 120.9, 121.3, 127.12, 127.14, 129.07, 129.10, 129.4, 129.5, 138.4, 138.6, 143.3, 143.6, 162.5, 162.6, 165.6, 165.7.

HR-MS (ESI): Calcd for $C_{36}H_{35}N_3NaO_7$ $[M+Na]^+$, 644.2373. Found, 644.2366.

(+)-**52a**: $[\alpha]_D^{25}$= +68.5 (*c* 0.040, $CHCl_3$)

(–)-**52a**: $[\alpha]_D^{25}$= –75.0 (*c* 0.040, $CHCl_3$)

***N,N'*-(((2*aS/R*,4*R/S*,4*aS/R*,6*R/S*,6*aS/R*)-4,6-Dimethylhexahydro-1,3,5-trioxa-2a^1-azacyclopenta[*cd*]pentalene-4,6-diyl)bis(3,1-phenylene))bis(2-methoxybenzamide) (50d)**

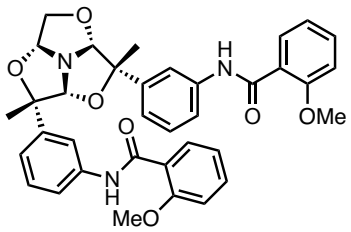

According to the synthetic protocol of **50a**, **35d** (10.0 mg, 0.0283 mmol) was converted to **50d** (16.2 mg, 92%) as a colorless solid.

IR (KBr, cm^{-1}) 3360, 2927, 1666, 1552, 1234, 1120, 1019.

^{1}H NMR (400 MHz, $CDCl_3$) δ 1.57 (s, 3H), 1.76 (s, 3H), 3.75 (s, 3H), 3.81 (dd, *J* = 2.8, 10.1 Hz, 1H), 3.93 (s, 3H), 4.22 (d, *J* = 10.1 Hz, 1H), 5.04 (s, 1H), 5.15 (s, 1H), 5.36 (d, *J* = 2.8 Hz, 1H), 6.86–6.97 (m, 5H), 7.13 (dd, *J* = 1.6, 1.6 Hz, 1H), 7.24–7.30 (m, 2H), 7.34–7.40 (m, 2H), 7.43 (dd, *J* = 8.0, 8.0 Hz, 1H), 7.52 (dd, *J* = 1.6, 1.6 Hz, 1H), 7.94–8.01 (m, 3H), 8.25 (dd, *J* = 1.6, 8.0 Hz, 1H), 9.75 (brs, 1H), 10.09 (brs, 1H).

^{13}C NMR (100 MHz, $CDCl_3$) δ 22.1, 24.1, 56.0, 56.5, 71.9, 86.6, 87.4, 94.7, 100.1, 101.9, 111.4, 111.5, 116.6, 119.1, 119.3, 119.4, 121.0, 121.15, 121.22, 121.38, 121.42, 121.5, 128.6, 128.9, 132.1, 132.3, 133.1, 138.2, 138.5, 141.1, 142.5, 157.2, 157.3, 163.2, 163.3. HR-MS (ESI): Calcd for $C_{36}H_{35}N_3NaO_7$ $[M+Na]^+$, 644.2373. Found, 644.2348.

***N,N'*-(((2*aS/R*,4*R/S*,4*aS/R*,6*R/S*,6*aS/R*)-4,6-Dimethylhexahydro-1,3,5-trioxa-2a^1-azacyclopenta[*cd*]pentalene-4,6-diyl)bis(3,1-phenylene))bis(3-methoxybenzamide) (51d)**

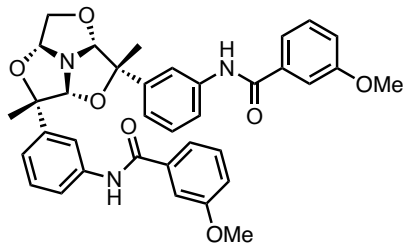

According to the synthetic protocol of **50a**, **36d** (10.0 mg, 0.0283 mmol) was converted to **51d** (14.3 mg, 81%) as a colorless solid.

IR (KBr, cm^{-1}) 3314, 2929, 1654, 1543, 1238, 1121, 1041.

^{1}H NMR (400 MHz, $CDCl_3$) δ 1.57 (s, 3H), 1.72 (s, 3H), 3.76–3.79 (m, 1H), 3.78 (s, 3H), 3.79 (s, 3H), 4.22 (d, *J* = 10.1 Hz, 1H), 4.95 (s, 1H), 5.19 (s, 1H), 5.35 (d, *J* = 2.8 Hz, 1H), 6.90–6.95 (m, 2H), 6.98–7.01 (m, 1H), 7.23–7.31 (m, 9H), 7.43 (dd, *J* = 7.6, 7.6 Hz, 1H), 7.69 (dd, *J* = 1.6, 7.6 Hz, 1H), 7.74–7.77 (m, 2H), 8.12 (brs, 1H), 8.13 (brs, 1H).

^{13}C NMR (100 MHz, $CDCl_3$) δ 22.9, 23.5, 55.5, 71.8, 87.1, 87.2, 94.8, 100.1, 101.9, 112.4, 112.5, 117.6, 117.8, 118.3, 118.8, 118.9, 119.2, 119.7, 120.5, 121.3, 122.6, 128.69, 128.74, 129.7, 129.8, 136.2, 136.6, 137.5, 137.9, 142.1, 142.2, 159.8, 159.9, 165.8, 166.1.

HR-MS (ESI): Calcd for $C_{36}H_{35}N_3NaO_7$ $[M+Na]^+$, 644.2373. Found, 644.2353.

***N,N'*-(((2*aS/R*,4*R/S*,4*aS/R*,6*R/S*,6*aS/R*)-4,6-Dimethylhexahydro-1,3,5-trioxa-2a^1-azacyclopenta[*cd*]pentalene-4,6-diyl)bis(3,1-phenylene))bis(4-methoxybenzamide) (52d)**

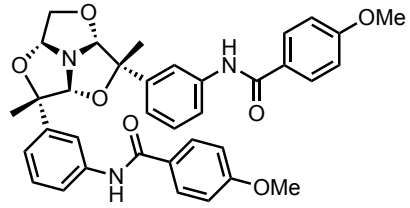

According to the synthetic protocol of **50a**, **37d** (10.0 mg, 0.0283 mmol) was converted to **52d** (15.0 mg, 85%) as a colorless solid.

IR (KBr, cm^{-1}) 3313, 2929, 1648, 1543, 1253, 1120, 1031.

^{1}H NMR (400 MHz, $CDCl_3$) δ 1.56 (s, 3H), 1.72 (s, 3H), 3.77 (dd, *J* = 2.8, 10.1 Hz, 1H), 3.79 (s, 3H), 3.82 (s, 3H), 4.21 (d, *J* = 10.1 Hz, 1H), 4.94 (s, 1H), 5.17 (s, 1H), 5.34 (d, *J* = 2.8 Hz, 1H), 6.79–6.84 (m, 3H), 6.88–6.91 (m, 1H), 7.22–7.28 (m, 3H), 7.41 (dd, *J* = 8.0, 8.0 Hz, 1H), 7.68–7.76 (m, 7H), 8.08 (brs, 1H), 8.11 (brs, 1H).

^{13}C NMR (100 MHz, $CDCl_3$) δ 22.8, 23.5, 55.47, 55.52, 71.7, 87.1, 87.2, 94.8, 100.1, 101.9, 113.9, 117.5, 119.2, 119.7, 120.6, 121.1, 122.4, 127.0, 127.4, 128.6, 128.7, 129.0, 129.1, 137.7, 138.2, 142.0, 142.1, 162.3, 162.4, 165.6, 165.8. HR-MS (ESI): Calcd for $C_{36}H_{35}N_3NaO_7$ $[M+Na]^+$, 644.2373. Found, 644.2366.

(+)-**52b**: $[\alpha]_D^{25}$= +55.0 (*c* 0.040, $CHCl_3$)

(–)-**52b**: $[\alpha]_D^{25}$= –55.0 (*c* 0.040, $CHCl_3$)

***N,N'*-(((2*aS/R*,4*S/R*,4*aS/R*,6*S/R*,6*aS/R*)-4,6-Dimethylhexahydro-1,3,5-trioxa-2a^1-azacyclopenta[*cd*]pentalene-4,6-diyl)bis(3,1-phenylene))bis(2-(dimethylamino)benzamide) (53a)**

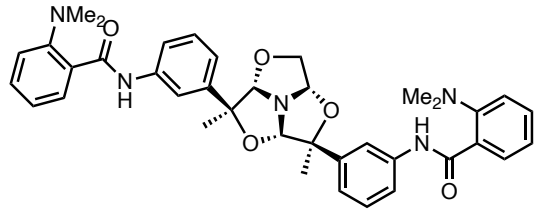

To a solution of **35a** (10.0 mg, 0.0283 mmol) in 1,2-dichlorimethane (1 mL) was added 2-(dimethylamino) benzoic acid (48 mg, 0.283 mmol), HATU (107.6 mg, 0.283 mmol) and DIPEA (49.3 μL, 0.283 mmol), then the mixture was stirred at room temperature for 15 h. After that, 1,2-dichlorimethane was removed in reduced pressure and the residue was diluted with ethyl acetate (5 mL), washed with water (10 mL) and brine (1 mL × 2). The combined organic layers were dried over anhydrous Na_2SO_4 and concentrated *in vacuo.* The residue was purified by preparative TLC (hexane/ethyl acetate = 1/1) to give the mixture of **53a** (17.0 mg, 93%) as a pale-yellow amorphous.

IR (KBr, cm^{-1}) 2934, 1670, 1552, 1109. ^{1}H NMR (400 MHz, $CDCl_3$) δ 1.73 (s, 3H), 1.74 (s, 3H), 2.79 (s, 6H), 2.84 (s, 6H), 3.82 (dd, *J* = 2.8, 10.1 Hz, 1H), 4.31 (d, *J* = 10.1 Hz, 1H), 5.13 (d, *J* = 2.8 Hz, 1H), 5.18 (s, 1H), 5.23 (s, 1H), 7.11–7.13 (m, 1H), 7.22–7.33 (m, 6H), 7.39 (dd, *J* = 8.0, 8.0 Hz, 1H), 7.45–7.51 (m, 4H), 7.81 (dd, *J* = 1.6, 1.6 Hz, 1H), 7.92 (dd, *J* = 1.6, 1.6 Hz, 1H), 8.21 (dd, *J* = 1.6, 8.0 Hz, 1H), 8.25 (dd, *J* = 1.6, 8.0 Hz, 1H), 12.10 (brs, 1H), 12.21 (brs, 1H).

^{13}C NMR (100 MHz, $CDCl_3$) δ 24.3, 45.57, 45.63, 71.4, 86.9, 87.4, 95.3, 99.8, 101.6, 116.9, 119.2, 120.3, 120.37, 120.43, 120.7, 125.05, 125.13, 127.68, 127.73, 129.2, 129.3, 131.7, 131.8, 132.50, 132.54, 139.2, 139.3, 143.6, 143.8, 152.21, 152.24, 164.3.

HR-MS (ESI): Calcd for $C_{38}H_{41}N_5NaO_5$ $[M+Na]^+$, 670.3005. Found, 670.2981.

***N,N'*-(((2*aS/R*,4*S/R*,4*aS/R*,6*S/R*,6*aS/R*)-4,6-Dimethylhexahydro-1,3,5-trioxa-2a^1-azacyclopenta[*cd*]pentalene-4,6-diyl)bis(3,1-phenylene))bis(3-(dimethylamino)benzamide) (54a)**

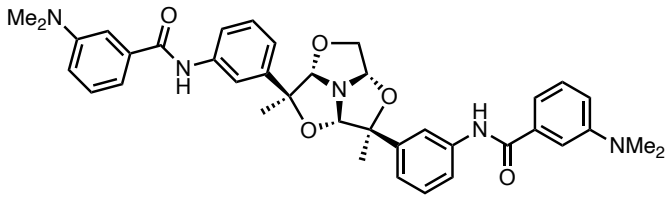

According to the synthetic protocol of **53a**, **36a** (10.0 mg, 0.0283 mmol) was converted to **54a** (8.5 mg, 46%) as a colorless amorphous.

IR (KBr, cm^{-1}) 2925, 1650, 1537, 1109.

^{1}H NMR (400 MHz, $CDCl_3$) δ 1.698 (s, 3H), 1.703 (s, 3H), 2.97 (s, 6H), 2.98 (s, 6H), 3.77 (dd, *J* = 2.8, 10.1 Hz, 1H), 4.27 (d, *J* = 10.1 Hz, 1H), 5.06 (d, *J* = 2.8 Hz, 1H), 5.13 (s, 1H), 5.24 (s, 1H), 6.81–6.86 (m, 2H), 7.02–7.04 (m, 1H), 7.08–7.10 (m, 1H), 7.16–7.29 (m, 6H), 7.33 (dd, *J* = 8.0, 8.0 Hz, 1H), 7.38 (dd, *J* = 8.0, 8.0 Hz, 1H), 7.55 (dd, *J* = 1.6, 8.0 Hz, 1H), 7.63–7.68 (m, 2H), 7.81–7.82 (m, 1H), 7.96 (brs, 1H), 7.97 (brs, 1H).

^{13}C NMR (100 MHz, $CDCl_3$) δ 24.1, 24.2, 40.6, 71.3, 86.8, 87.3, 95.3, 99.6, 101.5, 111.4, 113.8, 113.9, 115.58, 115.60, 117.0, 117.3, 119.3, 119.5, 121.1, 121.2, 129.38, 129.42, 129.46, 129.51, 135.8, 135.9, 138.49, 138.53, 143.5, 143.6, 150.86, 150.91, 166.8, 166.9.

HR-MS (ESI): Calcd for $C_{38}H_{41}N_5NaO_5$ $[M+Na]^+$, 670.3005. Found, 670.2986.

***N,N'*-(((2*aS/R*,4*S/R*,4*aS/R*,6*S/R*,6*aS/R*)-4,6-Dimethylhexahydro-1,3,5-trioxa-2a^1-azacyclopenta[*cd*]pentalene-4,6-diyl)bis(3,1-phenylene))bis(4-(dimethylamino)benzamide) (55a)**

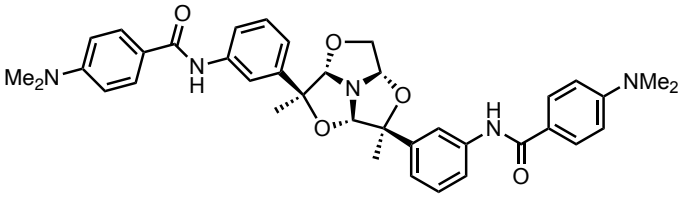

According to the synthetic protocol of **53a**, **37a** (10.0 mg, 0.0283 mmol) was converted to **55a** (10.8 mg, 59%) as a colorless amorphous.

IR (KBr, cm^{-1}) 2929, 1607, 1522, 1108.

^{1}H NMR (400 MHz, $CDCl_3$) δ 1.69 (s, 3H), 1.70 (s, 3H), 3.00 (s, 6H), 3.02 (s, 6H), 3.76 (dd, *J* = 2.8, 10.1 Hz, 1H), 4.26 (d, *J* = 10.1 Hz, 1H), 5.05 (d, *J* = 2.8 Hz, 1H), 5.12 (s, 1H), 5.28 (s, 1H), 6.59–6.61 (m, 2H), 6.64–6.67 (m, 2H), 7.13–7.17 (m, 2H), 7.31 (dd, *J* = 8.0, 8.0 Hz, 1H), 7.36 (dd, *J* = 8.0, 8.0 Hz, 1H), 7.54–7.57 (m, 1H), 7.62 (dd, *J* = 1.6, 1.6 Hz, 1H), 7.68–7.69 (m, 1H), 7.72–7.75 (m, 2H), 7.78–7.81 (m, 3H), 7.919 (brs, 1H), 7.923 (brs, 1H).

^{13}C NMR (100 MHz, $CDCl_3$) δ 24.0, 24.2, 40.2, 71.3, 86.8, 87.2, 95.2, 99.5, 101.5, 111.16, 111.21, 116.9, 117.3, 119.2, 119.5, 120.5, 120.7, 121.3, 128.7, 128.8, 129.3, 129.4, 138.8, 138.9, 143.2, 143.5, 152.66, 152.72, 165.8, 165.9.

HR-MS (ESI): Calcd for $C_{38}H_{41}N_5NaO_5$ $[M+Na]^+$, 670.3005. Found, 670.3021.

***N,N'*-(((2*aS/R*,4*R/S*,4*aS/R*,6*R/S*,6*aS/R*)-4,6-Dimethylhexahydro-1,3,5-trioxa-2a^1-azacyclopenta[*cd*]pentalene-4,6-diyl)bis(3,1-phenylene))bis(2-(dimethylamino)benzamide) (53d)**

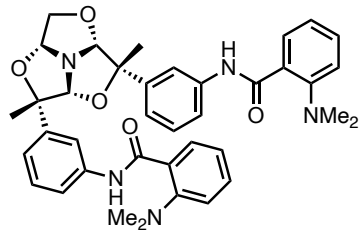

According to the synthetic protocol of **53a**, **35d** (10.0 mg, 0.0283 mmol) was converted to **53d** (8.7 mg, 47%) as a pale-red amorphous.

IR (KBr, cm^{-1}) 3449, 1665, 1559, 1120.

^{1}H NMR (400 MHz, $CDCl_3$) δ 1.60 (s, 3H), 1.74 (s, 3H), 2.71 (s, 6H), 2.74 (s, 6H), 3.80 (dd, *J* = 2.8, 10.1 Hz, 1H), 4.20 (d, *J* = 10.1 Hz, 1H), 5.01 (s, 1H), 5.22 (s, 1H), 5.36 (d, *J* = 2.8 Hz, 1H), 6.90–6.92 (m, 1H), 7.17–7.31 (m, 6H), 7.38–7.48 (m, 4H), 7.55–7.57 (m, 1H), 7.70 (dd, *J* = 1.6, 1.6 Hz, 1H), 7.83–7.85 (m, 1H), 8.14–8.17 (m, 2H), 12.04 (brs, 1H), 12.25 (brs, 1H).

^{13}C NMR (100 MHz, $CDCl_3$) δ 23.1, 23.8, 45.6, 71.8, 87.1, 87.3, 94.8, 100.0, 101.8, 116.9, 118.1, 119.1, 119.3, 120.35, 120.38, 121.2, 121.7, 125.0, 125.1, 127.67, 127.70, 128.5, 128.6, 131.6, 131.7, 132.4, 138.6, 141.8, 142.3, 152.2, 152.3, 164.2, 164.3.

HR-MS (ESI): Calcd for $C_{38}H_{41}N_5NaO_5$ $[M+Na]^+$, 670.3005. Found, 670.2981.

***N,N'*-(((2*aS/R*,4*R/S*,4*aS/R*,6*R/S*,6*aS/R*)-4,6-Dimethylhexahydro-1,3,5-trioxa-2a^1-azacyclopenta[*cd*]pentalene-4,6-diyl)bis(3,1-phenylene))bis(3-(dimethylamino)benzamide) (54d)**

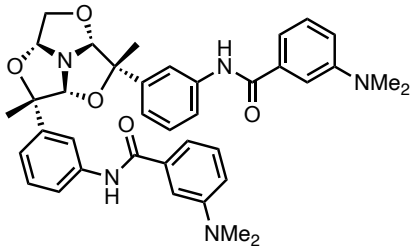

According to the synthetic protocol of **53a**, **36d** (10.0 mg, 0.0283 mmol) was converted to **54d** (8.5 mg, 46%) as a colorless amorphous.

IR (KBr, cm^{-1}) 2925, 1655, 1542, 1120.

^{1}H NMR (400 MHz, $CDCl_3$) δ 1.57 (s, 3H), 1.72 (s, 3H), 2.960 (s, 6H), 2.962 (s, 6H), 3.77 (dd, *J* = 2.8, 10.1 Hz, 1H), 4.22 (d, *J* = 10.1 Hz, 1H), 4.96 (s, 1H), 5.19 (s, 1H), 5.34 (d, *J* = 2.8 Hz, 1H), 6.79 (dd, *J* = 2.0, 8.0 Hz, 1H), 6.82 (dd, *J* = 2.0, 8.0 Hz, 1H), 6.89–6.91 (m, 1H), 6.98–7.33 (m, 9H), 7.42 (dd, *J* = 8.0, 8.0 Hz, 1H), 7.69–7.74 (m, 3H), 8.00 (brs, 1H), 8.02 (brs, 1H).

^{13}C NMR (100 MHz, $CDCl_3$) δ 22.9, 23.6, 40.6, 71.8, 87.1, 87.2, 94.8, 100.1, 101.9, 111.5, 113.9, 114.0, 115.49, 115.52, 117.3, 119.0, 119.1, 120.2, 121.2, 122.4, 128.6, 128.8, 129.30, 129.33, 135.7, 136.0, 137.8, 138.0, 142.07, 142.14, 150.8, 166.7, 166.9.

HR-MS (ESI): Calcd for $C_{38}H_{41}N_5NaO_5$ $[M+Na]^+$, 670.3005. Found, 670.3000.

***N,N'*-(((2*aS/R*,4*R/S*,4*aS/R*,6*R/S*,6*aS/R*)-4,6-Dimethylhexahydro-1,3,5-trioxa-2a^1-azacyclopenta[*cd*]pentalene-4,6-diyl)bis(3,1-phenylene))bis(4-(dimethylamino)benzamide) (55d)**

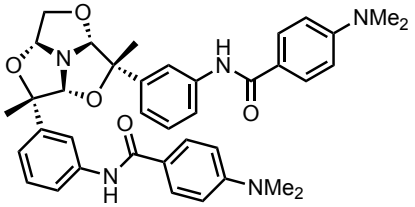

According to the synthetic protocol of **53a**, **37d** (10.0 mg, 0.0283 mmol) was converted to **55d** (28.9 mg, 52%) as a colorless solid.

IR (KBr, cm^{-1}) 2905, 1607, 1523, 1121.

^{1}H NMR (400 MHz, $CDCl_3$) δ 1.56 (s, 3H), 1.72 (s, 3H), 3.00 (s, 6H), 3.02 (s, 6H), 3.78 (dd, *J* = 2.8, 10.1 Hz, 1H), 4.23 (d, *J* = 10.1 Hz, 1H), 4.96 (s, 1H), 5.19 (s, 1H), 5.34 (d, *J* = 2.8 Hz, 1H), 6.61–6.64 (m, 4H), 6.86–6.88 (m, 1H), 7.17 (dd, *J* = 1.6, 1.6 Hz, 1H), 7.22–7.28 (m, 2H), 7.42 (dd, *J* = 8.0, 8.0 Hz, 1H), 7.65 (dd, *J* = 1.6, 1.6 Hz, 1H), 7.68–7.71 (m, 4H), 7.74–7.84 (m, 5H), 7.89 (brs, 1H).

^{13}C NMR (100 MHz, $CDCl_3$) δ 22.9, 23.6, 40.2, 71.8, 87.1, 87.3, 94.8, 100.2, 102.0, 111.2, 111.3, 117.1, 118.8, 119.0, 120.0, 120.7, 121.4, 121.6, 121.9, 128.6, 128.67, 128.73, 128.8, 138.2, 138.4, 142.01, 142.04, 152.66, 152.69, 165.7, 165.9.

HR-MS (ESI): Calcd for $C_{38}H_{41}N_5NaO_5$ $[M+Na]^+$, 670.3005. Found, 670.2997.

***N,N'*-(((2*aS/R*,4*S/R*,4*aS/R*,6*S/R*,6*aS/R*)-4,6-Dimethylhexahydro-1,3,5-trioxa-2a^1-azacyclopenta[*cd*]pentalene-4,6-diyl)bis(3,1-phenylene))dipicolinamide (56a)**

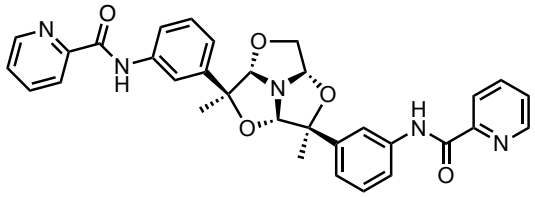

According to the synthetic protocol of **53a**, **35a** (10.0 mg, 0.0283 mmol) was converted to **56a** (17.3 mg, 100%) as a colorless amorphous.

IR (KBr, cm^{-1}) 2929, 1685, 1536, 1111.

^{1}H NMR (400 MHz, $CDCl_3$) δ 1.72 (s, 3H), 1.73 (s, 3H), 3.82 (dd, *J* = 2.8, 10.1 Hz, 1H), 4.32 (d, *J* = 10.1 Hz, 1H), 5.11 (d, *J* = 2.8 Hz, 1H) 5.20 (s, 1H), 5.22 (s, 1H), 7.16–7.18 (m, 1H), 7.27–7.30 (m, 1H), 7.36 (dd, *J* = 8.0, 8.0 Hz, 1H), 7.43 (dd, *J* = 8.0, 8.0 Hz, 1H), 7.45–7.51 (m, 2H), 7.74–7.76 (m, 2H), 7.81–7.83 (m, 1H), 7.87–7.93 (m, 3H), 8.26–8.32 (m, 2H), 8.57–8.58 (m, 1H), 8.63–8.65 (m, 1H), 10.0 (brs, 1H), 10.1 (brs, 1H). ^{13}C NMR (100 MHz, $CDCl_3$) δ 24.3, 71.3, 86.8, 87.3, 95.3, 99.6, 101.4, 116.4, 116.6, 118.9, 119.0, 121.0, 121.3, 122.5, 122.6, 126.64, 129.5, 129.6, 137.8, 137.9, 138.1, 138.2, 143.65, 143.74, 148.08, 148.12, 149.88, 162.1, 162.2.

HR-MS (ESI): Calcd for $C_{32}H_{29}N_5NaO_5$ $[M+Na]^+$, 586.2066. Found, 586.2039.

***N,N'*-(((2*aS/R*,4*S/R*,4*aS/R*,6*S/R*,6*aS/R*)-4,6-Dimethylhexahydro-1,3,5-trioxa-2a^1-azacyclopenta[*cd*]pentalene-4,6-diyl)bis(3,1-phenylene))dinicotinamide (57a)**

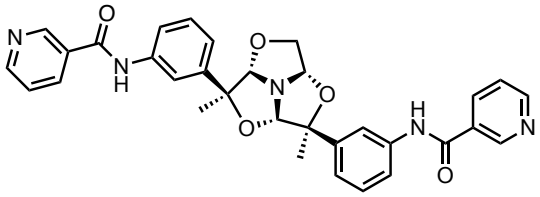

According to the synthetic protocol of **53a**, **36a** (10.0 mg, 0.0283 mmol) was converted to **57a** (16.0 mg, 100%) as a colorless amorphous.

IR (KBr, cm^{-1}) 3309, 2931, 1656, 1549, 1111.

^{1}H NMR (400 MHz, $CDCl_3$) δ 1.656 (s, 3H), 1.664 (s, 3H), 3.69 (dd, *J* = 2.8, 10.0 Hz, 1H), 4.22 (d, *J* = 10.0 Hz, 1H), 5.00 (d, *J* = 2.8 Hz, 1H), 5.06 (s, 1H), 5.20 (s, 1H), 7.20 (dd, *J* = 8.0, 8.0 Hz, 2H), 7.27–7.36 (m, 4H), 7.55–7.80 (m, 4H), 8.09–8.16 (m, 2H), 8.63–8.66 (m, 2H), 8.72 (brs, 1H), 8.76 (brs, 1H), 9.00–9.08 (m, 2H).

^{13}C NMR (100 MHz, $CDCl_3$) δ 24.00, 24.04, 71.3, 86.8, 87.2, 95.3, 99.6, 101.4, 117.6, 117.8, 119.8, 120.2, 121.6, 121.9, 123.76, 123.79, 129.5, 129.6, 130.80, 130.82, 135.57, 135.63, 137.9, 138.0, 143.4, 143.7, 148.0, 148.1, 152.37, 152.42, 164.3, 164.5.

HR-MS (ESI): Calcd for $C_{32}H_{29}N_5NaO_5$ $[M+Na]^+$, 586.2066. Found, 586.2063.

***N,N'*-(((2*aS/R*,4*S/R*,4*aS/R*,6*S/R*,6*aS/R*)-4,6-Dimethylhexahydro-1,3,5-trioxa-2a^1-azacyclopenta[*cd*]pentalene-4,6-diyl)bis(3,1-phenylene))diisonicotinamide (58a)**

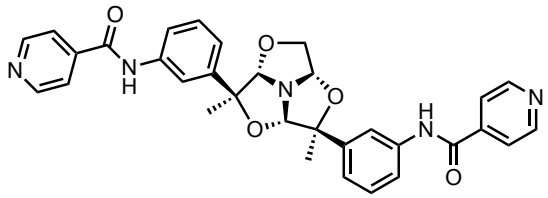

According to the synthetic protocol of **53a**, **37a** (10.0 mg, 0.0283 mmol) was converted to **58a** (14.2 mg, 89%) as a colorless amorphous.

IR (KBr, cm^{-1}) 3489, 2924, 1656, 1550, 1120.

^{1}H NMR (400 MHz, $CDCl_3$) δ 1.668 (s, 3H), 1.674 (s, 3H), 3.70 (dd, *J* = 2.8, 10.1 Hz, 1H), 4.23 (d, *J* = 10.1 Hz, 1H), 5.00 (d, *J* = 2.8 Hz, 1H), 5.07 (s, 1H), 5.19 (s, 1H), 7.22–7.24 (m, 2H), 7.33 (dd, *J* = 8.0, 8.0 Hz, 1H), 7.36 (dd, *J* = 8.0, 8.0 Hz, 1H), 7.54–7.67 (m, 7), 7.78–7.80 (m, 1H), 8.54 (brs, 1H), 8.60 (brs, 1H), 8.63 (d, *J* = 6.0 Hz, 2H), 8.67 (d, *J* = 6.0 Hz, 2H).

^{13}C NMR (100 MHz, $CDCl_3$) δ 24.0, 24.1, 71.3, 86.8, 87.2, 95.3, 99.6, 101.4, 117.5, 117.8, 119.7, 120.1, 121.0, 121.1, 121.9, 122.2, 129.6, 129.7, 137.6, 137.7, 142.08, 142.10, 143.5, 143.9, 150.68, 150.74, 164.1, 164.3.

HR-MS (ESI): Calcd for $C_{32}H_{29}N_5NaO_5$ $[M+Na]^+$, 586.2066. Found, 586.2076.

***N,N'*-(((2*aS/R*,4*R/S*,4*aS/R*,6*R/S*,6*aS/R*)-4,6-Dimethylhexahydro-1,3,5-trioxa-2a^1-azacyclopenta[*cd*]pentalene-4,6-diyl)bis(3,1-phenylene))dipicolinamide (56d)**

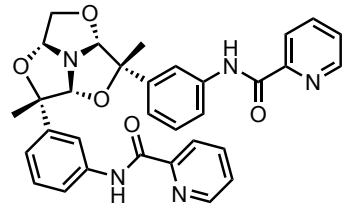

According to the synthetic protocol of **53a**, **35d** (10.0 mg, 0.0283 mmol) was converted to **56d** (30.6 mg, 96%) as a colorless amorphous.

IR (KBr, cm^{-1}) 2926, 1685, 1541, 1121.

^{1}H NMR (400 MHz, $CDCl_3$) δ 1.57 (s, 3H), 1.77 (s, 3H), 3.79 (dd, *J* = 2.8, 10.1 Hz, 1H), 4.26 (d, *J* = 10.1 Hz, 1H), 4.99 (s, 1H), 5.17 (s, 1H), 5.36 (d, *J* = 2.8 Hz, 1H), 6.91–6.94 (m, 1H), 7.27–7.31 (m, 2H), 7.40–7.43 (m, 3H), 7.55 (dd, *J* = 8.0, 8.0 Hz, 1H), 7.77–7.82 (m, 5H), 7.95 (dd, *J* = 2.0, 8.0 Hz, 1H), 8.12–8.15 (m, 3H), 8.52–8.53 (m, 1H), 8.62–8.63 (m, 1H), 9.91 (brs, 1H), 10.1 (brs, 1H).

^{13}C NMR (100 MHz, $CDCl_3$) δ 22.3, 23.7, 71.9, 87.11, 87.14, 94.8, 100.3, 102.0, 116.7, 118.0, 118.4, 119.0, 121.2, 122.2, 126.4, 128.8, 129.0, 137.6, 141.8, 142.3, 148.0, 148.1, 149.8, 161.9, 162.1.

HR-MS (ESI): Calcd for $C_{32}H_{29}N_5NaO_5$ $[M+Na]^+$, 586.2066. Found, 586.2043.

***N,N'*-(((2*aS/R*,4*R/S*,4*aS/R*,6*R/S*,6*aS/R*)-4,6-Dimethylhexahydro-1,3,5-trioxa-2a^1-azacyclopenta[*cd*]pentalene-4,6-diyl)bis(3,1-phenylene))dinicotinamide (57d)**

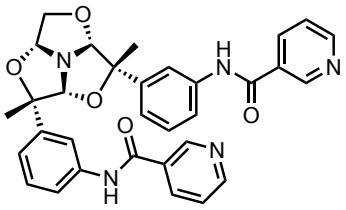

According to the synthetic protocol of **53a**, **36d** (10.0 mg, 0.0283 mmol) was converted to **57b** (14.5 mg, 91%) as a colorless amorphous.

IR (KBr, cm^{-1}) 3489, 2924, 16 56, 1550, 1120.

^{1}H NMR (400 MHz, $CDCl_3$) δ 1.56 (s, 3H), 1.71 (s, 3H), 3.74 (dd, *J* = 2.8, 10.0 Hz, 1H), 4.08 (d, *J* = 10.0 Hz, 1H), 4.95 (s, 1H), 5.18 (s, 1H), 5.33 (d, *J* = 2.8 Hz, 1H), 6.95–6.97 (m, 1H), 7.19–7.28 (m, 5H), 7.41 (dd, *J* = 8.0, 8.0 Hz, 1H), 7.67–7.69 (m, 1H), 7.80–7.82 (m, 2H), 7.91–7.93 (m, 1H), 8.03–8.05 (m, 1H), 8.50 (dd, *J* = 1.2, 4.4 Hz, 1H), 8.59 (dd, *J* = 1.2, 4.4 Hz, 1H), 8.72 (brs, 1H), 8.81–8.88 (m, 2H), 8.96 (brs, 1H).

^{13}C NMR (100 MHz, $CDCl_3$) δ 22.8, 23.4, 71.6, 87.06, 87.10, 94.7, 100.0, 101.9, 117.9, 119.7, 120.7, 121.3, 121.7, 123.0, 123.6, 123.7, 128.76, 128.84, 130.5, 131.3, 135.4, 135.8, 137.1, 137.7, 142.1, 147.9, 148.2, 152.0, 152.3, 164.3, 164.8.

HR-MS (ESI): Calcd for $C_{32}H_{29}N_5NaO_5$ $[M+Na]^+$, 586.2066. Found, 586.2081.

***N,N'*-(((2*aS/R*,4*R/S*,4*aS/R*,6*R/S*,6*aS/R*)-4,6-Dimethylhexahydro-1,3,5-trioxa-2a^1-azacyclopenta[*cd*]pentalene-4,6-diyl)bis(3,1-phenylene))diisonicotinamide (58d)**

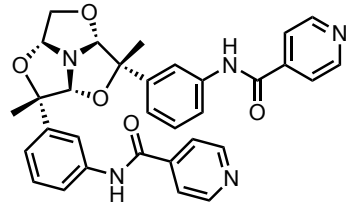

According to the synthetic protocol of **53a**, **37d** (10.0 mg, 0.0283 mmol) was converted to **58d** (6.3 mg, 39%) as a colorless amorphous.

IR (KBr, cm^{-1}) 2934, 1656, 1550, 1120.

^{1}H NMR (400 MHz, $CDCl_3$) δ 1.57 (s, 3H), 1.70 (s, 3H), 3.76 (dd, *J* = 2.8, 10.0 Hz, 1H), 4.03 (d, *J* = 10.0 Hz, 1H), 4.99 (s, 1H), 5.21 (s, 1H), 5.33 (d, *J* = 2.8 Hz, 1H), 6.94 (ddd, *J* = 1.2, 1.2, 8.0 Hz, 1H), 7.24–7.30 (m, 3H), 7.40 (d, *J* = 5.2 Hz, 2H), 7.45 (dd, *J* = 8.0, 8.0 Hz, 1H), 7.56 (d, *J* = 5.2 Hz, 2H), 7.62–7.63 (m, 1H), 7.73–7.80 (m, 2H), 8.42 (brs, 1H), 8.57 (d, *J* = 5.2 Hz, 2H), 8.65 (d, *J* = 5.2 Hz, 2H), 8.84 (brs, 1H).

^{13}C NMR (100 MHz, $CDCl_3$) δ 23.1, 23.8, 71.6, 87.09, 87.11, 94.7, 100.1, 101.9, 117.5, 119.6, 120.2, 121.1 (×4), 121.3, 122.0, 123.2, 128.9, 129.0, 136.8, 137.4, 141.9, 142.2, 142.3, 142.5, 150.5, 150.7, 164.2, 164.6.

HR-MS (ESI): Calcd for $C_{32}H_{29}N_5NaO_5$ $[M+Na]^+$, 586.2066. Found, 586.2057.

Chiral column analysis

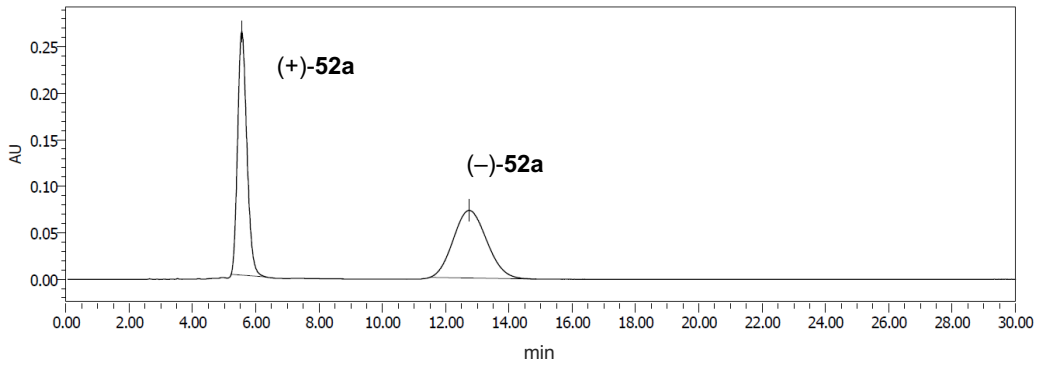

Figure S13. Chiral HPLC chromatogram of **52a** as racemic mixture with Chiralpak AD-H (Eluent: hexane/2-propanol = 1/1, Flow rate: 1 mL/min).

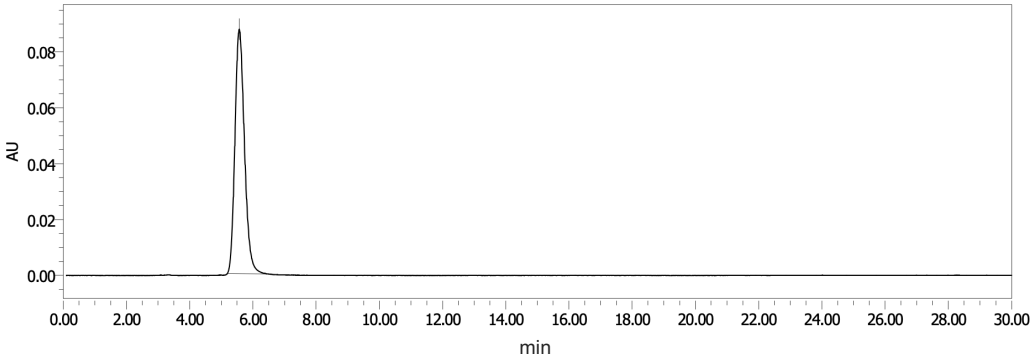

Figure S14. Chiral HPLC chromatogram of isolated **(+)-52a** with Chiralpak AD-H (Eluent: hexane/2-propanol = 1/1, Flow rate: 1 mL/min).

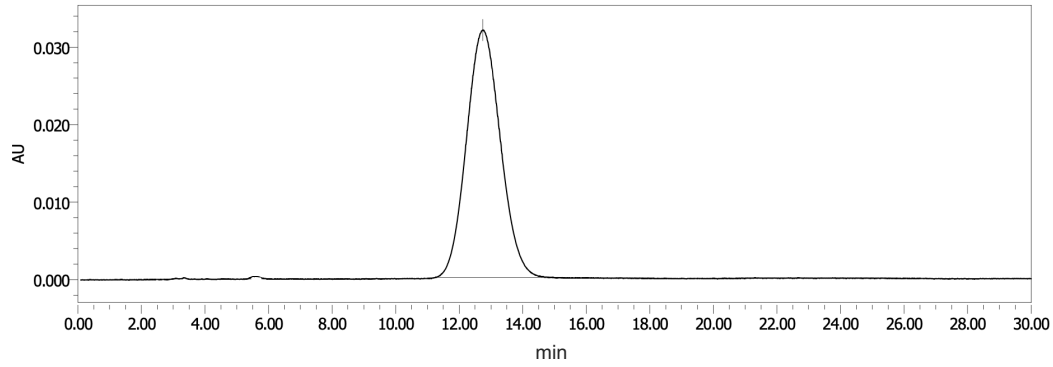

Figure S15. Chiral HPLC chromatogram of isolated **(–)-52a** with Chiralpak AD-H (Eluent: hexane/2-propanol = 1/1, Flow rate: 1 mL/min).

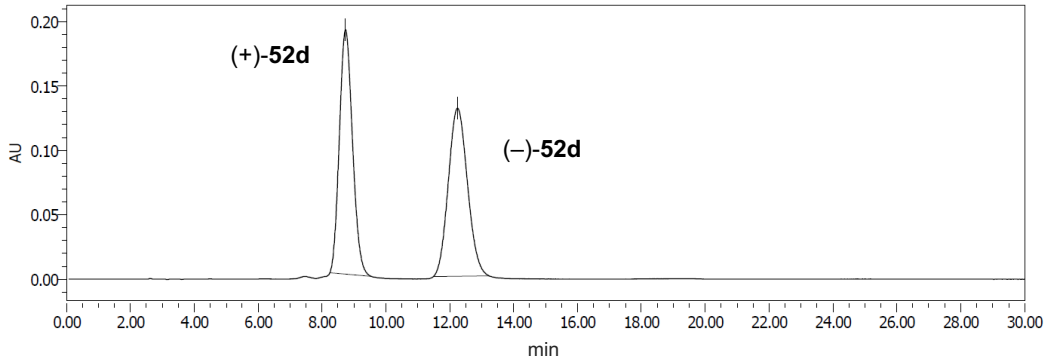

Figure S16. Chiral HPLC chromatogram of **52d** as racemic mixture with Chiralpak AD-H (Eluent: hexane/2-propanol = 3/2, Flow rate: 1 mL/min).

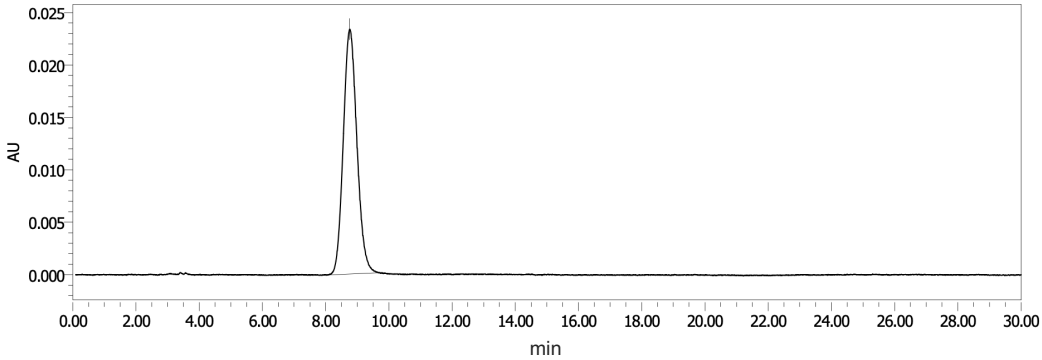

Figure S17. Chiral HPLC chromatogram of isolated (+)-**52d** with Chiralpak AD-H (Eluent: hexane/2-propanol = 3/2, Flow rate: 1 mL/min).

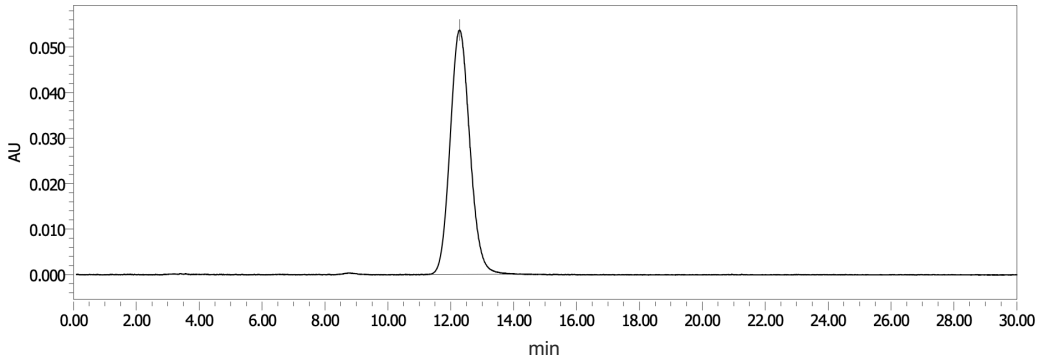

Figure S18. Chiral HPLC chromatogram of isolated (–)-**52d** with Chiralpak AD-H (Eluent: hexane/2-propanol = 3/2, Flow rate: 1 mL/min).

Calculation of the CD spectra of simplified models 52a and 52d.

Theoretical calculations of the CD spectra started with a preliminary MMFF conformational search of **52a** and **52d** using Molecular Operating Environment® (MOE) (CCG Inc., Montreal, Canada). The obtained conformers of **52a** and **52d** within 3 kcal/mol from the corresponding most stable conformers were further optimized by DFT calculation at wB97XD/6-311+g (d,p) computational level with the conductor-like polarizable continuum model (CPCM) for acetonitrile using Gaussian16 (Gaussian, Inc., USA). After removing the duplicate conformers, the CD spectra of the resultant stable conformers were calculated by time-dependent DFT/CAM-B3LYP/6-311+g(d,p), where the first 50 singlet-to-singlet electronic transitions were taken into account. On the basis of the predicted transitions, calculated CD spectra were simulated using Gaussian band shapes with 0.25 eV half-width at half height. The final spectra were obtained by weighted-average of the spectra for each conformer on the basis of its Boltzmann populations using SpecDis Version1.71(T. Bruhn, A. Schaumlöffel, Y. Hemberger, G. Pescitelli, SpecDis version 1.71, Berlin, Germany, 2017, http:/specdis-software.jimdo.com).

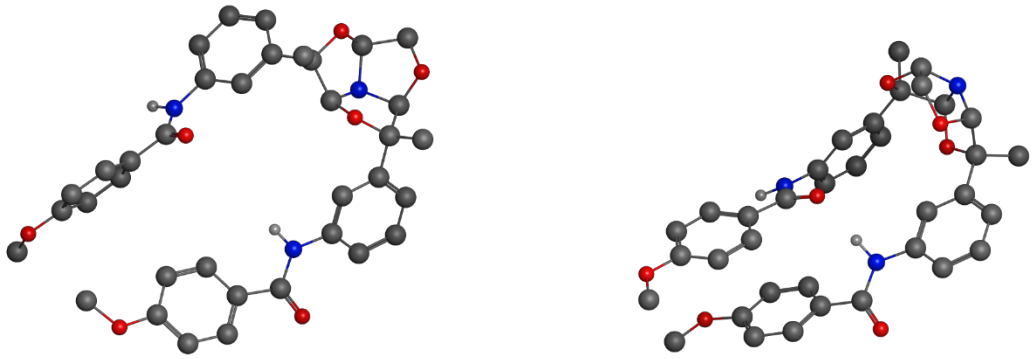

Figure S19. The most stable conformers of (2a*S*,4*S*,4a*S*,6*S*,6a*S*)-**52a** and (2a*S*,4*R*,4a*S*,6*R*,6a*S*)-**52d** predicted by TD-DFT/CAM-B3LYP/6-31G+g(d,p) using CPCM for acetonitrile.

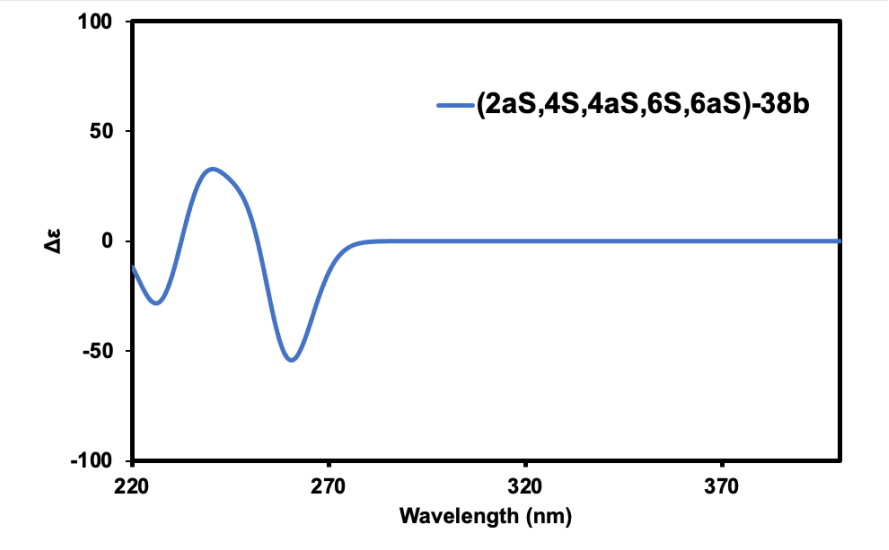

Figure S20. Estimated CD spectrum of (2a*S*,4*S*,4a*S*,6*S*,6a*S*)-**52a** using PCM for acetonitrile.

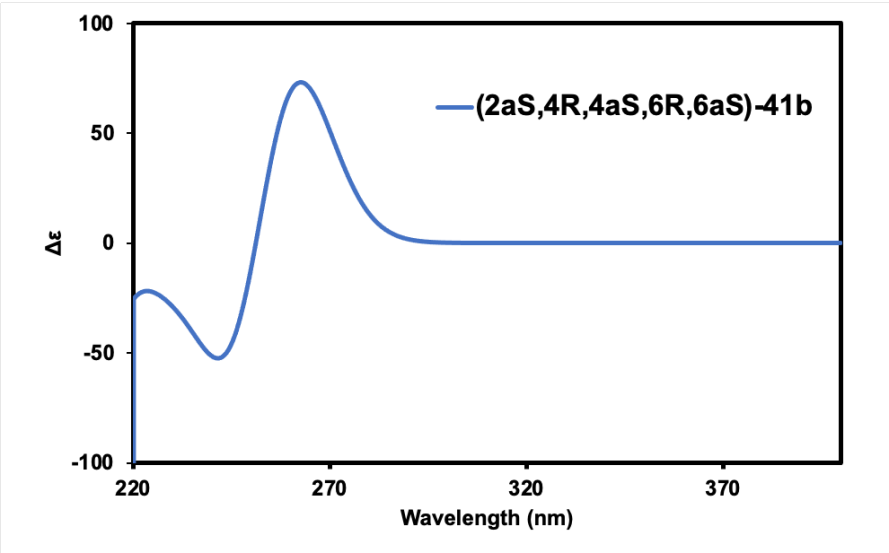

Figure S21. Estimated CD spectrum of (2a*S*,4*R*,4a*S*,6*R*,6a*S*)-**52d** using PCM for acetonitrile.

CD spectrum analysis of 57a and 57d

Measurements were performed at 20 °C using a 10 mm quartz cell in a volume of 3.5 mL. Compounds (1.0 mg) were dissolved in MeOH (5.0 mL). The instrument settings were bandwidth, 1.0 nm; data pitch, 0.2 nm; speed, 100 nm/min; accumulation, 16; and wavelengths, 400–200 nm.

Docking experiments

All the molecular modeling and docking operations were performed in the software Molecular Operating Environment® (MOE) ver. 2019.0102 (Chemical Computing Group, Inc., Montreal, Canada). Molecular docking calculations of eutomers (–)-**52a** and (+)-**52d** against OX_1R and OX_2R were performed using by default docking protocol implemented in MOE. The 3D atomic coordinates of the SB-334867/OX_1R crystal structure (PDB ID: 6TQ7)[85] were used for docking against OX_1R. The 3D atomic coordinates of OX_2R for docking were constructed based on the SB-334867/OX_1R crystal structure (PDB ID: 6TQ7) by threonine substitutions of $S103^{2.61}$ and $A127^{3.33}$ to reproduce the corresponding $T111^{2.61}$ and $T135^{3.33}$, respectively. The residues within 7 angstroms of SB-334867 were defined as the binding pockets of OX_1R and OX_2R. Before docking calculation, only the atomic coordinates of the generated hydrogen atoms were energetically optimized. The alpha spheres for molecular docking were placed in the defined binding pockets. For each compound, the pose with the best GBVI/WSA dG score was adopted as the representative docking pose.

***tert*-Butyl (4-((2*S/R*,2a*R/S*,4a*R/S*,6*S/R*,6a*R/S*)-2-(4-aminophenyl)-2,6-dimethylhexahydro-1,3,5-trioxa-2a^1-azacyclopenta[*cd*] pentalen-6-yl)phenyl)carbamate and *tert*-butyl (4-((2*S/R*,2a*R/S*,4a*R/S*,6*S/R*,6a*R/S*)-6-(4-aminophenyl)-2,6-dimethylhexahydro-1,3,5-trioxa-2a^1-azacyclopenta[*cd*]pentalen-2-yl)phenyl)carbamate (S1a)**

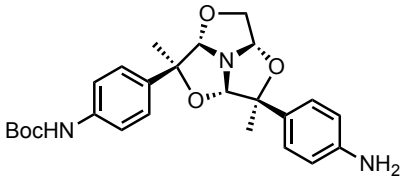

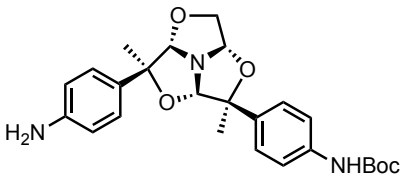

To a solution of **35a** (202 mg, 0.566 mmol) in 1,2-dichlorimethane (20 mL) was added Boc_2O (0.13 mL, 0.565 mmol) at 0 ºC and the mixture was stirred at room temperature for 36 h under Ar atmosphere. The reaction mixture was poured into saturated $NaHCO_3$ aqueous solution (20 mL) and extracted with $CHCl_3$ (100 mL, 80 mL, 60 mL). The combined organic layers were dried over anhydrous Na_2SO_4 and concentrated *in vacuo.* The residue was purified by silica gel chromatography (hexane/ethyl acetate = 1/1) to give **S1a** (62 mg, 20%) as a colorless solid.

IR (KBr, cm^{-1}) 3377, 2932, 1718, 1609, 1542, 1160, 1110, 718.

^{1}H NMR (400 MHz, $CDCl_3$) δ 1.36 (s, 3H), 1.56 (s, 3H), 1.52 (s, 4.5H), 1.58 (s, 4.5H), 3.66 (brs, 1H), 3.72 (brs, 1H), 3.78 (dd, *J* = 2.8, 10 Hz, 1H), 4.25 (d, *J* = 10 Hz, 1H), 5.03 (d, *J* = 2.8 Hz, 1H), 5.08 (s, 0.5H), 5.10 (s, 0.5H), 5.12 (s, 1H), 6.48 (brs, 0.5H), 6.52 (brs, 0.5H), 6.55–6.57 (m, 1H), 6.72–6.81 (m, 2H), 7.03–7.08 (m, 0.5H), 7.10–7.15 (m, 2H), 7.28–7.31 (m, 2H), 7.47 (brs, 0.5H).

^{13}C NMR (100 MHz, $CDCl_3$) δ 24.18 (×2), 24.20 (×2), 28.45 (×2), 71.18 (×2), 80.6 (×2), 86.7, 86.8, 87.21, 87.25, 95.0, 95.1, 99.4 (×2), 101.4 (×2), 111.7, 111.8, 114.2, 114.3, 115.2, 115.4, 117.7 (×2), 119.6, 119.8, 129.2, 129.3, 129.5, 129.6, 138.7 (×2), 138.8 (×2), 143.4, 143.5, 143.6, 143.8, 146.6, 146.7, 152.8 (×2).

HR-MS (ESI): Calcd for $C_{25}H_{31}N_3NaO_7$ $[M+Na]^+$, 476.21614. Found, 476.21429.

***tert*-Butyl (4-((2*R/S*,2a*S/R*,4a*S/R*,6*R/S*,6a*S/R*)-2-(4-aminophenyl)-2,6-dimethylhexahydro-1,3,5-trioxa-2a^1-azacyclopenta[*cd*] pentalen-6-yl)phenyl)carbamate and *tert*-butyl (4-((2*R/S*,2a*S/R*,4a*S/R*,6*R/S*,6a*S/R*)-6-(4-aminophenyl)-2,6-dimethylhexahydro-1,3,5-trioxa-2a^1-azacyclopenta[*cd*]pentalen-2-yl)phenyl)carbamate (S1d)**

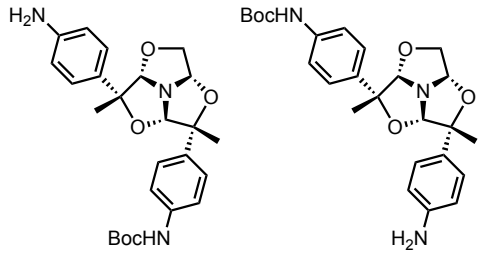

According to the synthetic protocol of **S1a**, **35d** (200 mg, 0.565 mmol) was converted to **S1d** (72 mg, 29%) as a colorless amorphous.

IR (KBr, cm^{-1}) 3419, 2929, 1716, 1614, 1549, 1161, 1120, 754.

^{1}H NMR (400 MHz, $CDCl_3$) δ 1.49 (s, 3H), 1.51 (s, 3H), 1.55 (s, 9H), 3.64 (brs, 2H), 3.77 (dd, *J* = 2.8, 10 Hz, 1H), 4.24 (d, *J* = 10 Hz, 1H), 5.01 (d, *J* = 2.8 Hz, 1H), 5.07–5.08 (m, 1H), 5.11–5.12 (s, 1H), 6.46 (brs, 0.5H), 6.53 (brs, 0.5H), 6.71–6.79 (m, 1H), 6.98–7.09 (m, 3.5H), 7.28–7.29 (m, 2H), 7.45 (brs, 0.5H).

^{13}C NMR (100 MHz, $CDCl_3$) δ 24.2 (×4), 27.9 (×2), 69.6 (×2), 79.9 (×2), 86.7 (×2), 87.17, 87.25, 95.0 (×2), 99.2 (×2), 101.3 (×2), 111.6 (×2), 114.2 (×2), 115.2, 115.6, 117.7 (×2), 119.5 (×2), 129.2 (×2), 129.5, 129.6, 138.7 (×4), 143.46 (×2), 143.51 (×2), 146.6, 146.7, 152.8 (×2).

HR-MS (ESI): Calcd for $C_{25}H_{31}N_3NaO_7$ $[M+Na]^+$, 476.21614. Found, 476.21664.

***N*-(4-((2*S/R*,2a*R/S*,4a*R/S*,6*S/R*,6a*R/S*)-6-(4-Aminophenyl)-2,6-dimethylhexahydro-1,3,5-trioxa-2a^1-azacyclopenta[*cd*]pentalen-2-yl)phenyl)-4-methoxybenzamide and *N*-(4-((2*S/R*,2a*R/S*,4a*R/S*,6*S/R*,6a*R/S*)-2-(4-aminophenyl)-2,6-dimethylhexahydro-1,3,5-trioxa-2a1-azacyclopenta[*cd*]pentalen-6-yl)phenyl)-4-methoxybenzamide (59a)**

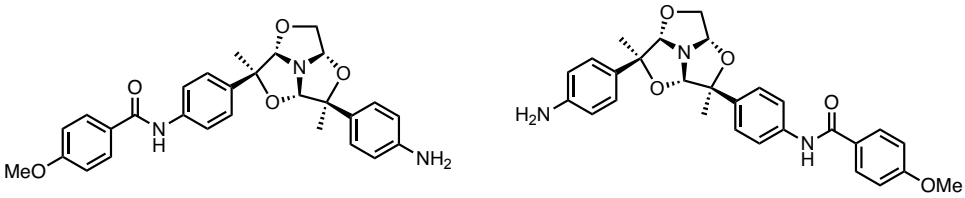

To a solution of **35a** (10.0 mg, 0.0283 mmol) in 1,2-dichlorimethane (1 mL) was added triethylamine (40 μL, 0.287 mmol) and 4-methoxybenzoyl chloride (152 μL, 1.13 mmol) and the mixture was stirred at room temperature for 1.5 h. After that, the reaction mixture was poured into saturated $NaHCO_3$ aqueous solution (30 mL) and extracted with $CHCl_3$ (40 mL, 30 mL, 20 mL). The combined organic layers were dried over anhydrous Na_2SO_4 and concentrated *in vacuo.* The residue was purified by silica gel chromatography ($CHCl_3$/MeOH = 40/1) to give the mixture of **59a** (80.2 mg, 42%) as a colorless solid.

IR (KBr, cm^{-1}) 3369, 2932, 1654, 1607, 1509, 1251, 1105, 1027, 704.

^{1}H NMR (400 MHz, $CDCl_3$) δ 1.66 (s, 3H), 1.69 (s, 3H), 3.76 (s, 3H), 3.78 (dd, *J* = 2.8, 11 Hz, 1H), 4.25 (d, *J* = 11 Hz, 0.5H), 4.28 (d, *J* = 11 Hz, 0.5H), 5.03 (d, *J* = 2.8 Hz, 0.5H), 5.04 (d, *J* = 2.8 Hz, 0.5H), 5.06 (s, 0.5H), 5.10 (s, 0.5H), 5.15 (s, 0.5H), 5.16 (s, 0.5H), 6.51–6.23 (m, 2H), 6.74–6.82 (m, 2H), 6.97–6.99 (m, 2H), 7.01–7.16 (m, 2H), 7.27–7.34 (m, 2H), 7.56–7.83 (m, 2H), 7.85–7.87 (m, 2H).

^{13}C NMR (100 MHz, $CDCl_3$) δ 24.2 (×2), 24.3 (×2), 55.6 (×2), 71.3 (×2), 86.8 (×2), 87.25 (×2), 87.31(×2), 95.1, 95.2, 99.4, 99.5, 101.4 (×2), 111.8 (×2), 114.1 (×2), 114.2 (×2), 114.4 (×2), 115.38, 115.41, 118.2 (×2), 119.4 (×2), 121.2 (×2), 128.1 (×2), 129.0 (×2), 129.4 (×2), 192.5, 129.6, 138.4 (×2), 138.5 (×2), 143.8 (×2), 146.7, 146.8, 162.7 (×2), 165.4 (×2).

HR-MS (ESI): Calcd for $C_{28}H_{29}N_3NaO_5$ $[M+Na]^+$, 510.20049. Found, 510.20041.

***N*-(4-((2*R/S*,2a*S/R*,4a*S/R*,6*R/S*,6a*S/R*)-6-(4-Aminophenyl)-2,6-dimethylhexahydro-1,3,5-trioxa-2a^1-azacyclopenta[*cd*]pentalen-2-yl)phenyl)-4-methoxybenzamide and *N*-(4-((2*R/S*,2a*S/R*,4a*S/R*,6*R/S*,6a*S/R*)-2-(4-aminophenyl)-2,6-dimethylhexahydro-1,3,5-trioxa-2a^1-azacyclopenta[*cd*]pentalen-6-yl)phenyl)-4-methoxybenzamide (59d)**

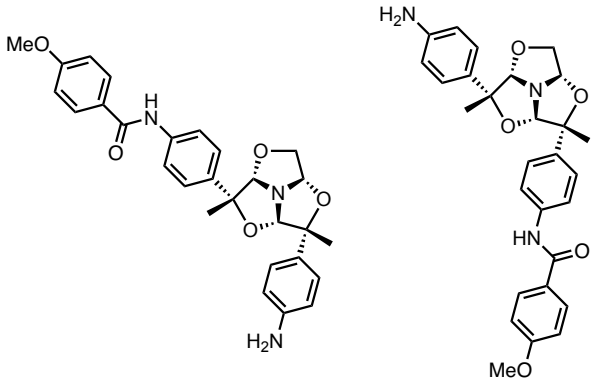

According to the synthetic protocol of **59a**, **35d** (200 mg, 0.565 mmol) was converted to **59d** (72 mg, 29%) as a colorless amorphous.

IR (KBr, cm^{-1}) 3368, 2928, 1654, 1608, 1509, 1252, 1119, 1030, 700.

^{1}H NMR (400 MHz, $CDCl_3$) δ 1.48 (s, 3H), 1.70 (s, 3H), 3.52 (brs, 2H), 3.75 (dd, *J* = 2.8, 11 Hz, 1H), 3.89 (s, 3H), 4.19 (d, *J* = 11 Hz, 1H), 4.89 (s, 1H), 5.11 (s, 1H), 5.31 (d, *J* = 2.8 Hz, 1H), 6.42–6.49 (m, 3H), 6.92–7.00 (m, 3H), 7.24–7.25 (m, 1H), 7.38–7.40 (m, 1H), 7.611–7.614 (m, 1H), 7.82–7.93 (m, 4H).

^{13}C NMR (100 MHz, $CDCl_3$) δ 22.4, 23.5, 23.7, 23.9, 55.2 (×2), 55.6, 55.7, 71.5, 71.7, 87.0, 87.1, 94.7 (×2), 100.1 (×2), 101.8 (×2), 102.0, 102.2, 112.6 (×2), 113.8, 114.0, 115.2 (×2), 118.7 (×2), 119.9 (×2), 121.8 (×2), 121.9, 122.2 127.1 (×2), 128.6, 129.1 (×2), 137.7 (×2), 1341.7 (×2), 141.8, 141.9, 142.4 (×2), 145.9 (×2), 146.2, 146.4, 162.4 (×2), 162.5. 162.6, 165.2 (×2), 165.5, 165.6.

HR-MS (ESI): Calcd for $C_{28}H_{29}N_3NaO_5$ $[M+Na]^+$, 510.20049. Found, 510.20141.

***N*-(4-((2*S/R*,2a*R/S*,4a*R/S*,6*S/R*,6a*R/S*)-2,6-Dimethyl-6-(4-(methylsulfonamido)phenyl)hexahydro-1,3,5-trioxa-2a^1-azacyclopenta[*cd*]pentalen-2-yl)phenyl)-4-methoxybenzamide and *N*-(4-((2*S/R*,2a*R/S*,4a*R/S*,6*S/R*,6a*R/S*)-2,6-dimethyl-2-(4-(methylsulfonamido)phenyl)hexahydro-1,3,5-trioxa-2a^1-azacyclopenta[*cd*]pentalen-6-yl)phenyl)-4-methoxybenzamide (60a)**

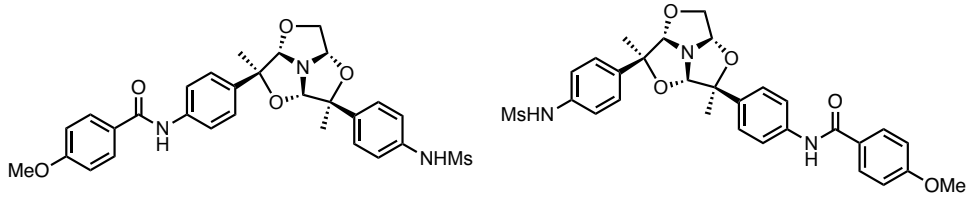

To a solution of **59a** (49.6 mg, 0.0937 mmol) in 1,2-dichlorimethane (5 mL) was added pyridine (1.25 mL) and methanesulfonyl chloride (22 μL, 0.281 mmol) at 0 ºC, and the mixture was stirred at room temperature for 8 h. After that, the reaction mixture was concentrated *in vacuo.* The residue was purified by preparative TLC ($CHCl_3$/MeOH = 3/1, hexane/ethyl acetate = 1/5) to give the mixture of **60a** (25.8mg, 46%) as a brown amorphous.

IR (KBr, cm^{-1}) 3422, 2931, 1607, 1509, 1323, 1252, 1150, 1112, 705.

^{1}H NMR (400 MHz, $CDCl_3$) δ 1.67 (s, 3H), 1.69 (s, 3H), 2.86 (s, 1.5H), 2.90 (s, 1.5H), 3.75 (dd, *J* = 2.8, 11 Hz, 1H), 3.85 (s, 1.5H), 3.86 (s, 1.5H), 4.23–4.27 (m, 1H), 4.98 (s, 0.5H), 5.02 (d, *J* = 2.8 Hz, 0.5H), 5.06 (d, *J* = 2.8 Hz, 0.5H), 5.09 (s, 0.5H), 5.22 (s, 0.5H), 5.27 (s, 0.5H), 6.96–7.04 (m, 3H), 7.14–7.23 (m, 3H), 7.29–7.36 (m, 3H), 7.46–7.68 (m, 2H), 7.85–7.89 (m, 2H), 8.02–8.07 (m, 1H).

^{13}C NMR (100 MHz, $CDCl_3$) δ 23.8, 23.9, 24.0, 24.2, 39.2, 39.3, 39.6, 39.7, 55.6 (×2), 71.4 (×2), 76.8, 77.1, 77.3, 77.5, 86.8, 87.0, 87.2, 87.3, 95.3, 95.4, 99.7, 100.1, 101.5, 101.8, 114.16, 114.21, 117.3, 117.5, 118.3, 118.5, 119.15, 119.21, 119.5, 119.8, 120.4, 120.5, 121.3, 121.7, 122.6, 126.5, 126.8, 127.0, 127.1, 129.2, 129.4, 129.5, 129.9, 130.1, 137.0, 137.4, 138.5, 138.6, 143.2, 143.5, 144.0, 144.7, 162.4, 162.8, 165.5, 166.0.

HR-MS (ESI): Calcd for $C_{29}H_{31}N_3NaO_7S$ $[M+Na]^+$, 588.17804. Found, 588.17649.

***N*-(4-((2*R/S*,2a*S/R*,4a*S/R*,6*R/S*,6a*S/R*)-2,6-Dimethyl-6-(4-(methylsulfonamido)phenyl)hexahydro-1,3,5-trioxa-2a^1-azacyclopenta[*cd*]pentalen-2-yl)phenyl)-4-methoxybenzamide and *N*-(4-((2*R/S*,2a*S/R*,4a*S/R*,6*R/S*,6a*S/R*)-2,6-dimethyl-2-(4-(methylsulfonamido)phenyl)hexahydro-1,3,5-trioxa-2a^1-azacyclopenta[*cd*]pentalen-6-yl)phenyl)-4-methoxybenzamide (60d)**

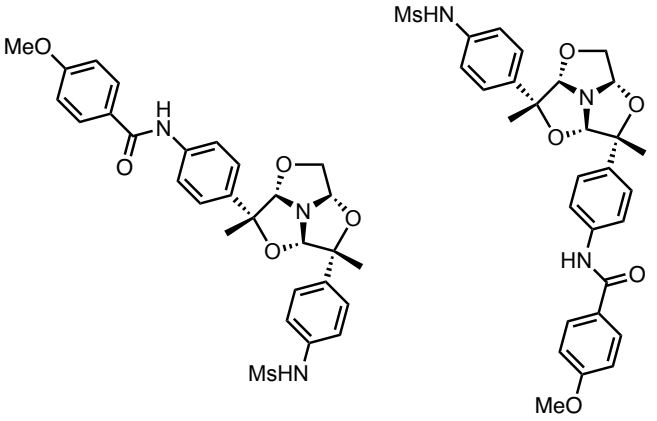

According to the synthetic protocol of **60a**, **59d** (10.8 mg, 0.022 mmol) was converted to **60d** (10 mg, 80%) as a brown amorphous.

IR (KBr, cm^{-1}) 3432, 2926, 1600, 1509, 1321, 1250, 1151, 1110, 708.

^{1}H NMR (400 MHz, $CDCl_3$) δ 1.58 (s, 3H), 1.71 (s, 3H), 2.79 (s, 3H), 2.90 (s, 1.5H), 3.76 (dd, *J* = 2.8, 11 Hz, 1H), 3.85 (s, 3H), 4.16 (d, 11 Hz, 1H), 4.80 (s, 1H), 5.17 (s, 1H), 5.34 (d, *J* = 2.8, 1H), 6.97–6.99 (m, 3H), 7.15–7.22 (m, 3H), 7.29–7.38 (m, 2H), 7.91–8.03 (m, 5H), 8.18 (brs, 1H).

^{13}C NMR (100 MHz, $CDCl_3$) δ 21.7, 21.8, 22.0, 23.0, 38.7 (×2), 55.6 (×2), 71.5 (×2), 86.54, 86.62, 86.8, 87.2, 94.3, 94.9, 99.9 (×2), 101.9 (×2), 114.2 (×4), 120.4 (×2), 121.6, 121.2, 121.4 (×2), 121.9 (×2), 122.6 (×2), 126.3, 126.5, 128.8 (×2), 129.5 (×2), 129.7 (×2), 129.9 (×2), 137.2, 137.3, 137.4, 137.5, 141.7, 141.8, 141.9, 142.1, 162.8, 162.9, 163.0 (×2), 166.8 (×2).

HR-MS (ESI): Calcd for $C_{29}H_{31}N_3NaO_7S$ $[M+Na]^+$, 588.17804. Found, 588.17765.

***tert*-Butyl (4-((2*S/R*,2a*R/S*,4a*R/S*,6*S/R*,6a*R/S*)-2-(4-(4-methoxybenzamido)phenyl)-2,6-dimethylhexahydro-1,3,5-trioxa-2a^1-azacyclopenta[*cd*]pentalen-6-yl)phenyl)carbamate and *tert*-butyl (4-((2*S/R*,2a*R/S*,4a*R/S*,6*S/R*,6a*R/S*)-6-(4-(4-methoxybenzamido)phenyl)-2,6-dimethylhexahydro-1,3,5-trioxa-2a^1-azacyclopenta[*cd*]pentalen-2-yl)phenyl)carbamate (61a)**

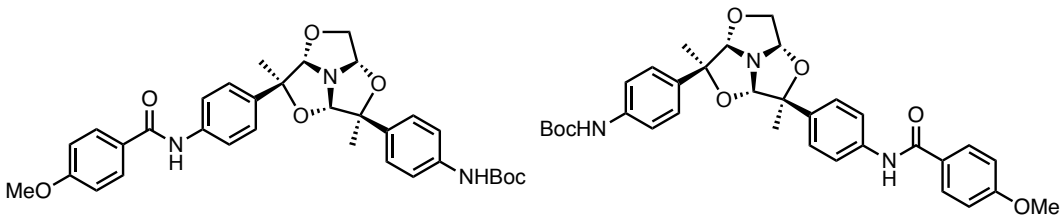

According to the synthetic protocol of **60a**, **59a** (50.0 mg, 0.110 mmol) was converted to **61a** (65.2 mg, 91%) as a brown amorphous.

IR (KBr, cm^{-1}) 3339, 2933, 1708, 1608, 1509, 1250, 1159, 1029, 705.

^{1}H NMR (400 MHz, $CDCl_3$) δ 1.48 (s, 3H), 1.51 (s, 3H), 3.02 (s, 9H), 3.84 (dd, *J* = 2.8 Hz, 11 Hz, 1H), 3.88 (s, 3H), 4.28 (d, *J* = 11 Hz, 1H), 5.02 (d, *J* = 2.8 Hz, 0.5H), 5.03 (d, *J* = 2.8 Hz, 0.5H), 5.11 (s, 0.5H), 5.13 (s, 0.5H), 5.17 (s, 0.5H), 5.19 (s, 0.5H), 6.97–7.01 (m, 5H), 7.30–7.56 (m, 3H), 7.83–7.88 (m, 3H), 8.01–8.12 (m, 3H).

^{13}C NMR (100 MHz, $CDCl_3$) δ 24.2 (×4), 28.4 (×6), 55.6 (×2), 71.2 (×2), 80.7 (×2), 86.7, 86.8, 87.2 (×2), 95.1, 95.2, 99.4, 99.5, 101.4 (×4), 114.05 (×2), 114.08 (×2), 115.4 (×2), 116.9, 117.1, 117.9 (×2), 119.4 (×2), 119.5, 119.6, 121.0, 121.2, 127.1, 127.2, 129.05, 129.08, 129.3 (×2), 129.4, 129.5, 138.4, 138.6. 138.7, 138.8, 143.46, 143.48, 143.7 (×2), 152.8 (×2), 162.6 (×2), 165.4, 165.5.

HR-MS (ESI): Calcd for $C_{33}H_{37}N_3NaO_7$ $[M+Na]^+$, 610.25292. Found, 610.25141.

***tert*-Butyl (4-((2*R/S*,2a*S/R*,4a*S/R*,6*R/S*,6a*S/R*)-2-(4-(4-methoxybenzamido)phenyl)-2,6-dimethylhexahydro-1,3,5-trioxa-2a^1-azacyclopenta[*cd*]pentalen-6-yl)phenyl)carbamate and *tert*-butyl (4-((2*R/S*,2a*S/R*,4a*S/R*,6*R/S*,6a*S/R*)-6-(4-(4-methoxybenzamido)phenyl)-2,6-dimethylhexahydro-1,3,5-trioxa-2a^1-azacyclopenta[*cd*]pentalen-2-yl)phenyl)carbamate (61d)**

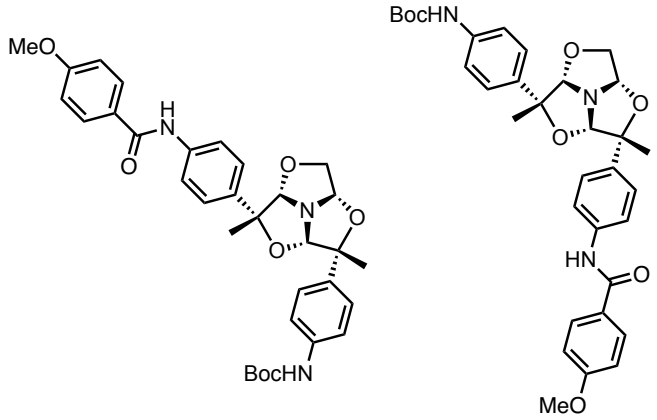

According to the synthetic protocol of **60a**, **59d** (65.0 mg, 0.143 mmol) was converted to **61d** (75.3 mg, 87%) as a brown amorphous.

IR (KBr, cm^{-1}) 3337, 2975, 2930, 1719, 1655, 1609, 1251, 1161, 1031, 700.

^{1}H NMR (400 MHz, $CDCl_3$) δ 1.43 (s, 9H), 1.52 (s, 3H), 1.71 (s, 3H), 3.75 (dd, *J* = 2.8 Hz, 11 Hz, 1H), 3.87 (s, 3H), 4.19 (d, *J* = 11 Hz, 1H), 4.94 (s, 1H), 5.14 (s, 1H), 5.33 (d, *J* = 2.8 Hz, 1H), 6.73–6.79 (m, 2H), 6.94–7.01 (m, 3H), 7.15–7.16 (m, 1H), 7.28–7.41 (m, 2H), 7.66 (brs, 1H), 7.85–7.86 (m, 2H), 7.88 (brs, 2H).

^{13}C NMR (100 MHz, $CDCl_3$) δ 22.6 (×2), 23.7 (×2), 28.4 (×6), 55.8 (×2), 71.2 (×2), 80.5 (×2), 87.0, 87.1, 87.0 (×2), 94.6, 94.7, 100.0 (×2), 101.9 (×2), 114.0 (×6), 114.2 (×2), 115.4 (×2), 119.8, 119.9, 121.3 (×2), 122.5 (×2), 128.6 (×2), 129.2 (×6), 137.7 (×2), 138.3 (×2), 141.5 (×2), 152.9 (×2), 162.6 (×2), 165.5 (×2).

HR-MS (ESI): Calcd for $C_{33}H_{37}N_3NaO_7$ $[M+Na]^+$, 610.25292. Found, 610.25195.

***N*-(4-((2*S/R*,2a*R/S*,4a*R/S*,6*S/R*,6a*R/S*)-6-(4-Acetamidophenyl)-2,6-dimethylhexahydro-1,3,5-trioxa-2a^1-azacyclopenta[*cd*]pentalen-2-yl)phenyl)-4-methoxybenzamide and *N*-(4-((2*S/R*,2a*R/S*,4a*R/S*,6*S/R*,6a*R/S*)-2-(4-acetamidophenyl)-2,6-dimethylhexahydro-1,3,5-trioxa-2a^1-azacyclopenta[*cd*]pentalen-6-yl)phenyl)-4-methoxybenzamide (S2a)**

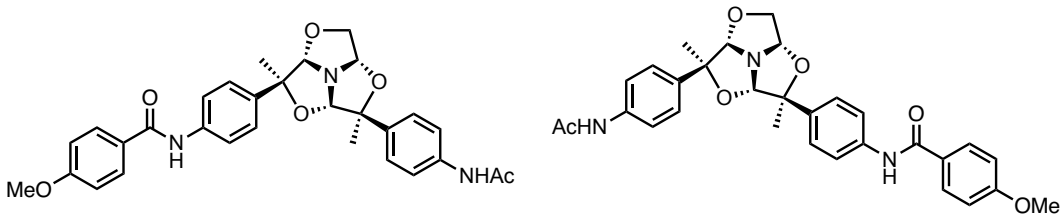

According to the synthetic protocol of **60a**, **59a** (14.9 mg, 0.033 mmol) was converted to **S2a** (8.0 mg, 46%) as a brown amorphous.

IR (KBr, cm^{-1}) 3419, 2932, 1649, 1608, 1548, 1509, 1485, 1430, 1253, 703.

^{1}H NMR (400 MHz, $CDCl_3$) δ 1.67 (s, 3H), 1.69 (s, 3H), 2.08 (s, 1.5H), 2.14 (s, 1.5H), 3.76 (dd, *J* = 2.8 Hz, 11 Hz, 1H), 3.87 (s, 3H), 4.25 (d, *J* = 11 Hz, 1H), 5.01 (d, *J* = 2.8 Hz, 0.5H), 5.02 (d, *J* = 2.8 Hz, 0.5H), 5.04 (s, 0.5H), 5.05 (s, 0.5H), 5.21 (s, 0.5H), 5.29 (s, 0.5H), 6.95–7.00 (m, 2H), 7.12–7.15 (m, 2H), 7.32–7.48 (m, 5H), 7.49 (brs, 1H), 7.82–7.86 (m, 3H), 7.89 (brs, 1H).

^{13}C NMR (100 MHz, $CDCl_3$) δ 23.8, 23.9, 24.1, 24.2, 24.7, 24.8, 55.62, 55.64, 71.3, 71.4, 86.8, 87.2, 95.3 (×2), 99.7 (×2), 101.4, 101.6, 114.0 (×2), 114.1 (×2), 116.8, 117.2, 117.3, 117.4, 119.0, 119.3, 119.4, 119.8 (×2), 120.8, 120.9, 121.3 (×2), 127.2, 127.3, 129.1(×2), 129.2, 129.3, 129.4, 129.45, 129.51, 138.2, 138.3, 138.4, 138.5, 143.2, 143.3, 143.6, 143.7, 162.6 (×2), 162.7, 165.5, 165.6, 168.5, 168.7.

HR-MS (ESI): Calcd for $C_{30}H_{31}N_3NaO_6$ $[M+Na]^+$, 522.21105. Found, 522.21051.

***N*-(4-((2*R/S*,2a*S/R*,4a*S/R*,6*R/S*,6a*S/R*)-6-(4-Acetamidophenyl)-2,6-dimethylhexahydro-1,3,5-trioxa-2a^1-azacyclopenta[*cd*]pentalen-2-yl)phenyl)-4-methoxybenzamide and *N*-(4-((2*R/S*,2a*S/R*,4a*S/R*,6*R/S*,6a*S/R*)-2-(4-acetamidophenyl)-2,6-dimethylhexahydro-1,3,5-trioxa-2a^1-azacyclopenta[*cd*]pentalen-6-yl)phenyl)-4-methoxybenzamide (S2d)**

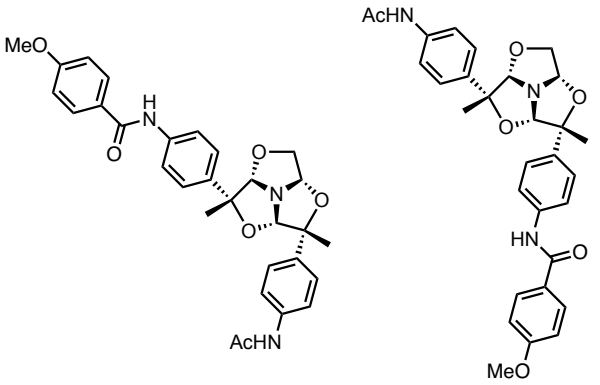

According to the synthetic protocol of **60a**, **59d** (13.2 mg, 0.027 mmol) was converted to **S2d** (14 mg, 96%) as a brown amorphous.

IR (KBr, cm^{-1}) 3435, 2932, 1645, 1508, 1487, 1252, 1119.

^{1}H NMR (400 MHz, $CDCl_3$) δ 1.52 (s, 3H), 1.72 (s, 3H), 1.96 (s, 3H), 3.76 (dd, *J* = 2.8 Hz, 11 Hz, 1H), 3.88 (s, 3H), 4.21 (d, *J* = 11 Hz, 1H), 4.90 (s, 1H), 5.15 (s, 1H), 5.34 (d, *J* = 2.8 Hz, 1H), 6.81–6.82 (m, 1H), 6.96–7.12 (m, 3H),7.20–7.24 (m, 2H), 7.42–7.43 (m, 1H), 7.73–7.76 (m, 3H), 7.82–7.87 (m, 3H), 8.15 (brs, 1H).

^{13}C NMR (100 MHz, $CDCl_3$) δ 22.7, 23.2, 24.5 (×2), 55.6 (×2), 71.7, 86.9, 87.1, 94.8 (×2), 100.1 (×2), 101.9 (×2), 114.1 (×6), 117.4(×2), 119.3 (×2), 120.4 (×2), 120.8 (×2), 121.5 (×2), 122.5 (×2), 127.0 (×2), 128.5 (×2), 128.7 (×2), 129.3 (×6), 137.4 (×2), 138.0 (×2), 141.7 (×2), 142.0 (×2), 162.7 (×2), 166.2 (×2), 168.9 (×2).

HR-MS (ESI): Calcd for $C_{30}H_{31}N_3NaO_6$ $[M+Na]^+$, 522.21105. Found, 522.21051.

Table S1. Assay results of OXR agonist activity of synthetic hetero-TriMER derivatives

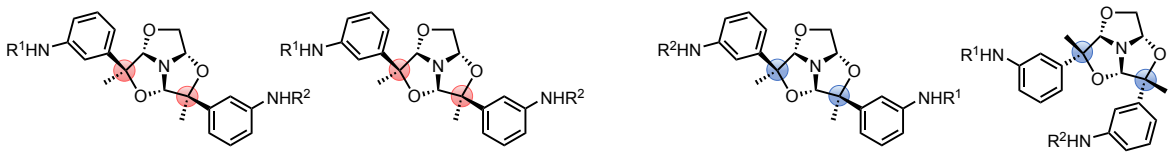

Type-I Type-IV

Comp.	Core type	R^1	R^2	% of OXA [a]	
				OX_1R	OX_2R
S1a	I	H	Boc	2.89	2.53
S1d	IV	H	Boc	3.82	3.68
59a	I	H	4-MeO-Bz	11.45	6.97
59d	IV	H	4-MeO-Bz	6.18	2.89
60a	I	SO_2Me	4-MeO-Bz	10.46	11.64
60d	IV	SO_2Me	4-MeO-Bz	5.84	2.84
61a	I	Boc	4-MeO-Bz	12.21	9.56
61d	IV	Boc	4-MeO-Bz	2.75	3.67
S2a	I	Ac	4-MeO-Bz	14.07	11.15
S2d	IV	Ac	4-MeO-Bz	1.24	4.03

[a] The value obtained at 10 μM was used. The agonist activity of orexin A (OXA) was set as 100%.

Table S2. Assay results of OXR agonist activity of synthetic hetero-TriMER derivatives

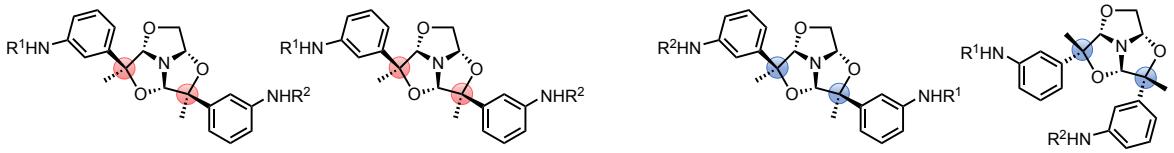

Type-I Type-IV

Comp.	Core type	R^1	R^2	% of OXA [a]	
				OX_1R	OX_2R
S1a	I	H	Boc	34.4	55.62
S1d	IV	H	Boc	6.89	76.07
59a	I	H	4-MeO-Bz	23.95	8.73
59d	IV	H	4-MeO-Bz	19.73	73.61
60a	I	SO_2Me	4-MeO-Bz	19.28	11.29
60d	IV	SO_2Me	4-MeO-Bz	16.42	75.33
61a	I	Boc	4-MeO-Bz	26.22	62.15
61d	IV	Boc	4-MeO-Bz	10.4	88.73
S2a	I	Ac	4-MeO-Bz	25.14	10.98
S2d	IV	Ac	4-MeO-Bz	8.4	85.39

[a] The value obtained at 10 μM was used. Orexin A (OXA) is set at 100% and evaluated how much inhibiting that with synthetic compounds. Darker red compounds have more potent OXR antagonistic activity.

2-((4-(2-(1,3-dioxoisoindolin-2-yl)ethyl)-4,6-dimethylhexahydro-1,3,5-trioxa-2a1-azacyclopenta[*cd*] pentalen-6-yl)methyl)isoindoline-1,3-dione (71a–d)

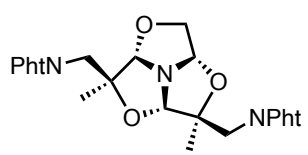

71a

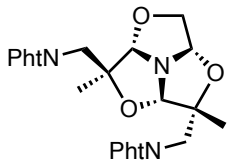

71b

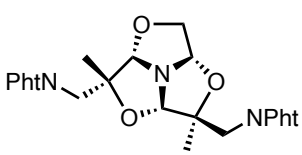

71c

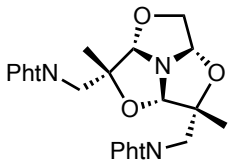

71d

To a solution of potassium *tert*-butoxide (2.92 g, 26.02 mmol) in anhydrous THF (40 mL) were added (methoxymethyl)triphenylphosphonium chloride (8.89 g, 25.93 mmol) at 0 °C under nitrogen flow. After stirring for 1 h, the mixture was added a solution of *N*-acetonylphthalimide (3.00 g, 14.76 mmol) in 20 mL of anhydrous THF and stirred at room temperature for 12 h. The reaction mixture was poured into water (15mL) and extracted with $CHCl_3$ (50 mL, 25 mL, 10 mL). The combined organic extracts were dried over anhydrous Na_2SO_4 and concentrated *in vacuo* to obtain the methyl enol ether 2.17 g as a yellow oil.

To a solution of the methyl enol ether in 1,2-dichloromethane (45 mL) was added mCPBA (2.42 g, 14.01 mmol) at 0 °C and stirred at room temperature for 1 h. The reaction mixture was concentrated *in vacuo.*

To a crude mixture in THF (10 mL) was added 2 M HCl aqueous solution (16 mL) at room temperature and the mixture was stirred at 70 °C for 13 h under Ar atmosphere. After cooling to room temperature, the mixture was neutralized with saturated $NaHCO_3$ aqueous solution (30 mL) and extracted with $CHCl_3$ (100 mL, 50 mL, 25 mL). The combined organic layers were dried over anhydrous Na_2SO_4 and concentrated *in vacuo* to obtain the crude mixture of α-hydroxyaldehyde (2.29 g), which was used in the next reaction without further purification.

To a solution of the crude mixture (2.29 g) in MeOH (45 mL) were added NH_4Cl (789.0 mg, 14.7 mmol) and NaOAc (2.42 g, 29.4 mmol) at room temperature and the mixture was refluxed for 6 h under Ar atmosphere. After cooling to room temperature, MeOH was removed under reduced pressure. The residue was poured into sat. $NaHCO_3$ aq. solution (25 mL) and extracted with $CHCl_3$ (100 mL, 50 mL, 25 mL). The combined organic layers were dried over anhydrous Na_2SO_4 and concentrated *in vacuo.* The residue was purified by silica gel chromatography (hexane/ethyl acetate = 1/1) to give the isomeric mixture (1.30 g) as a pale-yellow amorphous.

To a solution of the isomeric mixture (1.25 g) in $CHCl_3$ (30 ml) were added glycolaldehyde dimer (342 mg, 2.85 mmol) and 10-camphorsulfonic acid (1.32 g, 5.70 mmol) at room temperature and the mixture was stirred at the same temperature for 2 h under Ar atmosphere. The reaction mixture was poured into sat. $NaHCO_3$ aq. solution (30 mL) and extracted with $CHCl_3$ (100 mL, 50 mL, 20 mL). The combined organic layers were dried over anhydrous Na_2SO_4 and concentrated *in vacuo*. The residue was purified by silica gel column chromatography (hexane/ethyl

acetate = 5/1) and recrystallized (hexane/EtOAc) to obtain compound **71a** (341 mg, 10%), **71b** (111 mg, 3%), **71c** (201 mg, 5%) and **71d** (328 mg, 9%) as a colorless solid, respectively.

71a

IR (KBr, cm^{-1}) 3471, 3049, 2997, 2982, 2936, 2871, 1776, 1720, 1467, 1428, 1398, 1374, 1177, 1155, 1111, 1061, 736, 711.

^1H NMR (400 MHz, $CDCl_3$) δ 1.27 (s, 3H), 1.38 (s, 3H), 3.73 (d, *J* = 14.4 Hz, 2H), 3.77 (dd, *J* = 2.8, 10.0 Hz, 1H), 3.97 (d, *J* = 14.4 Hz, 1H), 3.98 (d, *J* = 14.4 Hz, 1H), 4.06 (d, *J* = 10.0 Hz, 1H), 4.76 (s, 1H), 5.29 (s, 1H), 5.59 (d, *J* = 2.8 Hz, 1H), 7.74 (dd, *J* = 3.2, 5.6 Hz, 2H), 7.76 (dd, *J* = 3.2, 5.6 Hz, 2H), 7.86 (dd, *J* = 3.2, 5.6 Hz, 2H), 7.89 (dd, *J* = 3.2, 5.6 Hz, 2H).

^{13}C NMR (100 MHz, $CDCl_3$) δ 17.9, 18.0, 41.48, 41.54, 71.6, 86.2, 86.3, 95.4, 98.0, 99.5, 123.5 (×2), 123.6 (×2), 132.1 (×4), 134.2 (×2), 134.3 (×2), 168.6 (×2), 168.7 (×2).

HR-MS (ESI): Calcd for $C_{26}H_{23}N_3NaO_7$ $[M + Na]^+$, 512.1434. Found: 512.1428.

71b

IR (KBr, cm^{-1}) 3472, 3023, 2987, 2926, 2903, 2868, 1776, 1715, 1612, 1466, 1429, 1393, 1161, 1142, 1114, 1076, 1060, 732, 716.

^1H NMR (400 MHz, $CDCl_3$) δ 1.27 (s, 3H), 1.38 (s, 3H), 3.74 (d, *J* = 14.4 Hz, 1H), 3.76 (dd, *J* = 2.8, 10.0 Hz, 1H), 3.88 (d, *J* = 14.8 Hz, 1H), 3.93 (d, *J* = 14.8 Hz, 1H), 4.08 (d, *J* = 14.8 Hz, 1H), 4.24 (d, *J* = 10.0 Hz, 1H), 4.75 (s, 1H), 5.12 (d, *J* = 2.8 Hz, 1H), 5.25 (s, 1H), 7.70 (dd, *J* = 2.8, 5.6 Hz, 2H), 7.76 (dd, *J* = 2.8, 5.6 Hz, 2H), 7.82 (dd, *J* = 2.8, 5.6 Hz, 2H), 7.90 (dd, *J* = 2.8, 5.6 Hz, 2H).

^{13}C NMR (100 MHz, $CDCl_3$) δ 18.0, 19.6, 41.6, 42.1, 71.6, 85.2, 86.8, 95.5, 99.2, 100.2, 123.4 (×2), 123.6 (×2), 132.1 (×2), 132.2 (×2), 134.0 (×2), 134.3 (×2), 168.5 (×2), 168.6 (×2).

HR-MS (ESI): Calcd for $C_{26}H_{23}N_3NaO_7$ $[M + Na]^+$, 512.1434. Found: 512.1418.

71c

IR (KBr, cm^{-1}) 3743, 3097, 3061, 3025, 2990, 2933, 2893, 2869, 1778, 1714, 1612, 1467, 1456, 1422, 1395, 1361, 1191, 1176, 1113, 1065, 1047, 755, 736, 710.

^{1}H NMR (400 MHz, $CDCl_3$) δ 1.28 (s, 3H), 1.42 (s, 3H), 3.69 (d, *J* = 14.0 Hz, 1H), 3.79 (dd, *J* = 2.8, 10.0 Hz, 1H), 3.91 (d, *J* = 14.0 Hz, 1H), 3.96 (d, *J* = 14.0 Hz, 1H), 4.13 (d, *J* = 10.0 Hz, 1H), 4.23 (d, *J* = 14.0 Hz, 1H), 4.74 (s, 1H), 4.88 (s, 1H), 5.51 (d, *J* = 2.8 Hz, 1H), 7.72 (dd, *J* = 2.8, 5.2 Hz, 2H), 7.73 (dd, *J* = 2.8, 5.2 Hz, 2H), 7.86 (dd, *J* = 2.8, 5.2 Hz, 4H).

^{13}C NMR (100 MHz, $CDCl_3$) δ 18.0, 18.9, 41.7, 41.8, 72.1, 85.2, 86.5, 95.1, 97.8, 101.3, 123.5 (×2), 123.6 (×2), 132.1 (×2), 132.2 (×2), 134.1 (×2), 134.3 (×2), 168.4 (×2), 168.6 (×2).

HR-MS (ESI): Calcd for $C_{26}H_{23}N_3NaO_7$ $[M + Na]^+$, 512.1434. Found: 512.1430.

71d

IR (KBr, cm^{-1}) 3474, 2979, 2951, 2937, 2909, 1775, 1719, 1611, 1542, 1509, 1466, 1395, 1191, 1115, 1055, 731, 712.

^{1}H NMR (400 MHz, $CDCl_3$) δ 1.20 (s, 3H), 1.28 (s, 3H), 3.80 (dd, *J* = 2.8, 10.0 Hz, 1H), 3.96 (d, *J* = 14.8 Hz, 1H), 3.99 (d, *J* = 14.8 Hz, 1H), 4.326 (d, *J* = 10.0 Hz, 1H), 4.331 (d, *J* = 14.8 Hz, 1H), 4.38 (d, *J* = 14.8 Hz, 1H), 4.75 (s, 1H), 4.85 (s, 1H), 5.11 (d, *J* = 2.8 Hz, 1H), 7.69–7.75 (m, 4H), 7.83–7.89 (m, 4H).

^{13}C NMR (100 MHz, $CDCl_3$) δ 19.0, 19.1, 41.8, 42.2, 72.1, 85.4, 85.8, 95.2, 100.1, 101.1, 123.40 (×2), 123.44 (×2), 132.2 (×4), 134.00 (×2), 134.04 (×2), 168.4 (×2), 168.6 (×2).

HR-MS (ESI): Calcd for $C_{26}H_{23}N_3NaO_7$ $[M + Na]^+$, 512.1434. Found: 512.1424.

4,6-Dimethylhexahydro-1,3,5-trioxa-2a^1-azacyclopenta[cd]pentalene-4,6-diyl)dimethanol (75a–d)

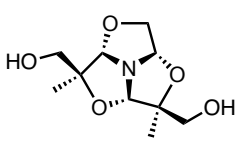

75a

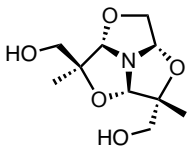

75b

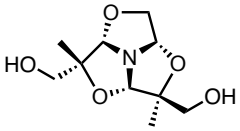

75c

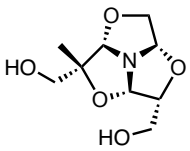

75d

To a solution of tosylmethyl isocyanide (TosMIC, 14.8 g, 75.9 mmol) in MeOH (120 mL) was added potassium *tert*-butoxide (8.52 g, 75.9 mmol) at 0 ºC under an argon atmosphere. After stirring for 10 min, the mixture was added benzyloxyacetone (**65**, 9.60 mL, 7.62 mmol) and stirred for 2 h at room temperature. The reaction mixture was poured into water (300 mL) and extracted with $CHCl_3$ (200 mL, 100 mL, 50 mL). The combined organic layers were dried over anhydrous Na_2SO_4 and concentrated *in vacuo* to obtain a crude mixture (21.6 g) as brown oil, which was used in the next reaction without further purification.

To a solution of the crude mixture (21.6 g) in THF (15 mL) was added 2 M HCl aqueous solution (24 mL) at room temperature and the mixture was stirred for 2.5 h at 60 ºC under an argon atmosphere. After cooling to room temperature, the residue was neutralized with sat. $NaHCO_3$ aqueous solution (40 mL). THF was removed under reduced pressure, and the product mixture was extracted with $CHCl_3$ (100 mL, 50 mL, 20 mL). The combined organic layers were dried over anhydrous Na_2SO_4 and concentrated *in vacuo* to obtain a mixture of α-hydroxyaldehyde **72** (2.18 g) as a brown oil, which was used in the next reaction without further purification.

To a mixture of **72** (2.18 g) in MeOH (40 mL) were added NH_4Cl (1.04 g, 19.4 mmol) and NaOAc (3.13 g, 38.1 mmol) at room temperature, and the mixture was refluxed for 3 h under an argon atmosphere. After cooling to room temperature, the residue was poured into water (50 mL). MeOH was removed under reduced pressure, and the product mixture was extracted with $CHCl_3$ (100 mL, 50 mL, 20 mL). The combined organic layers were dried over anhydrous Na_2SO_4 and concentrated *in vacuo*. The residue was purified by silica gel column chromatography (hexane/EtOAc = 2/1 to 1/1) to obtain oxazolinedimer **7** (1.23 g, 3.33 mmol) as a brown oil, which was used in the next reaction without further purification.

To a solution of oxazolinedimer **73** (1.23 g, 3.33 mmol) in $CHCl_3$ (30 mL) were added glycolaldehyde dimer (0.400 g, 3.33 mmol) and 10-camphorsulfonic acid (1.55 g, 6.66 mmol), and the mixture was stirred for 18 h under an argon atmosphere. The reaction mixture was poured into sat. $NaHCO_3$ aqueous solution (30 mL) and extracted with $CHCl_3$ (50 mL, 40 mL, 20 mL). The combined organic layers were dried over anhydrous Na_2SO_4 and concentrated *in vacuo*. The residue was purified by silica gel column chromatography (hexane/EtOAc = 5/1 to 3/1) to obtain a crude mixture of the isomeric mixture of **74** (1.13 g, 82%) as a colorless oil, which was used in the next reaction without further purification.

To a solution of isomeric mixture of **74** (1.13 g, 2.75 mmol) in MeOH (60 mL) was added 5% Pd/C (Degussa type, 1.03 g, 5 mol%) and the mixture was stirred for 17 h under a hydrogen atmosphere (balloon pressure). The reaction mixture was filtered with Celite and concentrated *in vacuo*. The residue was purified by silica gel column chromatography ($CHCl_3$/MeOH/EtOH = 40/1/1 to 20/1/1) to obtain **75a** (180 mg, 28%), **75b** (120 mg, 19%), **75c** (128 mg, 20%) and **75d** (154 mg, 24%) as a colorless oil, respectively.

75a

IR (neat, cm^{-1}) 2934, 1112, 1042.

^1H NMR (400 MHz, $CDCl_3$) δ 1.34 (s, 3H), 1.39 (s, 3H), 2.08 (brs, 1H), 2.63 (brs, 1H), 3.55–3.58 (m, 2H), 3.65–3.74 (m, 3H), 4.10 (d, J = 10 Hz, 1H) 4.65 (s, 1H), 4.95 (s, 1H), 5.20 (d, J = 2.8 Hz, 1H).

^{13}C NMR (100 MHz, $CDCl_3$) δ 16.5, 16.7, 65.9, 66.0, 71.8, 86.6, 86.7, 95.8, 98.0, 98.9.

HR-MS (ESI): Calcd for $C_{10}H_{17}NNaO_5$ $[M+Na]^+$, 254.10044. Found, 254.10112.

75b

IR (neat, cm^{-1}) 2933, 1113, 1042.

^1H NMR (400 MHz, $CDCl_3$) δ 1.29 (s, 3H), 1.39 (s, 3H), 1.88–1.91 (m, 1H), 2.51–2.53 (m, 1H), 3.55 (dd, J = 7.8, 11 Hz, 1H), 3.71–3.79 (m, 4H), 4.18 (d, J = 11 Hz, 1H), 4.65 (s, 1H), 4.93 (s, 1H), 5.18 (d, J = 2.8 Hz, 1H).

^{13}C NMR (100 MHz, $CDCl_3$) δ 16.4, 18.9, 65.3, 65.4, 71.3, 84.9, 87.2, 95.2, 98.5, 100.8.

HR-MS (ESI): Calcd for $C_{10}H_{17}NNaO_5$ $[M+Na]^+$, 254.10044. Found, 254.10027.

75c

IR (neat, cm^{-1}) 2924, 1115, 1042.

^1H NMR (400 MHz, $CDCl_3$) δ 1.32 (s, 3H), 1.35 (s, 3H), 1.85–1.86 (m, 1H), 2.38–2.41 (m, 1H), 3.54–3.58 (m, 1H), 3.71–3.75 (m, 2H), 3.83–3.85 (m, 2H), 4.12 (d, J = 10 Hz, 1H), 4.68 (s, 1H), 4.88 (s, 1H), 5.18 (d, J = 2.8 Hz, 1H).

^{13}C NMR (100 MHz, $CDCl_3$) δ 16.4, 19.0, 65.4, 65.5, 71.4, 84.8, 87.2, 95.2, 98.5, 101.0.

HR-MS (ESI): Calcd for $C_{10}H_{17}NNaO_5$ $[M+Na]^+$, 254.10044. Found, 254.09967.

75d

IR (neat, cm^{-1}) 2934, 1113, 1042. ^{1}H NMR (400 MHz, $CDCl_3$) δ 1.29 (s, 3H), 1.39 (s, 3H), 1.88–1.91 (m, 1H), 2.51–2.53 (m, 1H), 3.55 (dd, *J* = 7.8, 11 Hz, 1H), 3.71–3.79 (m, 4H), 4.18 (d, *J* = 11 Hz, 1H), 4.65 (s, 1H), 4.93 (s, 1H), 5.18 (d, *J* = 2.8 Hz, 1H). ^{13}C NMR (100 MHz, $CDCl_3$) δ 16.4, 18.9, 65.3, 65.4, 71.3, 84.9, 87.2, 95.2, 98.5, 100.8. HR-MS (ESI): Calcd for $C_{10}H_{17}NNaO_5$ $[M+Na]^+$, 254.10044. Found, 254.09961.

Determination of the relative configurations of the synthesized compounds.

The relative configurations of **75a**–**d** were determined by 2D-NMR. The observed NOE relationships of each compound were shown by arrows.

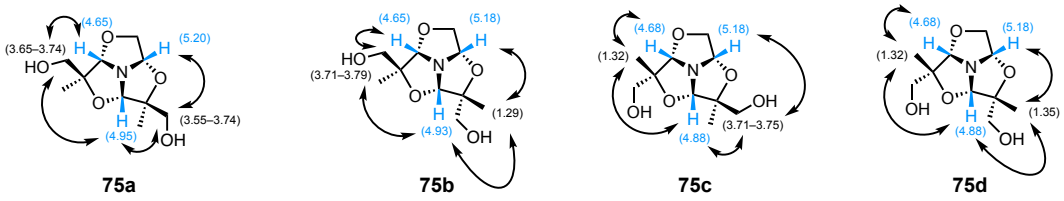

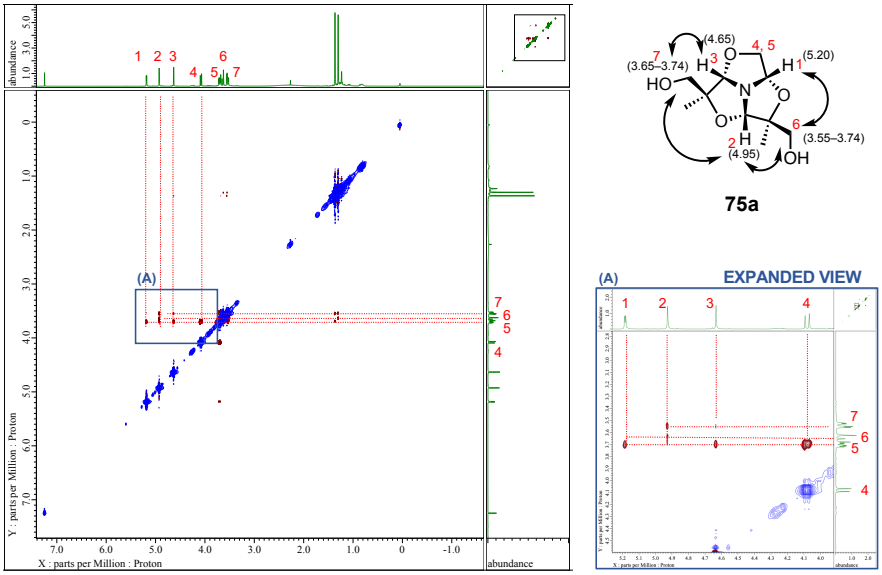

Figure S22. NOESY spectrum of **75a** (Type-I)

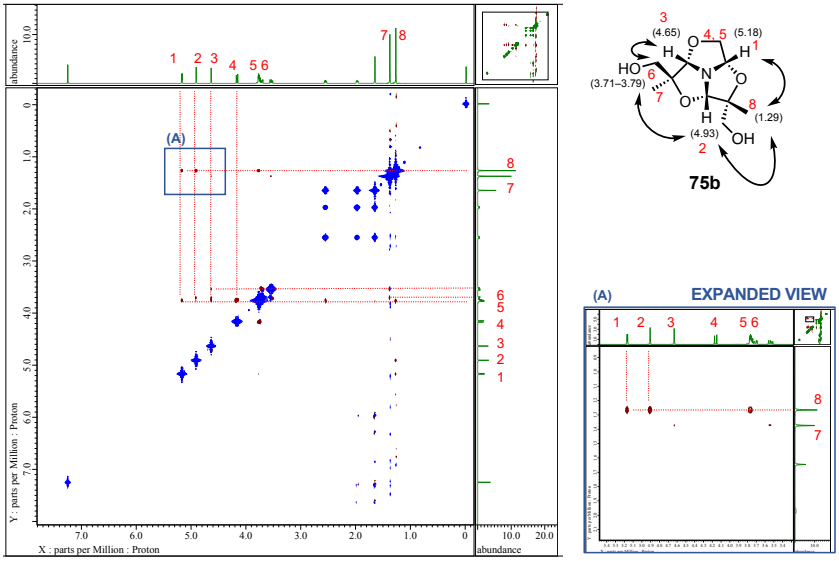

Figure S23. NOESY spectrum of **75b** (Type-II)

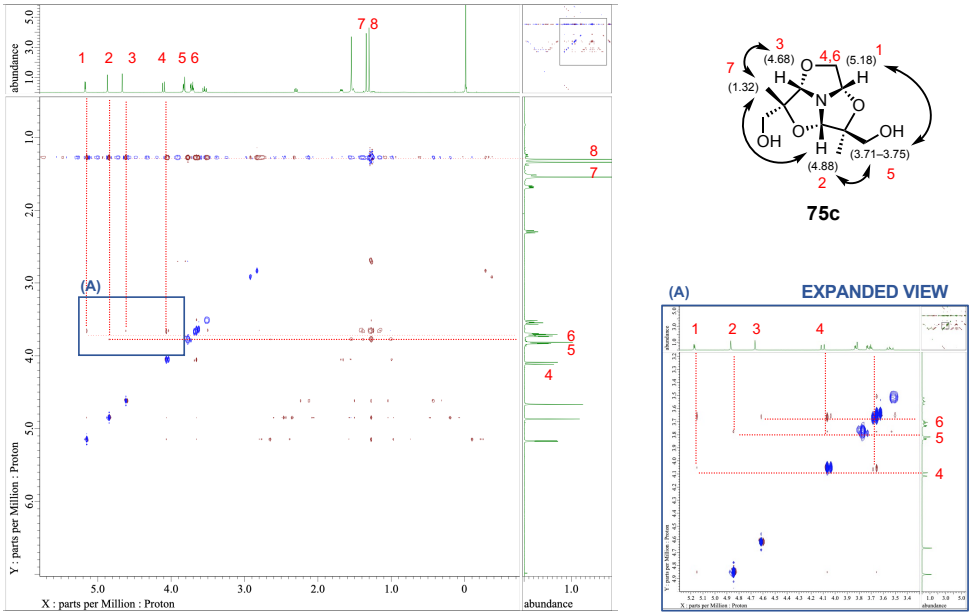

Figure S24. NOESY spectrum of **75c** (Type-III)

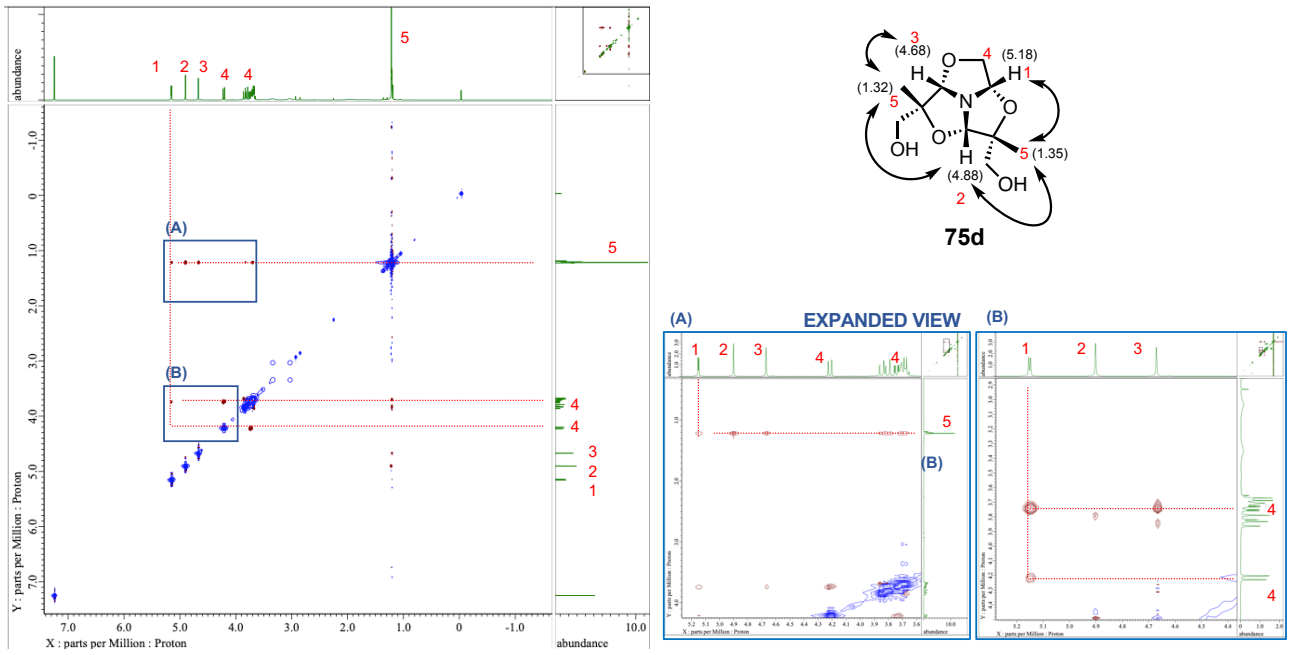

Figure S25. NOESY spectrum of **75d** (Type-IV)

((2a*S*/*R*,4*S*/*R*,4a*S*/*R*,6*S*/*R*,6a*S*/*R*)-4,6-Dimethylhexahydro-1,3,5-trioxa-2a^1-azacyclopenta[*cd*]pentalene-4,6-diyl)bis(methylene) dimethanesulfonate (76a)

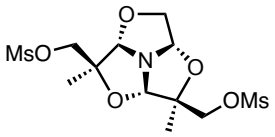

To a solution of alcohol **75a** (149 mg, 0.642 mmol) in dry DCM (5 mL) were added methanesulfonyl chloride (0.35 mL, 4.50 mmol) and dry pyridine (1.0 mL, 12.8 mmol), and the mixture was stirred for 2 h under an argon atmosphere. The reaction mixture was poured into sat. $NaHCO_3$ aqueous solution (50 mL) and extracted with $CHCl_3$ (50 mL, 30 mL, 20 mL). The combined organic layers were dried over anhydrous Na_2SO_4 and concentrated *in vacuo*. The residue was purified by silica gel column chromatography (hexane/EtOAc = 1/4) to obtain **76a** (182 mg, 81%) as a colorless amorphous.

IR (neat, cm^{-1}) 3442, 2939, 1645, 1460, 1353, 1173, 1114, 1055, 997, 969, 864, 832, 730.

^{1}H NMR (400 MHz, $CDCl_3$) δ 1.35 (s, 3H), 1.44 (s, 3H), 3.09 (s, 3H), 3.10 (s, 3H), 3.74 (dd, *J* = 2.8, 10 Hz, 1H), 4.08 (d, *J* = 10 Hz, 1H), 4.97 (d, *J* = 2.8 Hz, 1H), 4.09 (d, *J* = 11 Hz, 1H), 4.25 (d, *J* = 11 Hz, 1H), 4.26 (d, *J* = 11 Hz, 1H), 4.72 (s, 1H), 4.97 (s, 1H), 5.22 (d, *J* = 2.8 Hz, 1H).

^{13}C NMR (100 MHz, $CDCl_3$) δ 16.7, 16.9, 37.9 (×2), 70.7, 71.0, 71.8, 84.5, 84.7, 96.5, 98.1, 98.6.

HR-MS (ESI): Calcd for $C_{12}H_{21}NNaO_9S_2$ $[M+Na]^+$, 410.05554. Found, 410.05528.

((2a*S*/*R*,4*R*/*S*,4a*S*/*R*,6a*S*/*R*)-4,6-Dimethylhexahydro-1,3,5-trioxa-2a^1-azacyclopenta[*cd*]pentalene-4,6-diyl)bis(methylene) dimethanesulfonate (76b)

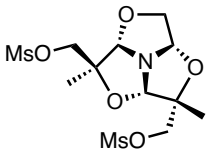

According to the synthetic protocol of **76a**, **75b** (186 mg, 0.804 mmol) was converted to **76b** (256 mg, 85%) as a colorless amorphous.

IR (neat, cm^{-1}) 3434, 3030, 1640, 1460, 1354, 1174, 1116, 1075, 968, 901, 864, 825, 754.

^{1}H NMR (400 MHz, $CDCl_3$) δ 1.31 (s, 3H), 1.36 (s, 3H), 3.06 (s, 3H), 3.09 (s, 3H), 3.74 (dd, *J* = 2.8, 11 Hz, 1H), 4.121 (d, *J* = 11 Hz, 1H), 4.123 (d, *J* = 11 Hz, 1H), 4.27 (d, *J* = 11 Hz, 1H), 4.37 (d, *J* = 11, 1H), 4.41 (d, *J* = 11, 1H), 4.65 (s, 1H), 4.92 (s, 1H), 5.21 (d, *J* = 2.8 Hz, 1H).

^{13}C NMR (100 MHz, $CDCl_3$) δ 16.9, 18.2, 37.4, 37.9, 70.7, 71.3, 72.2, 83.7, 84.5, 96.1, 97.3, 100.7.

HR-MS (ESI): Calcd for $C_{12}H_{21}N_1NaO_9S_2$ $[M+Na]^+$, 410.05554. Found, 410.05481.

((2a*S*/*R*,4*R*/*S*,4a*S*/*R*,6a*S*/*R*)-4,6-Dimethylhexahydro-1,3,5-trioxa-2a^1-azacyclopenta[*cd*]pentalene-4,6-diyl)bis(methylene) dimethanesulfonate (76c)

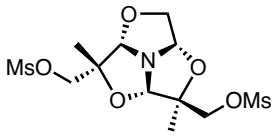

According to the synthetic protocol of **76a**, **75c** (200 mg, 0.864 mmol) was converted to **76c** (275mg, 82%) as a colorless amorphous.

IR (neat, cm^{-1}) 3434, 3028, 2940, 1640, 1460, 1354, 1174, 1114, 1076, 971, 830.

^{1}H NMR (400 MHz, $CDCl_3$) δ 1.38 (s, 3H), 1.42 (s, 3H), 3.06 (s, 3H), 3.09 (s, 3H), 3.79 (dd, *J* = 2.8, 11 Hz, 1H), 4.10 (d, *J* = 11 Hz, 1H), 4.13 (d, *J* = 10 Hz, 1H), 4.268 (d, *J* = 11 Hz, 1H), 4.272 (d, *J* = 11 Hz, 1H), 4.36 (d, *J* = 10 Hz, 1H), 4.71 (s, 1H), 4.90 (s, 1H), 5.17 (d, *J* = 2.8 Hz, 1H).

^{13}C NMR: (100 MHz, $CDCl_3$) δ 16.7, 18.4, 37.4 (×2), 38.0, 70.5, 71.4, 83.7, 85.1, 95.8, 98.1, 100.5.

HR-MS (ESI) Calcd for $C_{12}H_{21}N_1NaO_9S_2$ $[M+Na]^+$, 410.05554. Found, 410.05639.

((2a*S*/*R*,4*R*/*S*,4a*S*/*R*,6*R*/*S*,6a*S*/*R*)-4,6-Dimethylhexahydro-1,3,5-trioxa-2a^1-azacyclopenta[*cd*]pentalene-4,6-diyl)bis(methylene) dimethanesulfonate (76d)

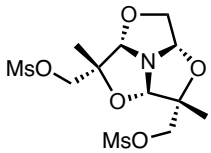

According to the synthetic protocol of **76a**, **75d** (236 mg, 1.02 mmol) was converted to **76d** (325 mg, 82%) as a colorless amorphous.

IR (neat, cm^{-1}) 3434, 3028, 2939, 1353, 1174, 1115, 1077, 968, 832.

^{1}H NMR (400 MHz, $CDCl_3$) δ 1.39 (s, 3H), 1.40 (s, 3H), 3.06 (s, 3H), 3.09 (s, 3H), 3.77 (dd, *J* = 2.8, 10 Hz, 1H), 4.13 (d, *J* = 10.0 Hz, 1H), 4.26 (d, *J* = 10 Hz, 1H), 4.35 (d, *J* = 10 Hz, 1H), 4.37 (s, 2H), 4.66 (s, 1H), 4.87 (s, 1H), 5.17 (d, *J* = 2.8 Hz, 1H).

^{13}C NMR (100 MHz, $CDCl_3$) δ 18.2, 18.3, 37.36, 37.43, 71.2 (×2), 71.8, 83.6, 84.2, 95.4, 99.7, 100.4.

HR-MS (ESI): Calcd for $C_{12}H_{21}NNaO_9S_2$ $[M+Na]^+$, 410.05554. Found, 410.05634.

((2a*S*/*R*,4*S*/*R*,4a*S*/*R*,6*S*/*R*,6a*S*/*R*)-4,6-Bis(azidomethyl)-4,6-dimethylhexahydro-1,3,5-trioxa-2a^1-azacyclopenta[*cd*]pentalene (77a)

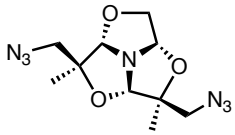

To a solution of **76a** (197 mg, 0.508 mmol) in dry DMSO (5 mL) was added sodium azide (1.00 g, 15.3 mmol) and the mixture was stirred for 2 h at 150 ºC under an argon atmosphere. After cooling to room temperature, the residue was poured into sat. $NaHCO_3$ aqueous solution (50 mL) and extracted with EtOAc (150 mL, 100 mL, 50 mL). The combined organic layers were washed with brine (100 mL), dried over anhydrous Na_2SO_4 and concentrated *in vacuo*. The residue was purified by silica gel column chromatography (hexane/EtOAc = 2/1) to obtain **77a** (127 mg, 89%) as a colorless oil.

IR (neat, cm^{-1}) 2934, 2100, 1112.

^{1}H NMR (400 MHz, $CDCl_3$) δ 1.35 (s, 3H), 1.42 (s, 3H), 3.27 (d, *J* = 12 Hz, 1H), 3.46 (d, *J* = 12 Hz, 1H), 3.49 (d, *J* = 12 Hz, 1H), 3.59 (d, *J* = 12 Hz, 1H), 3.74 (dd, *J* = 2.8, 10 Hz, 1H), 4.11 (d, *J* = 10 Hz, 1H), 4.61 (s, 1H), 4.83 (s, 1H), 5.18 (d, *J* = 2.8 Hz, 1H).

^{13}C NMR (100 MHz, $CDCl_3$) δ 17.6, 17.9, 55.6, 55.9, 71.9, 85.9, 86.1, 96.0, 98.4, 99.3.

HR-MS (ESI): Calcd for $C_{10}H_{15}N_7O_3$ $[M+H]^+$, 282.13146. Found, 282.13039.

((2a*S*/*R*,4*R*/*S*,4a*S*/*R*,6a*S*/*R*)-4,6-Bis(azidomethyl)-4,6-dimethylhexahydro-1,3,5-trioxa-2a^1-azacyclopenta[*cd*]pentalene (77b)

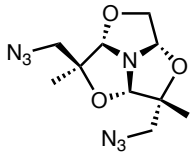

According to the synthetic protocol of **77a**, **76b** (200 mg, 0.516 mmol) was converted to **77b** (120 mg, 79%) as a colorless oil.

IR (neat, cm^{-1}) 2979, 2931, 2101, 1455, 1115.

^{1}H NMR (400 MHz, $CDCl_3$) δ 1.35 (s, 3H), 1.36 (s, 3H), 3.27 (d, *J* = 12 Hz, 1H), 3.476 (d, *J* = 12, 1H), 3.482 (d, *J* = 12, 1H), 3.59 (d, *J* = 12 Hz, 1H), 3.74 (dd, *J* = 2.8, 11 Hz, 1H), 4.11 (d, *J* = 11 Hz, 1H), 4.61 (s, 1H), 4.83 (s, 1H), 5.18 (d, *J* = 2.8 Hz, 1H).

^{13}C NMR (100 MHz, $CDCl_3$) δ 17.8, 18.8, 54.9, 55.8, 72.2, 85.1, 86.0, 95.7, 97.8, 100.7.

HR-MS (ESI): Calcd for $C_{10}H_{15}N_7Na_1O_3$ $[M+Na]^+$, 304.11341. Found, 304.11340.

((2a*S*/*R*,4*R*/*S*,4a*S*/*R*,6a*S*/*R*)-4,6-Bis(azidomethyl)-4,6-dimethylhexahydro-1,3,5-trioxa-2a^1-azacyclopenta[*cd*]pentalene (77c)

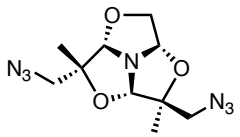

According to the synthetic protocol of **77a**, **76c** (250 mg, 0.645 mmol) was converted to **77c** (148 mg, 82%) as a colorless oil.

IR (neat, cm^{-1}) 2979, 2931, 2103, 1113.

^{1}H NMR (400 MHz, $CDCl_3$) δ 1.32 (s, 3H), 1.39 (s, 3H), 3.44 (d, *J* = 12 Hz, 1H), 3.45 (d, *J* = 12 Hz, 1H), 3.47 (d, *J* = 12 Hz, 1H), 3.48 (d, *J* = 12 Hz, 1H), 3.75 (dd, *J* = 2.8, 10 Hz, 1H), 4.11 (d, *J* = 10 Hz, 1H), 4.61 (s, 1H), 4.82 (s, 1H), 5.13 (d, *J* = 2.8 Hz, 1H).

^{13}C NMR (100 MHz, $CDCl_3$) δ 17.7, 19.1, 55.0, 55.6, 71.4, 85.1, 86.4, 95.4, 99.0, 100.2.

HR-MS (ESI): Calcd for $C_{10}H_{15}N_7O_3$ $[M+Na]^+$, 304.11341. Found, 304.11389.

((2a*S*/*R*,4*R*/*S*,4a*S*/*R*,6*R*/*S*,6a*S*/*R*)-4,6-Bis(azidomethyl)-4,6-dimethylhexahydro-1,3,5-trioxa-2a^1-azacyclopenta[*cd*]pentalene (77d)

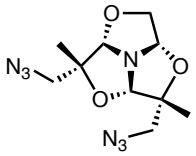

According to the synthetic protocol of **77a**, **76d** (235 mg, 0.607 mmol) was converted to **77d** (171 mg, 71%) as a colorless oil.

IR (neat, cm^{-1}) 3356, 2922, 2103, 1115.

^{1}H NMR (400 MHz, $CDCl_3$) δ 1.35 (s, 6H), 3.46 (d, *J* = 12 Hz, 1H), 3.50 (d, *J* = 12 Hz, 1H), 3.51 (d, *J* = 12 Hz, 1H), 3.57 (d, *J* = 12 Hz, 1H), 3.78 (dd, *J* = 2.8, 10 Hz, 1H), 4.13 (d, *J* = 12 Hz, 1H), 4.61 (s, 1H), 4.80 (s, 1H), 5.14 (d, *J* = 2.8 Hz, 1H).

^{13}C NMR (100 MHz, $CDCl_3$) δ 18.8, 18.9, 54.8 (×2), 71.8, 84.9, 85.6, 95.1, 99.4, 100.4.

HR-MS (ESI): Calcd for $C_{10}H_{15}N_7NaO_3$ $[M+Na]^+$, 304.11341. Found, 304.11242.

((2a*S*/*R*,4*S*/*R*,4a*S*/*R*,6*S*/*R*,6a*S*/*R*)-4,6-Dimethylhexahydro-1,3,5-trioxa-2a^1-azacyclopenta[*cd*]pentalene-4,6-diyl)dimethanamine (78a)

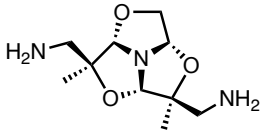

To a solution of **77a** (100 mg, 0.356 mmol) in MeOH (5 mL) was added 5% Pd/C (Degussa type, 0.100 g, 5 mol%) and the mixture was stirred for 3 h under a hydrogen atmosphere (balloon pressure). The reaction mixture was filtered with Celite and concentrated *in vacuo* to obtain **78a** (81.6 mg, quant.) as a pale-yellow oil.

IR (neat, cm^{-1}) 3366, 2935, 1607, 1117.

^{1}H NMR (400 MHz, CD_3OD) δ 1.32 (s, 3H), 1.39 (s, 3H), 2.28 (m, 2H), 3.05 (m, 2H), 3.30 (m, 2H), 3.32 (m, 2H), 3.75 (dd, *J* = 2.8, 10 Hz, 1H), 4.07 (d, *J* = 10 Hz, 1H), 4.60 (s, 1H), 4.77 (s, 1H), 5.12 (d, *J* = 2.8 Hz, 1H).

^{13}C NMR (100 MHz, CD_3OD) δ 16.7, 16.9, 44.6 (×2), 72.4, 79.5, 85.9, 96.2, 98.7, 100.3.

HR-MS (ESI): Calcd for $C_{10}H_{19}N_3NaO_3$ $[M+Na]^+$, 252.13241. Found, 252.13186.

((2a*S*/*R*,4*R*/*S*,4a*S*/*R*,6a*S*/*R*)-4,6-Bis(azidomethyl)-4,6-dimethylhexahydro-1,3,5-trioxa-2a^1-azacyclopenta[*cd*]pentalene (78b)

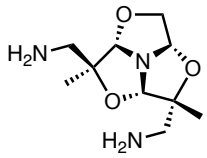

According to the synthetic protocol of **78a**, **77b** (103 mg, 0.366 mmol) was converted to **78b** (84.0 mg, quant.) as a pale-yellow oil.

IR (neat, cm^{-1}) 3376, 2934, 1583, 1115.

^{1}H NMR (400 MHz, CD_3OD) δ 1.27 (s, 3H), 1.29 (s, 3H), 2.57 (d, *J* = 13 Hz, 1H), 2.82 (d, *J* = 13 Hz, 1H), 2.90 (m, 2H), 3.31 (m, 2H), 3.35 (m, 2H), 3.71 (dd, *J* = 2.8, 10 Hz, 1H), 4.04 (d, *J* = 10 Hz, 1H), 4.63 (s, 1H), 4.75 (s, 1H), 5.06 (d, *J* = 2.8 Hz, 1H).

^{13}C NMR (100 MHz, CD_3OD) δ 16.8, 19.2, 48.4, 48.6, 72.6, 86.0, 87.4, 95.6, 98.7, 102.4.

HR-MS (ESI): Calcd for $C_{10}H_{19}N_3NaO_3$ $[M+Na]^+$, 252.13241. Found, 252.13193.

((2a*S*/*R*,4*R*/*S*,4a*S*/*R*,6a*S*/*R*)-4,6-Bis(azidomethyl)-4,6-dimethylhexahydro-1,3,5-trioxa-2a^1-azacyclopenta[*cd*]pentalene (78c)

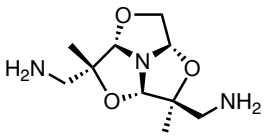

According to the synthetic protocol of **78a**, **77c** (100 mg, 0.356 mmol) was converted to **78c** (81.6 mg, quant.) as a pale-yellow oil.

IR (neat, cm^{-1}): 3373, 2928, 1583, 1115.

^{1}H NMR (400 MHz, CD_3OD) δ 1.25 (s, 3H), 1.33 (s, 3H), 2.56 (m, 1H), 2.83 (m, 1H), 2.90 (m, 4H), 3.31 (m, 2H), 3.73 (dd, *J* = 2.8, 10 Hz, 1H), 4.07 (d, *J* = 10 Hz, 1H), 4.52 (s, 1H), 4.77 (s, 1H), 5.15 (d, *J* = 2.8 Hz, 1H).

^{13}C NMR (100 MHz, CD_3OD) δ 16.6, 19.6, 48.6, 48.8, 72.2, 86.0, 87.7, 96.1, 100.2, 100.7.

HR-MS (ESI): Calcd for $C_{10}H_{19}N_3NaO_3$ $[M+Na]^+$, 252.13241. Found, 252.13234.

((2a*S*/*R*,4*R*/*S*,4a*S*/*R*,6*R*/*S*,6a*S*/*R*)-4,6-Dimethylhexahydro-1,3,5-trioxa-2a^1-azacyclopenta[*cd*]pentalene-4,6-diyl)dimethanamine (78d)

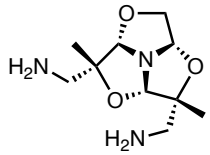

According to the synthetic protocol of **78a**, **77d** (101 mg, 0.361 mmol) was converted to **78d** (82.8 mg, quant.) as a pale-yellow oil.

IR (neat, cm^{-1}) 3312, 2912, 1611, 1115.

^{1}H NMR (400 MHz, $CDCl_3$) δ 1.35 (s, 6H), 2.41–2.54 (m, 1H), 2.82–2.85(m, 3H), 3.31–3.32 (m, 4H), 3.57 (d, *J* = 10 Hz, 1H), 4.13 (dd, *J* = 2.8, 10 Hz, 1H), 4.61 (s, 1H), 4.80 (s, 1H), 5.14 (d, *J* = 2.8 Hz, 1H).

^{13}C NMR (100 MHz, $CDCl_3$) δ 18.8, 18.9, 54.8 (×2), 71.8, 84.9, 85.6, 95.1, 99.4, 100.4.

HR-MS (ESI): Calcd for $C_{10}H_{19}N_3NaO_3$ $[M+Na]^+$, 252.13241. Found, 252.13171.

***N*,*N*'-(((2a*S*/*R*,4*S*/*R*,4a*S*/*R*,6*S*/*R*,6a*S*/*R*)-4,6-Dimethylhexahydro-1,3,5-trioxa-2a^1-azacyclopenta[*cd*]pentalene-4,6-diyl)bis(methylene)) diacetamide (79a)**

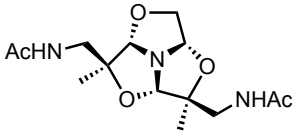

To a solution of amine **78a** (51.2 mg, 0.218 mmol) in pyridine (2 mL) was added acetic anhydride, (0.052 mL, 0.218 mmol) and the mixture was stirred for 2 h under an argon atmosphere. The reaction mixture was concentrated *in vacuo*. The residue was purified by silica gel column chromatography ($CHCl_3$/MeOH = 20/1 to 10/1) to obtain **79a** (56.0 mg, 82%) as a colorless amorphous.

IR (KBr, cm^{-1}) 3301, 2934, 1560, 1640, 1113.

^{1}H NMR (400 MHz, $CDCl_3$) δ 1.29 (s, 3H), 1.35 (s, 3H), 2.04 (s, 3H), 2.05 (s, 3H), 3.28 (dd, *J* = 4.4, 14 Hz, 1H), 3.33 (dd, *J* = 4.4, 14 Hz, 1H), 3.45 (dd, *J* = 8.0, 14 Hz, 1H), 3.54 (dd, *J* = 8.0, 14 Hz, 1H), 3.73 (dd, *J* = 2.8, 10 Hz, 1H), 4.07 (d, *J* = 10 Hz, 1H), 4.57 (s, 1H), 4.72 (s, 1H), 5.12 (d, *J* = 2.8 Hz, 1H), 5.64 (brs, 2H).

^{13}C NMR (100 MHz, $CDCl_3$) δ 17.1, 17.3, 23.4 (×2), 42.9, 43.1, 71.5, 85.6 (×2), 95.2, 98.0, 99.5, 170.6 (×2).

HR- MS (ESI): Calcd for $C_{14}H_{23}N_3NaO_5$ $[M+Na]^+$, 336.15354. Found, 336.15499.

***N*,*N*'-(((2a*S*/*R*,4*R*/*S*,4a*S*/*R*,6*R*/*S*,6a*S*/*R*)-4,6-Dimethylhexahydro-1,3,5-trioxa-2a^1-azacyclopenta[*cd*]pentalene-4,6-diyl)bis(methylene)) diacetamide (79d)**

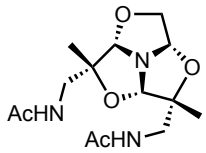

According to the synthetic protocol of **79a**, **78d** (53.1 mg, 0.227mmol) was converted to **79d** (65.4 mg, 92%) as a colorless amorphous.

IR (KBr, cm^{-1}) 3296, 2975, 1657, 1555, 1118.

^{1}H NMR (400 MHz, $CDCl_3$) δ 1.22 (s, 3H), 1.25 (s, 3H), 1.98 (s, 3H), 2.01 (s, 3H), 3.39–3.58 (m, 4H), 3.66 (dd, *J* = 2.8, 10 Hz, 1H), 4.02 (d, *J* = 10 Hz, 1H), 4.56 (s, 1H), 4.74 (s, 1H), 5.64 (d, *J* = 2.8 Hz, 1H), 6.18 (m, 2H).

^{13}C NMR (100 MHz, $CDCl_3$) δ 19.1, 19.8, 23.3, 23.4, 43.09, 43.15, 71.8, 84.4, 84.9, 94.8, 100.0, 101.2, 170.7 (×2).

HR- MS (ESI): Calcd for $C_{14}H_{23}N_3NaO_5$ $[M+Na]^+$, 336.15354. Found, 336.15384.

***N*,*N*'-(((2a*S*/*R*,4*S*/*R*,4a*S*/*R*,6*S*/*R*,6a*S*/*R*)-4,6-Dimethylhexahydro-1,3,5-trioxa-2a^1-azacyclopenta[*cd*]pentalene-4,6-diyl)bis (methylene)) bis(2,2-dimethylpropanamide) (80a)**

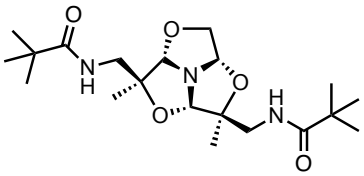

To a solution of amine **78a** (15.3 mg, 0.055 mmol) in dry DMF (1 mL) were added pivaloyl chloride (0.032 mL, 0.262mmol) and dry pyridine (0.053 mL, 0.262 mmol), and the mixture was stirred for 1.5 h under an argon atmosphere. The reaction mixture was poured into sat. $NaHCO_3$ aqueous solution (10 mL), concentrated *in vacuo* and extracted with $CHCl_3$ (30 mL, 20 mL, 10 mL). The combined organic layers were dried over anhydrous Na_2SO_4 and concentrated *in vacuo*. The residue was purified by silica gel column chromatography ($CHCl_3$/MeOH = 10/1) to obtain **80a** (16.4 mg, 61%) as a colorless amorphous.

IR (neat, cm^{-1}) 3376, 2972, 1643, 1535, 1115, 865.

^{1}H NMR (400 MHz, $CDCl_3$) δ 1.22 (m, 18H), 1.25 (s, 3H), 1.32 (s, 3H), 3.27 (dd, *J* = 4.1, 14 Hz, 1H), 3.33 (dd, *J* = 4.1, 14 Hz, 1H), 3.45 (dd, *J* = 7.3, 14 Hz, 1H), 3.52 (dd, *J* = 7.3, 14 Hz, 1H), 3.72 (dd, *J* = 2.8, 10 Hz, 1H), 4.08 (d, *J* = 10 Hz, 1H), 4.58 (s, 1H), 4.74 (s, 1H), 5.12 (d, *J* = 2.8 Hz, 1H), 5.86 (m, 2H).

^{13}C NMR (100 MHz, $CDCl_3$) δ 17.1, 17.2, 27.7 (×6), 39.0 (×2), 43.0, 43.1, 71.6, 85.9, 86.0, 95.3, 98.2, 100.0, 178.8 (×2).

HR-MS (ESI): Calcd for $C_{20}H_{35}N_3NaO_5$ $[M+Na]^+$, 420.24744. Found, 420.24613.

***N*,*N*'-(((2a*S*/*R*,4*R*/*S*,4a*S*/*R*,6*R*/*S*,6a*S*/*R*)-4,6-Dimethylhexahydro-1,3,5-trioxa-2a^1-azacyclopenta[*cd*]pentalene-4,6-diyl)bis (methylene)) bis(2,2-dimethylpropanamide) (80d)**

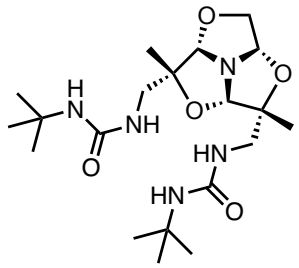

According to the synthetic protocol of **80a**, **78d** (15.0 mg, 0.055 mmol) was converted to **80d** (17.1 mg, 66%) as a brown oil.

IR (neat, cm^{-1}) 3443, 2961, 1648, 1530, 1115, 865.

^{1}H NMR (400 MHz, $CDCl_3$) δ 1.19 (m, 18H), 1.23 (s, 3H), 1.24 (s, 3H), 3.51 (dd, *J* = 4.6, 14 Hz, 1H), 3.53 (dd, *J* = 4.6, 14 Hz, 1H), 3.63 (dd, *J* = 6.9, 14 Hz, 1H), 3.74 (dd, *J* = 6.9, 14 Hz, 1H), 3.76 (dd, *J* = 2.8, 10 Hz, 1H), 4.10 (d, *J* = 10 Hz, 1H), 4.60 (s, 1H), 4.76 (s, 1H), 5.12 (d, *J* = 2.8 Hz, 1H), 6.03 (m, 1H), 6.23 (m, 1H).

^{13}C NMR (100 MHz, $CDCl_3$) δ 19.3, 19.5, 27.6 (×6), 38.8 (×2), 43.1, 43.2, 71.8, 84.7, 84.9, 94.8, 99.8, 101.2, 178.6 (×2).

HR-MS (ESI): Calcd for $C_{20}H_{35}N_3NaO_5$ $[M+Na]^+$, 420.24744. Found, 420.24567.

***N*,*N*'-(((2a*S*/*R*,4*S*/*R*,4a*S*/*R*,6*S*/*R*,6a*S*/*R*)-4,6-Dimethylhexahydro-1,3,5-trioxa-2a^1-azacyclopenta[*cd*]pentalene-4,6-diyl)bis(methylene)) dibenzamide (81a)**

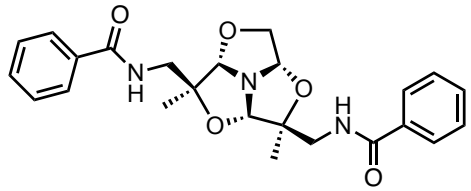

According to the synthetic protocol of **80a**, **78a** (12.6 mg, 0.055 mmol) was converted to **81a** (13.3 mg, 70%) as a brown oil.

IR (KBr, cm^{-1}) 3423, 2933, 1639, 1544, 1114, 709.

^{1}H NMR (400 MHz, $CDCl_3$) δ 1.37 (s, 3H), 1.43 (s, 3H), 3.52 (dd, *J* = 4.1, 14 Hz, 1H), 3.55 (dd, *J* = 4.1, 14 Hz, 1H), 3.64–3.80 (m, 3H), 4.11 (d, *J* = 10 Hz, 1H), 4.68 (s, 1H), 4.91 (s, 1H), 5.21 (d, *J* = 2.8 Hz, 1H), 6.42 (m, 2H), 7.42–7.53 (m, 6H), 7.77–7.81 (m, 4H).

^{13}C NMR (100 MHz, $CDCl_3$) δ 17.3, 17.6, 43.6 (×2), 71.6, 86.0 (×2), 95.4, 98.3, 99.6, 127.1 (×4), 128.8 (×4), 131.8 (×2), 134.4 (×2), 168.0 (×2).

HR-MS (ESI): Calcd for $C_{24}H_{27}N_3NaO_5$ $[M+Na]^+$, 460.18484. Found, 460.18307.

***N*,*N*'-(((2a*S*/*R*,4*R*/*S*,4a*S*/*R*,6*R*/*S*,6a*S*/*R*)-4,6-Dimethylhexahydro-1,3,5-trioxa-2a^1-azacyclopenta[*cd*]pentalene-4,6-diyl)bis(methylene)) dibenzamide (81d)**

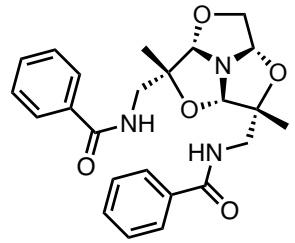

According to the synthetic protocol of **80a**, **78d** (10.0 mg, 0.0436 mmol) was converted to **81d** (10.2 mg, 54%) as a colorless amorphous.

IR (KBr, cm^{-1}) 3435, 2929, 1645, 1539, 1114, 754.

^{1}H NMR (400 MHz, $CDCl_3$) δ 1.325 (s, 3H), 1.331 (s, 3H), 3.55 (dd, *J* = 4.6, 14 Hz, 1H), 3.63 (dd, *J* = 4.6, 14 Hz, 1H), 3.80–3.87 (m, 2H), 4.02 (dd, *J* = 4.6, 14 Hz, 1H), 4.20 (d, *J* = 10 Hz, 1H), 4.68 (s, 1H), 4.87 (s, 1H), 5.18 (d, *J* = 2.8 Hz, 1H), 6.61 (m, 1H), 6.81 (m, 1H), 7.39–7.50 (m, 6H), 7.75–7.81 (m, 4H).

^{13}C NMR (100 MHz, $CDCl_3$) δ 19.5, 20.2, 43.6 (×2), 72.0, 84.7, 85.1, 94.9, 100.1, 101.5, 127.0 (×2), 127.1 (×2), 128.70 (×2), 128.74 (×2), 131.6, 131.7, 134.4, 134.6, 167.5, 167.6.

HR-MS (ESI): Calcd for $C_{24}H_{27}N_3NaO_5$ $[M+Na]^+$, 460.18484. Found, 460.18485.

***N*,*N*'-(((2a*S*/*R*,4*S*/*R*,4a*S*/*R*,6*S*/*R*,6a*S*/*R*)-4,6-Dimethylhexahydro-1,3,5-trioxa-2a^1-azacyclopenta[*cd*]pentalene-4,6-diyl)bis(methylene)) bis(2-methoxybenzamide) (82a)**

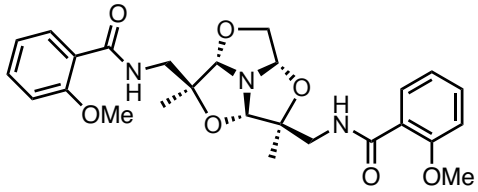

According to the synthetic protocol of **80a**, **78a** (20.0 mg, 0.0872 mmol) was converted to **82a** (35.2 mg, 95%) as a colorless amorphous.

IR (neat, cm^{-1}) 3423, 2926, 1626, 1449, 1325, 1144, 1113.

^{1}H NMR (400 MHz, $CDCl_3$) δ 1.40 (s, 3H), 1.44 (s, 3H), 3.55 (dd, *J* = 5.6, 14 Hz, 1H), 3.65 (d, *J* = 5.6 Hz, 2H), 3.74–3.78 (m, 2H), 3.94 (s, 3H), 3.97 (s, 3H), 4.12 (d, *J* = 10 Hz, 1H), 4.72 (s, 1H), 4.92 (s, 1H), 5.23 (d, *J* = 2.8 Hz, 1H), 6.97 (d, *J* = 8.2 Hz, 2H), 7.08 (m, 2H), 7.43–7.47 (m, 2H), 8.17–8.21 (m, 2H), Two NH protons are missing.

^{13}C NMR (100 MHz, $CDCl_3$) δ 17.5, 17.6, 43.5, 43.6, 56.07, 56.12, 71.5, 85.7, 85.8, 95.3, 98.2, 99.6, 111.5 (×2), 121.29 (×2), 121.33, 121.4, 132.4 (×2), 133.1 (×2), 157.6 (×2), 165.77, 165.81.

HR-MS (ESI): Calcd for $C_{26}H_{31}N_3NaO_7$ $[M+Na]^+$, 520.20597. Found, 520.20422.

***N*,*N*'-(((2a*S*/*R*,4*R*/*S*,4a*S*/*R*,6*R*/*S*,6a*S*/*R*)-4,6-Dimethylhexahydro-1,3,5-trioxa-2a^1-azacyclopenta[*cd*]pentalene-4,6-diyl)bis(methylene)) bis(2-methoxybenzamide) (82d)**

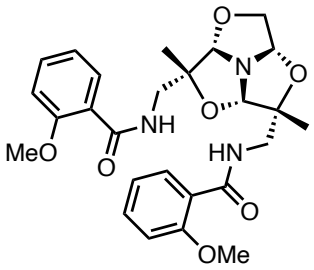

According to the synthetic protocol of **80a**, **78d** (10.0 mg, 0.0436 mmol) was converted to **82d** (21.8 mg, 90%) as a colorless amorphous.

IR (neat, cm^{-1}) 3003, 2935, 1650, 1537, 1114, 756.

^{1}H NMR (400 MHz, $CDCl_3$) δ 1.35 (s, 3H), 1.37 (s, 3H), 3.66 (dd, *J* = 5.0, 13 Hz, 1H), 3.78–3.84 (m, 2H), 3.899 (s, 3H), 3.904 (s, 3H), 3.95–4.02 (m, 2H), 4.20 (d, *J* = 10 Hz, 1H), 4.69 (s, 1H), 4.87 (s, 1H), 5.20 (d, *J* = 2.8 Hz, 1H), 6.94 (d, *J* = 8.2 Hz, 2H), 7.03–7.08 (m, 1H), 7.16–7.19 (m, 1H), 7.24–7.27 (m, 2H), 7.40–7.44 (m, 2H), Two NH protons are missing.

^{13}C NMR (100 MHz, $CDCl_3$) δ 19.6, 19.7, 43.4, 43.5, 56.0 (×2), 71.8, 85.2 (×2), 95.2, 100.0, 101.3, 111.3, 111.4, 121.3, 121.4, 125.4, 129.2, 132.4 (×2), 133.0 (×2), 157.6, 157.7, 165.5, 165.6.

HR-MS (ESI): Calcd for $C_{26}H_{31}N_3NaO_7$ $[M+Na]^+$, 520.20597. Found, 520.20466.

***N*,*N*'-(((2a*S*/*R*,4*S*/*R*,4a*S*/*R*,6*S*/*R*,6a*S*/*R*)-4,6-Dimethylhexahydro-1,3,5-trioxa-2a^1-azacyclopenta[*cd*]pentalene-4,6-diyl)bis(methylene)) bis(3-methoxybenzamide) (83a)**

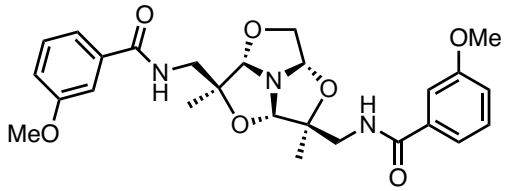

According to the synthetic protocol of **80a**, **78a** (20.0 mg, 0.0872 mmol) was converted to **83a** (36.2 mg, 94%) as a colorless amorphous.

IR (neat, cm^{-1}) 3394, 3004, 2936, 1466, 1298, 1163, 1023.

^{1}H NMR (400 MHz, $CDCl_3$) δ 1.34 (s, 3H), 1.41 (s, 3H), 3.55 (dd, *J* = 4.1, 14 Hz, 1H), 3.54 (dd, *J* = 4.1, 14 Hz, 1H), 3.65 (dd, *J* = 2.8, 10 Hz, 1H), 3.71–3.77 (m, 2H), 3.825 (s, 3H), 3.832 (s, 3H), 4.08 (d, *J* = 7.3, 10 Hz, 1H), 4.67 (s, 1H), 4.90 (s, 1H), 5.19 (d, *J* = 2.8 Hz, 1H), 6.54 (m, 2H), 7.02–7.05 (m, 2H), 7.30–7.38 (m, 6H).

^{13}C NMR (100 MHz, $CDCl_3$) δ 17.3, 17.5, 43.5, 43.6, 55.6 (×2), 71.6, 85.9, 86.0, 95.4, 98.2, 99.6, 112.6 (×2), 117.9 (×2), 118.8 (×2), 129.8 (×2), 135.8 (×2), 160.0 (×2), 167.9 (×2).

HR-MS (ESI): Calcd for $C_{26}H_{31}N_3NaO_7$ $[M+Na]^+$, 520.20597. Found, 520.20796.

***N*,*N*'-(((2a*S*/*R*,4*R*/*S*,4a*S*/*R*,6*R*/*S*,6a*S*/*R*)-4,6-Dimethylhexahydro-1,3,5-trioxa-2a^1-azacyclopenta[*cd*]pentalene-4,6-diyl)bis(methylene)) bis(3-methoxybenzamide) (83d)**

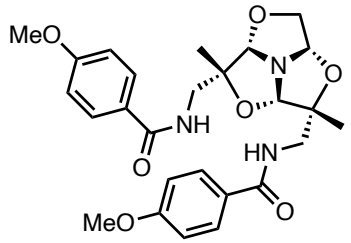

According to the synthetic protocol of **80a**, **78d** (10.0 mg, 0.0436 mmol) was converted to **83d** (20.1 mg, 92%) as a colorless amorphous.

IR (neat, cm^{-1}) 3393, 3003, 2936, 1651, 1537, 1298, 1240, 1115, 756.

^{1}H NMR (400 MHz, $CDCl_3$) δ 1.33 (s, 3H), 1.34 (s, 3H), 3.53 (dd, *J* = 4.6, 14 Hz, 1H), 3.64 (dd, *J* = 6.0, 14 Hz, 1H), 3.81–3.87 (m, 8H), 4.02 (dd, *J* = 8.2, 14 Hz, 1H), 4.21 (d, *J* = 10 Hz, 1H), 4.69 (s, 1H), 4.88 (s, 1H), 5.19 (d, *J* = 2.8 Hz, 1H), 6.64 (m, 1H), 6.85 (m, 1H), 7.03 (m, 2H), 7.29–7.38 (m, 6H).

^{13}C NMR (100 MHz, $CDCl_3$) δ 19.6, 20.2, 43.6 (×2), 55.5, 55.6, 72.0, 84.8, 85.0, 94.9, 100.0, 101.5, 112.4, 112.5, 117.8, 117.9, 118.7, 119.0, 129.7 (×2), 135.9, 136.1, 159.90, 159.93, 167.4, 167.5.

HR-MS (ESI): Calcd for $C_{26}H_{31}N_3NaO_7$ $[M+Na]^+$, 520.20597. Found, 520.20505.

***N*,*N*'-(((2a*S*/*R*,4*S*/*R*,4a*S*/*R*,6*S*/*R*,6a*S*/*R*)-4,6-Dimethylhexahydro-1,3,5-trioxa-2a^1-azacyclopenta[*cd*]pentalene-4,6-diyl)bis(methylene)) bis(4-methoxybenzamide) (84a)**

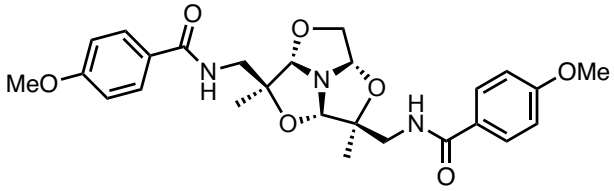

According to the synthetic protocol of **80a**, **78a** (20.0 mg, 0.0872 mmol) was converted to **84a** (21.4 mg, 98%) as a colorless amorphous.

IR (neat, cm^{-1}) 3423, 2933, 1637, 1607, 1255, 1113.

^{1}H NMR (400 MHz, $CDCl_3$) δ 1.35 (s, 3H), 1.41 (s, 3H), 3.49 (m, 2H), 3.67 (dd, *J* = 7.6, 14.0 Hz, 1H), 3.73–3.78 (m, 2H), 3.84 (s, 6H), 4.09 (d, *J* = 10 Hz, 1H), 4.66 (s, 1H), 4.88 (s, 1H), 5.19 (d, *J* = 2.8 Hz, 1H), 6.25–6.27 (m, 2H), 6.91–6.93 (m, 4H), 7.73–7.77 (m, 4H).

^{13}C NMR (100 MHz, $CDCl_3$) δ 17.3, 17.6, 43.6 (×2), 55.5 (×2), 71.6, 85.9, 86.0, 95.4, 98.3, 99.6, 113.9 (×4), 126.5 (×2), 128.9 (×4), 162.4 (×2), 167.4 (×2).

HR-MS (ESI): Calcd for $C_{26}H_{31}N_3NaO_7$ $[M+Na]^+$, 520.20597. Found, 520.20428.

***N*,*N*'-(((2a*S*/*R*,4*R*/*S*,4a*S*/*R*,6*R*/*S*,6a*S*/*R*)-4,6-Dimethylhexahydro-1,3,5-trioxa-2a^1-azacyclopenta[*cd*]pentalene-4,6-diyl)bis(methylene)) bis(4-methoxybenzamide) (84d)**

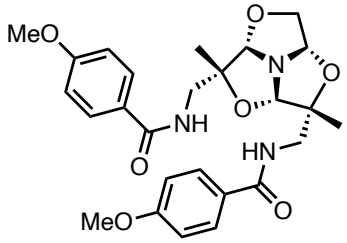

According to the synthetic protocol of **80a**, **78d** (17.0 mg, 0.0741 mmol) was converted to **84d** (35.7 mg, 97%) as a colorless amorphous.

IR (neat, cm^{-1}) 3328, 2931, 1642, 1607, 1255, 1115, 756.

^{1}H NMR (400 MHz, $CDCl_3$): δ 1.32 (s, 3H), 1.34 (s, 3H), 3.55 (dd, *J* = 4.1, 14.0 Hz, 1H), 3.64–3.69 (m, 2H), 3.80 (dd, *J* = 2.8, 10.1 Hz, 1H), 3.85 (s, 3H), 3.86 (s, 3H), 4.04 (dd, *J* = 7.8, 14.0 Hz, 1H), 4.16 (d, *J* = 10.1 Hz, 1H), 4.72 (s, 1H), 4.83 (s, 1H), 5.22 (d, *J* = 2.8 Hz, 1H), 6.21 (m, 1H), 6.75 (m, 1H), 6.93 (m, 4H), 7.73–7.77 (m, 4H).

^{13}C NMR (100 MHz, $CDCl_3$): δ 19.5, 20.3, 43.4, 43.5, 55.5 (×2), 72.0, 84.7, 85.1, 94.8, 100.1, 101.5, 113.8 (×2), 114.0 (×2), 126.7, 126.8, 128.8 (×2), 128.9 (×2), 162.25, 162.29, 167.0, 167.3.

HR-MS (ESI): Calcd for $C_{26}H_{31}N_3NaO_7$ $[M+Na]^+$, 520.20597. Found, 520.20588.

***N*,*N*'-(((2a*S*/*R*,4*S*/*R*,4a*S*/*R*,6*S*/*R*,6a*S*/*R*)-4,6-Dimethylhexahydro-1,3,5-trioxa-2a^1-azacyclopenta[*cd*]pentalene-4,6-diyl)bis(methylene)) bis(2-phenylacetamide) (85a)**

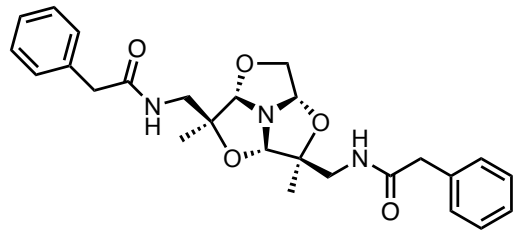

According to the synthetic protocol of **80a**, **78a** (20.0 mg, 0.0872 mmol) was converted to **85a** (11.8 mg, 30%) as a colorless amorphous.

IR (neat, cm^{-1}) 2931, 1650, 1552, 1115, 757.

^{1}H NMR (400 MHz, $CDCl_3$) δ 1.17 (s, 3H), 1.39 (s, 3H), 3.32–3.45 (m, 9H), 4.80 (d, *J* = 14 Hz, 1H), 4.84 (s, 1H), 5.10 (s, 1H), 5.22 (d, *J* = 2.8 Hz, 1H), 6.01 (m, 1H), 6.19 (m, 1H), 7.15–7.32 (m, 10H).

^{13}C NMR (100 MHz, $CDCl_3$) δ 17.0, 18.3, 53.0 (×2), 53.6 (×2), 71.4, 84.5, 85.6, 95.6, 99.0, 99.3, 121.1, 121.2 (×2), 125.9 (×2), 126.0, 128.3, 128.4, 128.9, 129.0, 130.5, 130.6, 172.2, 172.3.

HR-MS (ESI): Calcd for $C_{26}H_{31}N_3NaO_5$ $[M+Na]^+$, 488.21614. Found, 488.21534.

***N*,*N*'-(((2a*S*/*R*,4*R*/*S*,4a*S*/*R*,6*R*/*S*,6a*S*/*R*)-4,6-Dimethylhexahydro-1,3,5-trioxa-2a^1-azacyclopenta[*cd*]pentalene-4,6-diyl)bis(methylene)) bis(2-phenylacetamide) (85d)**

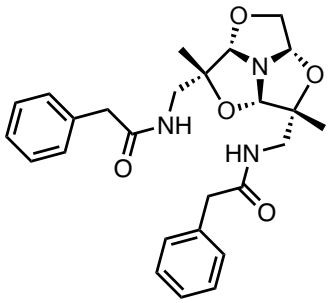

According to the synthetic protocol of **80a**, **78d** (10.0 mg, 0.0436 mmol) was converted to **85d** (18.0 mg, 89%) as a colorless amorphous.

IR (neat, cm^{-1}) 3370, 2928, 1651, 1115, 754.

^{1}H NMR (400 MHz, $CDCl_3$) δ 1.09 (s, 3H), 1.14 (s, 3H), 3.32–3.73 (m, 10H), 4.40 (s, 1H), 4.53 (s, 1H), 4.97 (d, *J* = 2.8 Hz, 1H), 5.94 (m, 1H), 6.04 (m, 1H), 7.18–7.35 (m, 10H).

^{13}C NMR (100 MHz, $CDCl_3$) δ 19.4, 19.6, 43.3, 43.4, 43.9, 44.0, 71.5, 84.2, 84.4, 94.8, 99.6, 101.2, 127.35, 127.37, 128.9, 129.0, 129.1 (×2), 129.5 (×2), 129.7 (×2), 134.9, 135.2, 1701.29, 171.33.

HR-MS (ESI): Calcd for $C_{26}H_{31}N_3NaO_5$ $[M+Na]^+$, 488.21614. Found, 488.21372.

***N*,*N*'-(((2a*S*/*R*,4*S*/*R*,4a*S*/*R*,6*S*/*R*,6a*S*/*R*)-4,6-Dimethylhexahydro-1,3,5-trioxa-2a^1-azacyclopenta[*cd*]pentalene-4,6-diyl)bis(methylene)) bis(3-phenylpropanamide) (86a)**

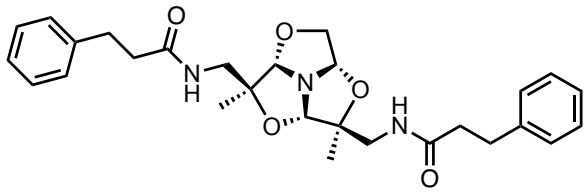

According to the synthetic protocol of **80a**, **78a** (20.0 mg, 0.0872 mmol) was converted to **86a** (42.2 mg, 98%) as a colorless amorphous.

IR (neat, cm^{-1}) 3310, 2931, 1650, 1152, 1116, 752.

^{1}H NMR (400 MHz, $CDCl_3$) δ 1.15 (s, 3H), 1.23 (s, 3H), 2.54 (m, 4H), 2.97 (t, *J* = 7.3, 2H), 2.98 (t, *J* = 7.3, 2H), 3.24 (dd, *J* = 3.7, 16.0 Hz, 1H), 3.25 (dd, *J* = 3.7, 16.0 Hz, 1H), 3.44 (dd, *J* = 7.3, 14 Hz, 1H), 3.51 (dd, *J* = 7.3, 14 Hz, 1H), 3.68 (dd, *J* = 3.2, 10 Hz, 1H), 4.02 (d, *J* = 10 Hz, 1H), 4.89 (s, 1H), 4.57 (s, 1H), 4.97 (d, *J* = 2.8 Hz, 1H), 5.49 (m, 2H), 7.18–7.31 (m, 10H).

^{13}C NMR (100 MHz, $CDCl_3$) δ 17.0, 17.2, 31.7 (×2), 38.5 (×2), 42.7, 42.8, 71.4, 85.4, 85.5, 95.1, 97.8, 99.4, 126.40, 126.44, 128.5 (×4), 128.7 (×4), 140.8 (×2), 172.6 (×2).

HR-MS (ESI): Calcd for $C_{28}H_{35}N_3NaO_5$ $[M+Na]^+$, 516.24744. Found, 516.24841.

***N*,*N*'-(((2a*S*/*R*,4*R*/*S*,4a*S*/*R*,6*R*/*S*,6a*S*/*R*)-4,6-Dimethylhexahydro-1,3,5-trioxa-2a^1-azacyclopenta[*cd*] pentalene-4,6-diyl)bis(methylene)) bis(3-phenylpropanamide) (86d)**

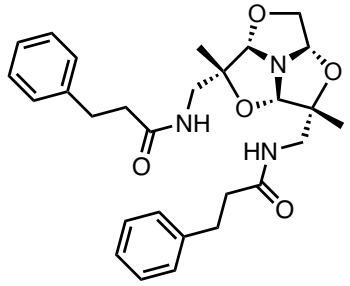

According to the synthetic protocol of **80a**, **78d** (5.00 mg, 0.0218 mmol) was converted to **86d** (18.0 mg, 62%) as a pale-yellow amorphous.

IR (neat, cm^{-1}) 3307, 2928, 1650, 1550, 1116, 753.

^{1}H NMR (400 MHz, $CDCl_3$) δ 1.12 (s, 3H), 1.13 (s, 3H), 2.48–2.52 (m, 4H), 2.96 (t, *J* = 7.6, 2H), 2.98 (t, *J* = 7.6, 2H), 3.42–3.61 (m, 4H), 3.66 (dd, *J* = 2.8, 10 Hz, 1H), 4.02 (d, *J* = 10 Hz, 1H), 4.41 (s, 1H), 4.55 (s, 1H), 5.04 (d, *J* = 2.8 Hz, 1H), 5.87 (m, 2H), 7.16–7.28 (m, 10H).

^{13}C NMR (100 MHz, $CDCl_3$) δ19.2, 19.6, 31.7, 31.9, 38.6 (×2), 43.16, 43.23, 71.8, 84.5, 84.9, 94.8, 99.9, 101.1, 126.3, 126.4, 128.52 (×4), 1289.67 (×4), 140.8, 141.0, 172.4, 172.5.

HR-MS (ESI): Calcd for $C_{28}H_{35}N_3NaO_5$ $[M+Na]^+$, 516.24744. Found, 516.24782.

(2*E*,2'*E*)-*N*,*N*'-(((2a*S*/*R*,4*S*/*R*,4a*S*/*R*,6*S*/*R*,6a*S*/*R*)-4,6-Dimethylhexahydro-1,3,5-trioxa-2a^1-azacyclopenta[*cd*]pentalene-4,6-diyl)bis (methylene))bis(3-phenylacrylamide) (87a)

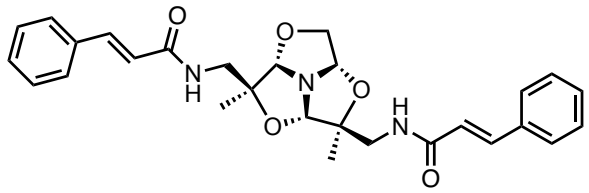

According to the synthetic protocol of **80a**, **78a** (20.0 mg, 0.0872 mmol) was converted to **87a** (32.8 mg, 77%) as a pale-yellow oil.

IR (neat, cm^{-1}) 3423, 2925, 1656, 1626, 1115.

^{1}H NMR (400 MHz, $CDCl_3$) δ 1.34 (s, 3H), 1.40 (s, 3H), 3.43 (dd, *J* = 4.6, 14 Hz, 1H), 3.50 (dd, *J* = 4.6, 14 Hz, 1H), 3.61 (dd, *J* = 6.8, 14 Hz, 1H), 3.68–3.73 (m, 2H), 4.08 (d, *J* = 10 Hz, 1H), 4.63 (s, 1H), 4.86 (s, 1H), 5.17 (d, *J* = 2.8 Hz, 1H), 6.24 (m, 2H), 6.50 (dd, *J* = 5.5, 16 Hz, 2H), 7.33–7.35 (m, 6H), 7.45–7.51 (m, 4H), 7.65 (dd, *J* = 5.5, 16 Hz, 2H).

^{13}C NMR (100 MHz, $CDCl_3$) δ 17.2,17.5, 43.1, 43.2, 71.5, 85.8, 85.9, 95.3, 98.1, 99.5, 120.3 (×2), 128.0 (×4), 129.0 (×4), 130.0 (×2), 134.7, 134.8, 141.8 (×2), 166.48, 166.52.

HR-MS (ESI): Calcd for $C_{28}H_{31}N_3NaO_5$ $[M+Na]^+$, 512.21614. Found, 512.21703.

(2*E*,2'*E*)-*N*,*N*'-(((2a*S*/*R*,4*R*/*S*,4a*S*/*R*,6*R*/*S*,6a*S*/*R*)-4,6-Dimethylhexahydro-1,3,5-trioxa-2a^{1}-azacyclopenta [*cd*]pentalene-4,6-diyl)bis (methylene))bis(3-phenylacrylamide) (87d)

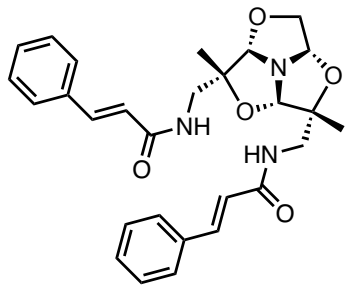

According to the synthetic protocol of **87a**, **78d** (5.00 mg, 0.0218 mmol) was converted to **87d** (5.62 mg, 52%) as a pale-yellow oil.

IR (neat, cm^{-1}) 3290, 2928, 1659, 1621, 1116, 756.

^{1}H NMR (400 MHz, $CDCl_3$) δ 1.3215 (s, 3H), 1.3221 (s, 3H), 3.65–3.74 (m, 3H), 3.79 (dd, *J* = 2.8, 8.2 Hz, 1H), 3.88 (dd, *J* = 8.2, 14 Hz, 1H), 4.18 (d, *J* = 10 Hz, 1H), 4.66 (s, 1H), 4.84 (s, 1H), 5.17 (d, *J* = 2.8 Hz, 1H), 6.24 (m, 1H), 6.34 (m, 1H), 6.47 (d, *J* = 16 Hz, 2H), 7.32–7.38 (m, 6H), 7.47–7.52 (m, 4H), 7.64 (dd, *J* = 2.3, 16 Hz, 2H).

^{13}C NMR (100 MHz, $CDCl_3$) δ 19.4, 20.1, 43.3 (×2), 72.0, 84.6, 85.2, 94.9, 100.1, 101.4, 120.80, 120.85, 127.98 (×2), 128.92 (×2), 128.94 (×2), 129.79 (×2), 129.83 (×2), 134.9 (×2), 141.4, 141.5, 166.3, 166.4.

HR-MS (ESI): Calcd for $C_{28}H_{31}N_3NaO_5$ $[M+Na]^+$, 512.21614. Found, 512.21362.

Di-*tert*-butyl(((2a*S*/*R*,4*S*/*R*,4a*S*/*R*,6*S*/*R*,6a*S*/*R*)-4,6-dimethylhexahydro-1,3,5-trioxa-2a^1-azacyclopenta [*cd*]pentalene-4,6-diyl)bis (methylene))dicarbamate (88a)

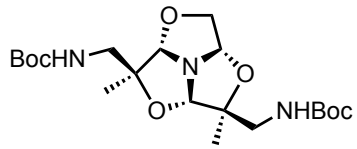

To a solution of amine **78a** (30.0 mg, 0.131 mmol) in pyridine (2 mL) was added di-*tert*-butyl dicarbonate, (0.35 mL, 4.50 mmol) and the mixture was stirred for 2 h under an argon atmosphere. The reaction mixture was poured into sat. $NaHCO_3$ aqueous solution (10 mL) and extracted with $CHCl_3$ (30 mL, 20 mL, 10 mL). The combined organic layers were dried over anhydrous Na_2SO_4 and concentrated *in vacuo*. The residue was purified by silica gel column chromatography ($CHCl_3$/MeOH = 20/1) to obtain **88a** (54.1 mg, 96%) as a colorless solid.

IR (KBr, cm^{-1}) 3360, 2979, 2932, 1712, 1515, 1455, 1392, 1367, 1155.

^{1}H NMR (400 MHz, $CDCl_3$) δ 1.28 (s, 3H), 1.35 (s, 3H), 1.45 (s, 18H), 3.23–3.32 (m, 4H), 3.72 (dd, *J* = 2.8, 9.6 Hz, 1H), 4.07 (d, *J* = 9.6 Hz, 1H), 4.56 (s, 1H), 4.70 (s, 1H), 4.76 (m, 2H), 5.10 (d, *J* = 2.8 Hz, 1H).

^{13}C NMR (100 MHz, $CDCl_3$) δ 17.3, 17.5, 28.8 (×6), 44.3, 44.5, 71.8, 80.05, 80.13, 85.96, 86.03, 95.4, 98.1, 99.7, 156.5 (×2).

HR-MS (ESI) Calcd for $C_{20}H_{35}N_3NaO_7$ $[M+Na]^+$, 452.2373. Found, 452.2357.

Di-*tert*-butyl(((2a*S*/*R*,4*R*/*S*,4a*S*/*R*,6a*S*/*R*)-4,6-dimethylhexahydro-1,3,5-trioxa-2a1-azacyclopenta[*cd*]pentalene-4,6-diyl)bis(methylene))dicarbamate (88b)

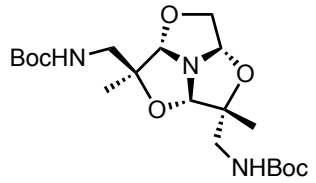

According to the synthetic protocol of **88a**, **78c** (8.20 mg, 0.0357 mmol) was converted to **88c** (14.3 mg, 81%) as a colorless amorphous.

IR (KBr, cm^{-1}) 3451, 3357, 2978, 2932, 1713, 1514, 1455, 1391, 1366, 1115.

^{1}H NMR (400 MHz, $CDCl_3$) δ 1.25 (s, 3H), 1.34 (s, 3H), 1.44 (s, 9H), 1.46 (s, 9H), 3.20–3.48 (m, 4H), 3.73 (dd, *J* = 2.8, 10 Hz, 1H), 4.09 (d, *J* = 10 Hz, 1H), 4.55 (s, 1H), 4.71–4.94 (m, 2H), 4.78 (s, 1H), 5.12 (d, *J* = 2.8 Hz, 1H).

^{13}C NMR (100 MHz, $CDCl_3$) δ 16.9, 19.4, 28.51 (×3), 28.53 (×3), 44.0, 44.6, 71.5 (×2), 79.3, 79.9, 84.8, 86.2, 95.3, 99.1, 100.1, 156.2, 156.5.

HR-MS (ESI): Calcd for $C_{20}H_{35}N_3NaO_7$ $[M+Na]^+$, 452.2373. Found, 452.2390.

Di-*tert*-butyl(((2a*S*/*R*,4*S*/*R*,4a*S*/*R*,6*R*/*S*,6a*S*/*R*)-4,6-dimethylhexahydro-1,3,5-trioxa-2a1-azacyclopenta[*cd*]pentalene-4,6-diyl)bis(methylene))dicarbamate (88c)

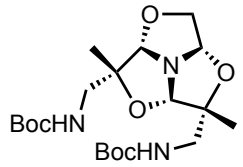

According to the synthetic protocol of **88a**, **78c** (7.46 mg, 0.0325 mmol) was converted to **88c** (13.0 mg, 93%) as a colorless amorphous.

IR (KBr, cm^{-1}) 3355, 2978, 1713, 1115.

^{1}H NMR (400 MHz, $CDCl_3$) δ 1.24 (s, 3H), 1.31 (s, 3H), 1.44 (s, 9H), 1.46 (s, 9H), 3.20–3.48 (m, 4H), 3.73 (dd, *J* = 2.8, 10 Hz, 1H), 4.09 (d, *J* = 10 Hz, 1H), 4.55 (s, 1H), 4.71–4.94 (m, 2H), 4.78 (s, 1H), 5.11 (d, *J* = 2.8 Hz, 1H).

^{13}C NMR (100 MHz, $CDCl_3$) δ 16.4, 19.0, 28.4 (×6), 44.0, 44.5, 71.2 (×2), 79.3, 80.0, 84.8, 85.2, 95.1, 99.1, 99.9, 156.25, 156.31.

HR-MS (ESI): Calcd for $C_{20}H_{35}N_3NaO_7$ $[M+Na]^+$, 452.23727. Found, 452.23825.

Di-*tert*-butyl(((2a*S*/*R*,4*R*/*S*,4a*S*/*R*,6*R*/*S*,6a*S*/*R*)-4,6-dimethylhexahydro-1,3,5-trioxa-2a^1-azacyclopenta [*cd*]pentalene-4,6-diyl)bis (methylene))dicarbamate (88d)

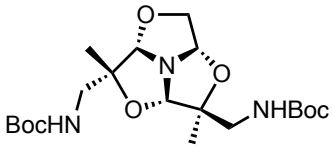

According to the synthetic protocol of **88a**, **78d** (12.0 mg, 0.0524 mmol) was converted to **88d** (30.2 mg, 97%) as a colorless amorphous.

IR (KBr, cm^{-1}) 3454, 3353, 2976, 2929, 1714, 1512, 1455, 1391, 1366, 1114, 756.

^{1}H NMR (400 MHz, $CDCl_3$) δ 1.42 (s, 6H), 1.46 (s, 18H), 3.39–3.46 (m, 4H), 3.70 (dd, *J* = 2.8, 10 Hz, 1H), 4.07 (d, *J* = 10 Hz, 1H), 4.55 (s, 1H), 4.75 (s, 1H), 4.84 (m, 1H), 4.94 (m, 1H), 5.08 (d, *J* = 2.8 Hz, 1H).

^{13}C NMR (100 MHz, $CDCl_3$) δ 19.3 (×2), 28.5 (×6), 44.6, 44.7, 71.8, 79.4, 79.5, 85.0, 85.1, 94.9, 100.0, 101.2, 156.4 (×2).

HR-MS (ESI): Calcd for $C_{20}H_{35}N_3NaO_7$ $[M+Na]^+$, 452.2373. Found, 452.2350.

Dimethyl(((2a*S*/*R*,4*S*/*R*,4a*S*/*R*,6*S*/*R*,6a*S*/*R*)-4,6-dimethylhexahydro-1,3,5-trioxa-2a^1-azacyclopenta[*cd*] pentalene-4,6-diyl)bis (methylene))dicarbamate (89a)

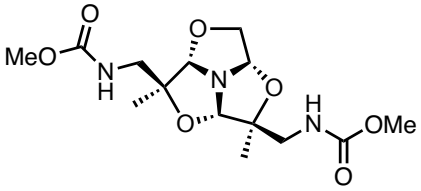

According to the synthetic protocol of **80a**, **78a** (15.0 mg, 0.0654 mmol) was converted to **89a** (21.6 mg, 96%) as a colorless amorphous.

IR (neat, cm^{-1}) 3337, 2937, 1710, 1542, 1258, 1115, 755.

^{1}H NMR (400 MHz, $CDCl_3$) δ 1.28 (s, 3H), 1.35 (s, 3H), 3.23–3.39 (m, 4H), 3.69–3.727 (m, 6H), 3.731 (dd, *J* = 2.3, 10 Hz, 1H), 4.07 (d, *J* = 10 Hz, 1H), 4.57 (s, 1H), 4.72 (s, 1H), 4.95 (m, 2H), 5.13 (d, *J* = 2.3 Hz, 1H).

^{13}C NMR (100 MHz, $CDCl_3$) δ 17.0, 17.2, 44.6, 44.7, 52.5 (×2), 71.5, 85.7 (×2), 95.2, 97.8, 99.3, 157.4 (×2).

HR-MS (ESI): Calcd for $C_{14}H_{23}N_3NaO_7$ $[M+Na]^+$, 368.14337. Found, 368.14313.

Dimethyl(((2a*S*/*R*,4*R*/*S*,4a*S*/*R*,6*R*/*S*,6a*S*/*R*)-4,6-dimethylhexahydro-1,3,5-trioxa-2a^1-azacyclopenta[*cd*]pentalene-4,6-diyl)bis (methylene))dicarbamate (89d)

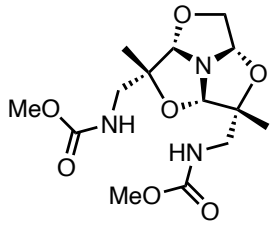

According to the synthetic protocol of **80a**, **78d** (20.0 mg, 0.0433 mmol) was converted to **89d** (18.2 mg, 75%) as a colorless amorphous.

IR (neat, cm^{-1}) 3338, 2919, 1714, 1537, 1250, 1114, 758.

^{1}H NMR (400 MHz, $CDCl_3$) δ 1.27 (s, 6H), 3.44–3.60 (m, 4H), 3.65–3.71 (m, 6H), 3.73 (dd, *J* = 2.8, 10 Hz, 1H), 4.10 (d, *J* = 10 Hz, 1H), 4.58 (s, 1H), 4.78 (s, 1H), 5.11 (d, *J* = 2.8 Hz, 1H), 5.11 (m, 1H), 5.20 (m, 1H).

^{13}C NMR (100 MHz, $CDCl_3$) δ 19.4, 19.6, 45.2 (×2), 52.3 (×2), 71.8, 84.7, 85.0, 95.0, 100.0, 101.3, 157.6 (×2).

HR-MS (ESI): Calcd for $C_{14}H_{23}N_3NaO_7$ $[M+Na]^+$, 368.14337. Found, 368.14221.

Divinyl(((2a*S*/*R*,4*S*/*R*,4a*S*/*R*,6*S*/*R*,6a*S*/*R*)-4,6-dimethylhexahydro-1,3,5-trioxa-2a^1-azacyclopenta[*cd*]pentalene-4,6-diyl)bis (methylene))dicarbamate (90a)

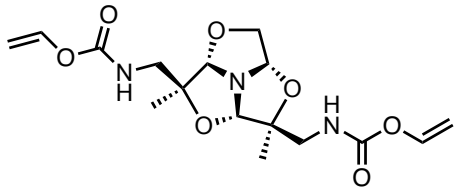

According to the synthetic protocol of **80a**, **78a** (10.0 mg, 0.0436 mmol) was converted to **90a** (9.20 mg, 53%) as a colorless amorphous.

IR (neat, cm^{-1}) 3337, 2396, 1710, 1537, 1253, 1157, 1116, 756.

^{1}H NMR (400 MHz, $CDCl_3$) δ 1.29 (s, 3H), 1.36 (s, 3H), 3.30–3.36 (m, 4H), 3.72 (dd, *J* = 2.8, 10 Hz, 1H), 4.07 (d, *J* = 10 Hz, 1H), 4.57–4.59 (m, 5H), 4.71 (s, 1H), 4.95 (m, 2H), 5.12 (d, *J* = 2.8 Hz, 1H), 5.22 (m, 2H), 5.34 (m, 2H), 5.89–5.96 (m, 2H).

^{13}C NMR (100 MHz, $CDCl_3$) δ 17.0, 17.2, 44.6, 44.7, 66.0 (×2), 71.5, 85.6 (×2), 95.2, 97.8, 99.4, 117.90, 117.99, 132.8 (×2), 156.6 (×2).

HR-MS (ESI): Calcd for $C_{18}H_{27}N_3NaO_7$ $[M+Na]^+$, 420.17467. Found, 420.17444.

Divinyl(((2a*S*/*R*,4*R*/*S*,4a*S*/*R*,6*R*/*S*,6a*S*/*R*)-4,6-dimethylhexahydro-1,3,5-trioxa-2a^1-azacyclopenta[*cd*] pentalene-4,6-diyl)bis (methylene))dicarbamate (90d)

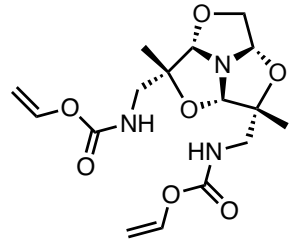

According to the synthetic protocol of **80a**, **78d** (20.0 mg, 0.0433 mmol) was converted to **90d** (12.3 mg, 58%) as a colorless amorphous.

IR (neat, cm^{-1}) 3584, 2932, 1720, 1519, 1232, 1113, 754.

^{1}H NMR (400 MHz, $CDCl_3$) δ 1.28 (s, 3H), 1.30 (s, 3H), 3.48–3.55 (m, 4H), 3.73 (dd, *J* = 2.8, 10 Hz, 1H), 4.10 (d, *J* = 10 Hz, 1H), 4.56–7.63 (m, 5H), 4.78 (s, 1H), 5.11 (d, *J* = 2.8 Hz, 1H), 5.20–5.31 (m, 6H), 5.89–5.96 (m, 2H).

^{13}C NMR (100 MHz, $CDCl_3$) δ 19.3, 19.5, 45.2 (×2), 65.8 (×2), 71.8, 84.8, 85.0, 95.0, 100.0, 101.2, 117.8, 118.0, 133.1 (×2), 156.8 (×2).

HR-MS (ESI): Calcd for $C_{18}H_{27}N_3NaO_7$ $[M+Na]^+$, 420.17467. Found, 420.17407.

Bis(2,2,2-trichloroethyl)(((2a*S*/*R*,4*S*/*R*,4a*S*/*R*,6*S*/*R*,6a*S*/*R*)-4,6-dimethylhexahydro-1,3,5-trioxa-2a^1-azacyclopenta[*cd*]pentalene-4,6-diyl)bis (methylene))dicarbamate (91a)

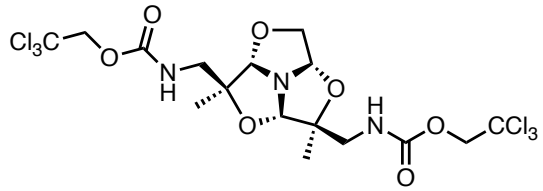

According to the synthetic protocol of **80a**, **78a** (15.0 mg, 0.0654 mmol) was converted to **91a** (32.1 mg, 53%) as a colorless amorphous.

IR (neat, cm^{-1}) 3436, 2938, 1736, 1525, 1246, 1154, 1116, 723.

^{1}H NMR (400 MHz, $CDCl_3$) δ 1.32 (s, 3H), 1.37 (s, 3H), 3.28–3.41 (m, 4H), 3.71 (dd, *J* = 2.8, 10 Hz, 1H), 4.08 (d, *J* = 10 Hz, 1H), 4.56 (s, 1H), 4.69–4.79 (m, 5H), 5.23 (d, *J* = 2.8 Hz, 1H), 5.19 (m, 2H).

^{13}C NMR (100 MHz, $CDCl_3$) δ 16.0, 16.2, 43.8, 43.9, 70.6, 73.8 (×2), 84.56, 84.61, 94.3, 94.6 (×2), 96.9, 98.4, 154.1 (×2).

HR-MS (ESI): Calcd for $C_{16}H_{21}N_3NaO_7$ $[M+Na]^+$, 599.94084. Found, 599.93934.

Bis(2,2,2-trichloroethyl)(((2a*S*/*R*,4*R*/*S*,4a*S*/*R*,6*R*/*S*,6a*S*/*R*)-4,6-dimethylhexahydro-1,3,5-trioxa-2a^1-azacyclopenta[*cd*]pentalene-4,6-diyl)bis (methylene))dicarbamate (91d)

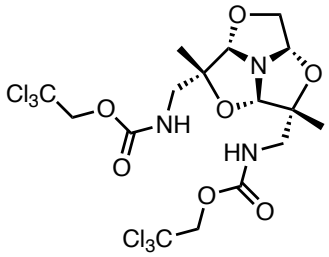

According to the synthetic protocol of **80a**, **78d** (20.0 mg, 0.0433 mmol) was converted to **91d** (29.6 mg, 63%) as a colorless amorphous.

IR (neat, cm^{-1}) 3437, 2931, 1739, 1520, 1228, 1116, 727.

^{1}H NMR (400 MHz, $CDCl_3$) δ 1.31 (s, 3H), 1.33 (s, 3H), 3.48–3.65 (m, 4H), 3.76 (dd, *J* = 2.8, 10 Hz, 1H), 4.14 (d, *J* = 10 Hz, 1H), 4.62 (s, 1H), 4.69–4.87 (m, 5H), 5.14 (d, *J* = 2.8 Hz, 1H), 5.40 (m, 1H), 5.46 (m, 1H).

^{13}C NMR (100 MHz, $CDCl_3$) δ 19.3, 19.4, 45.4 (×2), 71.8, 74.6, 74.7, 84.5, 85.1, 95.0, 95.7, 95.8, 100.1, 101.1, 155.2 (×2).

HR-MS (ESI): Calcd for $C_{16}H_{21}N_3NaO_7$ $[M+Na]^+$, 599.94084. Found, 599.93934.

Bibenzyl(((2a*S*/*R*,4*S*/*R*,4a*S*/*R*,6*S*/*R*,6a*S*/*R*)-4,6-dimethylhexahydro-1,3,5-trioxa-2a^1-azacyclopenta[*cd*] pentalene-4,6-diyl)bis (methylene))dicarbamate (92a)

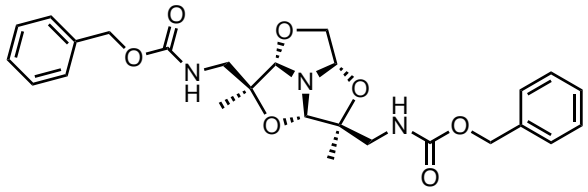

According to the synthetic protocol of **80a**, **78a** (15.0 mg, 0.0654 mmol) was converted to **92a** (33.2 mg, 99%) as a colorless amorphous.

IR (neat, cm^{-1}) 3339, 2935, 1529, 1455, 1251, 1115, 754.

^{1}H NMR (400 MHz, $CDCl_3$) δ 1.25 (s, 3H), 1.34 (s, 3H), 3.26–3.34 (m, 4H), 3.69 (dd, *J* = 2.8, 10 Hz, 1H), 4.04 (d, *J* = 10 Hz, 1H), 4.54 (s, 1H), 4.68 (s, 1H), 5.07–5.14 (m, 7H), 7.29–7.37 (m, 10H).

^{13}C NMR (100 MHz, $CDCl_3$) δ 17.0, 17.2, 44.6, 44.8, 67.1 (×2), 71.5, 85.6 (×2), 95.2, 97.8, 99.3, 128.2, 128.3 (×4), 128.4, 128.7 (×4), 136.4 (×2), 156.7 (×2).

HR-MS (ESI): Calcd for $C_{26}H_{31}N_3NaO_7$ $[M+Na]^+$, 520.20597. Found, 520.20376.

Dibenzyl(((2a*S*/*R*,4*R*/*S*,4a*S*/*R*,6*R*/*S*,6a*S*/*R*)-4,6-dimethylhexahydro-1,3,5-trioxa-2a^1-azacyclopenta[*cd*]pentalene-4,6-diyl)bis (methylene))dicarbamate (92d)

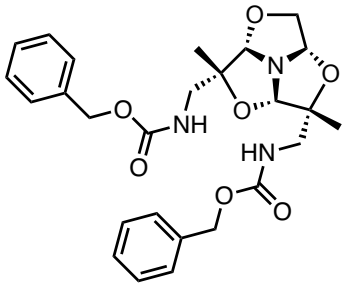

According to the synthetic protocol of **80a**, **78d** (20.0 mg, 0.0433 mmol) was converted to **92d** (18.9 mg, 88%) as a colorless amorphous.

IR (neat, cm^{-1}) 3337, 2932, 1720, 1519, 1232, 1114, 754.

^{1}H NMR (400 MHz, $CDCl_3$) δ 1.23 (s, 3H), 1.27 (s, 3H), 3.46–3.68 (m, 4H), 3.71 (dd, *J* = 2.8, 10 Hz, 1H), 4.04 (d, *J* = 10 Hz, 1H), 4.57 (s, 1H), 4.77 (s, 1H), 5.07–5.26 (m, 7H), 7.27–7.37 (m, 10H).

^{13}C NMR (100 MHz, $CDCl_3$) δ 19.4, 19.5, 45.2 (×2), 66.9, 67.0, 71.8, 84.8, 84.9, 95.0, 100.0, 101.2, 128.5 (×4), 128.6, 128.7 (×4), 136.6 (×2), 136.7, 156.9 (×2).

HR-MS (ESI): Calcd for $C_{26}H_{31}N_3NaO_7$ $[M+Na]^+$, 520.20597. Found, 520.20620.

***N*,*N*'-(((2a*S*/*R*,4*S*/*R*,4a*S*/*R*,6*S*/*R*,6a*S*/*R*)-4,6-Dimethylhexahydro-1,3,5-trioxa-2a^1-azacyclopenta[*cd*]pentalene-4,6-diyl)bis(methylene)) dimethanesulfonamide (93a)**

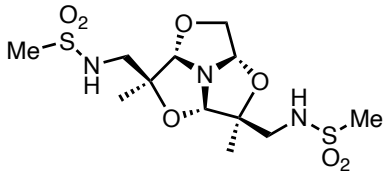

To a solution of amine **78a** (10.8 mg, 0.047 mmol) in dry pyridine (1 mL) was added methanesulfonyl chloride (0.014 mL, 0.181 mmol) and dry pyridine (1.0 mL, 12.8 mmol), and the mixture was stirred for 12 h under an argon atmosphere. The reaction mixture was poured into sat. $NaHCO_3$ aqueous solution (50 mL) and extracted with $CHCl_3$ (30 mL, 20 mL, 10 mL). The combined organic layers were dried over anhydrous Na_2SO_4 and concentrated *in vacuo*. The residue was purified by preparative TLC ($CHCl_3$/10% NH_3 in MeOH = 10/1) to obtain **93a** (5.07 mg, 28%) as a pale-yellow oil.

IR (neat, cm^{-1}) 2927, 1319, 1146, 1113, 758.

^{1}H NMR (400 MHz, $CDCl_3$) δ 1.35 (s, 3H), 1.42 (s, 3H), 3.02 (s, 3H), 3.03 (s, 3H), 3.06–3.12 (m, 2H), 3.35–3.42 (m, 2H), 3.75 (dd, *J* = 2.8, 10 Hz, 1H), 4.09 (d, *J* = 10 Hz, 1H), 4.56 (s, 1H), 4.69 (m, 1H), 4.78 (brs, 2H), 5.15 (d, *J* = 2.8 Hz, 1H).

^{13}C NMR (100 MHz, $CDCl_3$) δ 17.1, 17.4, 41.1 (×2), 46.7, 46.9, 71.7, 85.4 (×2), 95.5, 97.8, 99.3.

HR-MS (ESI): Calcd for $C_{12}H_{23}N_3NaO_7S_2$ $[M+Na]^+$, 408.08751. Found, 408.08689.

***N*,*N*'-(((2a*S*/*R*,4*R*/*S*,4a*S*/*R*,6*R*/*S*,6a*S*/*R*)-4,6-Dimethylhexahydro-1,3,5-trioxa-2a^1-azacyclopenta[*cd*]pentalene-4,6-diyl)bis(methylene)) dimethanesulfonamide (93d)**

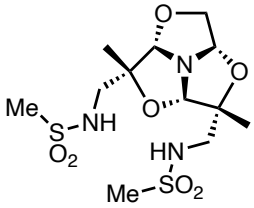

According to the synthetic protocol of **93a**, **78d** (20.0 mg, 0.0872 mmol) was converted to **93d** (11.2 mg, 33%) as a colorless amorphous.

IR (neat, cm^{-1}) 3286, 2932, 1319, 1147, 1115, 756.

^{1}H NMR (400 MHz, $CDCl_3$) δ 1.32 (s, 3H), 1.35 (s, 3H), 2.98 (s, 3H), 2.99 (s, 3H), 3.37 (dd, *J* = 6.9, 13 Hz, 1H), 3.37 (d, *J* = 6.9 Hz, 2H), 3.50 (dd, *J* = 6.9 Hz, 1H), 3.75 (dd, *J* = 2.8, 10 Hz, 1H), 4.15 (d, *J* = 10 Hz, 1H), 4.62 (s, 1H), 4.84 (s, 1H), 5.03 (t, *J* = 6.9 Hz, 1H), 5.16 (d, *J* = 2.8 Hz, 1H), 5.19 (t, *J* = 6.4 Hz, 1H).

^{13}C NMR (100 MHz, $CDCl_3$) δ 23.6, 24.4, 37.9 (×2), 52.7, 53.5, 77.5, 83.6 (×2), 93.3, 102.5, 103.0.

HR-MS (ESI): Calcd for $C_{12}H_{23}N_3NaO_7S_2$ $[M+Na]^+$, 408.08751. Found, 408.08725.

***N*,*N*'-(((2a*S*/*R*,4*S*/*R*,4a*S*/*R*,6*S*/*R*,6a*S*/*R*)-4,6-Dimethylhexahydro-1,3,5-trioxa-2a^1-azacyclopenta[*cd*]pentalene-4,6-diyl)bis(methylene)) (propane-1-sulfonamide) (94a)**

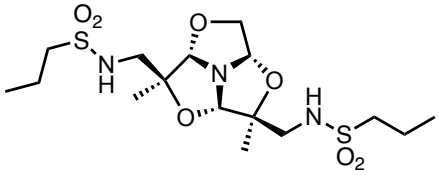

According to the synthetic protocol of **93a**, **78d** (10.0 mg, 0.0436 mmol) was converted to **94a** (8.50 mg, 44%) as a colorless amorphous.

IR (neat, cm^{-1}) 3287, 2936, 1321, 1142.

^{1}H NMR (400 MHz, $CDCl_3$) δ 1.07 (t, *J* = 6.9 Hz, 6H), 1.35 (s, 3H), 1.42 (s, 3H), 1.82–1.89 (m, 4H), 3.02–3.24 (m, 6H), 3.33 (dd, *J* = 4.1, 13 Hz, 1H), 3.34 (dd, *J* = 4.1, 13 Hz, 1H), 3.75 (dd, *J* = 2.8, 10 Hz, 1H), 4.08 (d, *J* = 10 Hz, 1H), 4.55 (s, 1H), 4.56–4.61 (m, 2H), 4.74 (s, 1H), 5.13 (d, *J* = 2.8 Hz, 1H).

^{13}C NMR (100 MHz, $CDCl_3$) δ 13.1 (×2), 17.1, 17.3, 17.5 (×2), 46.6, 46.8, 55.0, 55.1, 71.6, 85.4 (×2), 95.3, 97.6, 99.2.

HR- MS (ESI): Calcd for $C_{16}H_{31}N_3NaO_7S_2$ $[M+Na]^+$, 464.15011. Found, 464.15121.

***N*,*N*'-(((2a*S*/*R*,4*R*/*S*,4a*S*/*R*,6*R*/*S*,6a*S*/*R*)-4,6-Dimethylhexahydro-1,3,5-trioxa-2a^1-azacyclopenta[*cd*]pentalene-4,6-diyl)bis(methylene)) (propane-1-sulfonamide) (94d)**

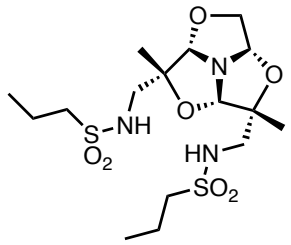

According to the synthetic protocol of **93a**, **78d** (17.0 mg, 0.0741 mmol) was converted to **94d** (10.6 mg, 32%) as a colorless amorphous.

IR (neat, cm^{-1}) 3288, 2934, 1323, 1117, 770.

^{1}H NMR (400 MHz, $CDCl_3$) δ 1.05–1.10 (m, 6H), 1.34 (s, 3H), 1.38 (s, 3H), 1.83–1.91 (m, 4H), 3.00–3.07 (m, 4H), 3.36–3.53 (m, 4H), 3.76 (dd, *J* = 2.8, 10 Hz, 1H), 4.16 (d, *J* = 10 Hz, 1H), 4.63 (s, 1H), 4.848 (s, 1H), 4.854 (m, 1H), 5.04 (m, 1H), 5.16 (d, *J* = 2.8 Hz, 1H).

^{13}C NMR (100 MHz, $CDCl_3$) δ 13.0, 13.1, 17.4, 17.5, 19.6, 19.7, 47.4, 47.7, 54.7, 55.0, 71.9, 83.9, 84.4, 95.2, 100.2, 101.5.

HR-MS (ESI): Calcd for $C_{16}H_{31}N_3NaO_7S_2$ $[M+Na]^+$, 464.15011. Found, 464.15065.

***N*,*N*'-(((2a*S*/*R*,4*S*/*R*,4a*S*/*R*,6*S*/*R*,6a*S*/*R*)-4,6-Dimethylhexahydro-1,3,5-trioxa-2a^1-azacyclopenta[*cd*]pentalene-4,6-diyl)bis(methylene)) (butane-1-sulfonamide) (95a)**

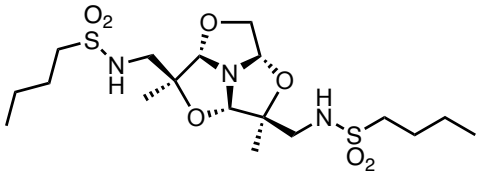

According to the synthetic protocol of **93a**, **78a** (10.0 mg, 0.0436 mmol) was converted to **95a** (11.4 mg, 56%) as a colorless amorphous.

IR (neat, cm^{-1}) 3281, 2935, 1324, 1112, 756.

^{1}H NMR (400 MHz, $CDCl_3$) δ 0.96 (t, *J* = 7.3 Hz, 3H), 0.98 (t, *J* = 7.3 Hz, 3H), 1.34 (s, 3H), 1.42 (s, 3H), 1.43–1.49 (m, 4H), 1.78–1.81 (m, 4H), 3.04–3.09 (m, 6H), 3.34 (d, *J* = 14 Hz, 1H), 3.35 (d, *J* = 14 Hz, 1H), 3.73 (brs, 1H), 3.74 (d, *J* = 2.8, 10 Hz, 1H), 4.08 (d, *J* = 10 Hz, 1H), 4.56 (s, 1H), 4.74 (brs, 1H), 4.76 (s, 1H), 5.14 (d, *J* = 2.8 Hz, 1H).

^{13}C NMR (100 MHz, $CDCl_3$) δ 13.7 (×2), 17.1, 17.4, 21.6 (×2), 25.7 (×2), 46.6, 46.8, 53.0, 53.1, 71.6, 85.5 (×2), 95.3, 97.7, 99.2.

HR-MS (ESI): Calcd for $C_{18}H_{35}N_3NaO_7S_2$ $[M+Na]^+$, 492.18141. Found, 492.18269.

***N*,*N*'-(((2a*S*/*R*,4*R*/*S*,4a*S*/*R*,6*R*/*S*,6a*S*/*R*)-4,6-Dimethylhexahydro-1,3,5-trioxa-2a^1-azacyclopenta[*cd*]pentalene-4,6-diyl)bis(methylene)) (butane-1-sulfonamide) (95d)**

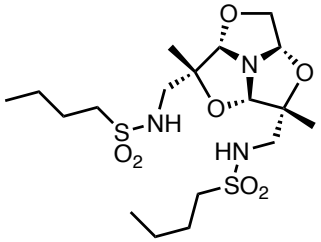

According to the synthetic protocol of **93a**, **78d** (20.0 mg, 0.0872 mmol) was converted to **95d** (16.7 mg, 41%) as a colorless amorphous.

IR (neat, cm^{-1}) 3283, 2961, 2934, 1325, 1143, 1115, 770.

^{1}H NMR (400 MHz, $CDCl_3$) δ 0.97 (m, 6H), 1.25–1.36 (m, 4H), 1.42–1.50 (m, 3H), 1.78–1.82 (m, 3H), 1.85–1.91 (m, 4H), 2.99–3.07 (m, 4H), 3.34–3.52 (m, 4H), 3.74 (dd, *J* = 2.8, 10 Hz, 1H), 4.14 (d, *J* = 10 Hz, 1H), 4.61 (s, 1H), 4.81 (m, 1H), 4.82 (s, 1H), 5.02 (m, 1H), 5.14 (d, *J* = 2.8 Hz, 1H).

^{13}C NMR (100 MHz, $CDCl_3$) δ 13.7 (×2), 19.6 (×2), 21.65, 21.70, 25.6, 25.7, 47.5, 47.7, 52.8, 53.1, 71.9, 84.0, 84.4, 95.2, 100.2, 101.5.

HR-MS (ESI): Calcd for $C_{18}H_{35}N_3NaO_7S_2$ $[M+Na]^+$, 492.18141. Found, 492.17944.

***N*,*N*'-(((2a*S*/*R*,4*S*/*R*,4a*S*/*R*,6*S*/*R*,6a*S*/*R*)-4,6-Dimethylhexahydro-1,3,5-trioxa-2a^1-azacyclopenta[*cd*]pentalene-4,6-diyl)bis(methylene)) (octane-1-sulfonamide) (96a)**

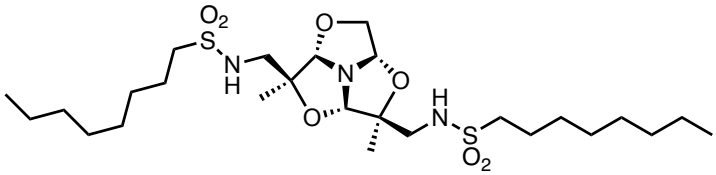

According to the synthetic protocol of **93a**, **78a** (10.0 mg, 0.0436 mmol) was converted to **96a** (6.00 mg, 28%) as a brown oil.

IR (neat, cm^{-1}) 3287, 2925, 1456, 1323, 1142, 1115.

^{1}H NMR (400 MHz, $CDCl_3$) δ 0.87 (t, *J* = 7.3 Hz, 6H), 1.26–1.40 (m, 26H), 1.78–1.81 (m, 4H), 3.02–3.06 (m, 6H), 3.34 (m, 2H), 3.74 (dd, *J* = 2.8, 10 Hz, 1H), 4.07 (d, *J* = 10 Hz, 1H), 4.45 (m, 2H), 4.54 (s, 1H), 4.72 (s, 1H), 5.11 (d, *J* = 2.8 Hz, 1H).

^{13}C NMR (100 MHz, $CDCl_3$) δ 14.2 (×2), 17.1, 17.3, 22.7 (×2), 23.8 (×2), 28.4 (×2), 29.0 (×2), 29.1 (×2), 31.8 (×2), 46.6, 46.8, 53.3, 53.4, 71.6, 85.3, 85.4, 95.3, 97.7, 99.2.

HR-MS (ESI): Calcd for $C_{26}H_{51}N_3NaO_7S_2$ $[M+Na]^+$, 604.30661. Found, 604.30730.

***N*,*N*'-(((2a*S*/*R*,4*R*/*S*,4a*S*/*R*,6a*S*/*R*)-4,6-Dimethylhexahydro-1,3,5-trioxa-2a^1-azacyclopenta[*cd*]pentalene-4,6-diyl)bis(methylene)) (octane-1-sulfonamide) (96b)**

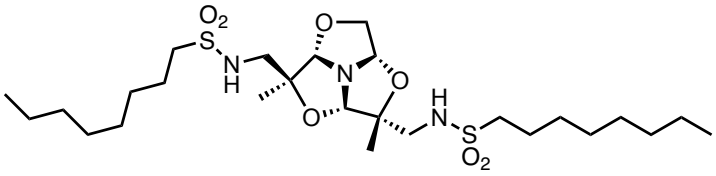

According to the synthetic protocol of **93a**, **78b** (10.0 mg, 0.0436 mmol) was converted to **96b** (8.62 mg, 36%) as a brown oil.

IR (neat, cm^{-1}) 3201, 2925, 14551, 1323, 1142, 1115, 776.

^{1}H NMR (400 MHz, $CDCl_3$) δ 0.912 (t, *J* = 7.3 Hz, 3H), 0.913 (t, *J* = 7.3 Hz, 3H),1.41 (m, 6H), 1.44–1.72 (m, 18H), 3.05–3.12 (m, 10H), 3.30–3.73 (m, 4H), 3.75 (dd, *J* = 2.8, 10 Hz, 1H), 4.11 (d, *J* = 10 Hz, 1H), 4.32 (s, 1H), 4.74 (s, 1H), 5.15–5.23 (m, 2H), 5.36 (d, *J* = 2.8 Hz, 1H).

^{13}C NMR (100 MHz, $CDCl_3$) δ 14.2 (×2), 17.1 (×2), 17.4 (×2), 22.7 (×2), 23.8 (×2), 28.4 (×2), 29.1, 29.2, 31.9 (×2), 46.7, 46.8, 53.3, 53.5, 71.6, 85.3, 85.4, 95.3, 97.8, 99.3.

HR-MS (ESI): Calcd for $C_{26}H_{51}N_3NaO_7S_2$ [M+Na]$^+$, 604.30661. Found, 604.30551.

***N*,*N*'-(((2a*S*/*R*,4*S*/*R*,4a*S*/*R*,6*R*/*S*,6a*S*/*R*)-4,6-Dimethylhexahydro-1,3,5-trioxa-2a^1-azacyclopenta[*cd*] pentalene-4,6-diyl)bis(methylene)) (octane-1-sulfonamide) (96c)**

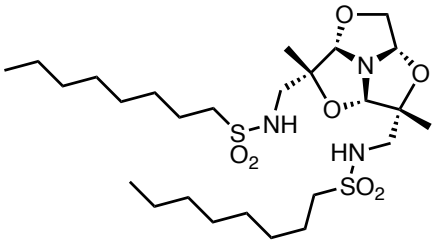

According to the synthetic protocol of **93a**, **78c** (10.0 mg, 0.0436 mmol) was converted to **96c** (8.44 mg, 34%) as a brown oil.

IR (neat, cm^{-1}) 3019, 2924, 1466, 1215, 1040, 770.

^{1}H NMR (400 MHz, $CDCl_3$) δ 0.970 (t, *J* = 7.3 Hz, 3H), 0.974 (t, *J* = 7.3 Hz, 3H),1.35 (m, 6H), 1.44–1.49 (m, 10H),1.78–1.83 (m, 10H), 3.05–3.12 (m, 8H), 3.30–3.73 (m, 4H), 3.75 (dd, *J* = 2.8, 10 Hz, 1H), 4.10 (d, *J* = 10 Hz, 1H), 4.54 (s, 1H), 4.77 (s, 1H), 5.04–5.07 (m, 2H), 5.11 (d, *J* = 2.8 Hz, 1H).

^{13}C NMR (100 MHz, $CDCl_3$) δ 14.2 (×2), 17.1 (×2), 17.4 (×2), 22.7 (×2), 23.8 (×2), 28.4 (×2), 29.1, 29.2, 31.9 (×2), 46.7, 46.8, 53.3, 53.5, 71.6, 85.3, 85.4, 95.3, 97.8, 99.3.

HR-MS (ESI): Calcd for $C_{26}H_{51}N_3NaO_7S_2$ [M+Na]$^+$, 604.30661. Found, 604.30642.

***N*,*N*'-(((2a*S*/*R*,4*R*/*S*,4a*S*/*R*,6*R*/*S*,6a*S*/*R*)-4,6-Dimethylhexahydro-1,3,5-trioxa-2a^1-azacyclopenta[*cd*]pentalene-4,6-diyl)bis(methylene)) (octane-1-sulfonamide) (96d)**

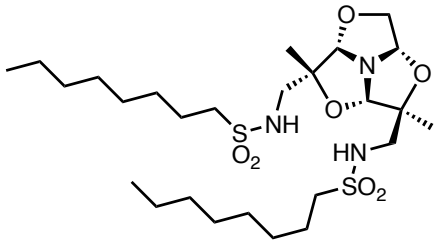

According to the synthetic protocol of **93a**, **78d** (10.0 mg, 0.0436 mmol) was converted to **96d** (5.30 mg, 21%) as a brown oil.

IR (neat, cm^{-1}) 3289, 2925, 1326, 1118.

^{1}H NMR (400 MHz, $CDCl_3$) δ 0.887 (m, 3H), 0.889 (m, 3H), 1.27–1.41 (m, 26H), 1.77–1.83 (m, 4H), 2.98–3.06 (m, 4H), 3.33–3.51 (m, 4H), 3.73 (dd, *J* = 2.8, 10 Hz, 1H), 4.13 (d, *J* = 10 Hz, 1H), 4.60 (s, 1H), 4.83 (m, 2H), 5.02 (m, 1H), 5.14 (d, *J* = 2.8 Hz, 1H).

^{13}C NMR (100 MHz, $CDCl_3$) δ 14.1 (×2), 19.3, 19.4, 22.7 (×2), 23.5 (×2), 23.7 (×2), 28.3, 28.4, 29.2, 31.8, 47.3, 47.5, 50.6 (×2), 53.0, 53.2, 71.8, 84.1, 84.4, 95.1, 99.9, 100.1.

HR-MS (ESI): Calcd for $C_{26}H_{51}N_3NaO_7S_2$ $[M+Na]^+$, 604.30661. Found, 604.30587.

***N*,*N*'-(((2a*S*/*R*,4*S*/*R*,4a*S*/*R*,6*S*/*R*,6a*S*/*R*)-4,6-Dimethylhexahydro-1,3,5-trioxa-2a^1-azacyclopenta[*cd*]pentalene-4,6-diyl)bis(methylene)) dibenzenesulfonamide (97a)**

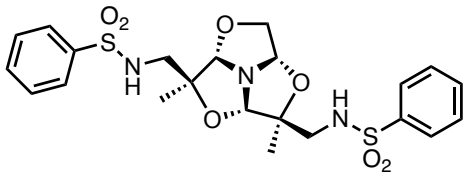

According to the synthetic protocol of **93a**, **78a** (10.0 mg, 0.0436 mmol) was converted to **97a** (3.40 mg, 15%) as a colorless amorphous.

IR (KBr, cm^{-1}) 3280, 2925, 1447, 1328, 1161, 1093, 755.

^{1}H NMR (400 MHz, $CDCl_3$) δ 1.20 (s, 3H), 1.34 (s, 3H), 2.86–3.06 (m, 4H), 3.61 (dd, *J* = 2.8, 10 Hz, 1H), 4.11 (d, *J* = 10 Hz, 1H), 4.40 (s, 1H), 4.46 (s, 1H), 4.69 (m, 1H), 4.75 (m, 1H), 4.80 (d, *J* = 2.8 Hz, 1H), 7.53–7.58 (m, 6H), 7.84–7.87 (m, 4H).

^{13}C NMR (100 MHz, $CDCl_3$) δ 19.5 (×2), 47.5, 47.7, 71.8, 84.4 (×2), 95.2, 100.0, 101.1, 127.1 (×2), 127.2 (×2), 129.2 (×2), 129.3 (×2), 132.7, 132.8, 140.2 (×2).

HR- MS (ESI): Calcd for $C_{22}H_{27}N_3NaO_7S_2$ $[M+Na]^+$, 532.11881. Found, 532.11764.

***N*,*N*'-(((2a*S*/*R*,4*R*/*S*,4a*S*/*R*,6*R*/*S*,6a*S*/*R*)-4,6-Dimethylhexahydro-1,3,5-trioxa-2a^1-azacyclopenta[*cd*]pentalene-4,6-diyl)bis(methylene)) dibenzenesulfonamide (97d)**

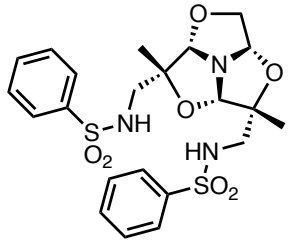

According to the synthetic protocol of **93a**, **78d** (10.0 mg, 0.0436 mmol) was converted to **97d** (6.20 mg, 28%) as a colorless amorphous.

IR (KBr, cm^{-1}) 3282, 2927, 1147, 1328, 1162, 1117, 755.

^{1}H NMR (400 MHz, $CDCl_3$) δ 1.29 (s, 3H), 1.37 (s, 3H), 3.15 (d, *J* = 7.3 Hz, 2H), 3.18 (dd, *J* = 1.4, 7.3 Hz, 2H), 3.65 (dd, *J* = 2.8, 10 Hz, 1H), 3.95 (d, *J* = 10 Hz, 1H), 4.53 (s, 1H), 4.77 (s, 1H), 4.99 (m, 1H), 5.06 (d, *J* = 2.8 Hz, 1H), 5.11 (m, 1H), 7.48–7.58 (m, 6H), 7.82–7.87 (m, 4H).

^{13}C NMR (100 MHz, $CDCl_3$) δ 19.4 (×2), 47.5, 47.7, 71.7, 84.4 (×2), 95.1, 100.0, 101.1, 127.1 (×2), 127.2 (×2), 129.2 (×2), 129.3 (×2), 132.7, 132.8, 140.2, 140.2.

HR-MS (ESI): Calcd for $C_{22}H_{27}N_3NaO_7S_2$ $[M+Na]^+$, 532.11881. Found, 532.11781.

1,1'-((2a*S*,4*S*,4a*S*,6*S*,6a*S*)-4,6-dimethylhexahydro-1,3,5-trioxa-2a^1-azacyclopenta[*cd*]pentalene-4,6-diyl)bis(*N*,*N*-dibenzylmethanamine) (99a)

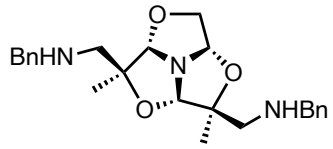

To a solution of diol **75a** (124 mg, 0.534 mmol) in dry DCM (2.5 mL) were added DIPEA (0.10 mL, 5.34 mmol), DMSO (0.760 mL, 10.7 mmol), and SO_3-py (850 mg, 5.34 mmol) then stirred at room temperature for 10 min. The reaction mixture was quenched by sat. $NaHCO_3$ aq. (20 mL) and extracted with $CHCl_3$ (50 mL, 30 mL, 20 mL). The combined organic layers were dried over anhydrous Na_2SO_4 and concentrated *in vacuo.*

To a solution of crude mixture in MeCN (2.4 mL) was added NH_2Bn (0.210 mL, 1.83 mmol), acetic acid (1 drop) and stirred at 60 ºC for 40 min. Subsequently, the mixture was added $NaBH_3CN$ (700 mg, 11.4 mmol) and stirred at same temperature. After cooling to room temperature, the reaction mixture was quenched by sat. $NaHCO_3$ aq. (20 mL) and extracted with $CHCl_3$ (100 mL, 50 mL, 20 mL). The combined organic layers were dried over anhydrous Na_2SO_4 and concentrated *in vacuo.* The residue was purified by silica gel column chromatography ($CHCl_3$/MeOH = 20/1) to obtain compound **99a** (85.6 mg, 32%, 2 steps) as a pale-yellow oil.

IR (neat, cm^{-1}) 3448, 2271, 1640, 1166, 1108.

^{1}H NMR (400 MHz, $CDCl_3$) δ 1.32 (s, 3H), 1.38 (s, 3H), 2.50–2.59 (m, 2H), 2.71–2.76 (m, 2H), 3.81 (dd, *J* = 2.8, 10 Hz, 1H), 3.91–4.01 (m, 5H), 4.56 (s, 1H), 4.61 (s, 1H), 4.95 (d, *J* = 2.8 Hz, 1H), 7.27–7.39 (m, 10H).

^{13}C NMR (100 MHz, $CDCl_3$) δ 17.6, 17.8, 53.1, 53.3, 54.30, 54.32, 71.6, 86.0, 86.2, 95.0, 98.3, 99.8, 128.2 (×2), 128.3 (×2), 128.50 (×2), 128.53 (×2), 128.9 (×2), 129.4 (×2).

HR-MS (ESI): Calcd for $C_{24}H_{29}N_3NaO_3$ $[M+Na]^+$, 432.22631. Found, 432.22628.

(2*aS/R*,4*S/R*,4*aS/R*,6*S/R*,6*aS/R*)-4,6-dimethyl-4,6-bis((4-phenyl-1H-1,2,3-triazol-1-yl)methyl)hexahydro -1,3,5-trioxa-2a^{1}-azacyclopenta[cd]pentalene (100a)

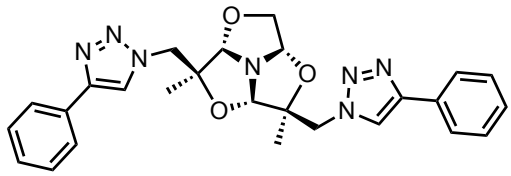

To a solution of **77a** (10.3 mg, 36.6 μmol) in dry THF (3 mL) were added phenylacetylene (20 μL, 0.183 mmol), copper iodide (74.0 mg, 0.366 mmol) and DIPEA (0.13 mL, 0.732 mmol), then stirred at 60 ºC for 12 h. After cooling to room temperature, the reaction mixture was quenched by sat. $NaHCO_3$ aq. (20 mL) and extracted with $CHCl_3$ (50 mL, 30 mL, 20 mL). The combined organic layers were dried over anhydrous Na_2SO_4 and concentrated *in vacuo.* The residue was purified by silica gel chromatography (hexane/ethyl acetate = 1/2) to give the mixture of **100a** (6.4 mg, 36%) as a colorless oil.

IR (neat, cm^{-1}) 2929, 1464, 1220, 1115, 768, 695.

^{1}H NMR (400 MHz, $CDCl_3$) δ 1.19 (s, 3H), 1.36 (s, 3H), 3.85 (dd, *J* = 3.2, 10 Hz, 1H), 4.22 (d, *J* = 10 Hz, 1H), 4.54 (m, 2H), 4.68 (s, 1H), 4.69 (d, *J* = 14 Hz, 1H), 4.80 (d, *J* = 14 Hz, 1H), 5.02 (s, 1H), 5.12 (d, *J* = 2.8 Hz, 1H).

^{13}C NMR (100 MHz, $CDCl_3$) δ 17.1, 18.4, 53.1, 53.6, 71.5, 84.5, 85.7, 95.7, 99.1, 99.4, 121.1, 121.2, 125.9, 126.0, 128.3, 129.0, 130.5, 130.7, 148.3.

HR-MS (ESI): Calcd for $C_{20}H_{35}N_3NaO_7$ $[M+Na]^+$, 508.20731. Found: 508.20882.

(2*aS/R*,4*S/R*,4*aS/R*,6*S/R*,6*aS/R*)-4,6-dimethyl-4,6-bis((4-phenyl-1H-1,2,3-triazol-1-yl)methyl)hexahydro -1,3,5-trioxa-2a^{1}-azacyclopenta[cd]pentalene (100c)

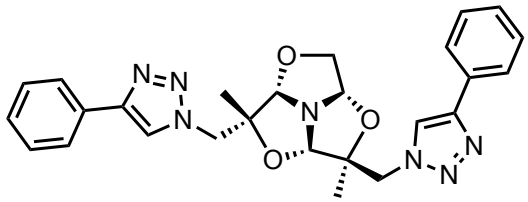

According to the synthetic protocol of **100a**, **77b** (10.0 mg, 0.0283 mmol) was converted to **100c** (5.80 mg, 38%) as a colorless oil.

IR (neat, cm^{-1}) 2929, 1484, 1383, 1119, 765.

^{1}H NMR (400 MHz, $CDCl_3$) δ 1.17 (s, 3H), 1.39 (s, 3H), 3.85 (dd, *J* = 2.8, 10.1 Hz, 1H), 4.23 (d, *J* = 10 Hz, 1H), 4.48 (d, *J* = 14 Hz, 1H), 4.55 (d, *J* = 14 Hz, 1H), 4.64 (d, *J* = 14 Hz, 1H), 4.80 (d, *J* = 14 Hz, 1H), 4.84 (s, 1H), 5.10 (s, 1H), 5.22 (d, *J* = 2.8 Hz, 1H), 7.30–7.43 (m, 2H), 7.79–7.87 (m, 4H), 7.95 (s, 6H).

^{13}C NMR (100 MHz, $CDCl_3$) δ 17.0, 18.3, 53.0, 53.6, 71.4, 84.5, 85.6, 95.6, 99.0, 99.3, 121.1, 121.2, 125.9, 126.0, 128.3, 128.4, 128.9, 129.0, 130.5, 130.6, 148.2, 148.3.

HR-MS (ESI): Calcd for $C_{26}H_{27}N_7Na_1O_3$ $[M+Na]^+$, 508.20731. Found: 508.20601.

((2*aS/R*,4*S/R*,4*aS/R*,6*S/R*,6*aS/R*)-4,6-dimethyl-4,6-bis((4-phenyl-1H-1,2,3-triazol-1-yl)methyl) hexahydro-1,3,5-trioxa-2a^{1}-azacyclopenta[cd]pentalene (100d)

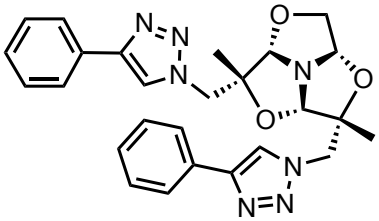

According to the synthetic protocol of **100a**, **77d** (10.5 mg, 0.0287 mmol) was converted to **100d** (22.5 mg, 70%) as a colorless oil.

IR (neat, cm^{-1}) 3137, 2905, 1610, 1464, 1387, 1121, 759.

^{1}H NMR (400 MHz, $CDCl_3$) δ 1.18 (s, 3H), 1.19 (s, 3H), 3.86 (dd, *J* = 2.8, 10 Hz, 1H), 4.29 (d, *J* = 10 Hz, 1H), 4.67–4.72- (m, 3H), 4.78 (dd, *J* = 5.0, 14 Hz, 2H), 4.85 (s, 1H), 5.18 (d, *J* = 2.8 Hz, 1H) 7.30–7.43 (m, 6H), 7.79–7.87 (m, 6H), 7.95 (s, 2H).

^{13}C NMR (100 MHz, $CDCl_3$) δ 18.3, 18.5, 53.8, 54.0, 71.9, 76.8, 84.3, 85.1, 95.4, 99.7, 100.4, 121.1, 125.8, 125.9, 128.3, 128.4, 129.0 (×2), 148.2, 148.3.

HR-MS (ESI): Calcd for $C_{26}H_{27}N_7Na_1O_3$ $[M+Na]^+$, 508.20731. Found: 508.20946.

Di-*tert*-butyl(((2a*S*/*R*,4*R*/*S*,4a*S*/*R*,6*R*/*S*,6a*S*/*R*)-4,6-Dimethylhexahydro-1,3,5-trioxa-2a^1-azacyclopenta [*cd*]pentalene-4,6-diyl)bis (methylene))bis(methylcarbamate) (98d)

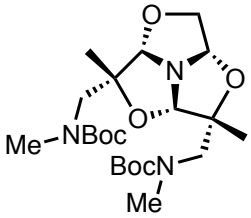

To a solution of carbamate **88d** (7.00 mg, 0.016 mmol) in dry DMF (1 mL) was added sodium hydride (0.019 g, 0.0792 mmol). After stirring for 10 min, methyl iodide (0.020 mL, 0.0326 mmol) and the mixture was stirred for 1 h under an argon atmosphere. The residue was poured into sat. $NaHCO_3$ aqueous solution (5 mL) and extracted with $CHCl_3$ (30 mL, 20 mL, 10 mL). The combined organic layers were dried over anhydrous Na_2SO_4 and concentrated *in vacuo*. The residue was purified by silica gel column chromatography (hexane/EtOAc = 1/1 to 1/2) to obtain **98d** (6.70 mg, 90%) as a colorless oil.

IR (neat, cm^{-1}) 2978, 2931, 1695, 1159, 756.

^{1}H NMR (400 MHz, $CDCl_3$) δ 1.23 (s, 3H), 1.26 (s, 3H),1.41 (s, 18H), 2.93 (s, 6H), 3.08–3.21 (m, 2H), 3.46–3.70 (m, 3H), 4.07 (d, *J* = 10 Hz, 1H), 4.84 (m, 1H), 4.94 (m, 1H), 5.08 (d, *J* = 2.8 Hz, 1H).

^{13}C NMR (100 MHz, $CDCl_3$) δ 19.1, 20.4, 29.6 (×3), 29.8 (×3), 43.7, 44.1, 50.1, 50.4, 71.9, 84.4, 85.1, 94.8, 100.5, 101.3, 157.9, 158.9.

HR-MS (ESI), Calcd for $C_{20}H_{37}N_5NaO_5$ $[M+Na]^+$, 427.28623. Found, 427.28412.

***N*,*N*'-(((2a*S*/*R*,4*R*/*S*,4a*S*/*R*,6*R*/*S*,6a*S*/*R*)-4,6-Dimethylhexahydro-1,3,5-trioxa-2a1-azacyclopenta[*cd*]pentalene-4,6-diyl)bis(methylene)) bis(*N*-methyloctane-1-sulfonamide) (99d)**

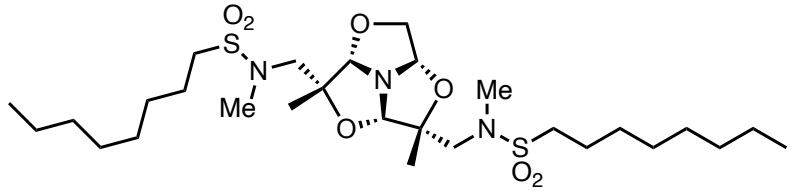

According to the synthetic protocol of **98d**, **96d** (30 mg, 0.152 mmol) was converted to **99d** (41 mg, 86%) as a colorless amorphous.

IR (neat, cm^{-1}) 3289, 2925, 1326, 1118.

^1H NMR (400 MHz, $CDCl_3$) δ 0.88 (m, 6H), 1.27–1.41 (m, 22H), 1.77–1.83 (m, 4H), 2.98–3.06 (m, 12H), 3.33–3.51 (m, 4H), 3.73 (dd, *J* = 2.8, 10 Hz, 1H), 4.13 (d, *J* = 10 Hz, 1H), 4.60 (s, 1H), 4.83 (m, 2H), 5.02 (m, 1H), 5.14 (d, *J* = 2.8 Hz, 1H).

^{13}C NMR (100 MHz, $CDCl_3$) δ 14.1 (×2), 18.6, 18.7, 23.5, 24.2, 25.4 (×2), 29.1(×2), 29.3 (×2), 31.6, 36.4 (×2), 47.1, 47.5, 51.3, 52.6, 70.3, 75.8, 76.1, 77.3, 80.5, 82.2, 90.3, 100.0, 101.3.

HR-MS (ESI): Calcd for $C_{28}H_{55}N_3NaO_7$ $[M+Na]^+$, 609.35631. Found, 609.35656.

1,1'-(((2a*S*/*R*,4*R*/*S*,4a*S*/*R*,6*R*/*S*,6a*S*/*R*)-4,6-Dimethylhexahydro-1,3,5-trioxa-2a^1-azacyclopenta[*cd*] pentalene-4,6-diyl)bis(methylene)) bis(3-(*tert*-butyl)urea) (101d)

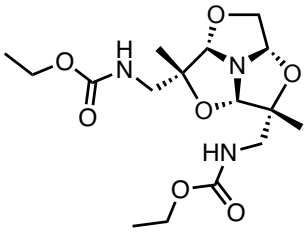

To a solution of amine **78d** (20.0 mg, 0.087 mmol) in THF (0.2 mL) was added *tert*-butyl isocyanate (0.12 mL, 0.872 mmol) and the mixture was stirred for 16 h under an argon atmosphere. The reaction mixture was concentrated *in vacuo*, and the residue was purified by preparative TLC ($CHCl_3$/MeOH = 10/1) to obtain **101d** (36.2 mg, 97%) as a colorless amorphous.

IR (KBr, cm^{-1}) 3360, 2979, 2932, 1712, 1515, 1455, 1392, 1367, 1155.

^{1}H NMR (400 MHz, $CDCl_3$) δ 1.22 (s, 3H), 1.24 (s, 3H), 1.31 (s, 9H), 1.32 (s, 9H), 3.23 (dd, *J* = 6.4, 14 Hz, 1H), 3.28 (dd, *J* = 6.4, 14 Hz, 1H), 3.59 (dd, *J* = 10, 14 Hz, 1H), 3.70 (dd, *J* = 2.8, 10 Hz, 1H), 3.76 (dd, *J* = 2.8, 6.4 Hz, 1H), 4.11 (d, *J* = 10 Hz, 1H), 4.55 (s, 1H), 4.74 (s, 1H), 5.00 (m, 1H), 5.11 (d, *J* = 2.8 Hz, 1H), 5.32 (m, 1H).

^{13}C NMR (100 MHz, $CDCl_3$) δ 19.1, 20.4, 29.6, 29.7, 29.8, 43.7, 44.1, 50.1, 50.5, 71.9, 84.4, 85.0, 94.8, 100.5, 101.3, 157.9, 158.9.

HR- MS (ESI) Calcd for $C_{20}H_{35}N_3NaO_7$ $[M+Na]^+$, 452.2373. Found, 452.2357.

Diethyl (((2a*S*,4*R*,4a*S*,6*R*,6a*S*)-4,6-dimethylhexahydro-1,3,5-trioxa-2a^1-azacyclopenta[*cd*]pentalene-4,6-diyl)bis(methylene))dicarbamate (102d)

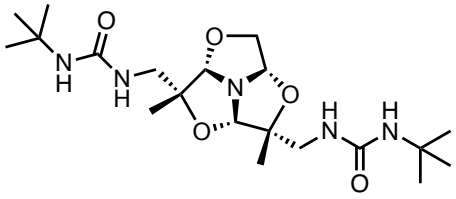

According to the synthetic protocol of **80a**, **78d** (25.0 mg, 0.0859 mmol) was converted to **102d** (29.4 mg, 92%) as a colorless oil.

IR (neat, cm^{-1}) 3338, 2968, 2876, 1720, 1533, 1240, 1115.

^{1}H NMR (400 MHz, $CDCl_3$) δ 1.21 (s, 3H), 1.22 (s, 3H), 1.25 (s, 6H), 3.40–3.68 (m, 4H), 3.71 (dd, *J* = 2.8, 10 Hz, 1H), 4.07–4.12 (m, 5H), 4.56 (s, 1H), 4.77 (s, 1H), 4.56 (m, 1H), 4.57 (m, 1H), 5.09 (d, *J* = 2.8 Hz, 1H), 5.12 (m, 1H).

^{13}C NMR (100 MHz, $CDCl_3$) δ 14.7 (×2), 19.2, 19.4, 45.0, 45.8, 61.0 (×2), 71.8, 84.8, 84.9, 95.0, 100.0, 101.2, 157.2 (×2).

HR-MS (ESI): Calcd for $C_{16}H_{27}N_3NaO_7$ $[M+Na]^+$, 396.17597. Found, 396.17542.

Dipropyl (((2a*S*,4*R*,4a*S*,6*R*,6a*S*)-4,6-dimethylhexahydro-1,3,5-trioxa-2a^1-azacyclopenta[*cd*]pentalene-4,6-diyl)bis(methylene))dicarbamate (103d)

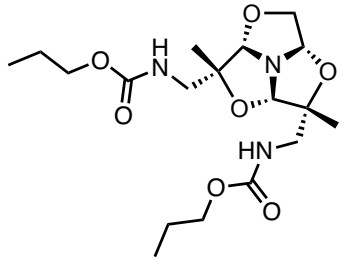

According to the synthetic protocol of **80a**, **78d** (36.0 mg, 0.143 mmol) was converted to **103d** (13.9 mg, 41%) as a colorless oil.

IR (neat, cm^{-1}) 3335, 2968, 2936, 1714, 1537, 1241, 1115.

^{1}H NMR (400 MHz, $CDCl_3$) δ 0.92 (t, *J* = 7.3 Hz, 6H), 1.27 (s, 6H), 1.61–1.66 (m, 4H), 3.47–3.71 (m, 4H), 3.73 (dd, *J* = 2.8, 10 Hz, 1H), 4.00–4.02 (m, 4H), 4.08 (d, 10 Hz, 1H), 4.58 (s, 1H), 4.77 (s, 1H), 5.01 (m, 1H), 5.10 (d, *J* = 2.8 Hz, 1H), 5.11 (m, 1H).

^{13}C NMR (100 MHz, $CDCl_3$) δ 10.5 (×2), 19.3, 19.5, 22.5, 45.0 (×2), 66.7 (×2), 71.8, 84.9, 85.1, 95.0, 100.0, 101.2, 157.4 (×2).

HR-MS (ESI): Calcd for $C_{18}H_{31}N_3NaO_7$ $[M+Na]^+$, 424.20597. Found, 424.20440.

Dibutyl (((2a*S*,4*R*,4a*S*,6*R*,6a*S*)-4,6-dimethylhexahydro-1,3,5-trioxa-2a^1-azacyclopenta[*cd*]pentalene-4,6-diyl)bis(methylene))dicarbamate (104d)

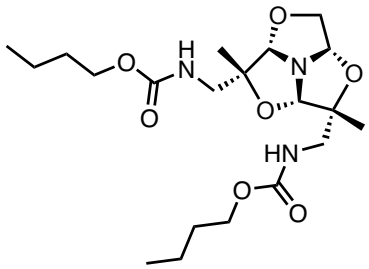

According to the synthetic protocol of **80a**, **78d** (22.0 mg, 0.0868 mmol) was converted to **104d** (27.0 mg, 73%) as a colorless oil.

IR (neat, cm^{-1}) 3338, 2959, 2934, 1721, 1530, 1242, 1115.

^{1}H NMR (400 MHz, $CDCl_3$) δ 0.89 (t, *J* = 7.3 Hz, 6H), 1.25 (s, 6H), 1.25–1.38 (m, 4H), 1.53–1.61 (m, 4H), 3.45–3.51 (m, 4H), 3.71 (dd, *J* = 2.8, 10 Hz, 1H), 4.04–4.06 (m, 5H), 4.56 (s, 1H), 4.76 (s, 1H), 5.00 (m, 1H), 5.085(d, *J* = 2.8 Hz, 1H), 5.092 (m, 1H).

^{13}C NMR (100 MHz, $CDCl_3$) δ 13.8, 19.2 (×2), 19.3, 19.4, 31.2 (×2), 45.0 (×2), 64.9, 65.0, 71.8, 84.8, 85.0, 95.0, 100.0, 101.2, 157.3 (×2).

HR-MS (ESI): Calcd for $C_{20}H_{35}N_3NaO_7$ $[M+Na]^+$, 452.23727. Found, 452.23532.

Di-isopropyl (((2a*S*,4*R*,4a*S*,6*R*,6a*S*)-4,6-dimethylhexahydro-1,3,5-trioxa-2a^1-azacyclopenta[*cd*] pentalene-4,6-diyl)bis(methylene))dicarbamate (105d)

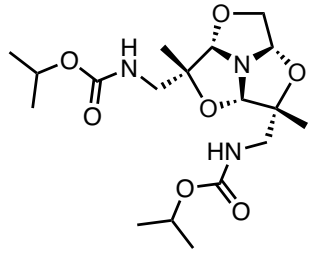

According to the synthetic protocol of **80a**, **78d** (22.5 mg, 0.0911 mmol) was converted to **105d** (4.7 mg, 40%) as a colorless oil.

IR (neat, cm^{-1}) 3339, 2979, 2934, 1713, 1531, 1247, 1112.

^{1}H NMR (400 MHz, $CDCl_3$) δ 1.21 (s, 6H), 1.23 (s, 6H), 1.27 (s, 6H), 3.47–3.55 (m, 4H), 3.73 (dd, *J* = 2.8, 10 Hz, 1H), 4.09 (d, 10 Hz, 1H), 4.58 (s, 1H), 4.78 (s, 1H), 4.87–4.93 (m, 3H), 5.03 (m, 1H), 5.10 (d, *J* = 2.8 Hz, 1H).

^{13}C NMR (100 MHz, $CDCl_3$) δ 19.3 (×2), 22.3 (×4), 45.0 (×2), 68.3 (×2), 71.8, 84.9, 85.1, 95.0, 100.0, 101.2, 156.8 (×2).

HR-MS (ESI): Calcd for $C_{18}H_{31}N_3NaO_7$ $[M+Na]^+$, 424.20597. Found, 424.20404.

Di-isobutyl (((2a*S*,4*R*,4a*S*,6*R*,6a*S*)-4,6-dimethylhexahydro-1,3,5-trioxa-2a^1-azacyclopenta[*cd*]pentalene-4,6-diyl)bis(methylene))dicarbamate (106d)

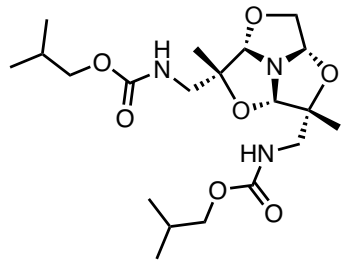

According to the synthetic protocol of **80a**, **78d** (26.7 mg, 0.0152 mmol) was converted to **106d** (4.1 mg, 63%) as a colorless oil.

IR (neat, cm^{-1}) 3342, 2961, 2935, 1714, 1520, 1238, 1115.

^{1}H NMR (400 MHz, $CDCl_3$) δ 0.87 (s, 6H), 0.88 (s, 6H), 0.93 (s, 6H), 1.89–1.94 (m, 2H), 3.47–3.53 (m, 4H), 3.75 (dd, *J* = 2.8, 10 Hz, 1H), 3.83–3.89 (m, 4H), 4.10 (d, *J* = 10 Hz, 1H), 4.59 (s, 1H), 4.80 (s, 1H), 5.03 (m, 2H), 5.12 (d, *J* = 2.8 Hz, 1H).

Di-neopentyl (((2a*S*,4*R*,4a*S*,6*R*,6a*S*)-4,6-dimethylhexahydro-1,3,5-trioxa-2a^1-azacyclopenta [*cd*]pentalene-4,6-diyl)bis(methylene))dicarbamate (107d)

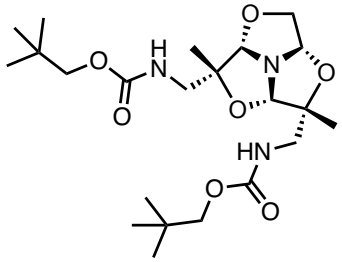

According to the synthetic protocol of **80a**, **78d** (26.7 mg, 0.0152 mmol) was converted to **107d** (4.1 mg, 63%) as a colorless oil.

IR (neat, cm^{-1}) 3336, 2958, 2870, 1713, 1519, 1236, 1116.

^{1}H NMR (400 MHz, $CDCl_3$) δ 0.93 (s, 18H), 1.23 (s, 6H), 3.48–3.53 (m, 4H), 3.75–3.85 (m, 5H), 4.11 (d, *J* = 10 Hz, 1H), 4.59 (s, 1H), 4.80 (s, 1H), 5.07–5.09 (m, 2H), 5.12 (d, *J* = 2.8 Hz, 1H).

^{13}C NMR (100 MHz, $CDCl_3$) δ 19.2, 29.4, 26.4 (×3), 26.5 (×3), 31.7 (×2), 45.1 (×2), 71.9, 74.4, 74.5, 84.9, 85.3, 94.9, 100.0, 101.1, 157.5 (×2).

HR-MS (ESI): Calcd for $C_{22}H_{39}N_3NaO_7$ $[M+Na]^+$, 480.26857. Found, 480.26666.

Diphenyl (((2a*S*,4*R*,4a*S*,6*R*,6a*S*)-4,6-dimethylhexahydro-1,3,5-trioxa-2a^1-azacyclopenta[*cd*]pentalene-4,6-diyl)bis(methylene))dicarbamate (108d)

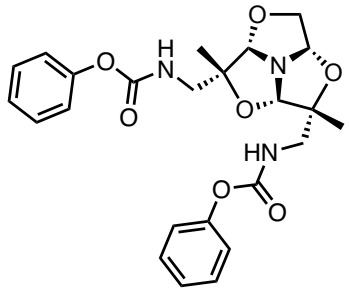

According to the synthetic protocol of **80a**, **78d** (28.5 mg, 0.113 mmol) was converted to **108d** (6.2 mg, 52%) as a pale-yellow oil.

IR (neat, cm^{-1}) 3434, 3345, 2925, 2856, 1739, 1492, 1206, 1116.

^{1}H NMR (400 MHz, $CDCl_3$) δ 1.35 (s, 6H), 3.48–3.69 (m, 4H), 3.80 (dd, *J* = 2.8, 10 Hz, 1H), 4.18 (d, *J* = 10 Hz, 1H), 4.67 (s, 1H), 4.88 (s, 1H), 5.18 (d, *J* = 2.8 Hz, 1H), 5.47 (m, 1H), 5.58 (m, 1H), 7.01–7.11 (m, 4H), 7.12–7.19 (m, 2H), 7.32–7.36 (m, 4H).

^{13}C NMR (100 MHz, $CDCl_3$) δ 19.5, 19.6, 45.4 (×2), 71.9, 84.8, 84.9, 95.0, 100.1, 101.4, 121.7 (×4), 125.4 (×2), 129.40 (×2), 129.43 (×2), 151.2 (×2), 155.3 (×2).

HR-MS (ESI): Calcd for $C_{24}H_{27}N_3NaO_7$ $[M+Na]^+$, 492.17467. Found, 492.17274.

***N*,*N*'-(((2a*S*,4*R*,4a*S*,6*R*,6a*S*)-4,6-dimethylhexahydro-1,3,5-trioxa-2a^1-azacyclopenta[*cd*]pentalene-4,6-diyl)bis(methylene))dipropionamide (109d)**

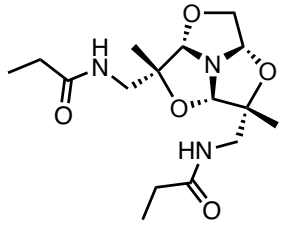

According to the synthetic protocol of **80a**, **78d** (10.0 mg, 0.0283 mmol) was converted to **109d** (2.05 mg, 21%) as a colorless oil.

IR (neat, cm^{-1}) 3300, 2937, 1651, 1555, 1113. ^1H NMR (400 MHz, $CDCl_3$): δ 1.19 (t×2, *J* = 7.3 Hz, 6H), 1.28 (s, 3H), 1.34 (s, 3H), 2.26 (q×2, *J* = 7.3 Hz, 4H), 2.28 (dd, *J* = 4.6, 14 Hz, 1H), 3.33 (dd, *J* = 4.6, 14 Hz, 1H), 3.47 (dd, *J* = 8.2, 14 Hz, 1H), 3.57 (dd, *J* = 8.2, 14 Hz, 1H), 3.73 (dd, *J* = 2.8, 10 Hz, 1H), 4.07 (d, *J* = 10 Hz, 1H), 4.57 (s, 1H), 4.73 (s, 1H), 5.12 (d, *J* = 2.8 Hz, 1H), 5.65 (m, 2H).

^{13}C NMR (100 MHz, $CDCl_3$): δ 10.0 (×2), 17.1, 17.3, 29.9 (×2), 42.8, 42.9, 71.5, 85.7(×2), 95.3, 98.1, 99.5, 174.3 (×2).

HR-MS (ESI): Calcd for $C_{16}H_{27}N_3NaO_5$ $[M+Na]^+$, 364.18484. Found, 364.18305.

***N*,*N*'-(((2a*S*,4*R*,4a*S*,6*R*,6a*S*)-4,6-dimethylhexahydro-1,3,5-trioxa-2a^1-azacyclopenta[*cd*]pentalene-4,6-diyl)bis(methylene))dipropionamide (110d)**

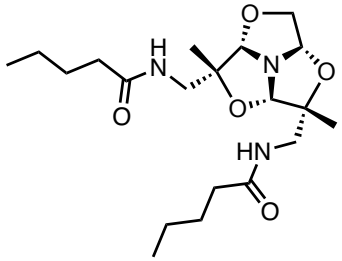

According to the synthetic protocol of **80a**, **78d** (10.0 mg, 0.0283 mmol) was converted to **110d** (5.10 mg, 30%) as a colorless oil.

IR (neat, cm^{-1}) 3307, 2931, 1651, 1554, 1114.

^{1}H NMR (400 MHz, $CDCl_3$): δ 0.93 (t×2, *J* = 7.3 Hz, 6H), 1.27 (s, 3H), 1.35 (m, 7H), 1.64 (m, 4H), 2.23 (t×2, *J* = 7.3 Hz, 4H), 3.28 (dd, *J* = 4.1, 14 Hz, 1H), 3.31 (dd, *J* = 4.1, 1 Hz, 1H), 3.47 (dd, *J* = 8.2, 14 Hz, 1H), 3.56 (dd, *J* = 8.2, 14 Hz, 1H), 3.72 (dd, *J* = 2.8, 10 Hz, 1H), 4.07 (d, *J* = 10 Hz, 1H), 4.57 (s, 1H), 4.72 (s, 1H), 5.11 (d, *J* = 2.8 Hz, 1H), 5.65 (m, 2H).

^{13}C NMR (100 MHz, $CDCl_3$): δ 13.9 (×2), 17.1, 17.3, 22.5 (×2), 27.9 (×2), 36.7 (×2), 42.7, 42.8, 71.5, 85.7, 85.7, 95.2, 98.0, 99.5, 173.6 (×2).

HR-MS (ESI): Calcd for $C_{20}H_{35}N_3NaO_5$ $[M+Na]^+$, 420.24744. Found, 420.24759.

***N*,*N*'-(((2a*S*,4*R*,4a*S*,6*R*,6a*S*)-4,6-dimethylhexahydro-1,3,5-trioxa-2a^1-azacyclopenta[*cd*]pentalene-4,6-diyl)bis(methylene))dioctanamide (111d)**

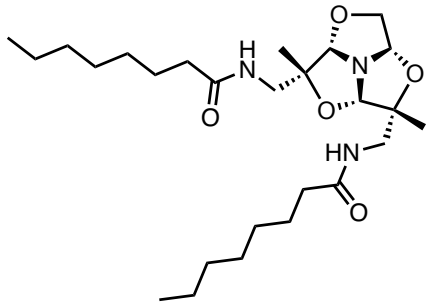

According to the synthetic protocol of **80a**, **78d** (10.0 mg, 0.0283 mmol) was converted to **111d** (18.3 mg, 98%) as a colorless oil.

IR (neat, cm^{-1}) 3306, 2926, 2856, 1651, 1555, 1115.

^{1}H NMR (400 MHz, $CDCl_3$) δ 0.88 (t×2, *J* = 7.6 Hz, 6H), 1.29 (m, 26H), 2.22 (m, 4H), 1.64 (m, 4H), 2.23 (t×2, *J* = 7.6 Hz, 4H), 3.28 (dd, *J* = 4.1, 14 Hz, 1H), 3.30 (dd, *J* = 4.1, 14 Hz, 1H), 3.47 (dd, *J* = 7.3, 14 Hz, 1H), 3.55 (dd, *J* = 7.8, 14 Hz, 1H), 3.72 (dd, *J* = 2.8, 10 Hz, 1H), 4.07 (d, *J* = 10 Hz, 1H), 4.57 (s, 1H), 4.73 (s, 1H), 5.12 (d, *J* = 2.8 Hz, 1H), 5.69 (m, 2H).

^{13}C NMR (100 MHz, $CDCl_3$) δ 14.2 (×2), 17.0 (×2), 17.3 (×2), 22.7 (×2), 26.0 (×2), 29.2, 29.5, 31.9 (×2), 37.1 (×2), 42.8, 43.0, 71.7, 85.9, 85.9, 95.3, 98.1, 99.6, 173.8 (×2).

HR-MS (ESI): Calcd for $C_{26}H_{47}N_3NaO_5$ $[M+Na]^+$, 504.34134. Found, 504.33920.

(*R*)-(2-Methyloxiran-2-yl)methanol ((*R*)-112)

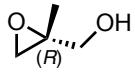

To a solution of activated MS 4A (10 g) in dry DCM (200 mL) were added $Ti(O^iPr)_4$ (8.6 mL, 45 mmol) and D-DIPT (11.3 mL, 54 mmol) at –20 ºC and the mixture was stirred for 10 min under an argon atmosphere. Then, β-metallyl alcohol (**113**, 22.5 mL, 0.45 mol) and cumene hydroperoxide (100 mL, 0.68 mmol) were added to a reaction mixture. After stirring for 19 h, a reaction mixture was diluted by Et_2O (120 mL) and added sat. Na_2SO_4 aqueous solution. (12 mL). After warming to room temperature and stirring for 3 h, the reaction mixture was filtered with Celite and concentrated *in vacuo*. The residue was purified by silica gel column chromatography (Petane/Et_2O = 1/1) and vacuum distillation (2 mmHg, 80 ºC) to obtain (*R*)-**112** (17.8 g, 45%) as a colorless oil.

IR (neat, cm^{-1}): 3407, 2930, 1045.

^1H NMR (400 MHz, $CDCl_3$) δ 1.35 (s, 3H), 2.27 (brs, 1H), 2.65 (d, *J* = 5.0 Hz, 1H), 2.91 (d, *J* = 5.0 Hz, 1H), 3.62 (d, *J* = 12 Hz, 1H), 3.71 (d, *J* = 12 Hz, 1H).

^{13}C NMR (100 MHz, $CDCl_3$) δ 18.2, 51.2, 57.4, 64.3.

HR-MS (ESI): Calcd for $C_4H_8Na_1O_2$ $[M+Na]^+$, 111.04220. Found, 111.04566.

$[\alpha]_{589}^{20}$ = +7.80 (c = 1.24, $CHCl_3$).

(*S*)-(2-methyloxiran-2-yl)methyl 4-nitrobenzoate ((*S*)-115)

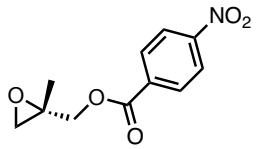

To a crude solution of activated MS 4A (3.5 g) in dry DCM (200 mL) were added $Ti(O^iPr)_4$ (1.9 mL, 10 mmol) and D-DIPT (2.5 mL, 12 mmol) at –20 ºC and the mixture was stirred for 10 min under an argon atmosphere. Then, β-metallyl alcohol (**113**, 5.0 mL, 0.10 mol) and cumene hydroperoxide (37 mL, 0.20 mmol) were added to a reaction mixture. After stirring for 6 h, a reaction mixture was added $P(OMe)_3$ (18 mL, 15 mmol) dropwise and stirred at –20 ºC for 1 h. After warming to room temperature, the mixture was added Et_3N (17 mL, 12 mmol) and 4-nitrobenzoyl chloride (18.6 g, 12 mmol). After stirring for 1 h, the reaction mixture was filtered with Celite and washed with 10%-Rochelle salt (Potassium sodium tartrate) aqueous solution (100 mL×2), sat. $NaHCO_3$ aqueous solution (100 mL×2) and brine (100 mL×2). The combined organic layers were dried over anhydrous Na_2SO_4 and concentrated *in vacuo*. The residue was purified by recrystallization and PTLC (DCM) to obtain (*S*)-**115** (11.8 g, 50%) as a colorless oil.

IR (neat, cm^{-1}): 3422, 1718, 1525, 1301, 1126, 718.

^1H NMR (400 MHz, $CDCl_3$) δ 1.50 (s, 3H), 2.77 (d, *J* = 4.6 Hz, 1H), 2.88 (d, *J* = 4.6 Hz, 1H), 4.25 (d, *J* = 12 Hz, 1H), 4.59 (d, *J* = 12 Hz, 1H), 8.23–8.26 (m, 2H), 8.30–8.32 (m, 2H).

^{13}C NMR (100 MHz, $CDCl_3$) δ 18.5, 51.9, 54.8, 68.6, 123.7 (×2), 130.9 (×2), 135.2, 150.7, 164.3.

HR-MS (ESI): Calcd for $C_{11}H_{12}N_1O_5$ $[M+H]^+$, 238.07155. Found, 238.07247.

((*S*)-2-Methyloxiran-2-yl)methyl (*S*)-3,3,3-trifluoro-2-methoxy-2-phenylpropanoate ((*S*)-116)

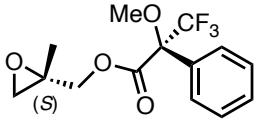

To a solution of epoxyalcohol (*R*)-**112** (40.0 mg, 0.055 mmol) in dry DMF (0.5 mL) were added (*S*)-(+)-MTPA chloride (42 μL, 0.227 mmol) and dry pyridine (35 μL, 12.8 mmol), and the mixture was stirred for 3.5 h under an argon atmosphere. The reaction mixture was poured into water (5 mL), concentrated *in vacuo*, and extracted with $CHCl_3$ (20 mL, 10 mL, 5 mL). The combined organic layers were dried over anhydrous Na_2SO_4 and concentrated *in vacuo*. The residue was purified by silica gel column chromatography ($CHCl_3$/MeOH = 100/1 to 50/1 and hexane EtOAc = 100/0 to 50/1) to obtain (*S*)-**116** (17.2 mg, 94%) as a colorless solid.

IR (neat, cm^{-1}): 2953, 1753, 1452, 1272, 1170, 1022.

^1H NMR (400 MHz, $CDCl_3$): δ 1.40 (s, 1.5H), 1.37 (s, 1.5H), 2.65–2.67 (m, 1H), 2.75 (d, *J* = 4.6 Hz, 0.5H), 2.78 (d, *J* = 4.6 Hz, 0.5H), 3.56 (s, 3H), 4.17 (d, *J* = 12 Hz, 0.5H), 4.24 (d, *J* = 12 Hz, 0.5H), 4.47 (d, *J* = 12 Hz, 0.5H), 4.50 (d, *J* = 12 Hz, 0.5H), 7.41–7.53 (m, 5H).

^{13}C NMR (100 MHz, $CDCl_3$) δ 18.3, 18.5, 51.7, 51.8, 54.5, 55.6, 68.3, 68.9, 127.5, 127.9, 128.6 (×2), 129.8, 132.1, 166.4.

HR-MS (ESI): Calcd for $C_{14}H_{15}F_3NaO_4$ $[M+Na]^+$, 327.08201. Found, 327.08321.

$[\alpha]_{589}^{20}$ = +7.80 (c = 1.24, $CHCl_3$).

(2-Methyloxiran-2-yl)methanol ((±)-112)

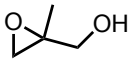

To a solution of β-metallyl alcohol **113** (5.00 mL, 48.5 mmol) in dry DCM (50 mL) was added *m*CPBA (16.7 g, 97.0 mmol) and stirred for 22 h under an argon atmosphere. A reaction mixture was poured into sat. Na_2SO_4 aqueous solution (12 mL). After warming to room temperature and stirring for 3 h, the reaction mixture was filtered with Celite and concentrated *in vacuo*. The residue was purified by silica gel column chromatography (Petane/Et_2O = 2/1 to 1/1) to obtain (±)-**112** (2.27 g, 35%) as a colorless oil.

IR (neat, cm^{-1}) 3407, 2930, 1045.

^1H NMR (400 MHz, $CDCl_3$) δ 1.37 (s, 3H), 2.27 (brs, 1H), 2.66 (d, *J* = 5.0 Hz, 1H), 2.92 (d, *J* = 5.0 Hz, 1H), 3.60 (d, *J* = 12 Hz, 1H), 3.73 (d, *J* = 12 Hz, 1H).

^{13}C NMR (100 MHz, $CDCl_3$) δ 18.2, 51.2, 57.4, 64.3.

HR-MS (ESI): Calcd for $C_4H_8NaO_2$ $[M+Na]^+$, 111.04220. Found, 111.04566.

(2-Methyloxiran-2-yl)methyl (2S)-3,3,3-trifluoro-2-methoxy-2-phenylpropanoate ((±)-116)

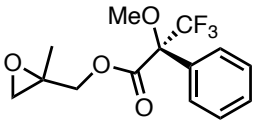

According to the synthetic protocol of (*S*)-**116**, (±)-**112** (20.0 mg, 0.227 mmol) was converted to (±)-**116** (66.8 mg, 97%) as a colorless oil.

IR (neat, cm^{-1}) 2952, 1753, 1495, 1452, 1272, 1171, 1023.

^1H NMR (400 MHz, $CDCl_3$) δ1.37 (s, 3H), 2.65–2.67 (m, 1H), 2.78 (d, *J* = 4.6 Hz, 1H), 3.56 (s, 3H), 4.24 (d, *J* = 12 Hz, 1H), 4.50 (d, *J* = 12 Hz, 1H), 7.41–7.53 (m, 5H).

^{13}C NMR (100 MHz, $CDCl_3$) δ 18.3, 18.5 (×2), 51.7, 51.9, 54.5, 55.6, 68.3, 68.9, 127.4, 128.6, 129.8, 132.0, 166.3.

HR-MS (ESI): Calcd for $C_{14}H_{15}F_3NaO_4$ $[M+Na]^+$, 327.08201. Found, 327.08169.

(*R*)-3-(Benzyloxy)-2-methylpropane-1,2-diol ((*R*)-117)

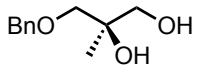

To a solution of alcohol (*R*)-**112** (5.00 g, 56.7 mmol) in a sealed tube were added benzyl alcohol (7.0 mL, 68.1 mmol) and cesium fluoride (172 mg, 1.13 mmol), and the mixture was stirred at 120 ºC for 22 h under an argon atmosphere. After cooling to room temperature, the residue was poured into water (50 mL) and extracted with EtOAc (100 mL, 50 mL, 30 mL). The combined organic layers were dried over anhydrous Na_2SO_4 and concentrated *in vacuo*. The residue was purified by silica gel column chromatography (hexane/EtOAc = 2/1 to 1/2) to obtain (*R*)-**117** (9.34 g, 84%) as pale-yellow oil.

IR (neat, cm^{-1}): 3397, 2866, 1454, 1099, 1054.

^1H NMR (400 MHz, $CDCl_3$) δ 1.15 (s, 3H), 2.34 (brs, 1H), 2.80 (brs, 1H), 3.43 (d, *J* = 8.7 Hz, 1H), 3.47 (dd, *J* = 4.6, 10 Hz, 1H), 3.52 (d, *J* = 8.7 Hz, 1H), 3.66 (dd, *J* = 4.6, 10 Hz, 1H), 4.56 (d, *J* = 13, 1H), 4.57 (d, *J* = 13, 1H), 7.31–7.39 (m, 5H).

^{13}C NMR (100 MHz, $CDCl_3$) δ 21.4, 68.8, 72.0, 73.9, 76.4, 127.8 (×2), 128.1, 128.7 (×2), 137.8.

HR-MS (ESI): Calcd for $C_{11}H_{16}NaO_3$ $[M+Na]^+$, 219.09971. Found, 219.09940.

$[\alpha]_{589}^{20}$ = –6.92 (c = 1.00, $CHCl_3$).

((2*S*,2a*S*,4*S*,4a*S*,6a*S*)-2,4-Dimethylhexahydro-1,3,5-trioxa-2a1-azacyclopenta[*cd*]pentalene-2,4-diyl) dimethanol ((–)-(2a*S*,4*S*,4a*S*,6*S*,6a*S*)-75a) and ((2a*R*,4*S*,4a*R*,6*S*,6a*R*)-4,6-dimethylhexahydro-1,3,5-trioxa-2a1-azacyclopenta[*cd*]pentalene-4,6-diyl)dimethanol ((+)-(2a*R*,4*S*,4a*R*,6*S*,6a*R*)-75d)

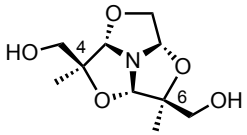

(*S*)-**Type I**
(–)-(2a*S*,4*S*,4a*S*,6*S*,6a*S*)-**75a**

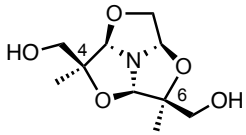

(*R*)-**Type IV**
(+)-(2a*R*,4*S*,4a*R*,6*S*,6a*R*)-**75d**

To a solution of diol (*R*)-**117** (1.24 g, 5.27 mmmol) in dry DCM (30 mL) were added activated MS 4A (2.08 g), *N*-methylmorpholine *N*-oxide (3.09 g, 26.4 mmmol) and tetrapropylammonium perruthenate (0.185 g, 0.527 mmol) at room temperature and the mixture was stirred for 12 h under an argon atmosphere. The residue was filtered with Celite and concentrated *in vacuo*, and α-hydroxyaldehyde (*S*)-**72** as a colorless oil, which was used in the next reaction without further purification.

According to the synthetic protocol of **75**, (*S*)-**72** (1.00 g, 2.34 mmol) was converted to (–)-(2a*S*,4*S*,4a*S*,6*S*,6a*S*)-**75a** (447 mg, 54%) as a colorless amorphous and (+)-(2a*R*,4*S*,4a*R*,6*S*,6a*R*)-**75d** (99.2 mg, 12%) as a colorless amorphous.

(–)-(2a*S*,4*S*,4a*S*,6*S*,6a*S*)-**75a**: $[\alpha]_{589}^{20}$ = –30.0 (c = 0.040, $CHCl_3$).

(+)-(2a*R*,4*S*,4a*R*,6*S*,6a*R*)-**75d**: $[\alpha]_{589}^{20}$ = +30.9 (c = 0.042, $CHCl_3$).

(*S*)-2-((Benzyloxy)methyl)-2-methyloxirane ((*S*)-114)

To a solution of sodium hydride (7.43 g, 170 mmol) in dry THF was added epoxyalcohol (*R*)-**112** (5.00 g, 56.7 mmol) dropwise at 0 ºC under an argon atmosphere, and the mixture was stirred at room temperature for 10 min. Then, benzyl bromide (8.08 mL, 68.0 mmol) was added dropwise at 0 ºC for 42 h. After warming to room temperature, the reaction mixture was poured into sat. NH_4Cl aqueous solution (100 mL) and extracted with Et_2O (100 mL, 100 mL, 50 mL). The combined organic layers were dried over anhydrous Na_2SO_4 and concentrated *in vacuo*. The residue was purified by silica gel column chromatography (hexane/Et_2O = 1/1) to obtain (*S*)-**114** (9.89 g, 98%) as a pale-yellow oil.

IR (neat, cm^{-1}): 2925, 1454, 1101.

^1H NMR (400 MHz, $CDCl_3$) δ 1.40 (s, 3H), 2.64 (d, *J* = 5.0 Hz, 1H), 2.76 (d, *J* = 5.0 Hz, 1H), 3.45 (d, *J* = 11 Hz, 1H), 3.58 (d, *J* = 11 Hz, 1H), 4.54 (d, *J* = 12 Hz, 1H), 4.60 (d, *J* = 12 Hz, 1H), 7.25–7.35 (m, 5H).

^{13}C NMR (100 MHz, $CDCl_3$): δ 18.6, 51.4 (×2), 56.0, 73.1, 73.4, 127.6 (×2), 128.3 (×2), 138.0.

HR-MS (ESI): Calcd for $C_{11}H_{14}NaO_2$ $[M+Na]^+$, 201.08915. Found, 201.08822.

(*S*)-3-(Benzyloxy)-2-methylpropane-1,2-diol ((*S*)-117)

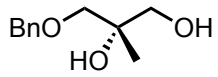

To a solution of epoxide (*S*)-**114** (1.80 g, 10.1 mmol) in *t*-BuOH was added 0.5 M NaOH aqueous solution (100 mL), and the mixture was stirred at 75 ºC for 15 h under an argon atmosphere. After cooling to room temperature, the residue was extracted with EtOAc (100 mL, 50 mL, 30 mL). The combined organic layers were washed with brine (30 mL), dried over anhydrous Na_2SO_4 and concentrated *in vacuo*. The residue was purified by silica gel column chromatography (hexane/EtOAc = 1/2) to obtain (*S*)-**117** (1.80 g, 91%) as a pale-yellow oil.

IR (neat, cm^{-1}): 3397, 2866, 1454, 1099, 1054.

^1H NMR (400 MHz, $CDCl_3$) δ 1.15 (s, 3H), 2.34 (brs, 1H), 2.80 (brs, 1H), 3.43 (d, *J* = 8.7 Hz, 1H), 3.47 (dd, *J* = 4.6, 10 Hz, 1H), 3.52 (d, *J* = 8.7 Hz, 1H), 3.66 (dd, *J* = 4.6, 10 Hz, 1H), 4.56 (d, *J* = 13, 1H), 4.57 (d, *J* = 13, 1H), 7.31–7.39 (m, 5H).

^{13}C NMR (100 MHz, $CDCl_3$) δ 21.4, 68.8, 72.0, 73.9, 76.4, 127.8 (×2), 128.1, 128.7 (×2), 137.8.

HR-MS (ESI): Calcd for $C_{11}H_{16}NaO_3$ $[M+Na]^+$, 219.09971. Found, 219.09940.

$[\alpha]_{589}^{20}$ = +8.25 (c = 1.00, $CHCl_3$).

((2*R*,2a*S*,4*R*,4a*S*,6a*S*)-2,4-Dimethylhexahydro-1,3,5-trioxa-2a1-azacyclopenta[*cd*]pentalene-2,4-diyl) dimethanol ((+)-(2a*R*,2a*S*,4*R*,4a*S*,6a*S*)-75a) and ((2*R*,2a*R*,4*R*,4a*R*,6a*R*)-2,4-dimethylhexahydro-1,3,5-trioxa-2a1-azacyclopenta[*cd*]pentalene-2,4-diyl)dimethanol ((–)-(2a*R*,4*S*,4a*R*,6*S*,6a*R*)-75d)

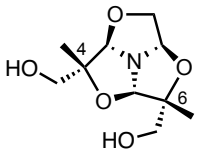

(*R*)-**Type I**
(+)-(2a*R*,4*R*,4a*R*,6*R*,6a*R*)-**75a**

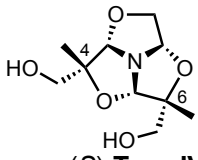

(*S*)-**Type IV**
(–)-(2a*S*,4*R*,4a*S*,6*R*,6a*S*)-**75d**

According to the synthetic protocol of (–)-(2a*S*,4*S*,4a*S*,6*S*,6a*S*)-**75a** and (+)-(2a*R*,4*S*,4a*R*,6*S*,6a*R*)-**75d**, (*S*)-**117** (1.08 g, 2.63 mmol) was converted to (+)-(2a*R*,4*R*,4a*R*,6*R*,6a*R*)-**75a** (538 mg, 58%) as a colorless oil and (–)-(2a*S*,4*R*,4a*S*,6*R*,6a*S*)-**75d** (121 mg, 13%) as a colorless oil.

(+)-(2a*R*,4*R*,4a*R*,6*R*,6a*R*)-**75a**: $[\alpha]_{589}^{20}$ = +43.2 (c = 0.044, $CHCl_3$).

(–)-(2a*S*,4*R*,4a*S*,6*R*,6a*S*)-**75d**: $[\alpha]_{589}^{20}$ = –39.6 (c = 0.048, $CHCl_3$).

Di-*tert*-butyl(((2a*S*,4*S*,4a*S*,6*S*,6a*S*)-4,6-dimethylhexahydro-1,3,5-trioxa-2a^1-azacyclopenta[*cd*] pentalene-4,6-diyl)bis(methylene))dicarbamate ((–)-88a)

According to the synthetic protocol of **88a**, (–)-(2a*S*,4*S*,4a*S*,6*S*,6a*S*)-**75a** was converted to (–)-**88a** (33.9 mg, 67% over 4 steps) as a colorless amorphous.

$[\alpha]_{589}^{20}$ = –39.3 (c = 0.056, $CHCl_3$).

Di-*tert*-butyl(((2a*R*,4*S*,4a*R*,6*S*,6a*R*)-4,6-dimethylhexahydro-1,3,5-trioxa-2a^1-azacyclopenta[*cd*] pentalene-4,6-diyl)bis(methylene))dicarbamate ((+)-88d)

According to the synthetic protocol of **88a**, (+)-(2a*R*,4*S*,4a*R*,6*S*,6a*R*)-**75d** was converted to (+)-**88d** (6.51 mg, 64% over 4 steps) as a colorless amorphous.

$[\alpha]_{589}^{20}$ = +56.2 (c = 0.048, $CHCl_3$).

***N*,*N*'-(((2a*S*,4*S*,4a*S*,6*S*,6a*S*)-4,6-Dimethylhexahydro-1,3,5-trioxa-2a^1-azacyclopenta[*cd*]pentalene-4,6-diyl)bis(methylene))bis(octane-1-sulfonamide) ((–)-96a)**

According to the synthetic protocol of **96a**, (–)-(2a*S*,4*S*,4a*S*,6*S*,6a*S*)-**75a** was converted to (+)-**96a** (5.70 mg, 26% over 4 steps) as a colorless amorphous.

$[\alpha]_{589}^{20}$ = –50.0 (c = 0.014, $CHCl_3$).

***N*,*N*'-(((2a*R*,4*S*,4a*R*,6*S*,6a*R*)-4,6-Dimethylhexahydro-1,3,5-trioxa-2a^1-azacyclopenta[*cd*]pentalene-4,6-diyl)bis(methylene))bis(octane-1-sulfonamide) ((+)-96d)**

According to the synthetic protocol of **96a**, (+)-(2a*R*,4*S*,4a*R*,6*S*,6a*R*)-**75d** was converted to (+)-**96d** (3.12 mg, 66% over 4 steps) as a colorless amorphous.

$[\alpha]_{589}^{20}$ = +64.9 (c = 0.040, $CHCl_3$).

Di-*tert*-butyl(((2a*R*,4*R*,4a*R*,6*R*,6a*R*)-4,6-dimethylhexahydro-1,3,5-trioxa-2a^1-azacyclopenta[*cd*] pentalene-4,6-diyl)bis(methylene))dicarbamate ((+)-88a)

According to the synthetic protocol of **88a**, (+)-(2a*R*,4*R*,4a*R*,6*R*,6a*R*)-**75a** was converted to (+)-**88a** (35.9 mg, 65% over 4 steps) as a colorless amorphous.

$[\alpha]_{589}^{20}$ = +56.3 (c = 0.048, $CHCl_3$).

Di-*tert*-butyl(((2a*S*,4*R*,4a*S*,6*R*,6a*S*)-4,6-dimethylhexahydro-1,3,5-trioxa-2a^1-azacyclopenta[*cd*] pentalene-4,6-diyl)bis(methylene))dicarbamate ((–)-88d)

According to the synthetic protocol of **88a**, (–)-(2a*S*,4*R*,4a*S*,6*R*,6a*S*)-**75d** was converted to (–)-**88d** (5.62 mg, 21% over 4 steps) as a brown oil.

$[\alpha]_{589}^{20}$ = –40.1 (c = 0.044, $CHCl_3$).

***N*,*N*'-(((2a*R*,4*R*,4a*R*,6*R*,6a*R*)-4,6-Dimethylhexahydro-1,3,5-trioxa-2a^1-azacyclopenta[*cd*]pentalene-4,6-diyl)bis(methylene))bis(octane-1-sulfonamide) ((+)-96a)**

According to the synthetic protocol of **96a**, (+)-(2R*S*,4*R*,4a*R*,6*R*,6a*R*)-**75a** was converted to (+)-**96a** (18.3 mg, 29% over 4 steps) as a colorless amorphous.

$[\alpha]_{589}^{20}$ = +64.6 (c = 0.048, $CHCl_3$).

***N*,*N*'-(((2a*S*,4*R*,4a*S*,6*R*,6a*S*)-4,6-Dimethylhexahydro-1,3,5-trioxa-2a^1-azacyclopenta[*cd*]pentalene-4,6-diyl)bis(methylene))bis(octane-1-sulfonamide) ((–)-96d)**

According to the synthetic protocol of **96a**, (–)-(2a*S*,4*R*,4a*S*,6*R*,6a*S*)-**75d** was converted to (+)-**96d** (19.0 mg, 26% over 4 steps) as a brown oil.

$[\alpha]_{589}^{20}$ = –63.3 (c = 0.030, $CHCl_3$).

Pharmacology

***In vitro* Ca^{2+} mobilization assay (Agonist activity)**[62]

Chinese hamster ovary (CHO)-K1 cells stably expressing human OX_1R ($CHOOX_1R$) or OX_2R ($CHOOX_2R$) were seeded in a 96-well-plate (10,000 cells/well) and incubated with 5% FBS/DMEM at 37 °C for 48 h. Then, cells were loaded with 5 μM fluorescent calcium indicator Fura 2-AM (Cayman Chemical) in Hanks balanced salt solution (HBSS: GIBCO) including 20 mM HEPES (Sigma-Aldrich), 2.5 mM Probenecid (WAKO), 5% CremophorEL (Fluka), and 0.1% BSA (SigmaAldrich) at 37 °C for 1 h. The cells were washed once and added with 75 μL of HBSS buffer. Then, cells were treated with 25 μL of various concentrations of test compounds or orexin A (OXA: diluted in PBS/0.1% BSA, Peptide Institute. Inc.). The increase of the intracellular Ca^{2+} concentration after the application of test compounds or OXA was monitored by FDSS 7000 system (Hamamatsu Photonics). The EC_{50} value of each compound was calculated by Graph Pad Prism 5J (MDF).

Luciferase assay (Agonist activity) [62]

$CHOOX_1R$ or $CHOOX_2R$ cells were seeded (10,000 cells/well) in a 96-well-plate and grown to confluence for 24 h. Cells were treated with indicated test compounds or OXA. OXA (diluted in PBS/0.1%BSA) was used positive control. Six hours later, the medium was removed by suction. The cell monolayer was lysed in 50 μL of Steay-Glo luciferase reagent (Promega) and luciferase activity was determined by ARVO x5 (PerkinElmer). The Steady-Glo reagent was diluted 10-fold in 25 mM Tris (pH 7.5)/10% Glycerol/1% triton X-100 as Working solution.

***In vitro* Ca^{2+} mobilization assay (Antagonist activity)**[78]

CHO-K1 cells stably expressing human OX_1R ($CHOOX_1R$) or OX_2R ($CHOOX_2R$) were seeded in a 96-well-plate (10 000 cells per well) and then were incubated with 5% fetal bovine serum (FBS)/Dulbecco's modified Eagle medium (DMEM) at 37 °C for 48 h. After the incubation, cells were loaded with 4 μM fluorescent calcium indicator Fura 2-AM (Cayman Chemical) in Hanks' balanced salt solution (HBSS, GIBCO) including 20 mM HEPES (Sigma-Aldrich), 2.5 mM Probenecid (WAKO), 5% CremophorEL (Fluka), and 0.1% bovine serum albumin (BSA) (Sigma-Aldrich) at 37 °C for 1 h. The cells were washed once and added with 50 μL of HBSS buffer. Cells were pretreated with 25 μL of various concentrations of test compounds for 15 min. After that, submaximal concentration of human orexin-A (OXA, 0.3 nM, Peptide Institute, Inc.) at 25 μL was added to the cells. The increase of the intracellular Ca^{2+} concentration was measured from the ratio of emission fluorescence of 510 nm by excitation at 340 or 380 nm using the Functional Drug Screening System 7000 system (Hamamatsu Photonics). The IC_{50} values

of compound to orexin A were calculated using GraphPad Prism 5J (MDF). Ki values were calculated by using the Cheng–Prusoff formula $K_i = IC_{50}/[1 + (L/EC_{50})]$, where IC_{50} is IC_{50} value of each test compound, L is orexin A concentration at IC_{50} experiments, EC_{50} is the half-maximal effective concentration of orexin A.

Opioid receptor binding

HEK cells stably expressing human μ, δ, or κ opioid receptors were provided from Drs. Uezono (The Jikei University School of Medicine, Japan) and Miyano (National Cancer Center Research Institute, Jaoan); these cell membranes were used for opioid receptor binding assay. Binding affinity for μ, δ, or κ opioid receptors in test compounds was measured by displacement of [^{3}H]-DAMGO, [^{3}H]-DPDPE, or [^{3}H]-U69,593 (each 2 nM), respectively. Nonspecific binding was measured in the presence of 10 μM unlabeled DAMGO, DPDPE, or U-69,593. Radioactivity in the test samples was determined by a MicroBeta scintillation counter with a 96-well microplate (PerkinElmer). The value of each test sample was calculated as $[(T_1 - T_0)/(T_2 - T_0)] \times 100$, where T_0 is the nonspecific binding, T_1 is the [^{3}H]-labeled ligand binding in the presence of various concentrations of test compounds (10^{-5}–10^{-11} M), and T_2 is the [^{3}H]-labeled ligand binding in the absence of respective test compounds. Sigmoidal concentration–response curve and K_i value were calculated by Prism software (version 6.05).

Caco-2 permeability assay

Assays and data analysis were performed by Eurofins Panlabs Inc., St. Charles, MO, USA according to the literature.[20]

Human liver microsome stability

Assays and data analysis were performed by Eurofins Panlabs Inc., St. Charles, MO, USA according to the literature.[80] The test compound was pre-incubated with pooled liver microsomes in phosphate buffer (pH 7.4) for 5 min in a 37 °C shaking water bath. The reaction was initiated by adding NADPH-generating system and incubated for 0, 15, 30, 45, and 60 min. The reaction was stopped by transferring the incubation mixture to acetonitrile/methanol. Samples were then mixed and centrifuged. Supernatants were used for HPLC-MS/MS analysis. Peak areas corresponding to the test compound were recorded and the compound remaining was calculated by comparing the peak area at each time point to time zero. The half-life was calculated from the slope of the initial linear range of the logarithmic curve of compound remaining (%) vs. time, assuming first-order kinetics. In addition, the intrinsic clearance (Cl_{int}) was calculated from the half-life.

***In vivo* experiments**

Animal experiments were carried out in a humane manner after receiving approval from the Institutional Animal Care and Use Committee of the University of Tsukuba and Tohoku University, and in accordance with the Regulation for Animal Experiments in our university and Fundamental Guideline for Proper Conduct of Animal Experiments and Related Activities in Academic Research Institutions under the jurisdiction of the Ministry of Education, Culture, Sports, Science, and Technology.

Determination of brain concentrations of 52a and 52d

C57BL/6J mice received i.p. administration of **52a** or **52d**. At the indicated time after administration, the mice were sacrificed, and the cerebral hemisphere of each mouse was collected, and homogenized in the 3:7 mixture of MeOH:MeCN including 100 pM risperidone as internal standard (5 mL: 1 g brain) with beads shaker (Precellys Evolution, Zirconia beads 1.0 mm (20 beads/tube), 2 ml tube, 8500 rpm, and 30 seconds). Then, the samples were centrifuged at 4°C and 17,360 g for 5 min, and 750 μL of supernatant was evaporated by centrifugation under vacuum, and the residue was reconstituted in 100 μL of 0.1% formic acid/90% water/10% acetonitrile. This solution was centrifuged at 4°C and 17,360 g for 5 min and the supernatant was subjected to LC-MS/MS analysis with an electrospray ionization–triple quadruple mass spectrometer (QTRAP5500; SCIEX, Framingham, MA) coupled to a UPLC system (Waters) equipped with a C18 column (ACQUITY UPLC BEH C18, 1.7 μm, 2.1 × 50 mm, Waters). Mobile phases A and B consisted of 0.1% formic acid in water and 0.1% formic acid in acetonitrile, respectively. The flow rate was 0.3 mL/min. The compounds were separated and eluted from the column with a linear gradient as follows: 1% B (0–1 min), rapidly increased to 100% B (1–3 min), maintained at 100% B (3–4 min), rapidly reduced to 0% B for 0.1 min (4–4.1 min), and then maintained at 1% B (4.1–6 min). The target compounds eluted from the UPLC column were detected by means of electrospray ionization in SRM mode. The SRM transitions were m/z 622.7→135.1 for **52a**, *m/z* 622.7→135.1 for , and *m/z* 411.2→191.1 for risperidone.

Sleep recordings

These protocols of sleep recording were described previously.[80,100] EEG/EMG recordings were performed for 12 consecutive hours in the dark phase. EEG/EMG data were analyzed as previously described[101], and EEG/EMG signals were scored in wakefulness, NREM sleep, and REM sleep state. All analyses were calculated by Sleep Sign (KISSEI COMTEC).

For (±)-**52a** intraperitoneal administration (i.p.) experiment, 8- to 12-wk-old male C57BL/6J mice (ID# 000664 from Charles River) were administered (±)-**52a** or vehicle (0.3 mL/30 g body weight) by intraperitoneal injection at ZT 12. DORA (±)-**52a** was dissolved in saline (50%), polyethylene glycol 400 (PEG400) (45%) and DMSO (5%) to a concentration of 1 mg/mL. Data are presented as the mean ± SEM of 8 mice.

Locomotor assay

4- to 6-wk-old male ICR mole mice (Japan SLC., Inc., Shizuoka, Japan) were individually placed in cages equipped with a running wheel and light-tight chamber under 12 h light/dark cycle (lights on 9:00 A.M. to 9:00 P.M.). The locomotor activity of mice was measured by infrared light beam-braking system locomotor recording system (wireless locomotor sensor: W03, wireless device USB Hub: DIG-807, software: SOF-860, BrainScience Idea. Co., Ltd., Osaka Japan). Briefly, a mouse was placed in a recording acrylic cage with an infrared beam sensor. Horizontal locomotor activity was tracked by invisible infrared light beams that do not interfere with the normal mouse behavior. Counts of horizontal locomotor activity were collected in 10 min intervals for 120 min after orexin A (3 nmol/mouse). Test compound (±)-**52d** (3 or 10 mg/kg, i.p.) was administered intraperitoneally 30 min before intracerebroventricular treatnt with orexin A. Statistical significance of total horizontal locomotor activity was determined by one-way ANOVA followed by Bonferroini test in GraphPad Prism software (version 6.05; GraphPad Software Inc., La Jolla, CA, USA). Data are presented as the mean ± SEM of 5–13 mice.

Intracerebroventricular administration of orexin A

Intracerebroventricular administration was performed according to the method described previously (Haley and McCormick, 1957). To make a hole in the skull for injection, 1–2 days before locomotor assay, mice were briefly anesthetized with isoflurane, and a 2 mm double needle (KN-386-4-4, Natsume Seisakusho, Tokyo, Japan) attached to a 25 μL Hamilton micro syringe was inserted into the unilateral injection site using a V-shaped holder to hold the head of the mouse. On the day of the locomotor assay, orexin A (3 nmol/mouse) was injected into the hole using 2 mm double needle attached to a 25 μL Hamilton micro syringe. The injection volume was 4 μL for each mouse.

References

(1) Payne, D. J.; Gwynn, M. N.; Holmes, D. J.; Pompliano, D. L. Drugs for Bad Bugs: Confronting the Challenges of Antibacterial Discovery. *Nat. Rev. Drug Discov.* **2007**, *6* (1), 29–40.

(2) Zhu, T.; Cao, S.; Su, P.-C.; Patel, R.; Shah, D.; Chokshi, H. B.; Szukala, R.; Johnson, M. E.; Hevener, K. E. Hit Identification and Optimization in Virtual Screening: Practical Recommendations Based on a Critical Literature Analysis. *J. Med. Chem.* **2013**, *56* (17), 6560–6572.

(3) Patrick, G. L. *An Introduction to Medicinal Chemistry*, 5th ed.; Oxford University Press: London, England, 2013.

(4) Merrifield, R. B. Solid Phase Peptide Synthesis. I. the Synthesis of a Tetrapeptide. *J. Am. Chem. Soc.* **1963**, *85* (14), 2149–2154.

(5) Hogan, J. C., Jr. Combinatorial Chemistry in Drug Discovery. *Nat. Biotechnol.* **1997**, *15* (4), 328–330.

(6) Schreiber, S. L. Target-Oriented and Diversity-Oriented Organic Synthesis in Drug Discovery. *Science* **2000**, *287* (5460), 1964–1969.

(7) Galloway, W. R. J. D.; Isidro-Llobet, A.; Spring, D. R. Diversity-Oriented Synthesis as a Tool for the Discovery of Novel Biologically Active Small Molecules. *Nat. Commun.* **2010**, *1* (1), 80.

(8) Lenci, E.; Trabocchi, A. Diversity‐oriented Synthesis and Chemoinformatics: A Fruitful Synergy towards Better Chemical Libraries. *European J. Org. Chem.* **2022**, *2022* (29). https://doi.org/10.1002/ejoc.202200575.

(9) Sauer, W. H. B.; Schwarz, M. K. Molecular Shape Diversity of Combinatorial Libraries: A Prerequisite for Broad Bioactivity. *J. Chem. Inf. Comput. Sci.* **2003**, *43* (3), 987–1003.

(10) Brown, D. G.; Bostrom, J. ChemInform Abstract: Analysis of Past and Present Synthetic Methodologies on Medicinal Chemistry: Where Have All the New Reactions Gone? *ChemInform* **2016**, *47* (31). https://doi.org/10.1002/chin.201631268.

(11) Roughley, S. D.; Jordan, A. M. The Medicinal Chemist's Toolbox: An Analysis of Reactions Used in the Pursuit of Drug Candidates. *J. Med. Chem.* **2011**, *54* (10), 3451–3479.

(12) Wirth, M.; Volkamer, A.; Zoete, V.; Rippmann, F.; Michielin, O.; Rarey, M.; Sauer, W. H. B. Protein Pocket and Ligand Shape Comparison and Its Application in Virtual Screening. *J. Comput. Aided Mol. Des.* **2013**, *27* (6), 511–524.

(13) Klein, H. F.; Hamilton, D. J.; de Esch, I. J. P.; Wijtmans, M.; O'Brien, P. Escape from Planarity in Fragment-Based Drug Discovery: A Synthetic Strategy Analysis of Synthetic 3D Fragment Libraries. *Drug Discov. Today* **2022**, *27* (9), 2484–2496.

(14) Karaki, F.; Umemoto, S.; Ashizawa, K.; Oki, T.; Sato, N.; Ogino, T.; Ishibashi, N.; Someya, R.; Miyano, K.; Hirayama, S.; Uezono, Y.; Fujii, H. A New Lead Identification Strategy: Screening an Sp3 -Rich and Lead-like Compound Library Composed of 7-Azanorbornane Derivatives. *ChemMedChem* **2019**, *14* (21), 1840–1848.

(15) Downes, T. D.; Jones, S. P.; Klein, H. F.; Wheldon, M. C.; Atobe, M.; Bond, P. S.; Firth, J. D.; Chan, N. S.; Waddelove, L.; Hubbard, R. E.; Blakemore, D. C.; De Fusco, C.; Roughley, S. D.; Vidler, L. R.; Whatton, M. A.; Woolford, A. J.-A.; Wrigley, G. L.; O'Brien, P. Design and Synthesis of 56 Shape-Diverse 3D Fragments. *Chemistry* **2020**, *26* (41), 8969–8975.

(16) Chawner, S. J.; Cases-Thomas, M. J.; Bull, J. A. Divergent Synthesis of Cyclopropane-Containing Lead-like Compounds, Fragments and Building Blocks through a Cobalt Catalyzed Cyclopropanation of Phenyl Vinyl Sulfide. *European J. Org. Chem.* **2017**, *2017* (34), 5015–5024.

(17) Nagase, H.; Kutsumura, N. Synthesis of Novel Triplets with a 1,3,5-Trioxazatriquinane Skeleton and Their Pharmacologies for Opioid Receptors. *Arch. Pharm. (Weinheim)* **2015**, *348* (6), 375–389.

(18) Nagase, H.; Ohshita, R.; Kutsumura, N.; Nagumo, Y.; Yamamoto, N.; Saitoh, T.; Hirayama, S. Synthesis of Novel 1,3-Dioxa-5-Thiazatriquinane and 1-Oxa-3,5-Dithiazatriquinane Derivatives and Their Pharmacologies. *Heterocycles* **2018**, *97* (2), 687.

(19) Nagase, H.; Watanabe, A.; Harada, M.; Nakajima, M.; Hasebe, K.; Mochizuki, H.; Yoza, K.; Fujii, H. Novel Synthesis of a 1,3,5-Trioxazatriquinane Skeleton Using a Nitrogen Clamp. *Org. Lett.* **2009**, *11* (3), 539–542.

(20) Watanabe, A.; Fujii, H.; Nakajima, M.; Hasebe, K.; Mochizuki, H.; Nagase, H. Synthesis of a New Opioid Ligand Having the Oxabicyclo[3.2.1]Octane Skeleton Using a New Rearrangement Reaction. *Bioorg. Med. Chem. Lett.* **2009**, *19* (9), 2416–2419.

(21) Nagase, H.; Fujii, H. Synthesis of Novel Basic Skeletons Derived from Naltrexone. In *Topics in Current Chemistry*; Topics in current chemistry; Springer Berlin Heidelberg: Berlin, Heidelberg, 2010; pp 187–237.

(22) Nagase, H.; Koyano, K.; Wada, N.; Hirayama, S.; Watanabe, A.; Nemoto, T.; Nakajima, M.; Nakao, K.; Mochizuki, H.; Fujii, H. Synthesis of Novel Triplet Drugs with 1,3,5-Trioxazatriquinane Skeletons and Their Pharmacologies. Part 2: Synthesis of Novel Triplet Drugs with the Epoxymethano Structure (Capped Homotriplet). *Bioorg. Med. Chem. Lett.* **2011**, *21* (20), 6198–6202.

(23) Nagase, H.; Watanabe, A.; Nemoto, T.; Nakajima, M.; Hasebe, K.; Mochizuki, H.; Fujii, H. Synthesis of Novel Triplet Drugs with 1,3,5-Trioxazatriquinane Skeletons and Their Pharmacologies. 1: Synthesis of Triplet Drugs with Morphinan Skeletons. *Bioorg. Med. Chem. Lett.* **2011**, *21* (13), 4023–4026.

(24) Wada, N.; Fujii, H.; Koyano, K.; Hirayama, S.; Iwai, T.; Nemoto, T.; Nagase, H. Synthesis of Novel Triplet Drugs with 1,3,5-Trioxazatriquinane Skeletons and Their Pharmacologies. 3: Synthesis of Novel Triplet Drugs with the Bis(Epoxymethano) or Bis(Dimethylepoxymethano) Structure (Double-Capped Triplet). *Bioorg. Med. Chem. Lett.* **2012**, *22* (24), 7551–7554.

(25) Hirayama, S.; Wada, N.; Kuroda, N.; Iwai, T.; Yamaotsu, N.; Hirono, S.; Fujii, H.; Nagase, H. Synthesis of a Novel Universal Opioid Receptor Agonist with the 1,3,5-Trioxazatriquinane Skeleton and Its Pharmacologies. *Bioorg. Med. Chem. Lett.* **2014**, *24* (20), 4895–4898.

(26) Hirayama, S.; Wada, N.; Nemoto, T.; Iwai, T.; Fujii, H.; Nagase, H. Synthesis and Pharmacology of a Novel κ Opioid Receptor (KOR) Agonist with a 1,3,5-Trioxazatriquinane Skeleton. *ACS Med. Chem. Lett.* **2014**, *5* (8), 868–872.

(27) Sakurai, T.; Amemiya, A.; Ishii, M.; Matsuzaki, I.; Chemelli, R. M.; Tanaka, H.; Williams, S. C.; Richardson, J. A.; Kozlowski, G. P.; Wilson, S.; Arch, J. R. S.; Buckingham, R. E.; Haynes, A. C.; Carr, S. A.; Annan, R. S.; McNulty, D. E.; Liu, W.-S.; Terrett, J. A.; Elshourbagy, N. A.; Bergsma, D. J.; Yanagisawa, M. Orexins and Orexin Receptors: A Family of Hypothalamic Neuropeptides and G Protein-Coupled Receptors That Regulate Feeding Behavior. *Cell* **1998**, *92* (4), 573–585.

(28) Sakurai, T.; Amemiya, A.; Ishii, M.; Matsuzaki, I.; Chemelli, R. M.; Tanaka, H.; Williams, S. C.; Richarson, J. A.; Kozlowski, G. P.; Wilson, S.; Arch, J. R.; Buckingham, R. E.; Haynes, A. C.; Carr, S. A.; Annan, R. S.; McNulty, D. E.; Liu, W. S.; Terrett, J. A.; Elshourbagy, N. A.; Bergsma, D. J.; Yanagisawa, M. Orexins and Orexin Receptors: A Family of Hypothalamic Neuropeptides and G Protein-Coupled Receptors That Regulate Feeding Behavior. *Cell* **1998**, *92* (5), 1 page following 696.

(29) Sakurai, T. Orexins and Orexin Receptors: Implication in Feeding Behavior. *Regul. Pept.* **1999**, *85* (1), 25–30.

(30) Harris, G. C.; Wimmer, M.; Aston-Jones, G. A Role for Lateral Hypothalamic Orexin Neurons in Reward Seeking. *Nature* **2005**, *437* (7058), 556–559.

(31) Aston-Jones, G.; Smith, R. J.; Moorman, D. E.; Richardson, K. A. Role of Lateral Hypothalamic Orexin Neurons in Reward Processing and Addiction. *Neuropharmacology* **2009**, *56 Suppl 1*, 112–121.

(32) Furlong, T. M.; Vianna, D. M. L.; Liu, L.; Carrive, P. Hypocretin/Orexin Contributes to the Expression of Some but Not All Forms of Stress and Arousal. *Eur. J. Neurosci.* **2009**, *30* (8), 1603–1614.

(33) Johnson, P. L.; Truitt, W.; Fitz, S. D.; Minick, P. E.; Dietrich, A.; Sanghani, S.; Träskman-Bendz, L.; Goddard, A. W.; Brundin, L.; Shekhar, A. A Key Role for Orexin in Panic Anxiety. *Nat. Med.* **2010**, *16* (1), 111–115.

(34) Johnson, P. L.; Molosh, A.; Fitz, S. D.; Truitt, W. A.; Shekhar, A. Orexin, Stress, and Anxiety/Panic States. *Prog. Brain Res.* **2012**, *198*, 133–161.

(35) Chemelli, R. M.; Willie, J. T.; Sinton, C. M.; Elmquist, J. K.; Scammell, T.; Lee, C.; Richardson, J. A.; Williams, S. C.; Xiong, Y.; Kisanuki, Y.; Fitch, T. E.; Nakazato, M.; Hammer, R. E.; Saper, C. B.; Yanagisawa, M. Narcolepsy in Orexin Knockout Mice. *Cell* **1999**, *98* (4), 437–451.

(36) Zhu, Y.; Miwa, Y.; Yamanaka, A.; Yada, T.; Shibahara, M.; Abe, Y.; Sakurai, T.; Goto, K. Orexin Receptor Type-1 Couples Exclusively to Pertussis Toxin-Insensitive G-Proteins, While Orexin Receptor Type-2 Couples to Both Pertussis Toxin-Sensitive and -Insensitive G-Proteins. *J. Pharmacol. Sci.* **2003**, *92* (3), 259–266.

(37) Marcus, J. N.; Aschkenasi, C. J.; Lee, C. E.; Chemelli, R. M.; Saper, C. B.; Yanagisawa, M.; Elmquist, J. K. Differential Expression of Orexin Receptors 1 and 2 in the Rat Brain. *J. Comp. Neurol.* **2001**, *435* (1), 6–25.

(38) Takakusaki, K.; Takahashi, K.; Saitoh, K.; Harada, H.; Okumura, T.; Kayama, Y.; Koyama, Y. Orexinergic Projections to the Cat Midbrain Mediate Alternation of Emotional Behavioural States from Locomotion to Cataplexy. *J. Physiol.* **2005**, *568* (Pt 3), 1003–1020.

(39) Hagan, J. J.; Leslie, R. A.; Patel, S.; Evans, M. L.; Wattam, T. A.; Holmes, S.; Benham, C. D.; Taylor, S. G.; Routledge, C.; Hemmati, P.; Munton, R. P.; Ashmeade, T. E.; Shah, A. S.; Hatcher, J. P.; Hatcher, P. D.; Jones, D. N.; Smith, M. I.; Piper, D. C.; Hunter, A. J.; Porter, R. A.; Upton, N. Orexin A Activates Locus Coeruleus Cell Firing and Increases Arousal in the Rat. *Proc. Natl. Acad. Sci. U. S. A.* **1999**, *96* (19), 10911–10916.

(40) Yamanaka, A.; Tsujino, N.; Funahashi, H.; Honda, K.; Guan, J.-L.; Wang, Q.-P.; Tominaga, M.; Goto, K.; Shioda, S.; Sakurai, T. Orexins Activate Histaminergic Neurons via the Orexin 2 Receptor. *Biochem. Biophys. Res. Commun.* **2002**, *290* (4), 1237–1245.

(41) Nakamura, T.; Uramura, K.; Nambu, T.; Yada, T.; Goto, K.; Yanagisawa, M.; Sakurai, T. Orexin-Induced Hyperlocomotion and Stereotypy Are Mediated by the Dopaminergic System11Published on the World Wide Web on 27 June 2000. *Brain Res.* **2000**, *873* (1), 181–187.

(42) Funato, H.; Tsai, A. L.; Willie, J. T.; Kisanuki, Y.; Williams, S. C.; Sakurai, T.; Yanagisawa, M. Enhanced Orexin Receptor-2 Signaling Prevents Diet-Induced Obesity and Improves Leptin Sensitivity. *Cell Metab.* **2009**, *9* (1), 64–76.

(43) Dergacheva, O.; Philbin, K.; Bateman, R.; Mendelowitz, D. Hypocretin-1 (Orexin A) Prevents the Effects of Hypoxia/Hypercapnia and Enhances the GABAergic Pathway from the Lateral Paragigantocellular Nucleus to Cardiac Vagal Neurons in the Nucleus Ambiguus. *Neuroscience* **2011**, *175*, 18–23.

(44) Dias, M. B.; Li, A.; Nattie, E. E. Antagonism of Orexin Receptor-1 in the Retrotrapezoid Nucleus Inhibits the Ventilatory Response to Hypercapnia Predominantly in Wakefulness. *J. Physiol.* **2009**, *587* (Pt 9), 2059–2067.

(45) Kukkonen, J. P.; Leonard, C. S. Orexin/Hypocretin Receptor Signalling Cascades. *Br. J. Pharmacol.* **2014**, *171* (2), 314–331.

(46) Boss, C.; Brisbare-Roch, C.; Jenck, F. Biomedical Application of Orexin/Hypocretin Receptor Ligands in Neuroscience. *J. Med. Chem.* **2009**, *52* (4), 891–903.

(47) Lebold, T. P.; Bonaventure, P.; Shireman, B. T. Selective Orexin Receptor Antagonists. *Bioorg. Med. Chem. Lett.* **2013**, *23* (17), 4761–4769.

(48) Boss, C.; Roch, C. Recent Trends in Orexin Research--2010 to 2015. *Bioorg. Med. Chem. Lett.* **2015**, *25* (15), 2875–2887.

(49) Roecker, A. J.; Cox, C. D.; Coleman, P. J. Orexin Receptor Antagonists: New Therapeutic Agents for the Treatment of Insomnia. *J. Med. Chem.* **2016**, *59* (2), 504–530.

(50) Cox, C. D.; Breslin, M. J.; Whitman, D. B.; Schreier, J. D.; McGaughey, G. B.; Bogusky, M. J.; Roecker, A. J.; Mercer, S. P.; Bednar, R. A.; Lemaire, W.; Bruno, J. G.; Reiss, D. R.; Harrell, C. M.; Murphy, K. L.; Garson, S. L.; Doran, S. M.; Prueksaritanont, T.; Anderson, W. B.; Tang, C.; Roller, S.; Cabalu, T. D.; Cui, D.; Hartman, G. D.; Young, S. D.; Koblan, K. S.; Winrow, C. J.; Renger, J. J.; Coleman, P. J. Discovery of the Dual Orexin Receptor Antagonist [(7R)-4-(5-Chloro-1,3-Benzoxazol-2-Yl)-7-Methyl-1,4-Diazepan-1-Yl][5-Methyl-2-(2H-1,2,3-Triazol-2-Yl)Phenyl]Methanone (MK-4305) for the Treatment of Insomnia. *J. Med. Chem.* **2010**, *53* (14), 5320–5332.

(51) Yoshida, Y.; Naoe, Y.; Terauchi, T.; Ozaki, F.; Doko, T.; Takemura, A.; Tanaka, T.; Sorimachi, K.; Beuckmann, C. T.; Suzuki, M.; Ueno, T.; Ozaki, S.; Yonaga, M. Discovery of (1R,2S)-2-{[(2,4-Dimethylpyrimidin-5-Yl)Oxy]Methyl}-2-(3-Fluorophenyl)-N-(5-Fluoropyridin-2-Yl)Cyclopropanecarboxamide (E2006): A Potent and Efficacious Oral Orexin Receptor Antagonist. *J. Med. Chem.* **2015**, *58* (11), 4648–4664.

(52) Treiber, A.; de Kanter, R.; Roch, C.; Gatfield, J.; Boss, C.; von Raumer, M.; Schindelholz, B.; Muehlan, C.; van Gerven, J.; Jenck, F. The Use of Physiology-Based Pharmacokinetic and Pharmacodynamic Modeling in the Discovery of the Dual Orexin Receptor Antagonist ACT-541468. *J. Pharmacol. Exp. Ther.* **2017**, *362* (3), 489–503.

(53) Haynes, A. C.; Chapman, H.; Taylor, C.; Moore, G. B. T.; Cawthorne, M. A.; Tadayyon, M.; Clapham, J. C.; Arch, J. R. S. Anorectic, Thermogenic and Anti-Obesity Activity of a Selective Orexin-1 Receptor Antagonist in Ob/Ob Mice. *Regul. Pept.* **2002**, *104* (1–3), 153–159.

(54) Lang, M.; Söll, R. M.; Dürrenberger, F.; Dautzenberg, F. M.; Beck-Sickinger, A. G. Structure-Activity Studies of Orexin a and Orexin B at the Human Orexin 1 and Orexin 2 Receptors Led to Orexin 2 Receptor Selective and Orexin 1 Receptor Preferring Ligands. *J. Med. Chem.* **2004**, *47* (5), 1153–1160.

(55) German, N. A.; Decker, A. M.; Gilmour, B. P.; Thomas, B. F.; Zhang, Y. Truncated Orexin Peptides: Structure-Activity Relationship Studies. *ACS Med. Chem. Lett.* **2013**, *4* (12), 1224–1227.

(56) Willie, J. T.; Chemelli, R. M.; Sinton, C. M.; Tokita, S.; Williams, S. C.; Kisanuki, Y. Y.; Marcus, J. N.; Lee, C.; Elmquist, J. K.; Kohlmeier, K. A.; Leonard, C. S.; Richardson, J. A.; Hammer, R. E.; Yanagisawa, M. Distinct Narcolepsy Syndromes in Orexin Receptor-2 and Orexin Null Mice. *Neuron* **2003**, *38* (5), 715–730.

(57) Lin, L.; Faraco, J.; Li, R.; Kadotani, H.; Rogers, W.; Lin, X.; Qiu, X.; de Jong, P. J.; Nishino, S.; Mignot, E. The Sleep Disorder Canine Narcolepsy Is Caused by a Mutation in the Hypocretin (Orexin) Receptor 2 Gene. *Cell* **1999**, *98* (3), 365–376.

(58) Peyron, C.; Faraco, J.; Rogers, W.; Ripley, B.; Overeem, S.; Charnay, Y.; Nevsimalova, S.; Aldrich, M.; Reynolds, D.; Albin, R.; Li, R.; Hungs, M.; Pedrazzoli, M.; Padigaru, M.; Kucherlapati, M.; Fan, J.; Maki, R.; Lammers, G. J.; Bouras, C.; Kucherlapati, R.; Nishino, S.; Mignot, E. A Mutation in a Case of Early Onset Narcolepsy and a Generalized Absence of Hypocretin Peptides in Human Narcoleptic Brains. *Nat. Med.* **2000**, *6* (9), 991–997.

(59) Thannickal, T. C.; Moore, R. Y.; Nienhuis, R.; Ramanathan, L.; Gulyani, S.; Aldrich, M.; Cornford, M.; Siegel, J. M. Reduced Number of Hypocretin Neurons in Human Narcolepsy. *Neuron* **2000**, *27* (3), 469–474.

(60) Schuld, A.; Blum, W. F.; Pollmächer, T. Low Cerebrospinal Fluid Hypocretin (Orexin) and Altered Energy Homeostasis in Human Narcolepsy. *Ann. Neurol.* **2002**, *51* (5), 660; author reply 660-1.

(61) Kubota, H.; Kanbayashi, T.; Tanabe, Y.; Ito, M.; Takanashi, J.-I.; Kohno, Y.; Shimizu, T. Decreased Cerebrospinal Fluid Hypocretin-1 Levels near the Onset of Narcolepsy in 2 Prepubertal Children. *Sleep* **2003**, *26* (5), 555–557.

(62) Nagahara, T.; Saitoh, T.; Kutsumura, N.; Irukayama-Tomobe, Y.; Ogawa, Y.; Kuroda, D.; Gouda, H.; Kumagai, H.; Fujii, H.; Yanagisawa, M.; Nagase, H. Design and Synthesis of Non-Peptide, Selective Orexin Receptor 2 Agonists. *J. Med. Chem.* **2015**, *58* (20), 7931–7937.

(63) Irukayama-Tomobe, Y.; Ogawa, Y.; Tominaga, H.; Ishikawa, Y.; Hosokawa, N.; Ambai, S.; Kawabe, Y.; Uchida, S.; Nakajima, R.; Saitoh, T.; Kanda, T.; Vogt, K.; Sakurai, T.; Nagase, H.; Yanagisawa, M. Nonpeptide Orexin Type-2 Receptor Agonist Ameliorates Narcolepsy-Cataplexy Symptoms in Mouse Models. *Proc. Natl. Acad. Sci. U. S. A.* **2017**, *114* (22), 5731–5736.

(64) Zhang, D.; Perrey, D. A.; Decker, A. M.; Langston, T. L.; Mavanji, V.; Harris, D. L.; Kotz, C. M.; Zhang, Y. Discovery of Arylsulfonamides as Dual Orexin Receptor Agonists. *J. Med. Chem.* **2021**, *64* (12), 8806–8825.

(65) Hong, C.; Byrne, N. J.; Zamlynny, B.; Tummala, S.; Xiao, L.; Shipman, J. M.; Partridge, A. T.; Minnick, C.; Breslin, M. J.; Rudd, M. T.; Stachel, S. J.; Rada, V. L.; Kern, J. C.; Armacost, K. A.; Hollingsworth, S. A.; O'Brien, J. A.; Hall, D. L.; McDonald, T. P.; Strickland, C.; Brooun, A.; Soisson, S. M.; Hollenstein, K. Structures of Active-State Orexin Receptor 2 Rationalize Peptide and Small-Molecule Agonist Recognition and Receptor Activation. *Nat. Commun.* **2021**, *12* (1), 815.

(66) Hino, T.; Saitoh, T.; Nagumo, Y.; Yamamoto, N.; Kutsumura, N.; Irukayama-Tomobe, Y.; Ishikawa, Y.; Tanimura, R.; Yanagisawa, M.; Nagase, H. Design and Synthesis of Novel Orexin 2 Receptor Agonists Based on Naphthalene Skeleton. *Bioorg. Med. Chem. Lett.* **2022**, *59* (128530), 128530.

(67) Iio, K.; Saitoh, T.; Ohshita, R.; Hino, T.; Amezawa, M.; Takayama, Y.; Nagumo, Y.; Yamamoto, N.; Kutsumura, N.; Irukayama-Tomobe, Y.; Ishikawa, Y.; Tanimura, R.; Yanagisawa, M.; Nagase, H. Discovery of Orexin 2 Receptor Selective and Dual Orexin Receptor Agonists Based on the Tetralin Structure: Switching of Receptor Selectivity by Chirality on the Tetralin Ring. *Bioorg. Med. Chem. Lett.* **2022**, 128555.

(68) Abdel-Magid, A. F. Orexin Receptor Agonists as Possible Treatment for Narcolepsy and Idiopathic Hypersomnia. *ACS Med. Chem. Lett.* **2022**, *13* (9), 1411–1412.

(69) Sabnis, R. W. Novel Macrocyclic Urea Orexin Receptor Agonists for Treating Sleep Disorders. *ACS Med. Chem. Lett.* **2022**, *13* (7), 1010–1011.

(70) Fujimoto, T.; Rikimaru, K.; Fukuda, K.; Sugimoto, H.; Masuda, K.; Ohyabu, N.; Banno, Y.; Tokunaga, N.; Kawamoto, T.; Tomata, Y.; Kumagai, Y.; Iida, M.; Nagano, Y.; Yoneyama-Hirozane, M.; Shimizu, Y.; Sasa, K.; Ishikawa, T.; Yukitake, H.; Ito, M.; Aoyama, K.; Matsumoto, T. Discovery of TAK-925 as a Potent, Selective, and

Brain-Penetrant Orexin 2 Receptor Agonist. *ACS Med. Chem. Lett.* **2022**. https://doi.org/10.1021/acsmedchemlett.1c00626.

(71) Yanagisawa, M. Small-Molecule Agonists for Type-2 Orexin Receptor. 20100150840:A1, June 17, 2010. https://patents.google.com/patent/US20100150840A1/en (accessed 2022-10-25).

(72) Iio, K.; Hashimoto, K.; Nagumo, Y.; Amezawa, M.; Hasegawa, T.; Yamamoto, N.; Kutsumura, N.; Takeuchi, K.; Ishikawa, Y.; Yanagisawa, M.; Nagase, H.; Saitoh, T. Design and Synthesis of Orexin 1 Receptor-Selective Agonists. *ChemRxiv*, 2022. https://doi.org/10.26434/chemrxiv-2022-fxx2d.

(73) Sabnis, R. W. Novel 5-Alkyl Pyrrolidine Orexin Receptor Agonists for Treating Sleep Disorders. *ACS Med. Chem. Lett.* **2020**, *11* (11), 2085–2086.

(74) Leino, T. O.; Turku, A.; Yli-Kauhaluoma, J.; Kukkonen, J. P.; Xhaard, H.; Wallén, E. A. A. Azulene-Based Compounds for Targeting Orexin Receptors. *Eur. J. Med. Chem.* **2018**, *157*, 88–100.

(75) Turku, A.; Leino, T. O.; Karhu, L.; Yli-Kauhaluoma, J.; Kukkonen, J. P.; Wallén, E. A. A.; Xhaard, H. Structure-Activity Relationships of 1-Benzoylazulenes at the OX1 and OX2 Orexin Receptors. *ChemMedChem* **2019**, *14* (9), 965–981.

(76) Willie, J. T.; Chemelli, R. M.; Sinton, C. M.; Tokita, S.; Williams, S. C.; Kisanuki, Y. Y.; Marcus, J. N.; Lee, C.; Elmquist, J. K.; Kohlmeier, K. A.; Leonard, C. S.; Richardson, J. A.; Hammer, R. E.; Yanagisawa, M. Distinct Narcolepsy Syndromes in Orexin Receptor-2 and Orexin Null Mice: Molecular Genetic Dissection of Non-REM and REM Sleep Regulatory Processes. *Neuron* **2003**, *38* (5), 715–730.

(77) Chou, T. C.; Lee, C. E.; Lu, J.; Elmquist, J. K.; Hara, J.; Willie, J. T.; Beuckmann, C. T.; Chemelli, R. M.; Sakurai, T.; Yanagisawa, M.; Saper, C. B.; Scammell, T. E. Orexin (Hypocretin) Neurons Contain Dynorphin. *J. Neurosci.* **2001**, *21* (19), RC168.

(78) Nagase, H.; Yamamoto, N.; Yata, M.; Ohrui, S.; Okada, T.; Saitoh, T.; Kutsumura, N.; Nagumo, Y.; Irukayama-Tomobe, Y.; Ishikawa, Y.; Ogawa, Y.; Hirayama, S.; Kuroda, D.; Watanabe, Y.; Gouda, H.; Yanagisawa, M. Design and Synthesis of Potent and Highly Selective Orexin 1 Receptor Antagonists with a Morphinan Skeleton and Their Pharmacologies. *J. Med. Chem.* **2017**, *60* (3), 1018–1040.

(79) Hidalgo, I. J.; Raub, T. J.; Borchardt, R. T. Characterization of the Human Colon Carcinoma Cell Line (Caco-2) as a Model System for Intestinal Epithelial Permeability. *Gastroenterology* **1989**, *96* (3), 736–749.

(80) Obach, R. S.; Baxter, J. G.; Liston, T. E.; Silber, B. M.; Jones, B. C.; MacIntyre, F.; Rance, D. J.; Wastall, P. The Prediction of Human Pharmacokinetic Parameters from Preclinical and in Vitro Metabolism Data. *J. Pharmacol. Exp. Ther.* **1997**, *283* (1), 46–58.

(81) Wager, T. T.; Chandrasekaran, R. Y.; Hou, X.; Troutman, M. D.; Verhoest, P. R.; Villalobos, A.; Will, Y. Defining Desirable Central Nervous System Drug Space through the Alignment of Molecular Properties, in Vitro ADME, and Safety Attributes. *ACS Chem. Neurosci.* **2010**, *1* (6), 420–434.

(82) Sakurai, T. The Role of Orexin in Motivated Behaviours. *Nat. Rev. Neurosci.* **2014**, *15* (11), 719–731.

(83) Smart, D.; Sabido-David, C.; Brough, S. J.; Jewitt, F.; Johns, A.; Porter, R. A.; Jerman, J. C. SB-334867-A: The First Selective Orexin-1 Receptor Antagonist. *Br. J. Pharmacol.* **2001**, *132* (6), 1179–1182.

(84) Porter, R. A.; Chan, W. N.; Coulton, S.; Johns, A.; Hadley, M. S.; Widdowson, K.; Jerman, J. C.; Brough, S. J.; Coldwell, M.; Smart, D.; Jewitt, F.; Jeffrey, P.; Austin, N. 1,3-Biarylureas as Selective Non-Peptide Antagonists of the Orexin-1 Receptor. *Bioorg. Med. Chem. Lett.* **2001**, *11* (14), 1907–1910.

(85) Rappas, M.; Ali, A. A. E.; Bennett, K. A.; Brown, J. D.; Bucknell, S. J.; Congreve, M.; Cooke, R. M.; Cseke, G.; de Graaf, C.; Doré, A. S.; Errey, J. C.; Jazayeri, A.; Marshall, F. H.; Mason, J. S.; Mould, R.; Patel, J. C.; Tehan, B. G.; Weir, M.; Christopher, J. A. Comparison of Orexin 1 and Orexin 2 Ligand Binding Modes Using X-Ray Crystallography and Computational Analysis. *J. Med. Chem.* **2020**, *63* (4), 1528–1543.

(86) Yin, J.; Mobarec, J. C.; Kolb, P.; Rosenbaum, D. M. Crystal Structure of the Human OX2 Orexin Receptor Bound to the Insomnia Drug Suvorexant. *Nature* **2015**, *519* (7542), 247–250.

(87) Yin, J.; Babaoglu, K.; Brautigam, C. A.; Clark, L.; Shao, Z.; Scheuermann, T. H.; Harrell, C. M.; Gotter, A. L.; Roecker, A. J.; Winrow, C. J.; Renger, J. J.; Coleman, P. J.; Rosenbaum, D. M. Structure and Ligand-Binding Mechanism of the Human OX1 and OX2 Orexin Receptors. *Nat. Struct. Mol. Biol.* **2016**, *23* (4), 293–299.

(88) Suno, R.; Kimura, K. T.; Nakane, T.; Yamashita, K.; Wang, J.; Fujiwara, T.; Yamanaka, Y.; Im, D.; Horita, S.; Tsujimoto, H.; Tawaramoto, M. S.; Hirokawa, T.; Nango, E.; Tono, K.; Kameshima, T.; Hatsui, T.; Joti, Y.; Yabashi, M.; Shimamoto, K.; Yamamoto, M.; Rosenbaum, D. M.; Iwata, S.; Shimamura, T.; Kobayashi, T. Crystal Structures of Human Orexin 2 Receptor Bound to the Subtype-Selective Antagonist EMPA. *Structure* **2018**, *26* (1), 7-19.e5.

(89) Malherbe, P.; Roche, O.; Marcuz, A.; Kratzeisen, C.; Wettstein, J. G.; Bissantz, C. Mapping the Binding Pocket of Dual Antagonist Almorexant to Human Orexin 1 and Orexin 2 Receptors: Comparison with the Selective OX1 Antagonist SB-674042 and the Selective OX2 Antagonist N-Ethyl-2-[(6-Methoxy-Pyridin-3-Yl)-(Toluene-2-Sulfonyl)-Amino]-N-Pyridin-3-Ylmethyl-Acetamide (EMPA). *Mol. Pharmacol.* **2010**, *78* (1), 81–93.

(90) Nogrady, C. T.; Weaver, D. *A Medicinal Chemistry: Molecular and Biochemical Approach*, 3rd ed.; Oxford University Press: Cary, NC, 2005.

(91) Saitoh, T.; Amezawa, M.; Horiuchi, J.; Nagumo, Y.; Yamamoto, N.; Kutsumura, N.; Ohshita, R.; Tokuda, A.; Irukayama-Tomobe, Y.; Ogawa, Y.; Ishikawa, Y.; Hasegawa, E.; Sakurai, T.; Uchida, Y.; Sato, T.; Gouda, H.; Tanimura, R.; Yanagisawa, M.; Nagase, H. Discovery of Novel Orexin Receptor Antagonists Using a 1,3,5-Trioxazatriquinane Bearing Multiple Effective Residues (TriMER) Library. *Eur. J. Med. Chem.* **2022**, *240* (114505), 114505.

(92) Yin, J.; Kang, Y.; McGrath, A. P.; Chapman, K.; Sjodt, M.; Kimura, E.; Okabe, A.; Koike, T.; Miyanohana, Y.; Shimizu, Y.; Rallabandi, R.; Lian, P.; Bai, X.; Flinspach, M.; De Brabander, J. K.; Rosenbaum, D. M. Molecular Mechanism of the Wake-Promoting Agent TAK-925. *Nat. Commun.* **2022**, *13* (1), 2902.

(93) Shao, H.; Zhu, Q.; Goodman, M. A New Asymmetric Synthesis of .Alpha.-Methylcysteines via Chiral Aziridines. *J. Org. Chem.* **1995**, *60* (4), 790–791.

(94) Hale, K. J.; Manaviazar, S.; Peak, S. A. Anomalous Enantioselectivity in the Sharpless Catalytic Asymmetric Dihydroxylation Reaction of 1,1-Disubstituted Allyl Alcohol Derivatives. *Tetrahedron Lett.* **1994**, *35* (3), 425–428.

(95) Katsuki, T.; Sharpless, K. B. The First Practical Method for Asymmetric Epoxidation. *J. Am. Chem. Soc.* **1980**, *102* (18), 5974–5976.

(96) Gao, Y.; Klunder, J. M.; Hanson, R. M.; Masamune, H.; Ko, S. Y.; Sharpless, K. B. Catalytic Asymmetric Epoxidation and Kinetic Resolution: Modified Procedures Including in Situ Derivatization. *J. Am. Chem. Soc.* **1987**, *109* (19), 5765–5780.

(97) Dale, J. A.; Mosher, H. S. Nuclear Magnetic Resonance Enantiomer Regents. Configurational Correlations via Nuclear Magnetic Resonance Chemical Shifts of Diastereomeric Mandelate, O-Methylmandelate, and .Alpha.-Methoxy-.Alpha.-Trifluoromethylphenylacetate (MTPA) Esters. *J. Am. Chem. Soc.* **1973**, *95* (2), 512–519.

(98) Cleveland, A. H.; Fronczek, F. R.; Kartika, R. Synthesis of Vicinal Dichlorides via Activation of Aliphatic Terminal Epoxides with Triphosgene and Pyridine. *J. Org. Chem.* **2018**, *83* (6), 3367–3377.

(99) Venkatakrishnan, A. J.; Deupi, X.; Lebon, G.; Tate, C. G.; Schertler, G. F.; Babu, M. M. Molecular Signatures of G-Protein-Coupled Receptors. *Nature* **2013**, *494* (7436), 185–194.

(100) Hasegawa, E.; Maejima, T.; Yoshida, T.; Masseck, O. A.; Herlitze, S.; Yoshioka, M.; Sakurai, T.; Mieda, M. Serotonin Neurons in the Dorsal Raphe Mediate the Anticataplectic Action of Orexin Neurons by Reducing Amygdala Activity. *Proc. Natl. Acad. Sci. U. S. A.* **2017**, *114* (17), E3526–E3535.

(101) Hasegawa, E.; Sakurai, T.; Mieda, M.; Hasegawa, E.; Yanagisawa, M.; Sakurai, T.; Mieda, M. Orexin Neurons Suppress Narcolepsy via 2 Distinct Efferent Pathways Find the Latest Version : Orexin Neurons Suppress Narcolepsy via 2 Distinct Efferent Pathways. **2014**, *124* (2), 604–616.

Acknowledgement

I am sincerely grateful to my supervisor Prof. Hiroshi Nagase and Prof. Noriki Kutsumura for their constant supervision and support. They always encouraged me and led me to achieve this research. Their accomplishments, knowledge, and humanity will forever be my goal.

I am deeply grateful to Dr. Tsuyoshi Saitoh as a mentor who understood me, gave me helpful advice, and afforded me enormous chances to learn. He listened carefully to what I wanted to say and taught me every technique of organic synthesis and medicinal chemistry. He made this research more attractive, and their outstanding approach to research and science is a source of inspiration. My sincere thanks also go to Dr. Yasuyuki Nagumo for supporting me in pharmacological experiments in this research. He also introduced the basis of pharmacology essential to this work to me and gave me many emotional supports. I gratefully appreciate Dr. Naoshi Yamamoto and Dr. Tomoya Sugai for giving me a careful, safe, and precise approach to organic synthesis and for their great warm support to me.

I want to express my deep gratitude to Prof. Masashi Yanagisawa, Dr. Yoko Irukayama-Tomobe, and Ms. Yukiko Ishikawa, Dr. Yasuhiro Ogawa (University of Tsukuba) for evaluating the orexin receptor agonistic activity of the TriMER derivatives. I also would like to thank Prof. Takeshi Sakurai, Dr. Emi Hasegawa (University of Tsukuba) for performing several *in vivo* assays for YNT-2293 and YNT-2294. I also would like to thank Dr. Yasuo Uchida, Mr. Tetsu Sato (Tohoku University) for performing *in vitro* permeability and stability of YNT-2293 and YNT-2294. I sincerely thank Dr. Ryuji Tanimura (TORAY) and Prof. Hiroaki Gouda (Showa pharmaceutical university) for performing docking simulations for orexin receptors.

I am grateful to my appreciation goes to Prof. Hideo Kigoshi, Prof. Junji Ichikawa, and Prof. Takahiro Sasamori for reviewing this thesis.

I would like to express my thanks to Dr. Ryuichiro Ohshita, Mr. Jumpei Horiuchi, Dr. Shigeto Hirayama, Dr. Keita Iio, Mr. Akihisa Tokuda, Ms. Kao Hashimoto, Mr. Toshiaki Kuribayashi, Mr. Shoma Takeda for their technical assistance with the experiments. I would like to sincerely thank members of the Nagase group, Ms. Naoko Yamada, Ms. Yuko Nito, Ms. Mami Nakamura, Ms. Miyuki Nakazawa, Dr. Shuji Ioka, Dr. Sayaka Ohrui, Dr. Yasuaki Koyama, Dr. Takahiro Okada, Dr. Yan Zhang, Dr. Kazunori Seki, Dr. Masahiro Yata, Ms. Yuko Suzuki, Mr. Kenta Maeda, Dr. Koki Katoh, Dr. Tsubasa Hino, Mr. Keita Kajino, Ms. Natsumi Sakamoto, Ms. Erika Miyazono, Mr. Hiroki Uchiyama, Mr. Rintaro Ohtani, Mr. Ryusuke Ohtsu, Mr. Yoshiaki Takayama, Ms. Ruburika Nagao, Mr. Taisei Hasegawa, Ms. Chika Tsuchihara, Mr. Tomoya Kakumoto, Ms. Arisa Shinkai, Ms. Yuki Sekiya, Mr. Daiki Tashiro for their kind assistance and friendships.

I would like to express my thanks to BUCHI for allowing to use the medium-pressure liquid chromatography system, Reveleris®. I would also like to my heartfelt appreciation to Faculty of Pure and Applied Sciences, and the Open Facility, Research Facility Center for Science and Technology, University of Tsukuba for allowing to use JASCO J-820 for CD spectrum measurements.

I am also grateful for the financial support of the Tokyo Biochemical Research Foundation (C-FINDs: Chugai Foundation for Innovative Drug discovery Science) and JST-SPRING (Japan Science and Technology Agency Support for Pioneering Research Initiated by the Next Generation).

Finally, I would like to express my heartfelt gratitude and appreciation to my family; mother, father, grandfather, sister Airi, and all my friends, who always stood by my side with support, assistance, and encouragement.

List of publications

1) Saitoh, T.,‡ **Amezawa, M.,**‡ Horiuchi, J.,‡ Nagumo, Y., Yamamoto, N., Kutsumura, N., Ohshita, R., Tokuda, A., Irukayama-Tomobe, Y., Ogawa, Y., Ishikawa, Y., Hasegawa, E., Sakurai, T., Gouda, H., Tanimura, R., Yanagisawa M., Nagase, H., Discovery of novel orexin receptor antagonists using a 1,3,5-trioxazatriquinans bearing multiple effective residues (TriMER) library, *Eur. J. Med. Chem.* **2022***, 240,* 114505. (‡: contributed equally)

2) **Amezawa, M.**, Yamamoto, N., Nagumo, Y., Kutsumura, N., Ishikawa, Y., Yanagisawa M., Nagase, H., Saitoh, T., Design and synthesis of novel orexin 2 receptor agonists with a 1,3,5- trioxazatriquinane skeleton, *Bioorg. Med. Chem. Lett.* **2023**, *82*, 129151.

Supplementary list of publications

1) Iio, K., Saitoh, T., Ohshita, R., Hino, T., **Amezawa, M.**, Takayama, Y., Nagumo, Y., Yamamoto, Y., Kutsumura, N., Irukayama-Tomobe, Y., Ishikawa, Y., Tanimura, R., Yanagisawa, M., Nagase, H., Discovery of orexin 2 receptor selective and dual orexin receptor agonists based on the tetralin structure: switching of receptor selectivity by chirality on the tetralin ring, *Bioorg. Med. Chem. Lett.* **2021**, *60*, 128555.

2) Iio, K., Hashimoto, K., Nagumo, Y., **Amezawa, M.**, Hasegawa, T., Yamamoto, Y., Kutsumura, N., Takeuchi, K., Ishikawa, Y., Yanagisawa, M., Nagase, H., Saitoh, T., Design and synthesis of orexin 1 receptor-selective agonists, *J. Med. Chem. under revision.* (*ChemRxiv* **2022**, doi: 10.26434/chemrxiv-2022-fxx2d.)

3) Lin, Y., Roy, K., Shuji, I., Otani, R., **Amezawa, M.**, Chérasse, Y., Kaushik, M. K., Klewe-Nebenius, D., Zhou, L., Oishi, Y., Saitoh, T., Lazarus, M., Positive allosteric adenosine A2A receptor modulation suppresses insomnia associated with mania- and schizophrenia-like behaviors in mice, *Front. Pharmacol. under revision.*